CHAPTER 1

GENERAL INTRODUCTION

1.0 Introduction

Reproductive biology has been reported to be the most crucial area of research for a successful domestication of any animal species (Addo, *et al.,* 2007). This is because the propagation of the species depends on it and most importantly, the maintenance of reproductive competence in captivity has been identified by experts as a cardinal marker of successful domestication (Zeuner, 1963; Dukelow, 1978; Fox, 1987; Adams, 1989). In the same vein, both the male and female genders in any mammalian species have reproductive characteristics that are crucial to facilitating and maximizing productivity (Hafez, 1980).

The basis for a sound knowledge of the male reproductive biology in any species lies in the detailed morpho-functional studies of its reproductive organs (Segatelli *et al.*, 2004) which entails, first, thorough morphological investigations of each segment of the tract at the gross, histological and ultra-structural levels in an attempt to understand the species-specific structural peculiarities of the organs, tissues and cell organelles in the male reproductive system. Secondly, it also involves the characterization and localization of hormones and peculiar cellular proteins that mediate and regulate male reproductive processes as well as their species-specific distributions in the different segments of the reproductive tract, by means of biochemical and immunohistochemistry assays, so as to understand and correlate physiological functions with structural morphology (Carpino *et al*., 2004; Lu *et al*., 2008; Joseph *et al*., 2011). Thirdly, it equally involves quantitative studies through morphometrical and stereological analysis of male reproductive tissues and cells which are not only valuable in the correlations of physiological or biochemical findings with morphological data (Segatelli *et al.*, 2004), but also allows for more

complete knowledge of spermatogenic process and reproductive structural behaviors under different conditions (Leal *et al.,* 2009; Machado-Junior *et al*., 2011).

The information from these studies has been used to characterize basic reproductive parameters peculiar to the species in question. For instance, in rodents like mice (Gomendio, *et al.*, 2006), gerbils (Segatelli, *et al.*, 2002) and African giant rat (Oke, 1988) detailed morphologic and morphometric analysis of the testis and epididymis have been used to characterize several specie-specific parameters, such as the gonadosomatic index, epididymal and seminiferous tubular diameters cum epithelial heights, sertoli and germ cell counts, number of germ cells supported by each Sertoli cell, the volume densities of seminiferous tubules and epididymis, the number of spermatogonial generations, the number of Sertoli cells per gram of testis and so on. These parameters have also served as yardstick in the evaluation of the reproductive efficiency in both wild (Almeida *et al*., 2006; Costa *et al*., 2008) and domesticated mammalian species (Franca *et al*., 1999; Neves *et al*., 2002; Ichihara and Pelliniemi, 2007). Similarly, changes in these parameters have equally been used to evaluate and/or determine the effects of some environmental (light, seasons, temperature, etc), pathological and pharmacological (drugs) conditions on the reproductive efficiency and competence in males (Ljungvall *et al.,* 2008; Abdelmalik, 2011) particularly of wild animals that are currently undergoing captive rearing and domestication (Ponchron *et al*., 2002; Busso, *et al.*, 2012).

At the same time, data from these studies also serve as aid in the genetic improvement and increase of parent stocks as well as intensification of production practices (Busso *et al*., 2012). According to Pukazhenthi and Wildt (2004), the knowledge of reproductive tract morphology and how it functions is, perhaps, the most important factor for the successful application of assisted reproductive techniques such as Artificial insemination and/or embryo

transfer in mammals. In *Chinchilla spp*, a wild hystricomorphic rodent that is currently undergoing captive-rearing and domestication in South America, genetic improvement was only made possible after a detailed knowledge of its reproductive tract morphology (Busso, *et al.*, 2012).

The greater cane rat (*Thryonomys swinderianus)*, popularly known as Grasscutter, is one of the wild rodents that are currently undergoing domestication and captive-rearing in parts of Africa. This herbivorous hystricomorphic rodent, found only in Africa yet (Addo *et al*., 2007), is vigorously hunted and exploited for food particularly in the West Africa sub-region. This is because its meat has an excellent taste and a comparatively high nutritive value (Asibey and Eyeson, 1975, Addo *et al.,* 2007). The mineral content of the tissue is similar to mutton (Ajayi and Tewe, 1980) with a comparably better carcass value which is low in fat but with high-quality lean meat, making it a meat-of-choice for people with cardiac problems. The meat yield and average dress weight are higher than for most species of livestock (Ajayi, 1994). Being one of the preferred and perhaps, the most expensive meat in West Africa (Asibey and Addo, 2000), it contributes to both local and export earning of many West African countries (GEPC 1995; Ntiamoa-Baidu, 1998). Also, as a rodent of African origin, the cane rat can become a good indigenous laboratory animal for biomedical research in Africa (Opara, 2010).

Consequent on these advantages of nutrition as well as financial and research potentials of the cane rat, efforts and resources are now being directed to its rearing/domestication and the recent trend in its farming is towards increased stocking and intensification of production (Adu *et al.*, 2005). However, the paucity of information on the reproductive biology (Yeboah and Adamu, 1995; Addo *et al.,* 2007) has slowed down the domestication process and has made parent stocking and intensified production difficult. Therefore, information on the reproductive

biology especially on the structure and functions of the male reproductive system in this animal is very imperative

1.1 Justification

Although there are some reports in literature regarding the ultra-structure of the efferent ducts (Aire and van der Merwe, 2003), the gonadosomatic index and the morphology of the Epididymis (Adebayo *et al.*, 2009; Adebayo & Olurode, 2010), accessory sex glands and penis in the greater cane rat (Adebayo *et al.,* 2009*a & b;* 2011), little is known about the reproductive biology particularly, the structural and functional anatomy of the reproductive system in the male cane rat. Therefore, the aim of this work is to provide detailed knowledge of the reproductive biology through the morpho-functional analysis of the male reproductive tract of the greater cane rat (*Thyronomys swinderianus*).

1.2. Objectives of the Study

The objectives of this research therefore are:

- To qualitatively and quantitatively characterize and fully describe the male reproductive tract – testis, efferent duct, epididymis and the accessory sex glands of the greater cane rat at gross, histological and ultra-structural levels.

- To evaluate the serum levels of five male sex hormones - testosterone, estrogen, progesterone, luteinizing hormone (LH) and the follicular stimulating hormone (FSH) in the male cane rat.

- To investigate the localization and the distribution of the two subtypes of estrogen (ERα and ERβ) and progesterone receptors along the different regions of the reproductive tract in the male cane rat.

- To morphometrically establish the following:
  i. The stages of the seminiferous epithelium cycle.
  ii. The frequencies of the stages.
  iii. The anthropometrical indices that can affect reproductive efficiency.

- To establish the possibility or otherwise of seasonal variation in reproductive efficiency by evaluating the effect of seasons on serum hormonal levels and testicular morphometric parameters.

CHAPTER 2

LITERATURE REVIEW

2.1. Anatomy of the Male Reproductive System

In all mammalian species, the four components of the male reproductive system are:

The two testes – the primary sex organs that function both as exocrine gland that produces the male germ cells and an endocrine gland that produces the male sex hormone, testosterone (Dyce *et al.*, 2002);

A paired excurrent duct system, each consisting of *Efferent ductules*, *Epididymis* and the *Deferent duct* which collect, modify, store and conduct spermatozoa from each testis (Dyce *et al.*, 2002);

The accessory sex glands – *vesicular gland, prostate* and *the bulbourethral glands* which secrete a nutritive and lubricating fluid medium called seminal fluid (Dyce *et al.*, 2002);

The penis - the copulatory organ that houses the major part of the urethra (Dyce *et al.*, 2002)

2.2. Development and Structure of the Testes

2.2.1 Embryonic development:

The development of the gonads begins in the embryo as a ridge-like thickening on the ventromedial face of the mesonephros while it is still the dominant embryonic excretory organ (Patten, 1959). This thickening, which begins as a single layer of coelomic epithelium, soon

rapidly becomes several layers thick, thereby causing this region to bulge into the embryonic coelom as the genital ridge (Arey, 1974). Histologically, at this stage, the genital ridge essentially consists of proliferating mesenchymal cells covered by epithelium. As the epithelium of the genital ridge proliferates it sends disorganized, densely packed cords of cells into the mesenchyme (Merchant – Larios, 1979). These epithelial cords which are called the primitive sex cords are subsequently invaded by the primordial germ cells which will later become the precursor of the gametes (Hahnel and Eddy, 1986).

The primodial germ cells originate from the extraembryonic mesoderm and endoderm of the yolk sac as well as the allantois close to the posterior end of the primitive streak. These mobile cells first migrate into the developing gut and at the level of the gonad, move actively out of the gut into the mesentery through which they reach the genital ridge where they subsequently invade the primitive sex cord (Fargeix *et al.*, 1981). Dyce *et al.* (2002) have also pointed out the possibility of carriage through the blood stream. During this migration the primodial germ cells divide mitotically and this continue even after their arrival at the genital ridge.

At this stage in the development, the resulting presumptive gonad is sexually undifferentiated either by gross inspection or by histology. Thus, it is referred to as the "indifferent" or "neuter" stage (Arey, 1974; Fargeix *et al.*, 1981). This neuter stage consists of thickened coelomic epithelium known as the cortex and a core of sex cords with some mesenchyme known as medulla (Hafez, 1987). However, as the gonads develop, the earliest indication that they will become a testis is provided by a marked mesenchymal condensation below the coelomic epithelium. This eventually forms a layer of connective tissue known as the tunica albuginea which separates the sex cords from the surface epithelium of the developing testes. The primitive sex cord, now isolated from the surface epithelium continues to grow in size

and in complexity of arrangement, forming a mass of cords that narrows at their distal tip to form the rete testes. These sex cords, now the seminiferous cords (Balinsky, 1981) are the forerunners of the seminiferous tubules (Dyce *et al.*, 2002).

Later in fetal life, the seminiferous cords become canalized, thereby creating a series of passage leading to the mesonephric ducts which have survived the general regression of the mesonephros to become the outlet for the gamete products of the testes. Therefore, the peripheral part of the cord becomes the seminiferous tubule, the central part (the narrow distal tip) becomes the rete and the mesonephric tubule becomes the efferent duct (Dyce *et al.*, 2002).

Within the seminiferous tubule at this stage, two cell lineages can be recognized: one provides the sustentacular cells that are precursors of the Sertoli cells; the second which is from the primodial germ cells differentiates into gonocytes that develop into the gametes postnatally. The mesenchyme surrounding the seminiferous tubules differentiates into connective tissue septae which extend to the tunica albuginea and converge towards an area occupied by the rete testes. Additional cell types which develop from the mesenchymal bed and lie between the seminiferous tubules are the interstitial cells and can be identified both in fetal and post natal life (Arey, 1974). While Fawcett and Burgos (1956) described interstitial cells as transformed fibroblasts that were responsible for the endocrine secretion of testosterone, Dyce *et al.* (2002) presumed their progenitors, like those of the Sertoli and primodial germ cells, migrate from the mesonephros during the fetal development to become embedded in the mesenchyme interstitium where they develop a second generation Leydig cells when the process of spermatogenesis is initiated at puberty.

The development of the testes which begins prenatally continues postnatally with the organ fully and functionally formed at puberty. According to Marty *et al,* (2003), the prenatal, early postnatal and prepubertal testes play a critical role in hormone production. This in turn regulates the differentiation of the male reproductive organ (Jost, 1953; Lasnitzki and Mizuno, 1977; Prins and Putz, 2008). Testosterone and its metabolites, 5α dihydrotestosterone (DHT) as well as estrogen play important roles in testicular development and functioning (Eddy *et al*, 1996; Matsumoto *et al*, 2005). However, recent findings have demonstrated that prenatal testosterone and DHT treatment during male fetal sexual differentiation have differential effects on post-puberal testicular and seminiferous tubular sizes in sheep (Recabarren *et al*, 2008; Bormann *et al*, 2011). Specified amount of these hormones are therefore essential for the prenatal, post natal and prepubertal testicular development.

The timing difference in the postnatal development of the testes in the different mammalian species (Connell, 1980; Ojeda *et al.*, 1980; Cortes *et al.*, 1987; Anderson *et al.*, 1998; Lemaster *et al.*, 2000) is also a factor that determines the testicular weight and the onset of spermatogenesis – a process that determines the reproductive ability and competence of the testes in adult animal.

2:2:2 Testicular Descent

During mammalian evolution, the male gonad has assumed a progressively lower position relative to the ovary and eventually taking up an extra abdominal location within the scrotum in most mammals (Bedford, 1978; Williams and Hutson, 1991). This process, known as testicular descent appears to be in multiple stages with various anatomical factors and hormonal

influences (Hutson *et al.*, 1997). The stages which were first proposed by Gier and Marion (1969) are: the initial displacement of gonads by the metanephros; the trans-abdominal movement to the groin and the final descent of the testes through the inguinal canal and down to the scrotum.

The process of testicular descent begins when the developing testes are moved downward by the developing metanephros and by its own weight. With this movement, the peritoneum on either side of the mesonephros is thrown into folds forming the cranial and the caudal ligament of the mesonephros. As development progresses, the cranial ligament which is now called the cranial suspensory ligament regresses, while the caudal ligament that becomes the gubernaculum enlarges. The caudal enlargement of the gubernaculum during relative trans-abdominal movement is known as the "swelling" reaction or "gubernacular outgrowth" and is caused by cell division and increase in glycosaminoglycans and hyaluronic acid (Heyns *et al.*, 1990). This gubernacular bulb enlargement and the traction applied by the bulb through the gubernacular cord leads to the trans-abdominal descent (Trans-abdominal phase) and the subsequent anchoring of the developing testes to the inguinal region (Hughes and Acerini, 2008).

The final descent through the inguinal canal to the scrotum (Inguino-scrotal phase) occurs when the gubernaculum bulges beyond the external inguinal ring while it simultaneously hollowed out by a peritoneal diverticulum called processus vaginalis (Backhouse, 1966; Heyns, 1987; Hughes and Acerini, 2008). With intra-abdominal pressure, the testis is forced through the canal dilated by the gubernacular bulb. According to Wensing (1986) the process of testicular descent is similar in most species but there are some timing and topographical differences. For instance, in gubernacular growth, mesenchymal regression, development of cremaster muscles and gubernacular bulb resorption take place after testicular migration in pigs and humans but

before migration in rodents. Also, the gestation time for complete testicular descent into the scrotum varies considerably amongst different mammals. The human testis is descended generally at birth, in common with the rabbit, pig and horse (Amann and Veeramachaneni, 2007). By contrast, cattle and deer have testes fully descended early in gestation whereas this is considerably delayed after birth in the dog (Hughes and Acerini, 2008). Irrespective of the timing, the two-phase process of transabdominal and inguinoscrotal descent are common to all mammalian species but are controlled by different mechanisms (Hughes and Acerini, 2008).

In most mammals, the inguinal canals close after the testes have rested in the scrotum. However, in some rodents these canals remain patent. In such rodents e.g. rabbit (Holtz, 1972), African giant rat (Oke and Aire, 1997; Akinloye, 2009), the opened inguinal canals and the complete encircling of the processus vaginalis by the cremaster muscle provide for the withdrawal of testes into the abdominal cavity, making scrotal, inguinal and abdominal locations of the testes possible.

2.2.3. The Structure of the Testis

The testes are paired ellipsoidal organs whose bulk bears no fixed proportion with the body size (Dyce *et al.*, 2002). As observed by Möller (1989), in mammals and birds, the size of the testis at sexual maturity is positively related to the rate of sperm production.

Enclosed in a pouch of skin known as Scrotum, testes have medial and lateral surfaces as well as free and attached (Epididymal) borders. Each testis is surrounded by the visceral layer of the vaginal processus and covered by a capsule of dense connective tissue called tunica albuginea. This tunic houses the vascular bed that feeds and drains the testis. It is thick in boar

and stallion and is sometimes referred to as tunica vasculosa in these species (Samuelson, 2007). According to Aire (2006) available data on capsular thickness varies among mammals as Davis *et al.* (1970) had earlier indicated that the thickness of the capsule varies from one testicular region to another. It has also been demonstrated that the capsule contains smooth muscles in some mammals (Davis *et al.,* 1970; Hargrove *et al.,* 1977). These muscles are probably responsible for the spontaneous and drug induced contractions that assist the movement of immobile testicular spermatozoa toward the epididymis in these mammals.

The capsule detaches septa and trabeculae (septulae testis) into the testicular parenchyma dividing it into lobules called lobuli testis. The septa are not always conspicuous but where it is well developed, it may either converge centrally to form mediastinum testis as in canine, ruminant and porcine (Setchell, 1977) or posteriorly towards the side bordering the epididymis as in equine, feline and rodents (Samuelson, 2007). The mediastinum testes (Corpus fibrosa) which occupy the long axis of the testis, is not only a thickened portion of the tunica albuginea but also contains rete testis as well as large lymphatics and vascular vessels.

Histologically, the lobules of the testis vary in number according to species (Samuelson, 2007). Each lobule holds the parenchyma which consists of one to four looping seminiferous tubules – the site for the production of spermatozoa. The ends of each tubule are connected to short straight ducts called the tubuli recti that guide the developing spermatozoa to the labyrinth of anastomosing channels - the rete testis. The rete begins a system of excretory duct called the excurrent duct of the male reproductive tract (Holtz, 1972; Aire, 2006; Samuelson, 2007).

2:2:3:1 Seminiferous Tubule

The seminiferous tubules constitute the exocrine portion of the testis which is in essence a cytogenous gland whose secretory products are whole cells (holocrine), the spermatozoa. This tubule, which may be branched or blind-ended (Bloom and Fawcett, 1975) is lined by a complex stratified epithelium composed of two cell type – supporting cells called Sertoli cells and spermatogenic cells.

2:2:3:2 Spermatogenic Cell

The motile spermatogenic cells comprise a series of differentiating cells that migrate continuously from the periphery of the tubule to the luminal free surface (Weiss, 1983) and are arranged in well defined concentric layers within the epithelium. These cells include, from the basal lamina to the lumen: Spermatogonia, primary spermatocytes, secondary spermatocytes, spermatids and spermatozoa (Roosen – Runge, 1961). The spermatogonia lie next to the basal lamina of the seminiferous epithelium between adjacent sustentacular cells. Their nuclei are round or slightly ovoid with nucleoli usually attached to the nuclear envelope. The proliferative activity of the epithelium is confined to the spermatogonia and spermatocytes near the base (Rowley *et al.*, 1971). The primary spermatocytes are readily recognized by their extensive cytoplasm and large nuclei containing coarse clumps or thin threads of chromatin. The secondary spermatocytes are much smaller than the primary spermatocytes and may contain pale granular chromatin. They have short duration and are infrequently found in sections of the seminiferous tubules (Weiss, 1983; Wheater *et al.*, 1990). By the process of meiosis, the secondary spermatocytes produce the spermatids which then proceed through a long metamorphosis known as spermiogenesis to become the spermatozoa.

The process of spermiogenesis involves four phases; the Golgi phase, the cap phase, acrosome phase and the maturation phase, at the end of which the reproductive cells become disengaged from the Sertoli cells to enter into the lumen of the tubule by another process called spermiation to become spermatozoa (Samuelson, 2007). Each seminiferous tubule, which is the site of the entire process of spermatogenesis, is about 1m in length and 0.5mm in diameter in the humans (Robaire *et al.,* 1995).

In mammalian species, the different generations of germ cells i.e. the spermatogonia, spermatocytes and the spermatids are organized into a series of well defined cellular associations. According to Weinbauer *et al*, (2001), these cell associations are referred to as stages of spermatogenesis (seminiferous epithelium stage) and they occur in cyclic pattern varying in number and duration in a species-specific manner. A seminiferous epithelium cycle is the sequence of events that occur from the disappearance of a given cellular association (stage) to its reappearance in a given area of the seminiferous epithelium while the time interval required for the completion of a series of cellular association at one point within the tubule is known as the duration of the seminiferous epithelium cycle (Segatelli *et al*, 2004). According to Segatelli *et al*, (2004) and Costa *et al*, (2010) identification of stages of seminiferous epithelium cycle and its durations are prerequisites for the estimation of the spermatogenic efficiency (daily sperm production/gram of testis) in any given mammalian species. The major criteria for stage identification resides in the knowledge of the morphological characteristic of the spermatids, in particular, their nuclei and acrosomal system.

Cellular associations of spermatogenesis have been described in both wild and domestic rodents like rat (Leblond and Clermont, 1952), mouse (Oakberg, 1956), golden hamster (Clermont, 1954), gerbil (Segatelli *et al*, 2002) and paca (Costa *et al*, 2010) with the duration

differing greatly among the species. Therefore, ultrastructural studies of the acrosomal formation and the characterization of the spermiogenic steps are very fundamental to stage identification especially in species where improved management and enhanced male reproductive capacity and artificial breeding programmes are desired (Comizzoli *et al*, 2000; Costa *et al*, 2010).

2:2:3:3 Sertoli Cell

Sertoli cells also known as sustentacular cells are the second type of cells found in the seminiferous epithelium. They are columnar cells resting upon the basal lamina and extending upwards through the full thickness of the epithelium to its free surface. As a group, Sertoli cells occupy much of the volume of the seminiferous tubules (Samuelson, 2007). The nuclei of the Sertoli cells are infolded to some extent in all species. The karyosome and peripheral clumps of heterochromatin that characterize the nuclei of most somatic cells are largely absent and the nucleoplasm is remarkably homogenous (Fawcett, 1975). The nucleolus is prominent and better observed in a thick section employed for light microscopy while ultrastucturally it may appear as a central mass with the laterally associated bodies (Pardue and Gall, 1970). The cytoplasm contains moderate number of mitochondria, many lipid droplets and relatively little rough endoplasmic reticulum. The presence of a highly ordered smooth endoplasmic reticulum, suggests that Sertoli cells are highly active in lipid biosynthesis (Wheater *et al.*, 1990).

The lateral sides of adjacent sustentacular cells form numerous infoldings as well as different types of cell junctions. The contact that form the junctions have been described in mouse and rats by Flickinger and Fawcett (1967) while Cheng and Mruk (2002) have reviewed the current status of research in the dynamics of cell junctions in the testes. The relationships of

the lateral sides of adjacent Sertoli cells are tightly linked to the development and activities of the spermatogenic cells (Weber *et al.,* 1983; Samuelson, 2007). According to Cheng and Mruk (2002) extensive interactions take place between Sertoli and germ cell in the seminiferous epithelium. These interactions co-ordinate the intermittent events of disassembly and re-assembly of Sertoli cell adherens and tight junctions as well as the Sertoli-germ cell adherens junctions that facilitate the movement of germ cells across the epithelium. Each Sertoli cell is able to support only a limited number of germ cells in a species-specific manner. In this regard, the number of the Sertoli cell established at puberty in mammals and the Sertoli cell efficiency are the best indicators of spermatogenic efficiency (the daily sperm production per gram of testis) (Hess *et al.*, 1993; Johnson, 1995; Franca and Russel, 1998; Costa *et al*, 2010).

In addition to supportive and sustaining roles, the Sertoli cells play a major role in the release of spermatids after spermatogenesis. They are responsible for the formation and maintenance of the blood-testis-barrier and for the secretion of intertubular fluid which mediates the transport of spermatozoa. The fluid is rich in inositol and glutamate which are also products of Sertoli cells (Schulze, 1984). The cells equally synthesize and secrete various proteins including the androgen binding protein (ABP) detected in rats (Hansson *et al.*, 1976). ABP found in rete fluid, epididymis and blood are utilized as an indicator of the metabolic activity of Sertoli cells (Hagenas and Ritzen, 1976).

Several hormones are secreted by Sertoli cells, major among which is inhibin, a steroidal hormone that acts upon both the hypothalamus and pituitary glands thereby controlling the secretion of FSH (Steinberger and Steinberger 1976; Lumpkin *et al.,* 1981). In rat, inhibin is known to inhibit DNA synthesis in the germ cell at the onset of spermatogenesis (Demoulin *et al.*, 1979; Setchell, 1980). Recent reports have also shown that testosterone and estrogen are

secreted by this cell in rat (Ichihara and Pelliniemi, 2007; Carreau *et al*, 2011). The other hormone is the antiparamesonephric hormone during the early development of the male. In Stallion, the number of the Sertoli cells has been reported to decline substantially as the animal ages (Samuelson, 2007).

2:2:3:3 Leydig Cell (Interstitial Cells)

The intertubular tissues of the adult testis are composed of loose connective tissue with a population of polygonal, fusiform and clear cells as well as rich networks of blood and lymphatic vessels (Burgos *et al.,* 1970; Oke, 1988; Wrobel and Bergmann, 2006). The large polygonal cell which has been described in a variety of mammal by Leydig (1850) is known as the interstitial or Leydig cells. Generally, the arrangement of the interstitial tissues showed marked species variations in terms of abundance of Leydig cells, amount of interlobular connective tissues and the location as well as the degree of development of the lymphatic system. The arrangement equally plays vital role in the interpretation of the physiology of the testis in any given mammalian species (Fawcett *et al.,* 1973; Wrobel and Bergmann, 2006).

The Leydig cells have single, eccentrically located nuclei which contained prominent nucleoli as well as a thin layer of condensed chromatin along their periphery (Schulze, 1984). The cytoplasm has a well developed smooth endoplasmic reticulum which consists of a labyrinth of anastomosing tubule of varying width and occupies a large area in each cell (Neaves, 1975; Aire, 1997). They also contain numerous mitochondria, prominent Golgi apparatus, centriole as well as a number of lipid droplets (Christensen, 1975). In humans, a specialized crystal (Reinke crystals) and lipofushin pigment granule are equally present (Weiss, 1983). The fine structural

arrangement of the Leydig cell organelles show some species characteristics which tend to be altered under different disease conditions (Ueno and Mori, 1990; Kianifard *et al*, 2012)

Functionally, the ultrastructure of Leydig cells betrays their roles in steroid synthesis. Their function of producing the male sex hormone, which was first suggested by Bouin and Ancel (1903) is now generally agreed upon - the cells produce majority of testosterone hormone from cholesterol. These cells which first become active during fetal life secrete considerable amount of testosterone which governs the differentiation of male sex organs. The fetal Leydig cells regress before birth but develop again at or before the onset of puberty in a species-specific manner (Hagenas, 1977; Marty *et al.*, 2003). According to Akingbemi (2005), Leydig cells also play a role in the secretion of testicular estrogen in man, stallion and boar. However, recent studies on rat have led to the assertion that Leydig cells are the major source of estrogen in adult life (Carreau *et al*, 2006; 2011)

The secretory activities of the Leydig cells are under the control of a pituitary gonadotrophic hormone, luteinizing hormone (also known as Interstitial Cell Stimulating Hormone) (Wheater *et al.*, 1990) and show some species variations. In seasonal breeders, the cells thereof follow a seasonal breeding scheme in which the testes, during one period of the year, are more or less atrophic with atrophic Leydig cells and regressed germinal epithelium. On the other hand, in non–seasonal breeders (like man and laboratory rats) there are continuous spermatogenic and Leydig cell activities throughout the year (Christensen, 1975; Chaves *et al.*, 2012).

Other component cells of the interstitium include very few macrophages that are closely associated with few single or a group of Leydig cells. In most mammals, these cells are

structurally and functionally coupled (Bergh, 1987; Gayton *et al.*, 1994). Some blood-derived cells such as lymphocytes, plasma and mast cells may also be seen in the interstitium of some species (Christensen and Fawcett, 1977; Aire, 2006).

2:3. The Development and Structures of the Excurrent Duct System

The excurrent duct system comprises the various ducts that transport spermatozoa and fluid produced by the seminiferous epithelium. They exist within the testes, the intratesticular duct and outside the testes, the extratesticular ducts. The intratesticular ducts comprise the tubuli recti and the rete testis (RT) units while the extratesticular ducts are made up of the efferent duct unit and the epididymal duct unit which in turn comprises the ductus conjugen (connecting duct), the ductus epididymidis (Epididymal duct) and the ductus deferens (the deferent duct) (Aire 2006).

2:3:1 Embryonic Development

Although the entire excurrent ducts develop from the mesonephros, the different parts of the duct system differentiate at different times (Roosen – Runge, 1961). While the intratesticular duct system develops as the testes differentiate from the mesonephros, the extratesticular duct system develops from the few mesonephric tubules that survived the general regression of the mesonephros (Dyce *et al*., 2002). As the seminiferous cords are being formed, they connect to a plexus or network within the testis. On the other side, the plexus makes contact with the blind ends of the few surviving mesonephric ducts. This is then followed in later fetal life, by canalization of the cords, thereby creating a series of passages leading to the mesonephric/ Wolffian duct which become the outlet for the gamete product of the testes (Patten, 1959; Larios and Mendoza, 2001). Subsequently, as the peripheral parts of the cords become the seminiferous tubules, the central part becomes the rete testis while the mesonephric tubules become the efferent ducts. In the same vein, the first part of the mesonephric/Wolffian duct undergoes convolution and transforms into the duct of the epididymis within its dense connective tissue

while the remaining part retains a straight course and acquires thicker investment of smooth muscle to become the ductus deferens which initially opens into the cloaca part that becomes the urogenital sinus (Dyce *et al*., 2002; Moore and Persaud, 2003; Hannema and Hughes, 2007). The major morphogenic events during Wolffian duct/epididymal duct development are the elongation and coiling of the duct (Hannema and Hughes, 2007). The process of elongation is likely a product of potential mechanisms such as cell proliferation coupled with directed cell rearrangements, along with the interactions between the Wolffian duct epithelium and the surrounding mesenchyme cells (Hinton *et al.*, 2011).

2:3:2. The Structures and Functions of the Excurrent Ducts.

2:3:2:1. The Intratesticular Duct System

Tubuli Recti:

The tubuli recti are the generally straight tubules that connect the highly convoluted seminiferous tubule to the rete testis. These tubules vary in length and can become tortuous as they progress distally towards the rete testis (Fawcett, 1975). As the terminal ends of the seminiferous tubules join the tubuli recti, they narrow in diameter, become depleted of germinal elements and lined only by Sertoli cells that become distally replaced by simple squamous to cuboidal epithelium. As the tubule nears the rete, the epithelial lining may become more columnar and apically modified with microvilli and cilia as well as lymphocytes and macrophages (Samuelson, 2007).

Rete Testis:

The anatomy of the adult rete testis varies greatly in different mammals (Roosen Runge, 1961). The distribution of rete testis in mammals also varies between species being septal and mediastinal in rat (Hermo and Dworkin, 1988), guinea pig (Fawcett and Dym, 1974), goat (Ezeasor, 1986; Goyal *et al.*, 1992) and bull (Hees *et al.*, 1989). Generally, however, the rete is a labyrinth-like network of anastomosing channels which function to receive from the tubuli recti, the inactive spermatozoa produced by the seminiferous tubules. Based on location, the rete testis can be divided into three parts namely intratesticular, intratunical and extratesticular parts, although this has been a subject of controversy (Roosen-Runge, 1961).

Roosen-Runge (1961) earlier reported that in rats, the intratesticular part is the largest and is not a network of fine canals but essentially a cavity, a flattened tube lying on the testes tubules and interrupted near the midline by occasional pillars of connective tissues lined with epithelium. However, though the intratesticular rete is rarely observed in birds, where present (in birds) and in mammals, it constitutes a minor part of the duct (Amann *et al.*, 1977; Roosen-Runge and Holstein 1978, Budras and Meier 1981). The pillars of connective tissues named chordae retis by Roosen-Runge and Holstein, (1978) may be a common feature of the RT in many species and probably act as transluminal coupling devise for contractile system of myofibroblast (Hees *et al.*, 1989) as do the *trabeculae septomarginales* of the heart (Aire, 2006).

The intracapsular and extracapsular portions of the rete testis are made up of rete channels that have epithelial linings similar to the intratesticular portion. The intracapsular rete connects the intratesticular rete with an extratesticular extension near the cranial end of the testis.

An extratesticular portion appears to be found in only a few mammalian species e.g man (Roosen-Runge and Holstein, 1978) and goat (Goyal *et al.*, 1992).

Histologically, the rete epithelium is simple squamous to low columnar (Hees *et al.*, 1989). The epithelium contains only non-ciliated cell type from which a single cilium projects. As observed by Hees *et al.* (1989), the solitary central cilium that exhibits the 9 + 2 axonemal structure and sensory in function, appears to be a common feature in rete cells in animals and man. Other cell types that may be found in the epithelium are the intraepithelial lymphocytes as well as occasional ciliated cells (Aire, 2006).

Functionally, the rete testis epithelium secretes 65% of the total testicular fluid (Tuck *et al.*, 1970). The network of the rete testis lacunae are surrounded and held together by a substantial amount of dense connective tissues which contain scattered myofibroblasts that lied beneath the epithelium (Samuelson, 2007). They act (by relaxation) to suck fluids from the seminiferous tubules and to move (by contraction) the testicular fluids forward into the efferent ducts (Aire, 2006).

2:3:2:2 The Extratesticular Duct System

The Efferent Duct Unit:

The structure of the efferent ducts varies not only from one species to another but also between the segments of the ducts in the same species (Aire and van der Merwe, 2003). Generally, the efferent duct unit is made up of 8-20 or more, short tubules that lead spermatozoa to the ductus epididymis (Samuelson, 2007). According to Ilio and Hess (1994), the efferent

ducts are unique in that they are the only duct unit of the male reproductive tract that is lined by a ciliated epithelium in addition to non ciliated cells.

The structure and the ultrastructure of the non ciliated cell components also vary from one species to another. For instance, in laboratory animals, there is a single non-ciliated cell type (Robaire and Hermo, 1988), two cell types in birds (Aire *et al.*, 1979; Aire, 1980) and three cell types in man, bull, goat, dog and greater cane rat (Morita, 1966; Goyal and Hrudka, 1981; Gray *et al.*, 1983; Goyal *et al.*, 1992; Ilio and Hess, 1994 and Aire and van der Merwe, 2003). Though, the significance of this difference is not clearly understood, Aire and van de Merwe (2003) opined that the varying structural features have functional significance and relevance. This classification of the non-ciliated cells in the efferent duct is based on the variation in the disposition and the number of vacuoles and/or granules in the cells. It is equally not clearly known whether or not these organelle differences influence the function of these cells in mammals but there appears to be an obvious dichotomy in function between the two non-ciliated cell types in birds (Clulow and Jones, 1988; Aire, 2006).

From the work of Aire and van der Merwe (2003) on the greater cane rat (*Thryonomys swinderianus*), it was reported that the efferent ducts emerge from the testes and run relatively straight course from the rete testis on the craniomedial aspects of the testes. They then became wavy and highly convoluted as they approach the epididymis where they subsequently open individually into the initial segment of the epididymis.

Histologically, three segments of the efferent duct were identified in the greater cane rats, based on their content of non-ciliated cell types (Aire and van der Merwe, 2003). Type I non-ciliated cells which are exclusively present in the long proximal part of the duct, exhibit a well

developed subapical endocytic apparatus as well as numerous oval or pleomorphic dense bodies. The type II non-ciliated cells predominate in the middle part of the duct and display a poorly developed subapical endocytic apparatus but contain large numerous vacuoles and dense bodies. The type III non-ciliated cells found in the epithelium of the terminal part are poorly endowed with a subapical endocytic apparatus and contain no conspicuous endocytic vesicle or vacuole but only a few small dense bodies, if at all. Though the ciliated cells of the efferent ducts have uniformly spaced cilia, interspersed with a few short and thinner microvilli than the non-ciliated cells and projecting into the duct, the relative frequency of the ciliated cells varies along the length of the duct. However, the work of Aire and van der Merwe (2003) did not count or establish the number of the short tubules that make up the efferent duct in the greater cane rat.

Functionally, it is now known that the epithelia of the efferent ducts modify their through-flow in many ways including but not limited to, sperm maturation and viability, fluid absorption and storage of spermatozoa (Joseph *et al,* 2011). Micropunctures studies in mammals indicate that the efferent duct reabsorb most of the testicular fluid entering the excurrent duct of the testis (Crabo, 1965; Jones, 1980; Clulow *et al.*, 1994; Man *et al.*, 1997, Lu *et al.,* 2008). According to Jones (1988), the rate of fluid absorption by the efferent ducts is much higher in birds than mammals since it takes spermatozoa 8 minutes to traverse the entire efferent duct of a Japanese quail as opposed to 45 minutes that it will takes to traverse the duct in the rat (English and Dym, 1981). Hees *et al,* (1987) equally observed that estrogen seems to have a profound effect on the ability of the efferent duct to reabsorb luminal fluid in mouse. Recent immunolocalization and gene expression of the alpha and beta estrogen receptors in the efferent duct have now established the role of estrogen in the development and normal functioning of the efferent duct (Joseph *et al.*, 2011).

Although the efferent ducts consistently show intense immunostaining for the two estrogen receptors across all species, the labeling of the different epithelial cells of the efferent ducts differ among species. In most species, the ciliated cells are known for being estrogen responsive in both male and female (Hess and Carnes, 2004; Schon *et al,* 2009) but in some species such as marmoset, the ciliated cells of the efferent duct exhibit reduced immunostaining (Shayu *et al,* 2005). According to Joseph *et al,* (2011), the complete understanding of the role of estrogen in the efferent ducts depends on the characterization of the distribution pattern of its receptors in the efferent ducts in as many as possible mammalian species.

In the rats, Morales and Hermo (1983) have demonstrated that the non-ciliated cells are capable of internalizing specific substance from the duct lumen in both absorptive and fluid phase endocytosis. It is also capable of absorbing testicular protein secreted into the testicular fluid (Veeramachenani and Amann, 1991; Clulow *et al.*, 1994).

The Epididymal Duct Unit

The mammalian epididymis is closely attached to the testis extending from one pole of the testes to the other and consisting of basically one duct arranged in a highly convoluted manner. The duct folds into a well organized structure comprising of many segments, each with distinct morphology and function (Robaire *et al,* 2006). The adult epididymis reaches over 1m in the mouse, 3m in the rat, an admirable 6m in humans and an extraordinary 15-18m in the stallion (Maneely, 1959; Jiang *et al.*, 1994; Stoltenberg *et al.*, 1998; Turner, 2008).

The pattern of attachment of the efferent ducts to the epididymis varies between animal species (Guttroff *et al.*, 1992). In most mammals, the efferent ducts have multiple points of entry into the rete testis. In rodents, these ducts converge into a common duct that feed into the initial

segment of the epididymis while in large mammals, including the humans, parallel efferent ducts form multiple entries into the head of the epididymis. Multiple entry patterns have also been reported in greater cane rat (Aire and van der Merwe, 2003). According to Joseph *et al.*, (2009), this enormous variation between species leaves many questions about the ways in which efferent duct connections to the rete testis and the epididymis are made.

The division of the epididymis into different regions or segments has been the topic of considerable discussion in several reports (Oke, 1988; Hinton and Turner, 2003; Robaire and Hinton, 2002; Robaire *et al.*, 2006). Conventionally and grossly, in most mammals, three easily recognized regions can be observed namely: Head (caput), Body (corpus) and Tail (cauda) epididymis. According to Oke (1988), the difficulties caused by the division into head, body and tail led to a new terminology of initial, middle and terminal segments introduced and advocated by Glover and Nicander (1971). However Joseph *et al.*, (2011) reported that the epididymal tube can be grouped into roughly five gross anatomical segments: Initial segment, Caput, Corpus, Cauda epididymis and the Vas deferens.

In animals which have testes whose long axis is vertical, the caput epididymis (head) is located close to the proximal pole of the testes while the tail is distal in position. The body is usually a narrow isthmus joining the head and tail together. The tail segment usually projects beyond the distal end of the testis to occupy the lowest and coolest part of the scrotum which normally exists at temperature 1.5 – 4^{o}C cooler than the adjacent testis (Brooks, 1973; Turner, 2008).

Histological characteristics allow for the easy identification of the anterior and posterior extremities of the mammalian epididymis. The thickness of the epididymal epithelium varies

with the thickest portion in the proximal caput and the thinnest in the caudal region. Conversely, the luminal diameter and the thickness of the peritubular smooth muscle increases from the proximal to the distal regions (Lasserre *et al*., 2001; Toshimori, 2003). Few sperm are found in the initial segment, but a large mass of sperm aggregates are located in the cauda (Yanagimachi *et al.,* 1985; Cornwall, 2009).

Histologically, the epididymis is divided into regions based on their cell types and population. These regions are physiologically different as they contain different luminal protein which may differ from one animal to another (Franca *et al*, 2005; Robaire *et al*, 2006). According to Dacheux *et al*, (2005) and Turner, (2008), in general, five physiological regions are distinguished as follows: (i) the proximal caput or the initial segment, (ii) the middle caput, (iii) the distal caput and the proximal corpus, (iv) the distal corpus and (v) the cauda epididymis. These physiological regions are however, different from the anatomical regions of the epididymis (Arroteia *et al*., 2012).

In all of these segments, the epididymal duct is lined with an epithelium composed of principal and basal cells. Other cells, such as apical, narrow, clear and halo cells are also present in this duct in a segment-specific manner. The cell population at the epithelium of the initial segment is comprised of principal cells, basal cells, narrow and apical cells (Reid and Cleland, 1957; Joseph *et al*, 2011). Narrow and apical cells of the initial segment and intermediate zone have a unique morphology and function that overlaps somewhat with clear cells (Adamali and Hermo, 1996). Nuclei of these cells are oval to spherical, and reside in the apical region of the cell. The narrow cell cytoplasm tapers between principal cells as it touches the basement membrane, but its apical cytoplasm may bulge slightly into the lumen with numerous vacuoles, endocytic vesicles, lysosomes, and mitochondria. These cells are somewhat different in their

biochemical components in that while carbonic anhydrase II (CAR2) is found only in the narrow cells, lysosomal enzymes, cathepsin D and beta-hexosaminidase A are present in both narrow and apical cells (Hermo *et al*, 2000). Narrow and apical cells equally show subtle differences in their expressions of specific components of the endocytic-lysosomal pathway. However, functionally, both cell types appear to be responsible for H^+ secretion and bicarbonate resorption in rat and mouse (Pushkin *et al*, 2000; Bagnis *et al*, 2001).

Beyond the initial segment, narrow and apical cell population drastically reduces with only about 1% in the cauda epididymis (Adamali and Hermo, 1996). On the other hand, clear cells are seen interspersed between the principal cells in the caput, corpus and cauda epididymis. Clear cells are large endocytic cells characterized by numerous coated pits at the apical region, vesicles, endosomes, multivesicular bodies, lysosomes, as well as lipid droplets (Robaire *et al.*, 2006; Abou-haila and Tulsiani, 2009). The endocytic activity of clear cells is greater than that of any other cell type in the epididymis, and is particularly active in the cauda segment. These cells are responsible for the uptake of a number of different proteins excreted by the epididymal epithelium, as well as the contents of the cytoplasmic droplet (Hermo *et al.*, 1988; Vierula *et al.*, 1995). Clear cells also secrete protons and express NHE3 (*Slc9a3*) and V-ATPase (*Atp6v1e1*) (Da Silva *et al.*, 2007; Shum *et al.*, 2009).

Principal cells are the most abundant and extensively studied cell type found in the epididymal epithelium constituting approximately 80% of the total epithelial cell population in the initial segment. The number of principal cells gradually decreases to 65% of the total epithelial cell population in the cauda epididymis (Robaire & Hermo, 1988). These columnar cells present prominent stereocilia and extend into the lumen. Ultrastructurally, the supranuclear region of this cell type contains large stacks of Golgi saccules, mitochondria, multivesicular

bodies and apical dilated membranous elements, while the infranuclear region is densely packed with rough endoplasmic reticulum (Robaire *et al*., 2000, Dacheux *et al*., 2005). Principal cells are responsible for the bulk of the proteins that are secreted into the lumen and are directly involved in the control of luminal protein concentrations. They frequently exhibit blebs of cytoplasm emanating from their apical cell surface. These cells also form tight junctions with one another, and as such, form the blood-epididymis barrier (Robaire *et al*., 2006; Cornwall, 2009).

Basal cells are the second most abundant cell type found in the epididymal epithelium, constituting 15-20% of the total epithelial cell population of the epididymis. They are triangular and flat cells that reside in the base of the epithelium. Basal cells cannot access the luminal compartment. They have elongated or round shaped nuclei, and they are in close association with the overlying principal cells or other basal cells through the presence of cytoplasmic extensions (Robaire *et al*., 2000; Cornwall, 2009; Arroteia *et al*, 2012). Because of this contact with the basement membrane, basal cells form an extensive cellular sheet surrounding the epididymal epithelium (Robaire *et al*., 2006; Cornwall, 2009). Although basal cells are extratubular in origin, some findings have suggested that the cells may have a role within the processes of the epithelial immune system and in the regulation of electrolytes by principal cells. As reported by Shum *et al*, (2009), basal cells express angiotensin II type 2 receptor, which, when activated by angiotensin II, increases proton secretion by adjacent clear cells. However, the exact functions of these cells are not yet clear (Robaire *et al*., 2006; Arroteia *et al*, 2012).

Halo cells are usually located in the base of the epithelium where it does not touch the basement membrane. These cells contain variable numbers of dense core granules, pale cytoplasm, (relative to other cells of the epithelium), sparse organelles and heterochromatic

nucleus. They develop in the immune system from a combination of B and T lymphocytes and monocytes (Dacheux *et al*., 2005; Robaire *et al*., 2006; Samuelson, 2007).

The principal function of the epididymis is to provide a luminal environment that transforms spermatozoa into fully mature cells. In addition to sperm ‘‘maturation,’’ the epididymis also plays an important role in sperm transport, protection, and storage (Robaire *et al*., 2000, 2006). The formation of this luminal environment is the result of net secretory and absorptive processes of the epithelium, which continually changes along the duct (Robaire *et al*., 2006; Sullivan *et al.,* 2007). These changes include net water, Na^+, Cl^-, and HCO_3^- reabsorption, K^+ secretion, and luminal acidification (Turner, 2002). In general, the secretions function to protect, stabilize, or modify the sperm surface, with the end product being spermatozoa that are viable, motile, and able to fertilize an egg (Turner, 2002; Robaire *et al*., 2006; Roberts *et al*, 2006).

The epididymis function is controlled by several hormones and growth factors with testosterone recognized as a primary stimulus for epididymal development and sperm maturation. Recent studies have also shown that estrogen and its receptors seem to participate in the regulation of narrow cells in the initial segment of the epididymis and clear cells in the remaining segments (Hess *et al.,* 2001; Lazari *et al.,* 2009). According to Samuelson (2007), change in normal hormone exposure of androgen, estrogen and quite possibly progestin during prepuberal development in dogs can result in alteration of both epithelium and the surrounding peritubular tissue which could alter the functional capability of the epididymis. Immunolocalization of the protein receptors of these hormones along the epididymal tract is a prerequisite to understanding their different involvements in the development and functioning of the epididymis in the different mammalian species (Joseph *et al.*, 2011).

The Ductus Deferens

The ductus deferens which is the caudal straight part of the epididymal duct extends from the cauda epididymis to the ejaculatory duct.

Histologically, it consists from within outward, of three tunica namely; tunica mucosa, tunica muscularis and tunica adventitia, and lack distinct tunica submucosa (Hasan *et al.,* 1974; Samuelson, 2007).

According to Khan *et al,* (2003), the ductus deferens reveals across the mammalian group, some common basic structures but at the same time, it also presents some striking species-specific differences by which it could be identified. In all species, the mucosal linings have longitudinal folds resulting in irregular outline of the lumen. The fold is formed by the laminae propria and the overlying epithelium. Wall thickness was found to be almost equal to the diameter of the lumen in rat and humans (Khan *et al.,* 2003). In the human, two folds of mucosa namely crest and papillae were present (Di Fiore, 1989). In goats and buffalo these folds were not prominent and less in number and were placed at regular interval. While in rats the mucosal folds were very variable, in rabbits, the duct was characterized by plethora of complex mucosal folds (Khan *et al.,* 2003).

The epithelial lining also presents variations among the species ranging from simple cuboidal and low columnar in rabbit to pseudostratified columnar with short stereociliated principal cells in others. Like the ductus epididymis, the base of the epithelium is attached to a thin layer of a well vascularised loose connective tissue (Khan *et al.,* 2003).

The tunica muscularis is prominent in all species (Khan *et al.,* 2003). In large herbivorous species, the tunica muscularis includes obliquely positioned smooth muscles that intermingle

with circular and longitudinal layers. Externally the serosal lining completes the construction of this duct (Samuelson, 2007). Towards the end of the ductus deferens the first accessory gland of the male reproductive tract is formed, known as the gland of the vas deferens or Ampulla (Banks, 1974; Samuelson, 2007).

2:4. The Development and Structure of the Male Accessory Sex Glands

2:4:1. The Development of Prostate Gland

In contrast to most male accessory sex glands which develop from the Wolffian ducts (mesodermal), the prostate gland originates from the urogenital sinus and is an endodermal structure (Hamilton, 1975). As reported by Prins and Putz, (2008), the development of the gland though a continuous process can be divided into five (5) distinct stages namely, the stage of determination, initiation or budding, branching morphogenesis, differentiation and pubertal maturation.

Determination stage involves the expression of the molecular signals that commit a specific field of the urogenital sinus to a prostatic fate and occurs before a morphological evidence of a developing structure (Prins and Putz, 2008). Initiation stage commences as the sinus epithelial cells form outgrowth or buds that penetrate the surrounding urogenital sinus mesenchyme in the ventro-dorsal and lateral direction caudal to the bladder. In rodents where the prostate gland is rudimentary at birth but undergoes the majority of its development during the first 15 days of life, this stage of its development occurs during fetal life. For instance, in mouse the initial outgrowth of epithelial buds occur between fetal day 16.5 – 17.5 in a 19 day gestation strain (Sugimura *et al.,* 1986) while in the rat it occurs at 18.5 in a 21 day gestation strain (Hayashi *et al.,* 1991). At birth, the ventral, dorsal and lateral rodent prostate lobes primarily consist of unbranched, solid elongating buds or ducts with subsequent outgrowth and patterning occurring postnatally. Also at this stage, proliferation of epithelial cells, occur primarily at the leading edge i.e. the distal tip of the duct (Prins *et al.*, 1992).

The stage of branching morphogenesis begins when the elongating buds contact the prostate mesenchymal pads that are peripheral to the periurethral smooth muscle (Prins and Putz, 2008). As reported by Timms *et al.* (1994), it is at this point that the secondary, tertiary and further branch points are established, with continued proximal-to-distal outgrowth and complexity. The pattern of the branching is lobe - specific, with ventral branching preceding that in the dorsolateral lobes by 3 - 4 days (Hayashi *et al.*, 1991). However, the morphogenesis of the entire complex is completed between day 15 – 30 postnatally in rat (Hayashi *et al.*, 1991).

The stage of epithelial and mesenchymal cell differentiation is coordinated with branching morphogenesis and occurs in the proximal to distal direction (Prins and Birch, 1995, Hayward *et al.,* 1996). In rat prostrate, it has been documented that epithelial differentiation into basal and luminal cells has changing patterns of cytokeratins as well as alterations in androgen receptor expression as early marker (Hayward *et al.*, 1996). Canalization of the solid epithelial cords is concomitant with differentiation into basal and luminal cell layers and is initiated in the proximal ducts around 5 days postnatal, extending to the distal tips by day 12. Between days 10 and 15, functional differentiation commences as defined by the synthesis of secretory products by differentiated luminal epithelial cells (Prins and Birch 1995).

The prostatic mesenchyme also undergoes differentiation as the epithelial differentiation progresses. As the epithelial duct of the urogenital sinus penetrates the prostatic mesenchymal pads, the cells of the pad condensate around the tip, forming a distinctive pattern along the length of the basement membrane (Prins and Putz, 2008). In rats, between day 3 and 5, cells adjacent to the duct form the periductal layer of smooth muscle cells while interductal cells differentiate into mature fibroblast. The periductal cell layer tapers with the growing proximal duct, forming a single layer of smooth muscle cell at the distal tip of the mature prostrate (Chang *et al.*, 1999).

As the prostrate undergoes the stage of branching morphogenesis, a branched vascular bed forms which becomes the vasculature within the prostatic stromal element and capillary beds that extend to the ductal basement membrane (Shabsigh *et al.*, 1999).

2:4:2 The Structure of Prostate gland.

The prostate is a compact musculo – glandular organ in contact with the inferior surface of the urinary bladder (Weiss, 1983). In the adult, it surrounds the initial portion of the prostatic urethra, as it leaves the urinary bladder and consists of three groups of gland arranged somewhat concentrically around the urethra (Ross and Romrell, 1985).

Grossly, the gland consists of two parts, the corpus prostata and the pars disseminata. However, these regions are not equally developed in all species (Banks 1974; Sandberg *et al.*, 1980). The body of the prostate (corpus prostata) which is located peripherally to and completely surrounds the pelvic urethra is particularly well developed in carnivores and stallions. In ruminants, the body is less pronounced than that of the other domestic animals. In the bull, the glandular tissue exists intermittently among a bundle of smooth muscle within the tunica muscularis whereas in the ram it is essentially non-existent (Banks, 1974; Pierre-Point *et al.*, 1975; Samuelson, 2007).

The prostate gland of the adult rat is considered to be formed by discrete paired ventral lobes at the neck of the urinary bladder, a dorsal and lateral group, also at the urinary bladder neck and a cranial or anterior lobe (coagulating gland) which lies in the curvature of the seminal vesicle. However the dorsolateral prostate is often examined due to lack of distinct border between these glands (Price, 1963; Hamilton, 1975, Sandberg *et al.*, 1980; Marty *et al.*, 2003).

In some wild rodents, the cranial or anterior lobe is more developed taking up structures that are distinct from the other prostate lobes. The replica of the anterior prostate in mouse (Harmelin *et al.,* 2005) is the coagulating glands in the African giant rat (Oke and Aire, 1996) and viscacha (Chaves *et al*., 2011). Giving its level of structural variation from the other prostate lobes in these wild species, Oke and Aire (1996) have advocated its classification as a distinct, separate gland from the prostate.

Histologically, the body of the prostrate is externally lined by a capsule of dense irregular connective tissue that becomes continuous with the stroma being primarily propria-submucosa (Wrobel and Bergmann, 2006). According to Samuelson (2007), much of the glandular parenchyma of the gland is located within the body, consisting of multiple compound tubuloalveolar secretory segments that individually wind through the propria-submucosa and its disseminate part and directly empty their secretions into the urethra.

The glandular epithelium and the duct are composed of cuboidal or low columnar cells. The secretory epithelial cells have apical blebs which indicate an apocrine type of secretory activity (Wrobel and Bergmann, 2006). Acidophilic granules and lipid droplets may be present in these cells. At the entrance or opening into the urethra, the duct system is lined by transitional epithelium (Samuelson, 2007). The cells of the epithelium have basally located nuclei and a large Golgi apparatus. The basement membrane is thin and rests on a stroma of connective tissues, smooth muscle fibres and blood vessels (Wrobel and Bergmann, 2006). Basal cells are often present (Price and William-Ashman, 1961; Samuelson, 2007).

The role of testosterone in the growth and normal functioning of the prostate has been well established (Flickinger, 1977; Luke and Coffey, 1994; Chaves *et al*., 2011). Following

castration, the epithelial cells lose their secretory granules which were restored by the administration of testosterone (Flickinger, 1977). Recent studies have shown that estrogen has significant direct and indirect effects on prostate gland development and homeostasis as well as playing a role in the etiology of prostatic diseases. The direct effects of this hormone are mediated through prostatic estrogen receptors alpha (ERα) and beta (ERβ) with expression levels changing over time and with disease progression (Prins and Korach, 2008; Lazari *et al.,* 2009). The distribution of these receptors among the prostate epithelium and stroma also vary among species. While endogenous estrogen is important for normal prostatic growth and development, exposure to estrogenic substances during development can also cause up-regulation of stromal ERα and progesterone receptors (PR) in the prostate gland (Williams *et al.*, 2001; Goyal *et al.*, 2007).

The prostatic secretion is a colourless fluid, p.H 6.5, rich in proteolytic enzymes. The most potent enzyme is fibrinolysin which plays a role in the liquefaction of the semen. Acid phosphatase also occurs in high concentrations in the prostatic fluid providing a reliable and sensitive test for accessing prostatic function (McNeal, 1981). Concretions of the secretory product of the prostate may be found in the alveoli and duct. The secretion of the prostrate is known to increase the motility of spermatozoa and affect the seminal concentration as well as contribute to the formation of vaginal plug (Oke, 1988; Lu *et al.*, 2008).

2:4:3. Development of Vesicular gland

The seminal vesicle is a paired accessory sex gland of mesodermal origin (Prins and Putz, 2008). It is considered to be derived from an evagination of a saccule from the caudal end of each mesonephric or Wolffian duct (Weisner, 1934; Price 1956; Burnes, 1961), and later become

short tube which is directed dorsolaterally and cranially and afterward develops lumen (Cunha and Lung, 1979). Branching of these tubular organs is followed by canalization of the glands and this varies to an extent with age. According to Aitken (1959), in the ram, at this stage of canalization, the vesicular glands are found to be provided with stratified epithelium which normally consists of two layers. While in the older embryo, the epithelium is simple columnar with nuclei located near the luminal surface. The epithelial height ranges from 18-31µm and was found to increase with age to reach 35-40 µm in the late embryo (Prins and Putz, 2008) .

In rats, the basic pattern of seminal vesicle formation is present at day 10 post-natal. Lumen formation occurs over a relatively protracted period from day 2-15 post natal and secretory granules become evident at day 16. The seminal vesicles markedly increase in size between days 11 and 24 and continue to grow until adult stage and secretory properties are attained between days 40 and 50 (Brooks *et al.*, 1973; Marty *et al.*, 2003).

2:4:4. The Structure of Vesicular gland.

The vesicular gland (seminal vesicle) consists of a lobulated compound gland that has a central duct surrounded radially by branching tubular to tubuloalveolar adenomeres (Samuelson, 2007). This gland shows structural and ultrastructural diversities among the different mammalian species. While it is absent in species like carnivores (Strzezek *et al*., 2000), it shows structural variations across species where it is present. In humans, horse, and rat, they are saccularly shaped; in pig and bull they are compact and multilobulated (Samuelson, 2007; Badia *et al*., 2006), and in some rodent species they exhibit a branched tubular structure (Mollineau *et al*., 2009; Ayres de Menezes *et al.*, 2010). The seminal vesicles in the adult rat are distal to the ampulla of the ductus deferens and secrete through the ejaculatory duct into the floor of the

urethra near a region corresponding to the colliculus seminalis or veru montanum. The ejaculatory duct blends, near their opening with the ducts of the seminal vesicle (Oke, 1988). In some animals, however, no ejaculatory duct is present and the seminal vesicle secrete directly into the pelvic urethra (Price and William-Ashman, 1961; Chaves *et al*., 2011).

Histologically, the wall of the vesicular gland is composed of three layers; a mucosa; an intermediate muscle layer which is thinner than that of the ductus deferens and arranged in two layers – an inner circular layer and an outer longitudinal layer; an external adventitia rich in elastic fibres. The mucosa is intricately folded inwards to form numerous irregularly shaped chambers or crypts that open into the large central cavity of the gland (Ross and Romrell, 1985). The overall configuration of the gland is that of a pinnately arranged structure, in which a central duct is present and from which radially branching secretory ends emanate (Banks, 1974).

The vesicular glandular epithelium is made up of principal and basal cells, with varying types and number among different mammalian species. The principal cells are simple columnar or pseudo-stratified columnar (Oke and Aire, 1997; Cakir and Karatas, 2004; Badia *et al*., 2006) or simple cuboidal (Chaves *et al*., 2011). While two types of principal cells have been reported in the seminal vesicles of humans (Riva and Aum¨uller, 1994) and several mammalian species like Brazilian zebus (Cardoso *et al.,* 1979), bulls (Amselgruber and Feder, 1986), buck and rams (Skinner *et al.,* 1968; Wrobel, 1970), guinea pigs (Veneziale *et al.,* 1974), three has been reported in pig (Badia *et al*., 2006). Ultrastructurally, the principal cells contain well-developed rough endoplasmic reticulum and Golgi apparatus as well as abundance of mitochondria. These suggest that principal cells of this gland are concerned with intense protein synthesis and secretions (Murakami and Yokoyama, 1989; Badia *et al.,* 2006). The cytoplasm of the epithelial

cells also contains secretion granules and a yellowish lipochrome pigment (Dym and Fawcett, 1970; Samuelson, 2007).

The Tunica muscularis, which varies in amount, consist of inner circular and outer longitudinal layers. The lamina propria-submucosa is provided with a plexus of nerve fibres and contains small sympathetic ganglia (Wislocki 1949, Fawcett 1975, Samuelson 2007).

The secretory cells produce a yellowish, viscid, alkaline fluid which is rich in sugar (fructose) that provides energy for the spermatozoa and make the semen viscous (Wheater *et al.*, 1990) as well as fibrinogen, vitamin C and lipids (Banks, 1974, Samuelson, 2007). The gland produces and elaborates abundant amount of fluids for the transportation and nourishment of spermatozoa in the seminal plasma as well as the formation of a vaginal stopper in some rodents (Chaves, *et al*., 2011). In pigs, these glands produce 80-90% of the seminal plasma proteins that protect and increase sperm viability and fertilizing capacity (Badia *et al*., 2006). Therefore, information on the morpho-physiology of these glands is imperative especially in wild species that are undergoing domestication and captive-rearing (Adaro, *et al.,* 2001; Chaves, *et al.,* 2012).

2:4:5. Development of Bulbourethral Gland.

The bulbourethral gland is also known as the Cowper's gland named after the 17th century English Surgeon, William Cowper (Chughtai *et al.,* 2005).. The paired gland develops from the intermediate urogenital sinus that has a different inductive capacity of its mesenchyme from that of the prostate (Patten, 1956; Chughtai *et al.,* 2005).. The gland sprouts below the urethra, just below the prostate as it develops, and under the influence of many endocrine and paracrine glands, most significantly the dihydrotestosterone (DHT) (Chughtai *et al.,* 2005).

2:4:6 The Structure of Bulbourethral gland.

The two main Cowper's glands are situated within the urogenital diaphragm with a second pair of accessory glands situated in the bulbospongiosal tissue (Frandson 1974; Chughtai *et al.,* 2005). The main Cowper's duct enters the ventral surface of the bulbourethra near the midline by piercing the spongiosum. The bulbourethra extends from the inferior urogenital diaphragm to the suspensory penile ligament superiorly and penoscrotal junction inferiorly.

The secretory unit consists of well demarcated lobules of small, compact tubuloalveolar gland, as in stallion and bull or compact tubuli as in boar and cats (Samuelson, 2007). The units radiate from a central excretory duct into which accessory ducts opens and are lined by pseudostratified columnar epithelium (Chughtai *et al.,* 2005) which become transitional epithelium before connecting to the urethra. The duct is also entrapped with fascicles of muscles. The gland has a thin connective tissue capsule and the secretory cells are composed of simple columnar epithelium (Samuelson, 2007).

The secretion of this gland, which is often released before ejaculation, generally clears the urethra of urine and subsequently aid in lubricating the vagina (Samuelson, 2007). However, the secretion from the Cowper's gland is said to contain glycoproteins that are involved in the immune defense of the genitourinary tract in man (Chughtai *et al,* 2005). In the rodents and boar, the secretions of this gland forms gelatinous copulatory plugs which prevents semen back flow in the females (Dunker and Aumuller, 2002; Badia *et al*, 2006). Moreover, in boars (Larsson *et al.*, 1976; Badia *et al.,* 2005) and goats (Gupta and Singh, 1982; Badia *et al*, 2006), although it has not been fully elucidated, it seems that the glycoconjugates secreted by the bulbourethral glands probably play a role in sperm metabolism by attaching to the sperm plasma membrane.

As with the diversity of compositions and functions of the secretion of the bulbourethral glands, so also are the structural diversities among the different mammalian species (Badia *et al*, 2006). While it is completely absent in dogs and aquatic mammals (Dyces *et al*, 2002), it is poorly developed in man (Jequier, 1995) but well developed in pig (Badia *et al*, 2006). Since the structural development of this gland determine its contribution to the ejaculate and consequently its role in reproduction (Dyce *et al*, 1999), it is pertinent to evaluate the structure of this gland in wild mammalian species that are currently undergoing captive rearing and domestication.

2:5. HORMONAL REGULATION OF THE MALE REPRODUCTIVE SYSTEM

It has been recognized that several hormones play vital roles in the development and functioning of the male reproductive system as well as in the regulation of its responses to different environmental and disease conditions (Min and Lee, 2010).

2.5.1. *Testosterone*

In the male, testosterone is the primary hormone that regulates the process of spermatogenesis as well as the growth and secretory activities of the male gonads, the excurrent ducts and accessory sex glands (Kalra and Kalra, 1979; Robaire *et al.*, 2007). This hormone, produced by the Leydig cells, is prominent from the fetal to adult life of all mammalian males, with its level surging at different stages in the development and growth of the reproductive tract in a species-specific manner (Anderson *et al.*, 1998; Claudio *et al.*, 1999; Marty *et al.*, 2003). While testosterone is principally produced by the Leydig cells of the testicular interstitium, Sertoli cells are now been recognized as another source of androgen (Gendt *et al*., 2004; Ichihara and Pelliniemi, 2007)

As enumerated by Emanuella and Emanuella, (2002), the biosynthesis of testosterone begins with the cleavage of 6-carbon group from cholesterol to form pregnenolone. This reaction, which is catalyzed by P450-linked side chain cleavaging enzyme (P450scc – found majorly in the mitochondria of steroid producing cells), occurs in the presence of steroidogenic acute regulating protein (StAR). The formed pregnenolone is converted to progesterone by the enzyme, 3β-hydroxysteriod dehydrogenase (3-β HSD) ((Emanuella and Emanuella, 2002)). Through the action of 17,20 lyase enzyme, the progesterone is then converted to androstenedione

which is further reduced by 17 ketoreductase enzyme (17β- HSD) to produce testosterone as illustrated in Figure A (Emanuella and Emanuella, 2002).

The action of testosterone on its target organs is said to be carried out by its active metabolite, dihydrotestosterone (DHT) which is formed through the action of specific enzyme, 5α- reductase (Luke and Coffey, 1994; Thompson, 2001). This action is principally mediated through specific binding of DHT to androgen receptors (AR) which are ubiquitously distributed in the male reproductive organ (Umar *et al.*, 2003; Chaves *et al.*, 2011; Arroteia *et al.*, 2012).

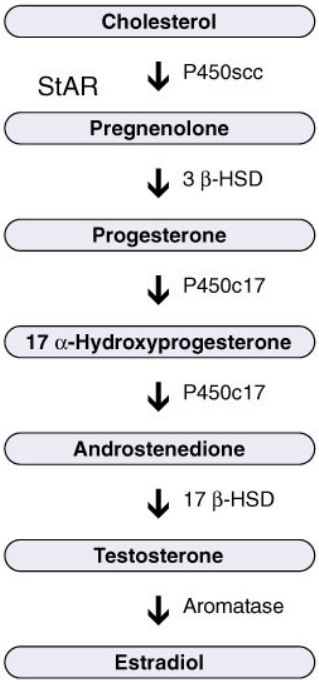

Figure A: Testosterone biosynthetic pathway. Multiple enzymes are necessary to synthesize testosterone. These are shown to the right of the arrows. The arrows indicate the different steroid precursors of testosterone that are synthesized at each step (Emanuella and Emanuella, 2002).

2.5.2. *Estrogen*

In time past, estrogen was considered to be female-only hormone but has now been found to plays key roles in the development and maintenance of reproductive function and fertility (Carreau *et al.*, 2008) as well as in pathological processes observed in tissues of the reproductive system (Prins and Korach, 2008). Recent evidences have also shown that the highly organized and coordinated spermatogenic processes are controlled by a well-regulated estrogen–androgen hormonal balance. Alteration of this endocrine balance, which can be caused by obesity, has equally been shown to disrupt or impair spermatogenesis and epithelial morphology of the epididymis in both humans and rodents (Hess, 2003; MacDonald *et al.,* 2010; Carreau *et al*., 2011).

As illustrated above (Fig. A), estrogen is produced from androgen by an irreversible reaction catalyzed by P450 aromatase (CYP19A1) enzyme. There are several sites of estrogen production along the male reproductive tract which includes the testis (Hess, 2003) and prostate gland (Prins and Korach, 2008). Like its androgen counterpart, the action of estrogen is mediated by its two receptors – estrogen receptor alpha (ERα) and beta (ERβ). According to Joseph *et al*, (2011) estrogen and its two receptors, ERα and ERβ, show a high degree of species variability in their pattern of distribution along the genital tract and often revealed a different topography in the multiple cell types of the male genital organs. From the recent work of Walker *et al*, (2012), estrogen receptors (ERα and ERβ) do not only mediate endogenous estrogen but also mediate the toxicological and pathological effects of exogenous estrogen as well as interference with androgen action as a result of early-life estrogenic exposure (Walker *et al.,* 2012). Exogenous estrogen exposure at developmental stages has been reported to cause up-regulation of stromal

ERα, induction of progesterone receptors (PR) expression and feminization of some male reproductive organs (Williams *et al.,* 2001; Goyal *et al.,* 2007; Walker *et al.,* 2012).

2.5.3. *Progesterone*

Although the presence of progesterone has been observed in the serum of male rat, guinea pig, dog and human (Kalra and Kalra, 1977; Connolly and Resko, 1989; Alollio *et al*., 1995; Frank *et al*., 2003), its role in the male reproductive tract is largely unknown. As illustrated above (Fig. A), progesterone is a product in the testosterone biosynthesis pathway in the male mediating its effect through the progesterone receptor (PR). As reported by Witts *et al*, (1994) progesterone is involved in the modulation of species-specific androgen-dependent sexual behavior in the males through its effect on the hypothalamus. This effect was mediated by PR which has been abundantly localized in the medial preoptic and ventro-medial nuclei of the hypothalamus (Witts *et al.,* 1994). The recent work of Baidi *et al*, (2011) and Timo *et al*, (2011) have also shown that, in humans, this hormone is involved in the control of chemotaxis, hypermotility and acrosomal exocytosis of sperm in the female reproductive tract by stimulating Ca^{2+} influx in the sperm.

According to Colegrove *et al*, (2009) progesterone receptors (PR) have been identified in some segments of the genital tract as well as in the epithelium and stroma of both the penis and prepuce of the male sea lions, primates and humans. However, the import of this receptor in these organs is yet unknown simply because few studies have examined the expression, distribution and function of progesterone receptor in the mammalian males (Luetjens *et al*., 2006; Colegrove *et al*., 2009).

2.5.4. *Luteinizing and Follicle Stimulating Hormone (LH & FSH)*

Luteinizing and Follicle stimulating hormones are two gonadotrophic hormones that control the biosynthesis of androgens and estrogen in the reproductive system (Emanuella and Emanuella, 2002). Produced from the hypophysis under the influence of the luteinizing hormone-releasing hormone (LHRH), LH and FSH are released into the general circulation to act primarily at the level of the gonads (Russel and Clermont, 1977; Ichihara and Pelliniemi, 2007).

In the male, LH stimulates testosterone production from the Leydig cells. According Ghosh *et al*, (1991), the degeneration of the preleptotene and pachytene spermatocytes as well as the abnormal manchette in elongated spermatids found in hypophysectomized rat, are attributable to lack of LH. The effect of FSH in the male is more on the Sertoli cells where it regulates Sertoli cell-intracellular testosterone production. In addition, FSH stimulates the secretion of androgen-binding proteins (ABP) which transport testosterone produced in the Leydig cells to the site of spermatogenesis (Ichihara and Pelliniemi, 2007). In human, FSH has also been found to be important in epididymal sperm maturation (Emanuella and Emanuella, 2002).

Serum levels of LH and FSH varies with age, stage of spermatogenesis and level of functional development of the hypothalamo-hypophysial unit in a given species (Lee *et al*., 1975; Genaro *et al.,* 2007). Evaluation of the serum levels of these hormones can serve as veritable tools in assessing normal physiological condition as well as complementary diagnostic tools for some reproductive abnormalities in the males (Jaszczak *et al*., 2010)

2:6. Morphometric Analysis of Male Reproductive System

In the past, morphometric studies were restricted to qualitative description of tissue structures and therefore they are subjective. In the recent years, the application of morphometric and stereological techniques has increased in biomedical research and are now being recognized as the new approach in morphological studies (Mukerjee and Rajan, 2006).

Although the basic structure of the testis, for instance, is highly conserved among vertebrates (Capel, 2000) specific characteristic of the testicular structure might be found for a particular species. In this regard quantitative data are now being used to answer important questions about testicular function and to provide a more complete understanding of spermatogenesis in the different species (Russell *et al.*, 1990; Franca and Russell, 1998).

Also, according to Cheng and Mruk (2002), recent advances in biochemistry, cell biology and molecular biology have shifted attention to understanding some key events that regulate spermatogenesis such as Sertoli-germ cell communication and junctional dynamics. To this end, accurate testicular morphometric information will not only provide means of assessing the efficiency of the testis and indirectly reproduction status of the male animal (Oke, 1988), it is also valuable for correlation of spermatogenic process with physiological and biochemical findings (Gaytan *et al.*, 1986; Franca and Russel, 1998; Abdelmalik, 2011). It is in this regard that quantitative investigation and analysis become pertinent in reproductive biology.

Several quantitative studies on male reproductive system have been reported in literature (Holtz 1972; Oke 1988; Akinloye 2001; Massanyi *et al.*, 2003; Mukerjee and Rajan, 2006; Oluwole 2008; Abdelmalik 2011). While some relate to the measurement of both gross and histological parameters of the male reproductive organ such as gonadosomatic index, relative

germinal volume, seminiferous tubular diameter, Epididymal epithelial height, morphometry of accessory organs and so on, others are involved with the process of spermatogenesis considering Germ cells, Sertoli cells and Leydig cells at both histological and ultrastructural levels in different mammals (Abdelmalik, 2011). Linear body measurements have equally been used to estimate body conditions that can affect reproductive performance (Pala *et al*., 2005; Engeland *et al*., 2007).

Gross and histomorphometric values of the different segments of the male reproductive tract are species specific and vary in seasons (Oke, 1988); changes in toxicity and poisoning (Akinloye, 2001; Oluwole, 2008) and stress condition (Mukerjee and Rajan, 2006). For most quantitative investigations of spermatogenesis, identification of the stages of cycle of seminiferous epithelium and the knowledge of its duration are required (Franca and Godinho, 2003; Berndtson, 1977).

The cycle of seminiferous epithelium are the sequence of events that occur from the disappearance of a given cell association to its reappearance in a given area of the seminiferous tubule (Leblond and Clermont, 1952). The time interval required for one complete series of cellular associations to appear at one point within the tubule is called duration of the seminiferous epithelium cycle. The major criteria for stage identification reside in the morphological characteristic of spermatid in particular, their nucleus and acrosomic system (Russel *et al.,* 1990; Hess *et al.,* 1990). One popular method of characterizing the stages of the cycle, which is simple and less arbitrary is the tubular morphology system and is based on the shape and location of the spermatids nuclei, presence of meiotic division and overall seminiferous epithelium composition. In the same vein, several methods have been used to estimate the duration of the seminiferous epithelium cycle (Smithwick *et al.,* 1996; Rosiepen *et*

al., 1997; Weinbauer *et al.*, 1998; Franca *et al.*, 1999). However tritriated thymidine, a labelled precursor of DNA is classically utilized as a germ cell marker in order to determine the duration of spermatogenesis (Barr, 1973; Neves *et al.*, 2002; Franca and Godinho, 2003; Costa *et al*., 2010).

With the stages and duration of seminiferous epithelium cycle, parameter such as spermatogenic efficiency, daily sperm production per testis and per gram of testes as well as Sertoli efficiency and germ cell apoptosis, which are species specific, can be estimated and characterized. These have also been done in several animals. For instance in rat, spermatogenic cycle is in 14 stages while the duration takes 12-14 days (Leblond and Clermont, 1952). In mouse, 12 stages and 8-9 days duration was observed (Russel *et al.*, 1990). In cats, the cycle length ranges from 9-12 days and 8 stages was observed (Franca and Godinho, 2003).

According to Franca and Godinho (2003), of the approximately 4000 mammalian species alive, testicular quantitative analysis has been estimated for only approximately 1% of them. This underscores the need for this analysis particularly in some wild rodents that are currently being domesticated (Pucek *et al.*, 1993; Busso *et al*., 2012).

2:7. Reproductive Biology of the greater cane rat (*Thryonomys swinderianus*)

The maintenance of reproductive competence in captivity is the most crucial and cardinal marker of successful domestication (Zeuner, 1963; Fox, 1987; Adams, 1989). According to Hafez (1980), among thousand mammalian species known, reproductive biology has been studied in only 25 species. Some of these species are characterized by peculiar reproductive phenomenon such as restricted sexual seasons, absence of estrous, presence of menstruation and ovulation during pregnancy. Both the male and female genders in mammalian species have reproductive characteristics that are crucial to facilitating and maximizing productivity.

In the female, reproductive characteristics noted as crucial are: oestrous cycle, ovulation, mating, pregnancy, parturition, embryonic mortality, fetal mortality, perinatal mortality (Betteridge, 1986; Short, 1990), gestation length, litter size, birth weight, age at puberty, birth interval, mating system, breeding season and reproductive lifespan (Short, 1990). The work of Addo *et al*, (2003, 2007) have provided valuable information on the reproductive biology of female Grasscutter specifically in the area of detection of mating, diagnosis of pregnancy and detection of imminent parturition using methods like perineal examination, post mating, abdominal palpation, monitoring of change in body weight during gestation, biological pregnancy assay and unobstructive observation of pregnant animals for changes in behaviour and posture as parturition approaches (Hafez, 1980; Arrington, 1972; Arthur *et al.*, 1989; UFAN 1989). Adu (2003) has also established the pattern of parturition and mortality in weaned captive Greater cane rat.

In the male, crucial reproductive characteristic are testes size, structural peculiarity of the reproductive organs, semen and sperm morphology and quality among others (Betteridge, 1986).

According to Segatelli *et al.* (2004), the basis for a sound knowledge of the male reproductive biology in any species lies in a detailed morpho-functional analysis of the testes and the spermatogenic efficiency of the species in question. Male reproductive parameters such as gonadotropic index (the ratio of the weight of the testes to the body weight), seminiferous epithelium cycle length, and daily sperm production are also valuable indices for the efficiency of spermatogenesis in the male gender (Franca and Godinho, 2003).

CHAPTER 3

MORPHOLOGICAL STUDIES OF THE TESTIS, EFFERENT DUCT, EPIDIDYMIS AND ACCESSORY SEX GLANDS IN THE GREATER CANE RAT (*Thryonomys swinderianus*)

3.1 Materials and Methods

3.1.1. Study Locations

The gross and histological aspects of the morphological studies were done in the Anatomy laboratories of the Department of Veterinary Anatomy, College of Veterinary Medicine, Federal University of Agriculture, Abeokuta and the Department of Veterinary Anatomy, Faculty of Veterinary Medicine, University of Ibadan, Ibadan, Nigeria while the ultra-structural studies and morphometric analysis were done at the Microscopy and Microanalysis laboratories of School of Anatomical sciences, Faculty of Health sciences, University of the Witwatersrand, Johannesburg and Department of Veterinary Anatomy, Faculty of Veterinary Sciences, University of Pretoria, Onderstepoort, Pretoria both in South Africa. The experimental protocol was approved by the ethical committee in animal research, University of Ibadan, Ibadan Nigeria.

3.1.2 Animals

A total of thirteen (13) adult male greater cane rats were used in this part of the study. The animals were obtained from Good health Farms in Igbesa, Ogun state and Pavemgo grasscutter Farms in Ibereko near Badagry, Lagos State where they were littered and raised in captivity with known ages, reproductive and medical records. The ages of the animals range from 13 – 24 months weighing between 1.4kg – 3.5kg (1400 – 3500g). All the animals had brownish perineal staining which is usually used as index of sexual maturity in male cane rat

(Adu and Yeboah, 2003). They were housed at the Grasscutter domestication unit, College of Veterinary Medicine, Federal University of Agriculture, Abeokuta, for seven days to acclimatize and were maintained on the combination of maize, cassava and ground nut cake with salt to taste. They were also provided with Elephant grass stems and water was given *ad libitum*.

3.1.3 Sample Collection and Tissue Processing

3.1.3.1 Gross Evaluation and Morphometry

Four (4) animals were used for the gross evaluation of the reproductive tract. Each animal was weighed alive and sacrificed after anaesthesia with chloroform in a closed container. The abdominal wall was dissected open through a mid ventral abdominal incision to evaluate and study the reproductive organs and their anatomical relationships *in situ*. The ischiatic arch was then completely disarticulated to further expose the reproductive organs. The positions of the organs were carefully noted and photographed. Individual organs: testes, epididymides, the ductus deferens, seminal vesicles (vesicular gland), prostate, bulbourethral (Cowper's) glands were then carefully dissected out collectively and individually.

For the gross morphometry, the weights and linear measurements, which comprise length, width and circumference of the testis and epididymis, were taken using analytical weighing balance and vernier caliper respectively. The volumes of the testes, epididymis and the accessory organs were found by water displacement method as described by Scherle, (1970) and adapted by Hughes (2005). Where the organ was curved, the measurement was taken using thread and ruler. The average of the left and right measurements were taken and recorded as each organ's measurement.

3.1.3.2 Histology and Histomorphometry

Five animals were used for histological study with each anaesthesized with chloroform in a closed container. The abdominal wall was immediately dissected open through a mid-ventral abdominal incision and the thoracic cage opened to expose the heart. To properly perfuse the reproductive organs, blood was first drained from the entire system by flushing the vessels with heparinized ringer's solution at the proportion of 0.5ml heparin in 500ml of ringer's as described by Hess and Moore (2001). An 18G x 3/4" butterfly needle was introduced into the left ventricle and the blood was drained through a slit opening made at the right atrium. The needle was then connected (through a perfusion line) to the heparinized ringer's solution, to clear and avoid blood-clotting in the smaller capillaries, by gravity and the residual pumping of the heart. With the needle in place the system was perfused-fixed with phosphate buffered 4% paraformaldehyde at pH 7.4 (Mettler-DELTA 320, Switzerland). This fixative was prepared by first, dissolving 80g of paraformaldehyde in 400ml of distilled water and heating at 85^0C to obtain a clear solution. After cooling the solution to room temperature, 500ml of phosphate buffered saline was then added and the total volume brought to 1litre with distilled water (Hess and Moore, 2001). The fixation line was removed after the colour of testis and epididymis had turned pale with the disappearance of the capsular blood vessels. The entire reproductive system was then removed after disarticulating the ischiatic arch, immersed and separated into different organs in the same fixative. Subsequently, each organ – testis, efferent duct, epididymis, vas deferens, prostate, vesicular and Cowper's glands were cut into pieces from which tissue samples was collected and further immersed, in separate containers, in the same fixative for 24hours.

The collected samples were processed using the automatic tissue processor (Shandon Citadel1000, Rankin Biomedical Co. USA). To achieve dehydration, the tissues were passed

through graded concentrations of alcohol: 70% for 1hour, 90% thrice for 1hour each, and absolute alcohol (100%) thrice for 1 hour, 2hours, and 1hour respectively. They were then cleared twice in chloroform for 2 hours each and embedded by passing through the four changes of paraffin wax at 60^{o}C. Serial paraffin sections of 4µ thick were obtained on the microtome (Leica, 2035 Biocut, Germany). These were mounted on clear albuminized slides after floating on a warm water bath and then dried in an oven and stained with haematoxylin & eosin (H & E) and Periodic acid Schiff stain (PAS). Some of these paraffin sections were used for immunohistochemistry (as described in chapter 4 of this thesis).

All the slides were examined under the light microscope (Axioskop 2 plus, Carl Zeiss, Germany). On the slides, histological features of each organ were studied and their histomorphometry was determined using a photomicroscope (Axio-Skop-2-Plus, ZEISS, Germany) with AxioVision Release 4.8.1 software package. Changes in the shape of the nucleus and acrosome of germ cells during their development in the testicular seminiferous epithelium were also visualized so as to characterize the stages of the cycle of the seminiferous epithelium in this animal.

3.1.3.3 Ultrastructural Studies

For the ultrastructural studies, four (4) animals were used and each was anaesthesized with chloroform in a closed container. The abdominal wall was immediately dissected open through a mid ventral abdominal incision and the thoracic cage opened to expose the heart. To properly perfuse the reproductive organs, blood was first drained from the entire system by flushing the vessels with heparinzed ringer's solution at the proportion of 0.5ml heparin in 500ml of ringer's as described by Hess and Moore (2001). After introducing an 18G x 3/4" butterfly needle, connected to a perfusion line, into the left ventricle, the blood was drained and the

vessels flushed with the heparinized ringer's solution through a slit opening made at the right atrium by gravity and the residual pumping of the heart. With the needle in place the system was then perfused-fixed with phosphate buffered 2% paraformaldehyde – 2.5% glutaraldehyde fixative at pH 7.4 (Mettler-DELTA 320, Switzerland) based on Glauert (1972). This fixative was prepared by first dissolving 2g of paraformaldehyde in 100ml of the phosphate buffer using heat and continuous stirring. After rapid cooling, 10ml of 25% glutaraldehyde was then added and the pH adjusted to 7.4. The mixture was afterall made-up to 100ml of the fixative. The fixation line was removed when the colour of testis and epididymis had turned whitish with the disappearance of the capsular blood vessels as recommended by Hess and Moore (2001). The testes and epididymides were quickly removed, minced into 1mm pieces and completely immersed in the same fixative. Afterward, the entire reproductive system was removed following disarticulation of the ischiatic arch, immersed and separated into different organs in the same fixative. Subsequently, all the organs – testis, efferent duct, epididymis, vas deferens, prostate, vescicular and cowper's glands were minced into 1mm pieces from which tissue samples were taken and further immersed in the same fixative but in separate containers for another 24 hours. The tissues were rinsed in the phosphate buffer twice at 30 minutes interval after fixation and then post-fixed for 1hour in 1% Osmium tetraoxide which was prepared by reconstituting the 2ml 4% ampoule (SP-CHEM, USA) with 6ml phosphate buffered solution. To remove the surplus Osmium, the tissues were further buffer-rinsed before dehydration.

The tissue samples were dehydrated in 70% alcohol for 20 minutes, twice in 95% alcohol for 20minutes each and twice in absolute alcohol for 20 minutes each. They were then cleared in propylene oxide twice for 20 minutes each. Epon-Araldite Resin mixture (resin), which was used to infiltrate and embed the tissues, was prepared by mixing 5.62g of Araldide CY212, 7.75g of

Epon812 and 15.0g of DDSA (Dodecenyl Succinic Anhydride) for 15minute by inverting bottle by hand after which 0.71g of DMP-30 (Tri(dimethylaminomethyl) phenol) was added and mixed for another 20minutes before use. The tissues were then infiltrated in a mixture of propylene and resin (the prepared mixture) at graded ratio of 3:1 for an hour, 1:1 for another hour, 1:3 for yet another one hour and finally in the resin only, overnight. The tissues were fully embedded in freshly prepared resin in separate numbered blocks and incubated (MEMMERT, Model U3D, Germany) at 60^0C for 24 hours.

The embedded tissue blocks were serially sectioned on an Ultra-microtome (Ultracut Reichert-Jung, Austria) with glass knives prepared from 38 mm glass strips using the LKB Knife Maker (Model 7801A Stockholm, Sweden). Firstly, semi-thin sections of the tissues cut at 1µm, were transferred to a drop of water on a glass slide, dried on a hot plate at 80^0C for about 25-40seconds and stained in Toulidine Blue-Pyronin Y which was a mixture of 1% Pyronin Y and 1% Toulidine Blue in 1% sodium tetraborate (Borax). These were then observed under the light microscope (Neovar 2, Reichert-Jung, Austria) for general orientation and to select areas for ultrathin sectioning. The ultrathin sections of the tissues were then cut from the selected areas at 60 – 90nm using glass knives. The gold-coloured sections were picked with looped wire strand and placed on uncoated 200 mesh copper wire grids for staining.

A combination of saturated solution of Uranyl acetate in methanol and 1% lead citrate in 4% concentrated sodium hydroxide (NaOH) was used to stain the ultrathin sections on the grids. The Uranyl acetate solution was prepared by dissolving Uranyl acetate powder (Merck Darmastadt, Germany) in absolute methanol by inverting the bottle by hand until saturation was achieved. The saturated solution was then spinned for 10 minutes at 3000 rpm. The lead citrate solution was also prepared by first dissolving 1g of lead citrate salt (Laboratory Reagent, British

Drug House, UK) in 100 ml distilled water after which 4 ml of concentrated NaOH was added. The solution was also spinned for 10 minutes at 3000 rpm. The procedure entails staining the grids initially with the prepared Uranyl acetate solution for 3minutes and rinsing the grids 3times in 50% methanol (by carefully holding each grid with a fine forceps and dipping it 10 times in each solution of 50% methanol). The grids were then allowed to dry for 10 minutes. This was immediately followed by staining with the prepared lead citrate solution for 2 minutes. The grids were afterward rinsed in diluted NaOH solution (1 drop of NaOH in 50ml of distilled water), followed by distilled-water rinsing 3 times (through careful dipping of each grid 10times into distilled water each time). The grids were allowed to dry for another 10minutes and viewed under the Transmission Electron Microscope (TEM) (CM 10, Phillips, Netherlands) at 80 KV with the electron micrographs produced using the Soft imaging System (SIS – iTEM) software package installed on a computer (SONY, JAPAN) attached to the microscope.

3.1.4 Statistical Analysis

All values obtained were expressed in mean ± standard deviation (*n = 13*) and evaluated with ANOVA. The mean differences were sorted using Duncan post hoc test. Data were also subjected to Pearson's correlation analysis. All stastical analyses were carried out using Paleontological statistics version 2.15 (PAST) data analysis tool.

3.2 RESULTS

3.2.1 Testis

3.2.1.1 Gross Appearance

The paired testes in the greater cane rat were suspended in individual scrotal sac located caudo-ventral to the penis. The scrotum was simply a skin-fold that had brownish staining but generally lack hair (Fig. 1a). The inguinal ring and canal were opened and the testes were sometimes seen either in the scrotum or the abdominal cavity especially in animals under stress such as excitement and physical restraint (Fig. 1b).

The cream-whitish coloured testis was ovoid to oblong in shape and present blunt cranial and caudal extremities. The caudal pole is relatively broader than the cranial border and has the gubernacular testis attached to it which extends into the scrotal sac (Fig. 2a). The capsule (tunica albuginea) is smooth, transparent and fairly uniformly ramified by straight blood vessels with the presence of larger vessels at the cranial pole (Fig. 2b). The testis was observed to be thickened on the craniomedial aspect where the efferent duct emerges from the rete testis. This area corresponds to the mediastinum testis which is both subcapsular and capsular. This thickening extends about 10mm from the cranial pole and about one-fifth of the length of the testis (Fig. 3). The parenchyma pouts through an incision on the capsule which indicates that it is contained under moderate pressure within the capsule.

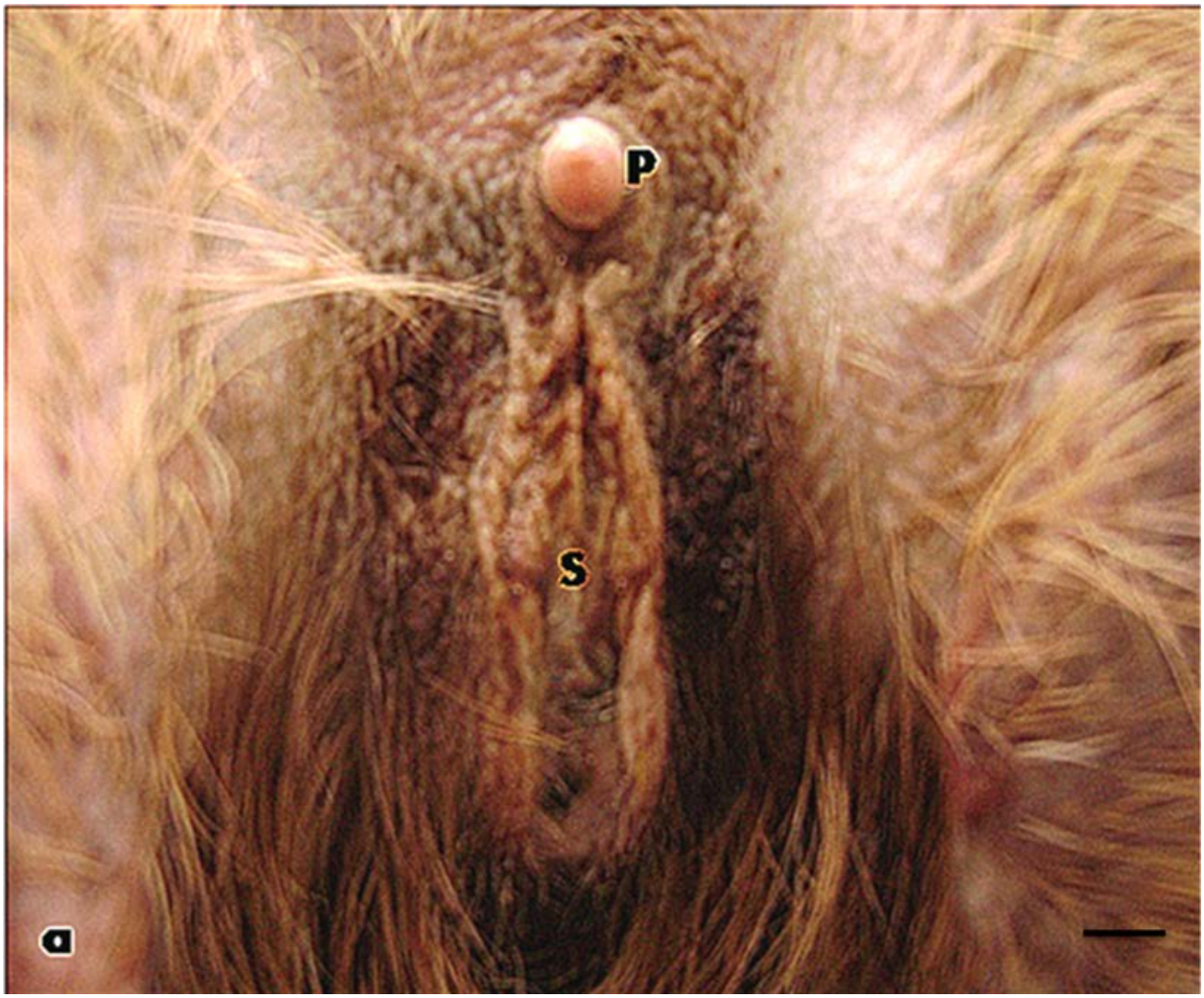

Figure 1a: Photograph of the perineal area of the male greater cane rat showing the scrotum and penis. Note the perineal staining on the scrotum (S) and the penis (P). Mag X5. **Scale bar = 2mm**

Figure 1b: Photograph of the abdominal cavity of the greater cane rat. Note the testes (T) in the abdominal cavity and the distended urinary bladder (B). Mag. X5. **Scale bar = 2mm**

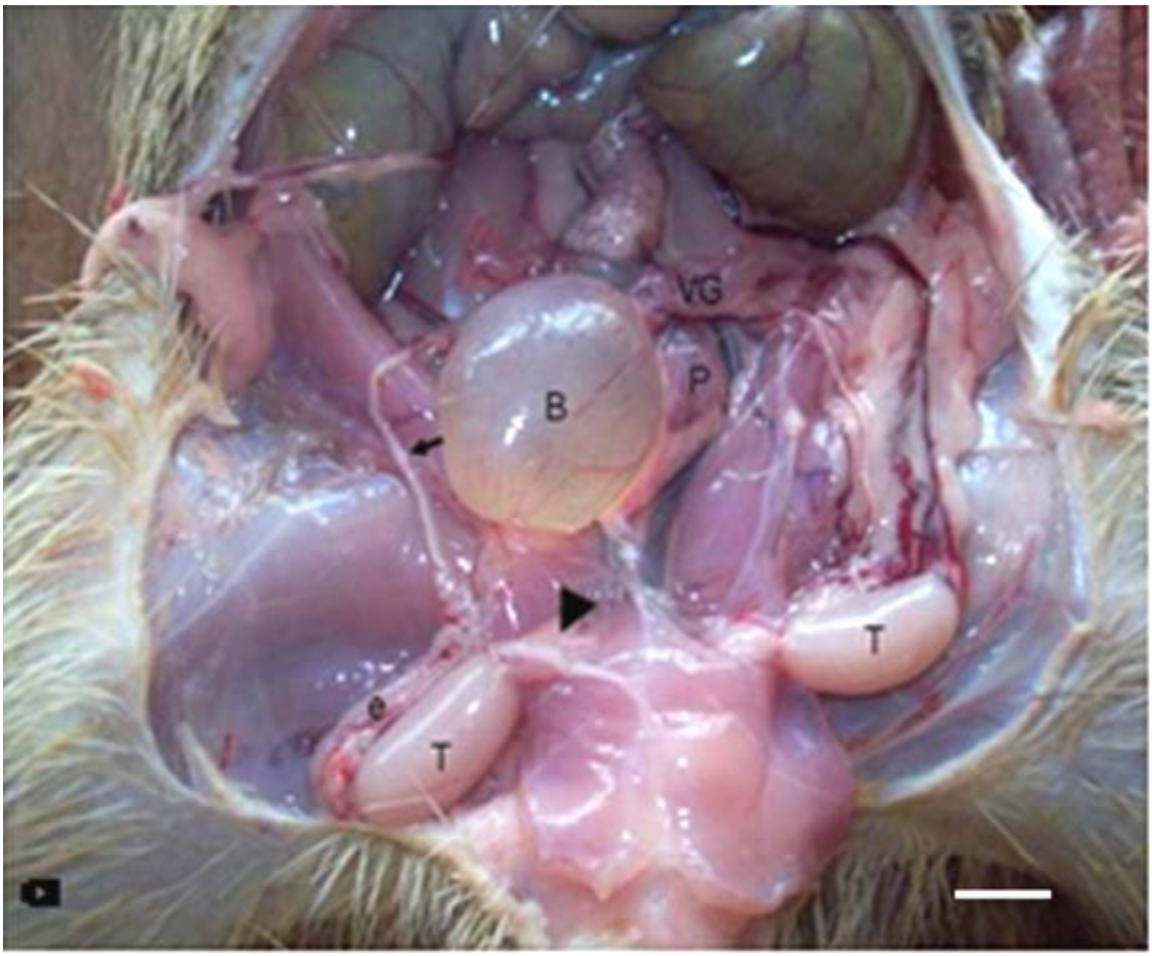

Figure 2a: Photograph of the male reproductive organ in the Greater cane rat *in situ*. Note the milk-white elongated ovoid testis (T), the distended urinary bladder (B) the ventral view of the prostate gland (P) and the vesicular gland (VG). The arrow indicates the deferent duct while the arrow head shows the gubernaculum testis attached to caudal pole. Mag X5. **Scale bar = 2mm**

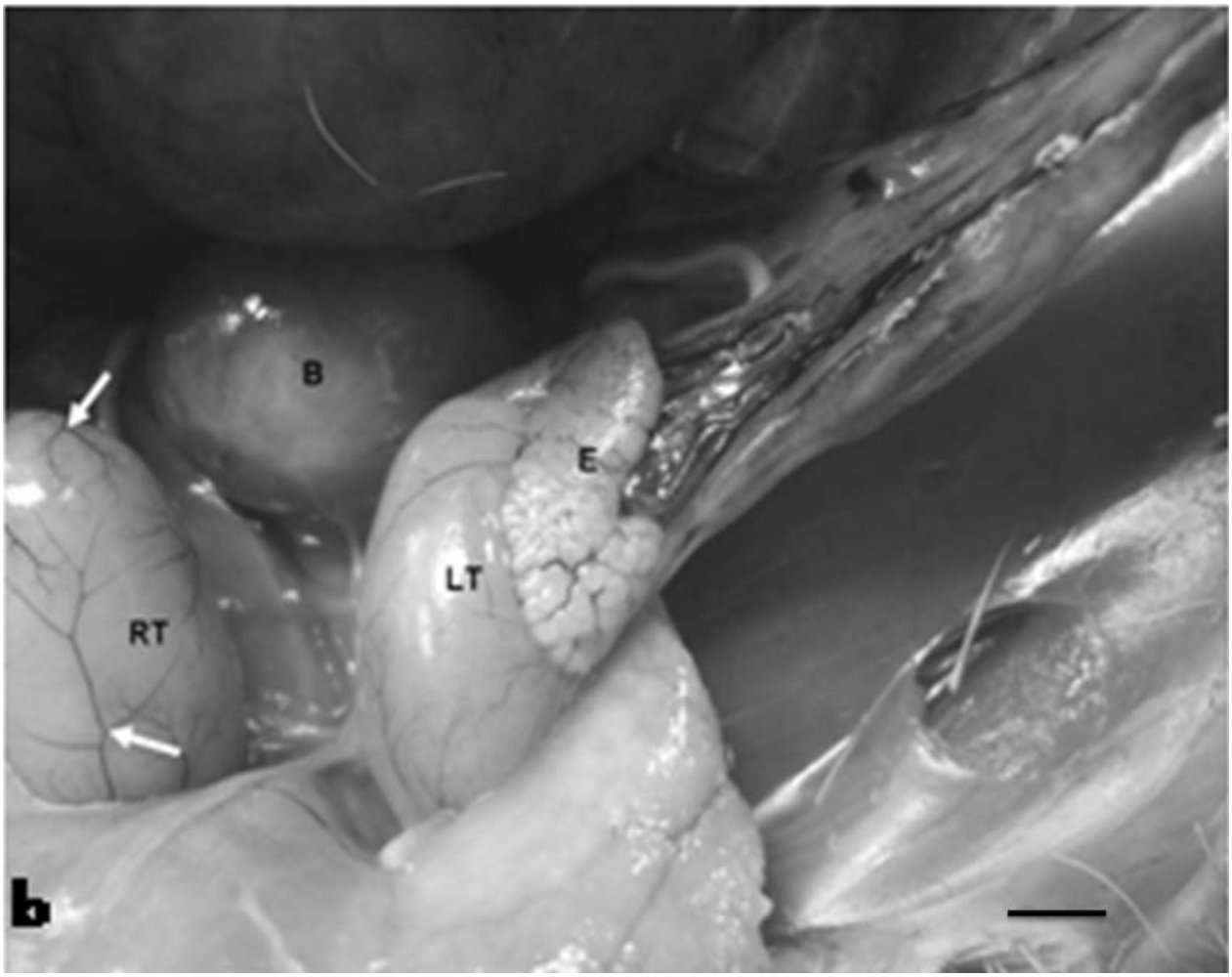

Figure 2b: Photograph of the male reproductive organ in the greater cane showing the right (RT) and left (LT) testes with the capsules ramified by blood vessels (white arrows), the epididymis (E) and the urinary bladder (B). **Scale bar = 2mm**

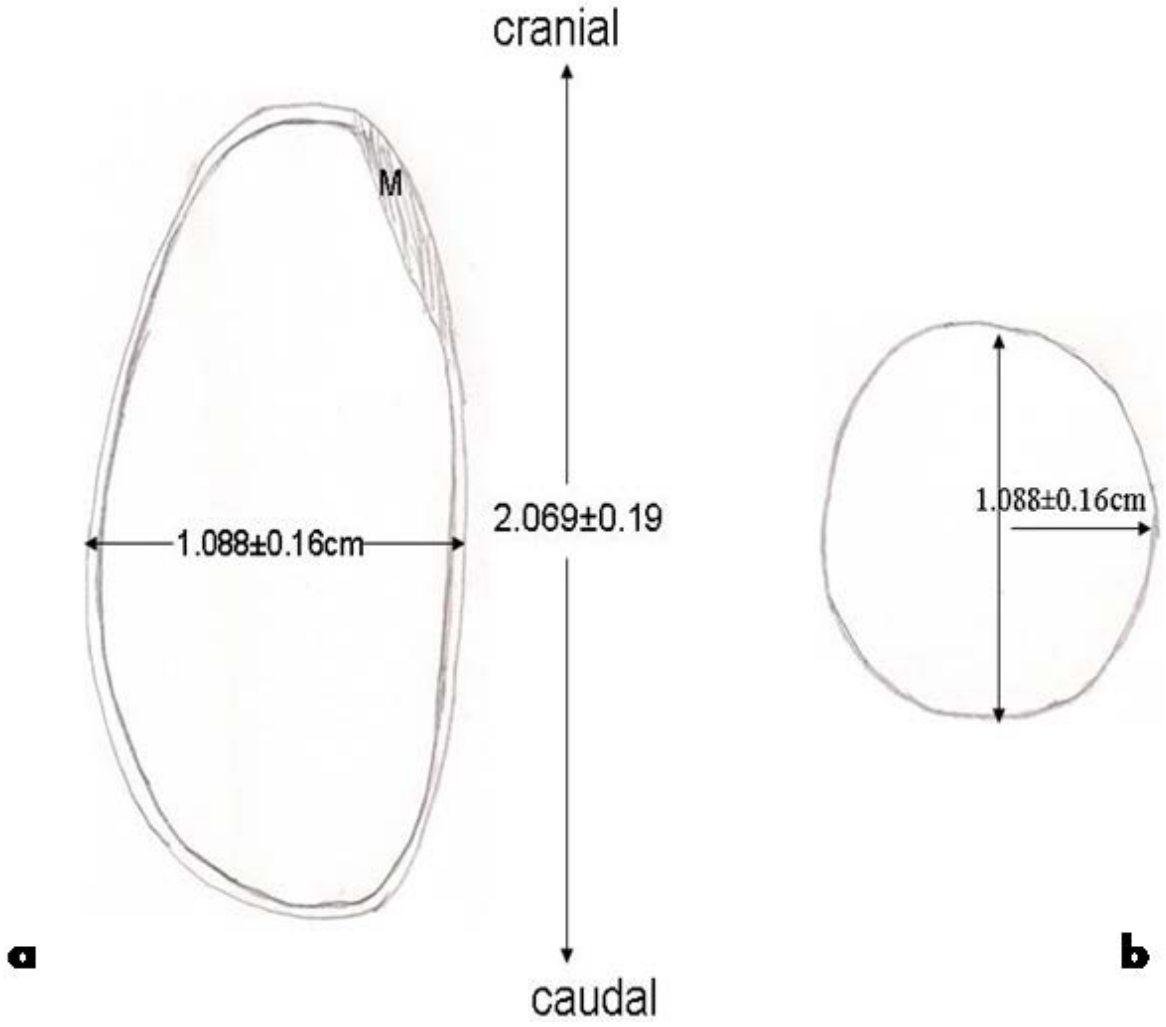

Figure 3: Schematic diagram of the shape and linear dimensions of the testis of the greater cane rat. In **(a**), note the mediastinum testis (M) on the longitudinal section of the testis. The (**b**) diagram shows the transverse section. Diagram is not drawn to scale.

3.2.1.2 Histological Appearance

Cross sections of the testis revealed the capsule (tunica albuginea) was made up of dense connective tissue that sends inconspicuous septae into the parenchyma which was composed mainly of seminiferous tubules (Fig. 4). Each tubule, in cross section, is generally roundish showing germinal epithelium containing all cellular stages of spermatogenesis. The spaces between the tubules were filled with interstitial tissues made up of connective tissue, Leydig's cells and various sized blood vessels, capillaries and lymphatics (Fig. 5). The germinal epithelium was composed of concentric layer of spermatogonia, spermatocytes and spermatids together with the Sertoli cells (Fig. 5). Different sections of the seminiferous tubules showed different successive cellular associations between the spermatogonia, spermatocytes and spermatids.

Three types of spermatogonia, A, intermediate (In) and B were identified based on their size, shape and nuclear morphology (Fig. 6). The A-type spermatogonia had oval-shaped euchromatic nuclei that contained several dot-like nucleoli. The nuclei of the Intermediate-type spermatogonia were also oval with more heterochromatin and several dot-like nucleoli. The B-type spermatogonia were relatively smaller with spherical nuclei having larger amount of heterochromatin and dot-like nucleoli.

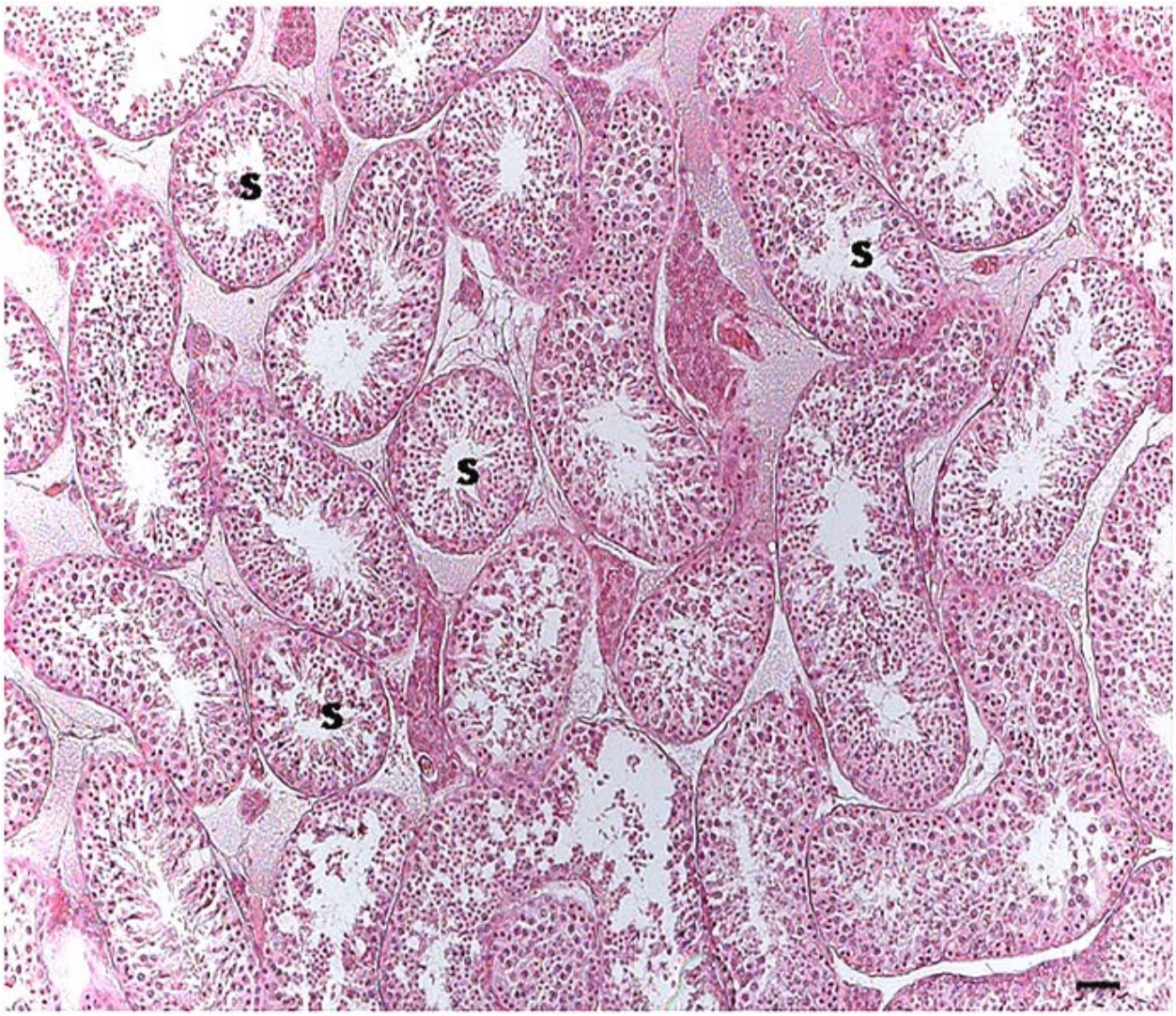

Figure 4: Photomicrograph of the section of the testis of the greater cane rat. Note the numerous generally roundish seminiferous tubules (S). **H&E,** Mag X100. **Scale bar = 50µm**.

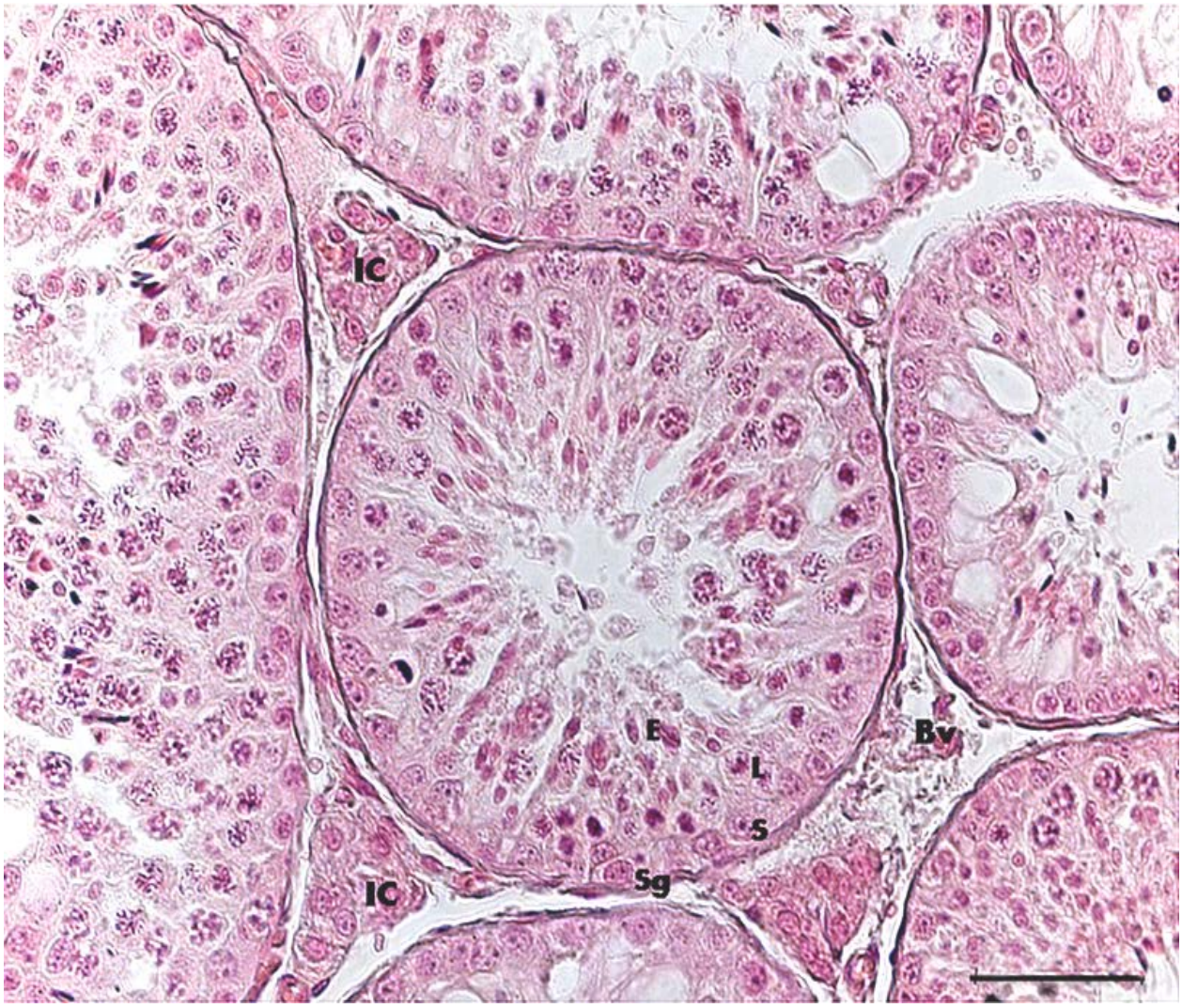

Figure 5: Photomicrograph of the seminiferous tubule in the greater cane rat showing the Sertoli cells (S), spermatogonia (Sg), spermatocytes (L) and the elongated spermatids (E). Note the interstitial cell of Leydig (IC) with the blood vessel (Bv) in between the seminiferous tubules. **H&E,** Mag X400. **Scale bar = 50µm**.

The spermatocytes at various meiotic steps were also observed in the germinal epithelium (Fig. 5&6). The preleptotene spermatocytes had smaller nuclei with larger heterochromatic crust than the B-type spermatogonia while the leptotene spermatocytes had irregular shaped nuclei with contraction of the chromatin at the centre of the cells. The zygotene and pachytene spermatocytes were characterized by enlargement of the nucleus, spreading of the chromosomes over the nucleus and the increasing visibility of the nucleolus. The nuclear enlargement gets to the maximum in the diplotene step spermatocytes (Fig. 6). Typical spermiogenic processes which entail the transformation of the spermatocytes to the round spermatids and subsequently to elongated spermatids that finally become the spermatozoa were observed in the tubular epithelium (Fig.6). The Sertoli cells are irregularly shaped and evenly spaced with nuclei that had prominent nucleoli (Fig. 5&6). The Leydig's cells in the interstitium were round and also possess nuclei with conspicuous nucleoli (Fig. 5).

In the greater cane rat, the mediastinum testis is composed of dense connective tissue, lymphatic and blood vessels as well as the rete testis which appears as labyrinths of anastomosing channels (Fig. 7a). The rete channels were lined by simple squamous epithelium (Fig. 7b)

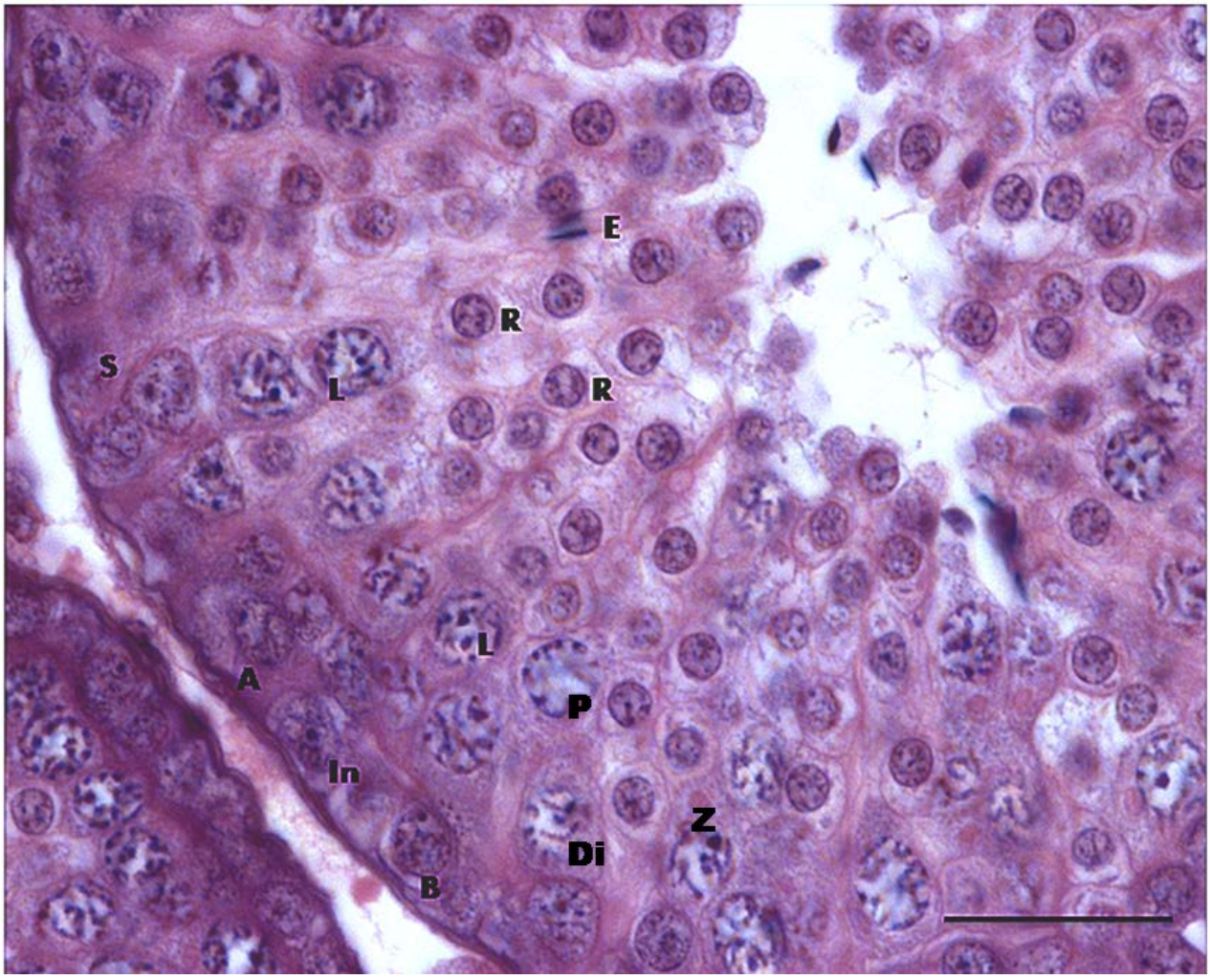

Figure 6: Photomicrograph of the seminiferous tubule in the greater cane rat showing the Sertoli cells (S), A, intermediate (In) and B spermatogonia, leptotene (L), pachytene (P), zygotene (Z) and Diplotene (Di) spermatocytes (L), round (R) and the elongated spermatids (E). **H&E,** Mag. X1000. **Scale bar = 20µm**.

Figure 7a: Photomicrograph of the Mediastinum testis in the greater cane rat showing the rete testis channels (RT), the large lymphatic vessel (L) and the mediastinal dense connective tissue (M), **H&E,** Mag. X100. **Scale bar = 50µm**.

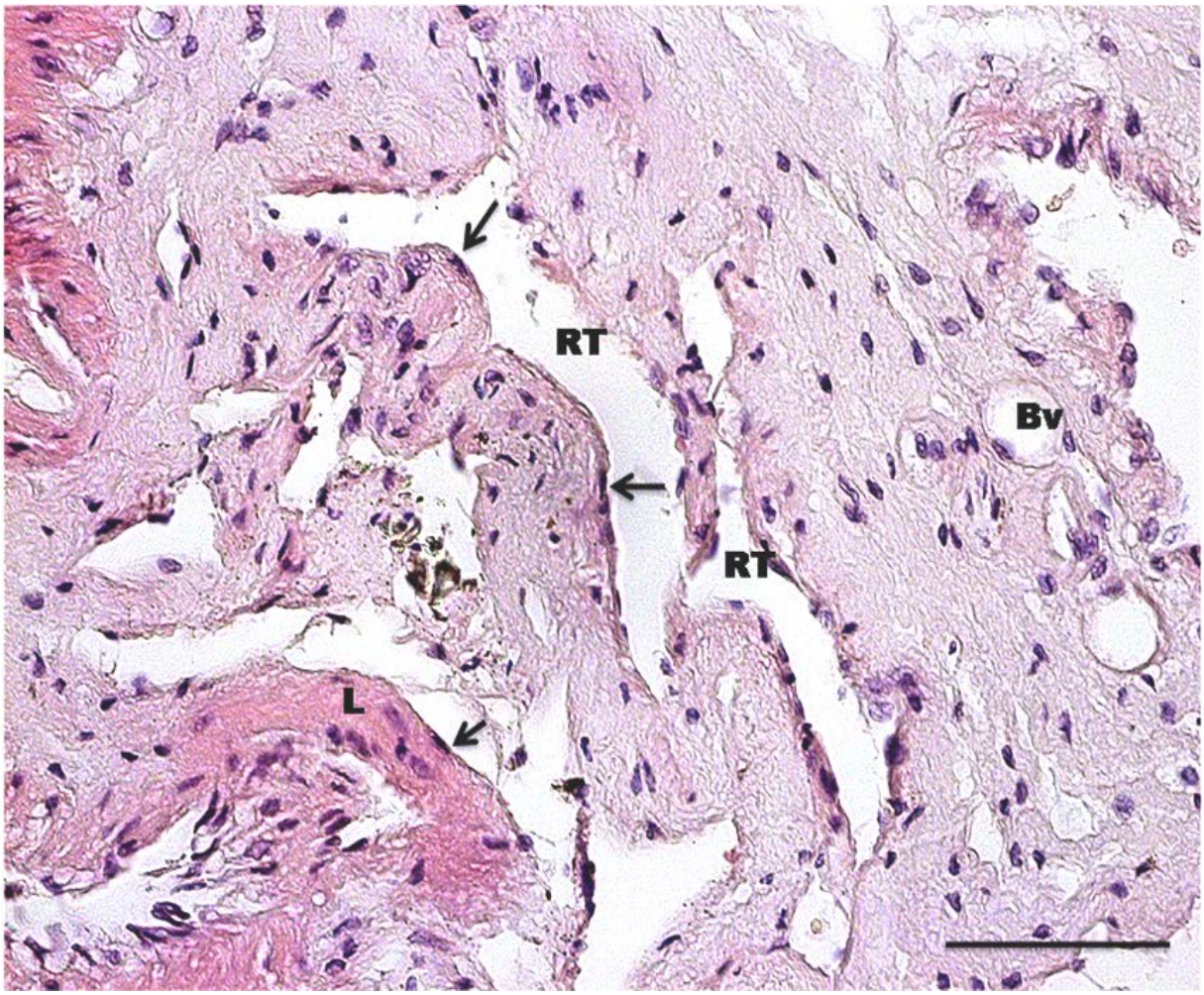

Figure 7b: Photomicrograph of the rete testis in the greater cane rat showing the rete channels (RT) lined with squamous epithelium (arrows), the large lymphatic vessels (L) and blood vessels (Bv), **H&E, Scale bar = 50µm**.

3.2.1.3 *Ultrastructure of the Spermatogenic Cells*

3.2.1.3.1 Spermatogonial Cells

Ultrastructurally, the A-type spermatogonia which were attached to the basal lamina by electron-lucent interdigitations had cytoplasm with granular appearance (Fig. 8a). The cytoplasm contained abundant round to oblong shaped mitochondria and some elongated cistrenae of the endoplasmic reticulum (Fig. 8a). The oblong-shaped nucleus contained several granule-like nucleoli with some of its heterochromatin condensed into small dots and a small amount heterochromatin flattened along the nuclear membrane giving the nucleus a general granular outlook (Fig 8a). Anchoring junctional complexes was observed between the plasma membrane of the A-type spermatogonia and the adjacent Sertoli cell (Fig. 8a)

The ultrastructure of the intermediate-type spermatogonium was quite similar to that of the A-type, only that the nucleus was relatively oval with less number but more prominent nucleoli (Fig. 8b). The cytoplasm also contained abundant round and elongated mitochondria as well as rod-shaped centrioles. Some of the In-type can be seen still joined to the daughter cells depending on their stage of division. Temporary junctions were equally present between the In-type and the adjacent spermatocytes (Fig. 8b)

For the B-type spermatogonia, the nucleus was smaller and more spherical than that of the In-type. It contained larger amount of heterochromatin condensed into flakes along the nuclear membrane and a more prominent nucleolus. The cytoplasm is also studded with abundant round and oblong-shaped mitochondria (Fig. 8c).

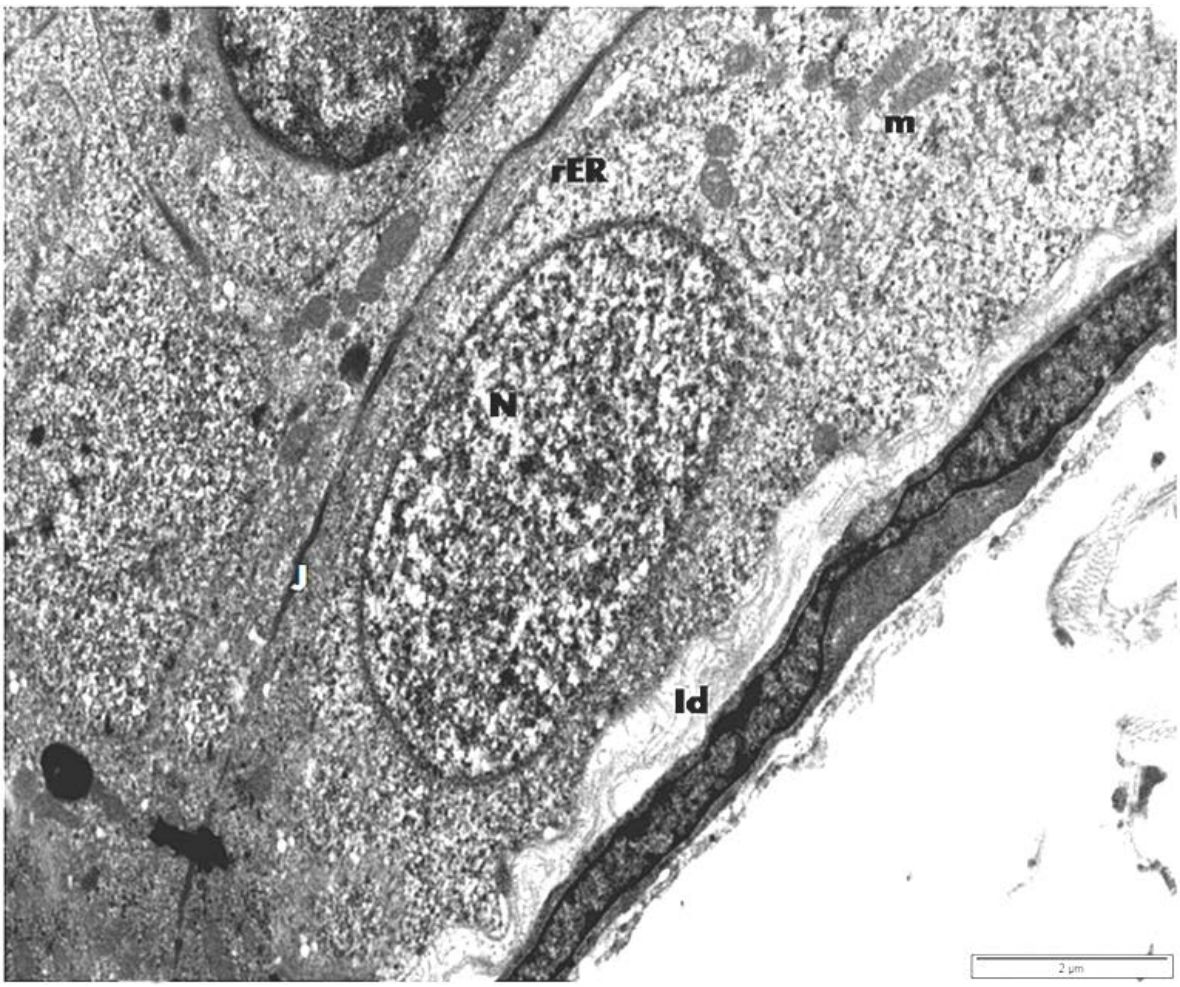

Figure 8a: Electron micrograph of the A-type spermatogonium in the testis of the greater cane rat. Note the presence of mitochondria (m), cisternae of rough endoplasmic reticulum (rER), granular nucleus (N), Junctional complex (J) and interdigitations (Id) with basal lamina.. Picture taken with Phillips CM10 TEM at 80 KV. Mag. X 20,000. **Scale bar = 2µm**

Figure 8b: Electron micrograph of the Intermediate (In)-type spermatogonium in the testis of the greater cane rat. Note the presence of mitochondria (m), granular nucleus (N) with nucleolus (Nu), tubular centrioles (C) and interdigitations (Id) with basal lamina. Possible evidence of cleavage furrow is also shown (arrow). Picture taken with Phillips CM10 TEM at 80 KV. Mag. X 20,000. **Scale bar = 2µm**.

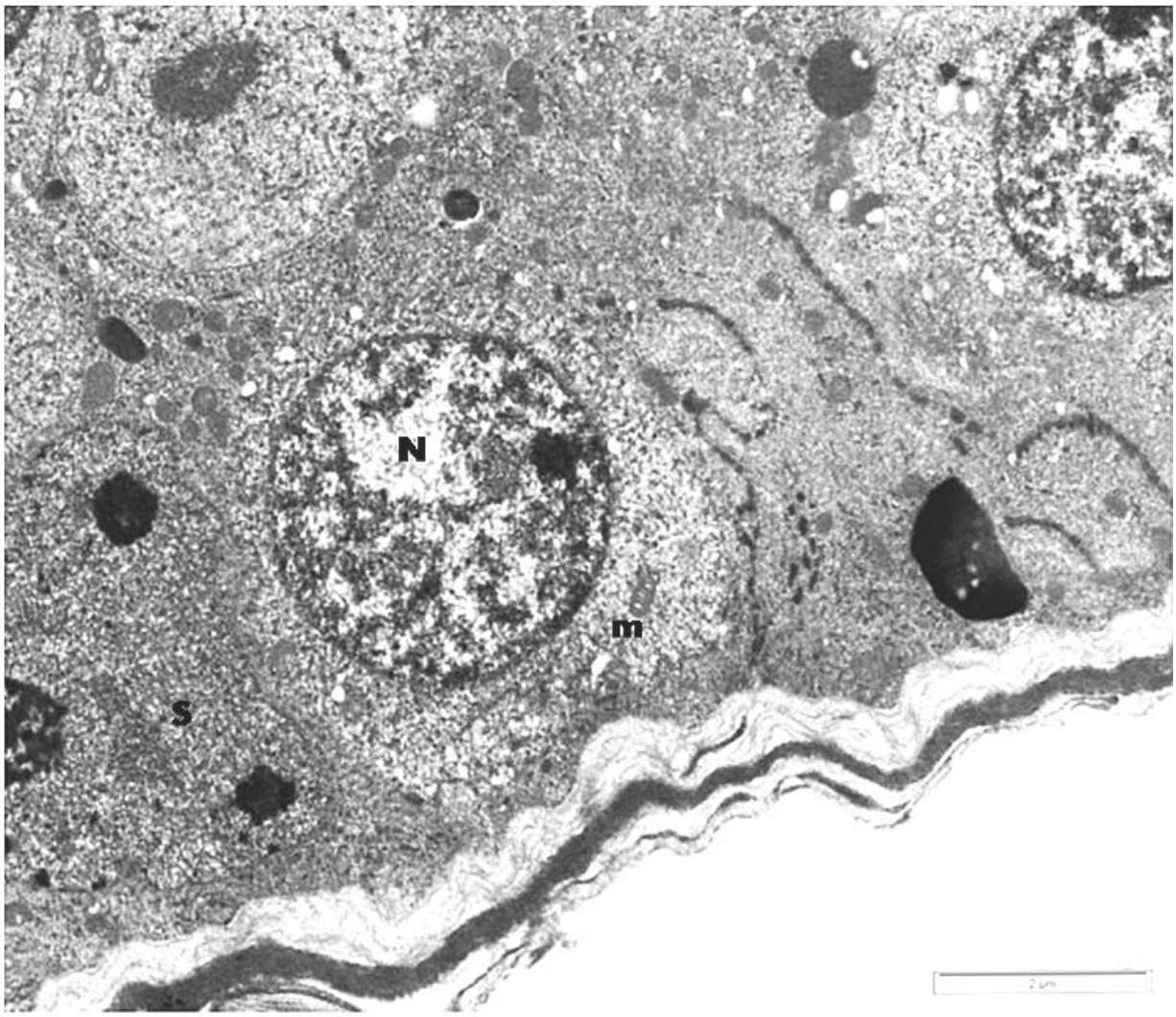

Figure 8c: Electron micrograph of the B-type spermatogonia in the testis of the greater cane rat showing the basal part. Note the presence of mitochondria (m), round nucleus (N). Part of the Sertoli cell is also shown (S). Picture taken with Phillips CM10 TEM at 80 KV. Mag. X 20,000. **Scale bar = 2µm**.

3.2.1.3.2 Spermatocytes

Except for the characteristic changes in the nuclear chromatin arrangements in the different division stages, the general ultrastructural architecture of the spermatocytes showed ovate to spheroidal nuclei with irregular patches of dense chromatin or chromosomal core which sometimes had synaptinemal complexes (Fig. 9). The cytoplasm contained numerous mitochondria and scattered endoplasmic reticulum cisternae. Golgi complexes and paired tubular centrioles were also present (Fig. 9).

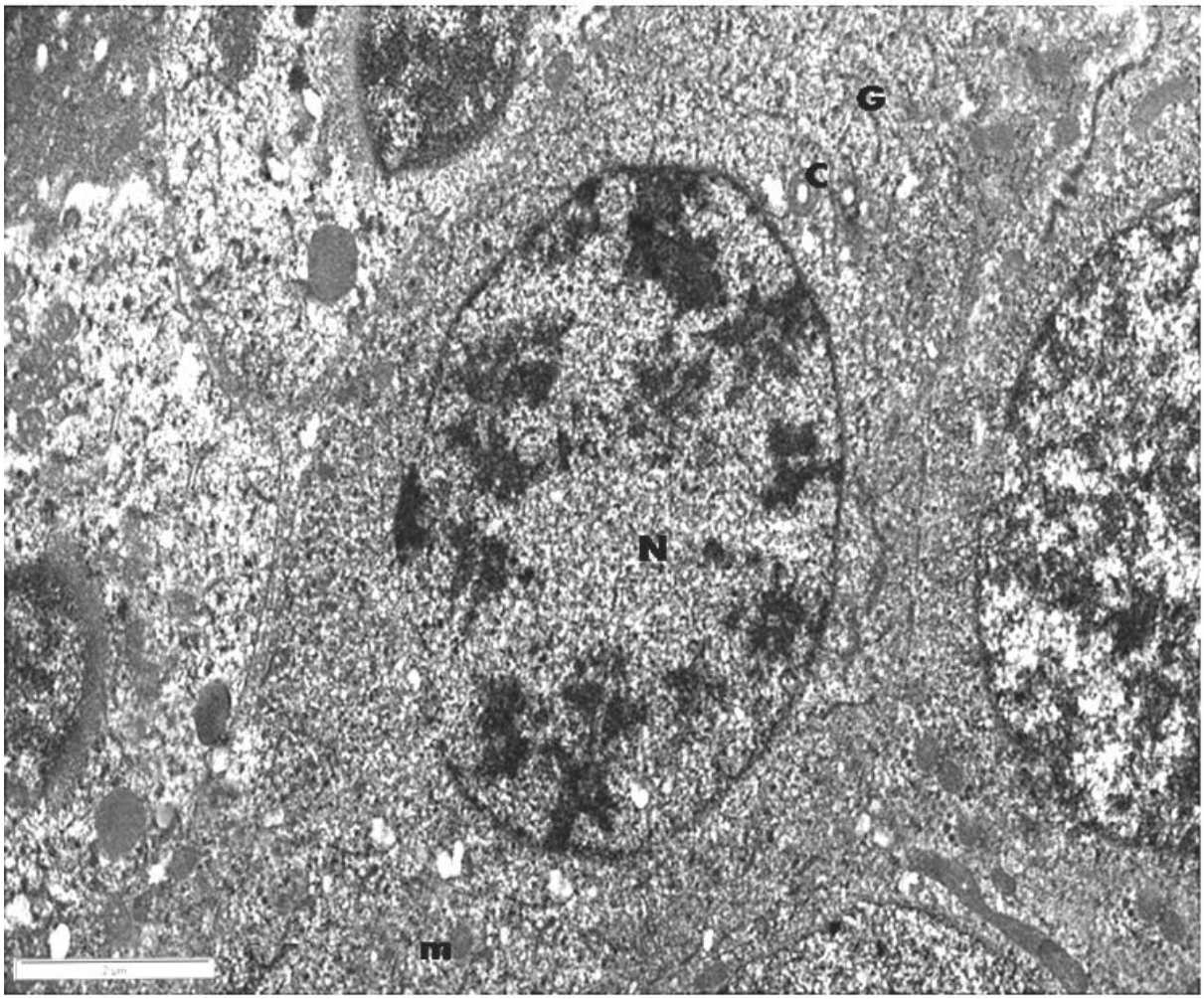

Figure 9: Electron micrograph of a representative spermatocyte in the testis of the greater cane rat showing oval nucleus (N) with dense chromatin, mitochondria (m), tubular centrioles (C) and some Golgi cisternae (G). Picture taken with Phillips CM10 TEM at 80 KV. Mag. X 20,000. **Scale bar = 2µm**.

3.2.1.3.3 Spermatids and Acrosome Formation

The transformation of the spermatids into the spermatozoa which involves the development of the acrosomal system and changes in the nuclear morphology as well as in cellular conformation occurred in twelve (12) steps in the greater cane rat (Fig. 10a-l). The steps can be distributed among the four spermiogenic phases as follows: the first three steps (Fig. 10a-c) constitute the *Golgi* phase; the *cap* phase consisted of the next three steps (Fig. 10d-f). While the three consecutive steps (Fig. 10g-i) make up the *acrosomal* phase, the last three steps (Fig. 10j-l) are the *maturation* phase.

The three spermatids in the Golgi phase had spheriodal nuclei with varying chromatin distributions. In the newly formed spermatid after the second meiotic division, the chromatin in its round nucleus was distributed as irregular patches with thin peripheral layer (Fig. 10a). In the cytoplasm, which was apparently less electron dense, Golgi complexes were beginning to appear at the Golgi zone near the nucleus..

In the step 2- spermatids (Fig. 10b), the round nuclei had irregularly dispersed chromatin with less at the periphery and the nuclear membrane tends to increase in thickness. In the cytoplasm, the proacrosomal granules began to transform into the acrosomal vesicle with the two parallel centriole taking position near the Golgi zone. There was also the presence of cisternae of endoplasmic reticulum, ribosomal granules and numerous mitochondria that exhibit typical linear cristae.

In the third step spermatid, the acrosomal granule attaches to the nuclear envelope with the development of the acrosomal vesicles (Fig. 10c). In the step 4-spermatid, acrosomal granule which is now closely attached to the nucleus exhibits a thickening at the area of contact and

flattens over the nucleus without indenting it (Fig. 10c). At this step, the nucleus has irregularly dispersed chromatin.

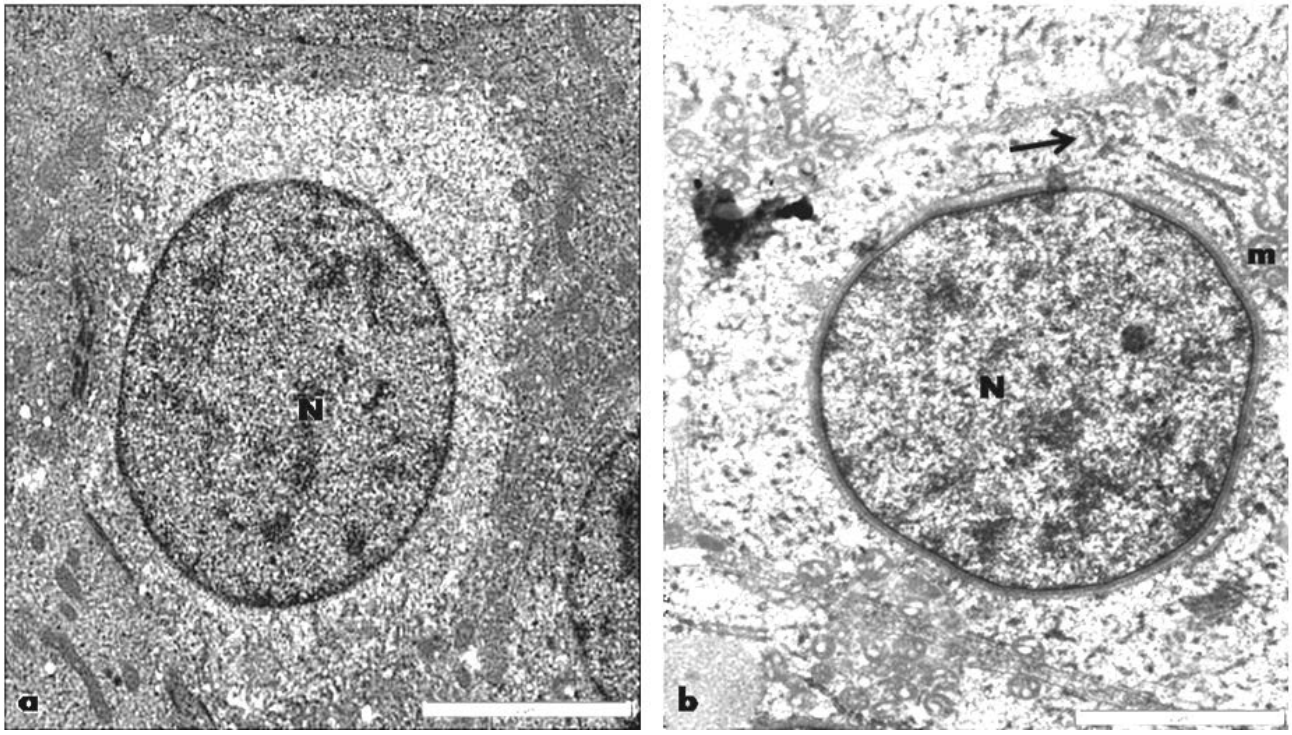

Figure 10a&b: Electron micrographs of step1 and 2 spermatids in the greater cane rat. **(a)** Step 1-spermatid with spherical nucleus (N) having irregularly distributed chromatin patches. **(b)** Step 2-spermatid with the formation of the Golgi zone and acrosomal vesicles (arrow). Mitochondria (m) are also shown. Picture taken with Phillips CM10 TEM at 80 KV. Mag. X 20,000. **Scale bar = 2µm**.

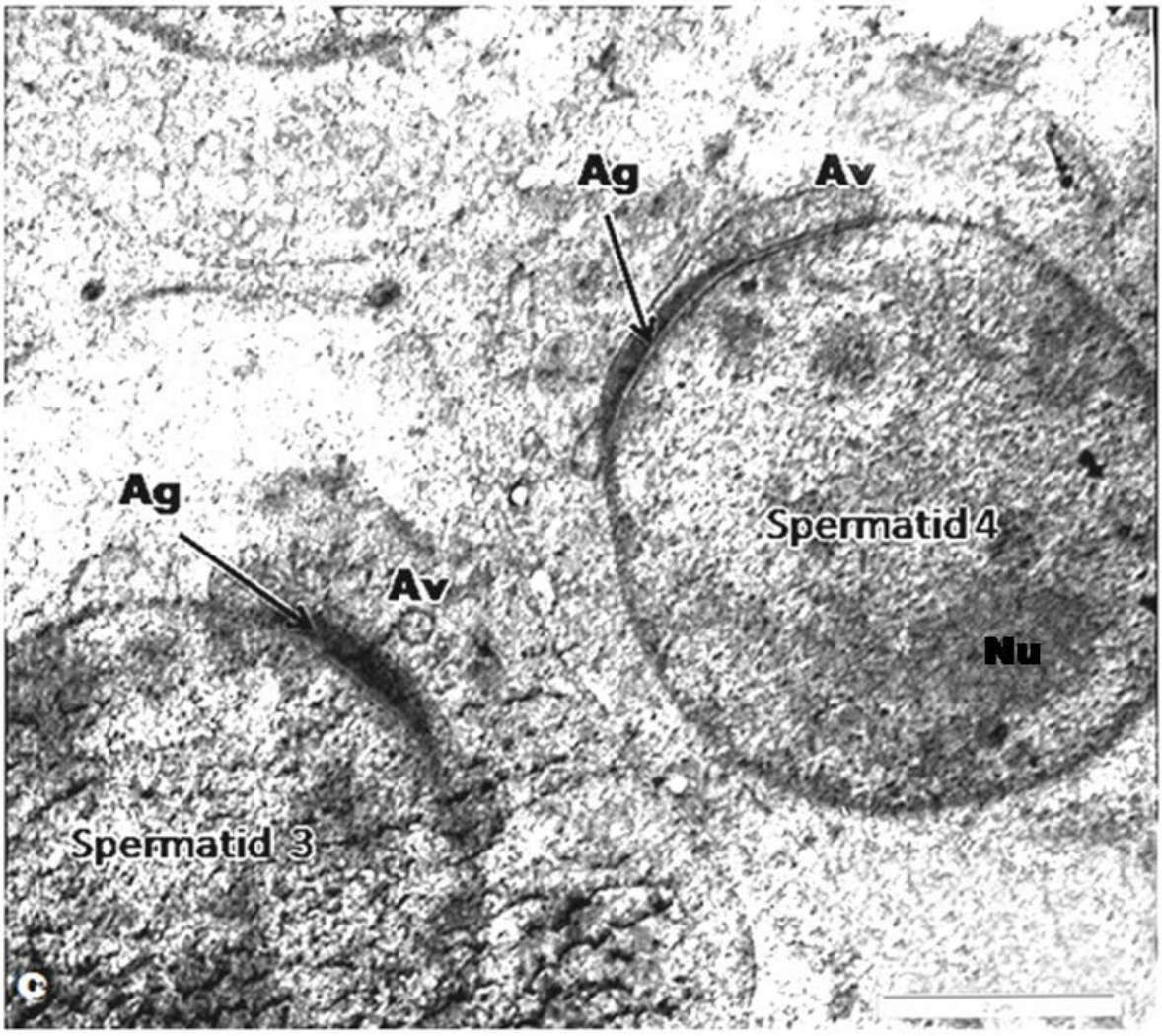

Figure 10c: Electron micrographs of steps 3 and 4 spermatids in the greater cane rat. Step 3-spermatid has the acrosomal granules (Ag) attached to the nucleus and the acrosomal cap (Av) formed on it while in Step 4-spermatid the attached acrosomal granule flattens over the nucleus and thickens at point of contact. Note in Spermatid 4, the flattening of the acrosomal vesicle, the irregularly distributed chromatin patches and the prominent nucleolus (Nu). Picture taken with Phillips CM10 TEM at 80 KV. Mag. X 20,000, **Scale bar = 2µm**.

The main feature of step 5 and 6 spermatids was the formation of the acrosomal cap by the acrosomal vesicle spreading over the round nucleus (Fig. 10d &e). In the step 5-spermatid, while the nucleus remains spherical, its chromatin begins condensation with the centrioles moving away from the acrosomal system (Fig. 10d). The spreading of the acrosomal cap continues in steps 6 spermatids with increasing accumulation of the mitochondria around the acrosomal area. The acrosomal granule also begins to spread over the nucleus in this step and the Golgi complex begins to move away from the acrosomal system (Fig. 10e). The nucleus in this step remains round with increasing chromatin condensation (Fig. 10e).

In the step 7 spermatids the acrosomal cap had extended to cover half of the nucleus with the acrosomic granule spreading along thereby making the acrosomal system have a homologous appearance (Fig. 10f). The expanded margin of the acrosomal vesicle also indents the nucleus to form a marginal fossa. At the same time, the spheroidal nucleus begins to change with the head area becoming conical. The spermatids also became oriented with the acrosomal system towards the basement membrane. Several axonemal fibres begin to appear in the cytoplasm with the tubular centrioles at the point of formation of the tail. The step 8-spermatids are characterized with increased nuclear elongation and condensation (Fig. 10g) with the cytoplasm also becoming conical. The spermatid nucleus with its acrosomal system begins to migrate towards the periphery of the cell. The first evidence of a flagellar axoneme at development becomes apparent at this step (Fig. 10g).

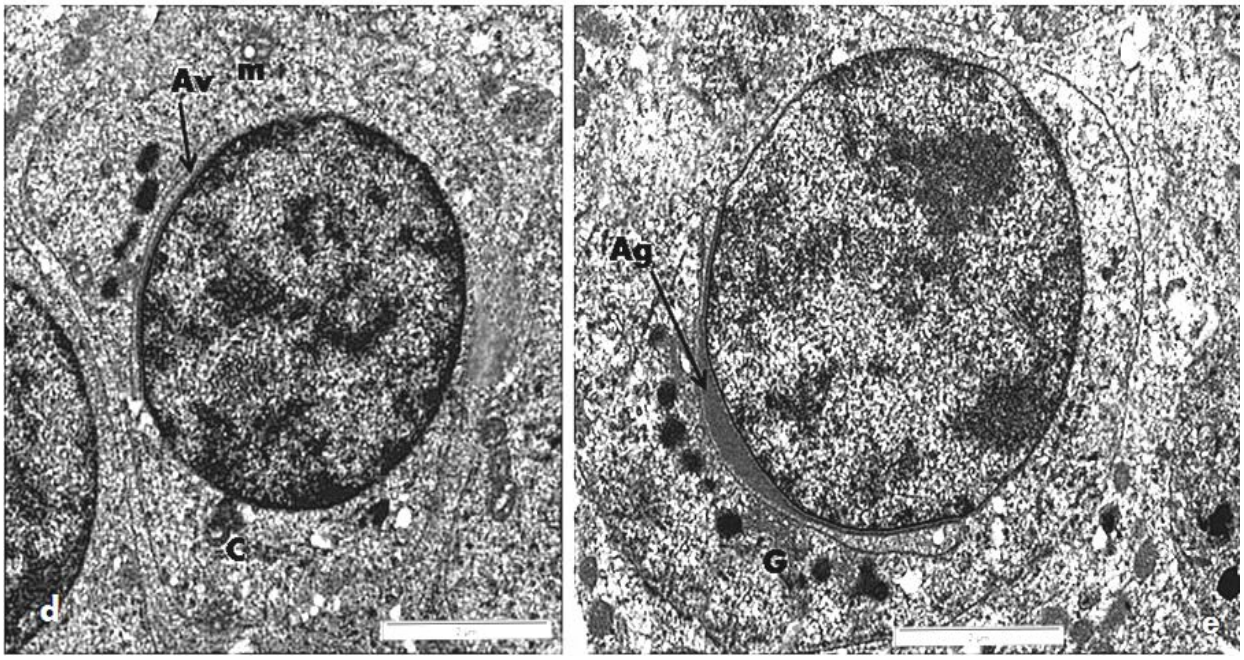

Figure 10d &e: Electron micrographs of step 5 and 6 spermatids in the greater cane rat. In **(d),** Step 5-spermatid acrosomal vesicle (Av) spreads over the nucleus. Note the nuclear condensation and presence of mitochondria (m). In step 6 spermatid **(e)**, note the spreading over of the acrosomal granule (Ag) and the moving away of the Golgi from the acrosomal system. Picture taken with Phillips CM10 TEM at 80 KV. Mag. X 20,000, **Scale bar = 2µm**.

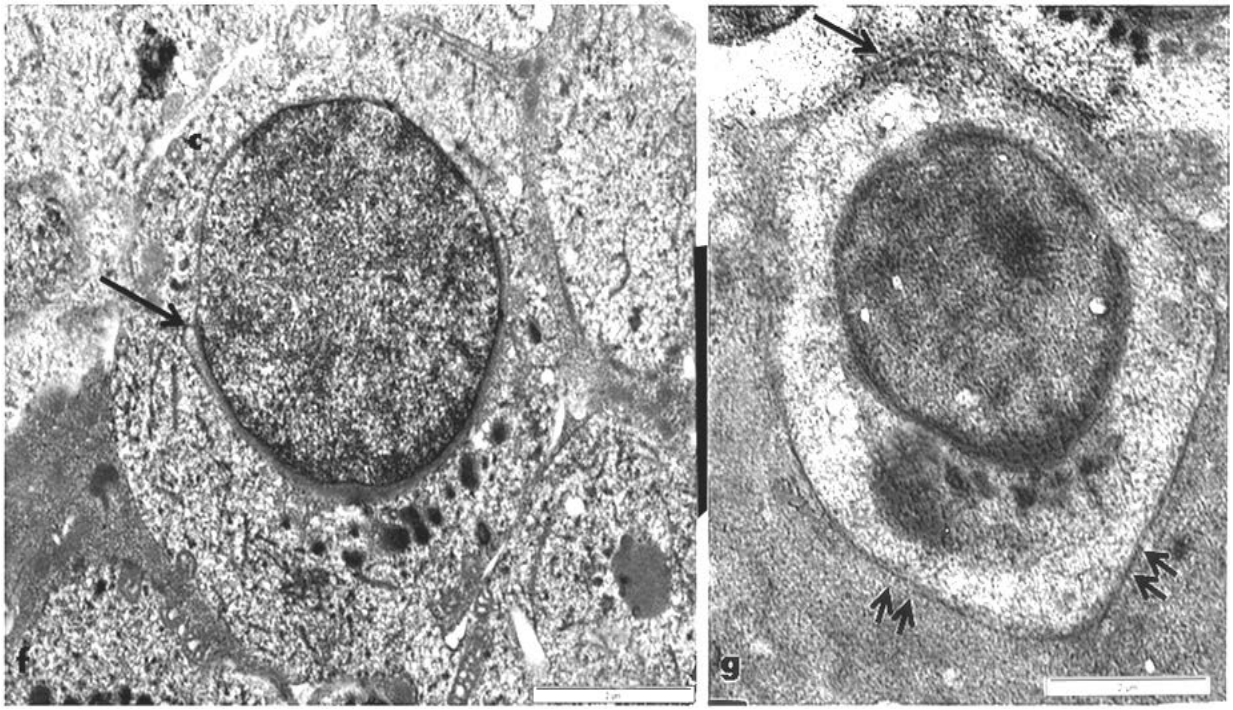

Figure 10f&g: Electron micrographs of steps 7 and 8 spermatids in the greater cane rat. **(f)** Step 7-spermatid has homologous acrosomal system with cap covering half of the nucleus. Note the marginal fossa (arrow) formed by the expanded cap margin and the location of the centriole (c). **(g)** Step 8-spermatid becoming elongated with acrosomal system moving close to the cell membrane (double arrows). Note the beginning of flagellar axoneme development (long arrow). Picture taken with Phillips CM10 TEM at 80 KV. Mag. X 20,000, **Scale bar = 2µm**.

As the acrosomal system dorsal elongation and nuclear condensation continue in the step 9 spermatid, the acrosomal system connects the cell membrane. At the same time, the bulk of the cytoplasm flows towards the other pole of the cell where the flagellum develops (Fig. 10h). In this step, the cytoplasm contains mitochondria that tend to gather at the region of the future middle piece of the spermatozoon. As the nuclear elongation continues, the acrosomal cap also continues its posterior extension to the caudal end of the nuclei in these spermatids.

The continued elongation and condensation gave the nuclei in the 10-step spermatid its elongated shape (Fig. 10i). In this spermatid the expanded acrosomal cap margins become apparent moving posterior and forming marginal fossa as the nucleus elongates, while occasional small vacuoles begin to appear in the more dense and compact nuclei. The formation of the spermatic tail with axonemal fibres appears within the cytoplasmic residues still persisting in this step.

In the step11 spermatid, rostral acrosomal extension which involved the anterolateral regions of the acrosomal cap becomes visible (Fig. 10j). Between the inner border of the acrosome and the nuclear envelope, the perforatium and the sub-acrosomal space are equally present. With the nuclear elongation, the marginal fossa moves caudally, thereby demarcating the equatorial segment from the middle segment of the acrosomal cap. The nuclear vacuoles were also on the increase (Fig. 10j).

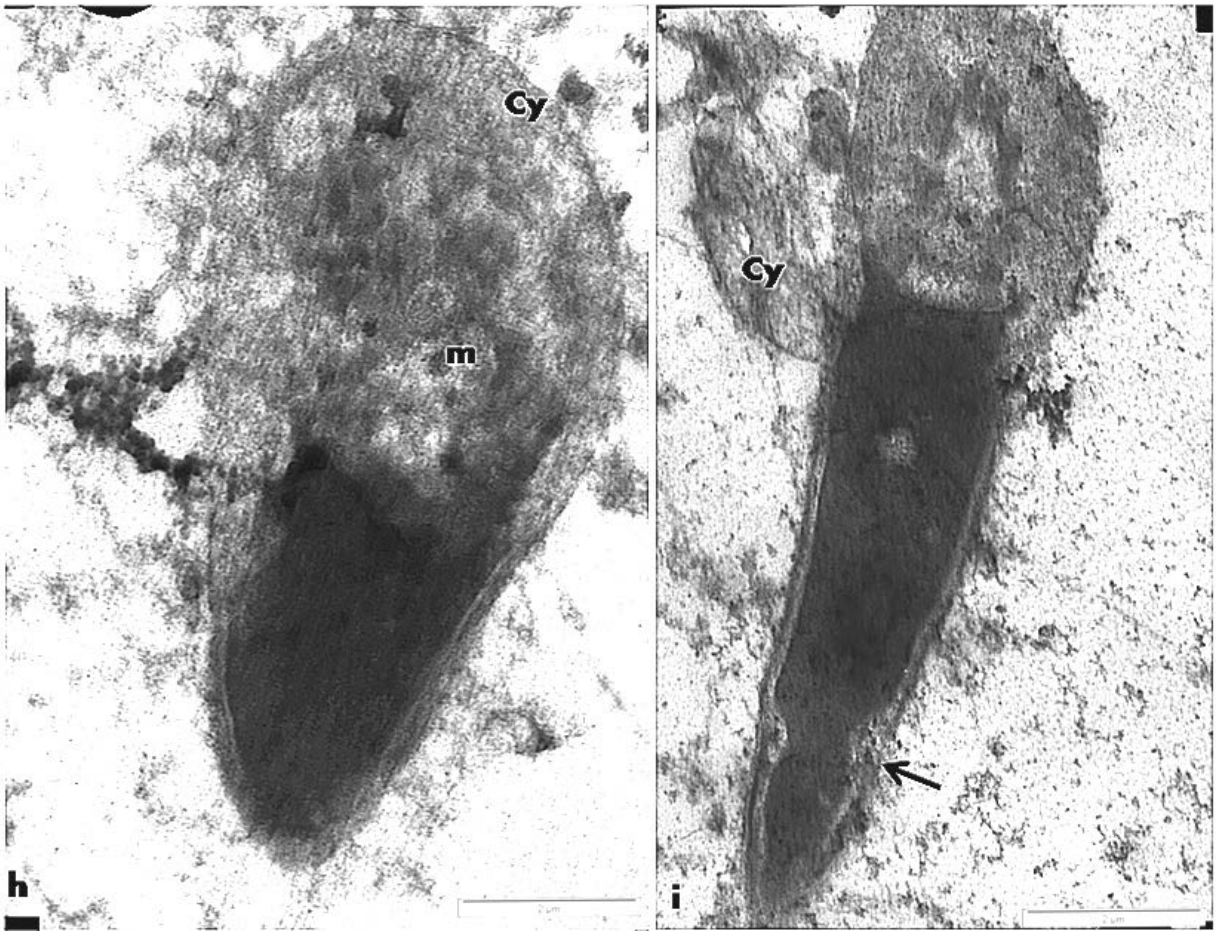

Figure 10h&i: Electron micrographs of steps 9 and 10 spermatids in the greater cane rat. In Step 9-spermatid **(h),** the nucleus abuts the cell membrane and the cytoplasm (Cy) moves towards the lumen. Note the mitochondria (m) in the cytoplasm. In **(i),** Step 10-spermatid become elongated spermatid with cytoplasmic residue (Cy) still hanging on it. Note the marginal fossa (arrow). Picture taken with Phillips CM10 TEM at 80 KV. Mag. X 20,000, **Scale bar = 2µm**

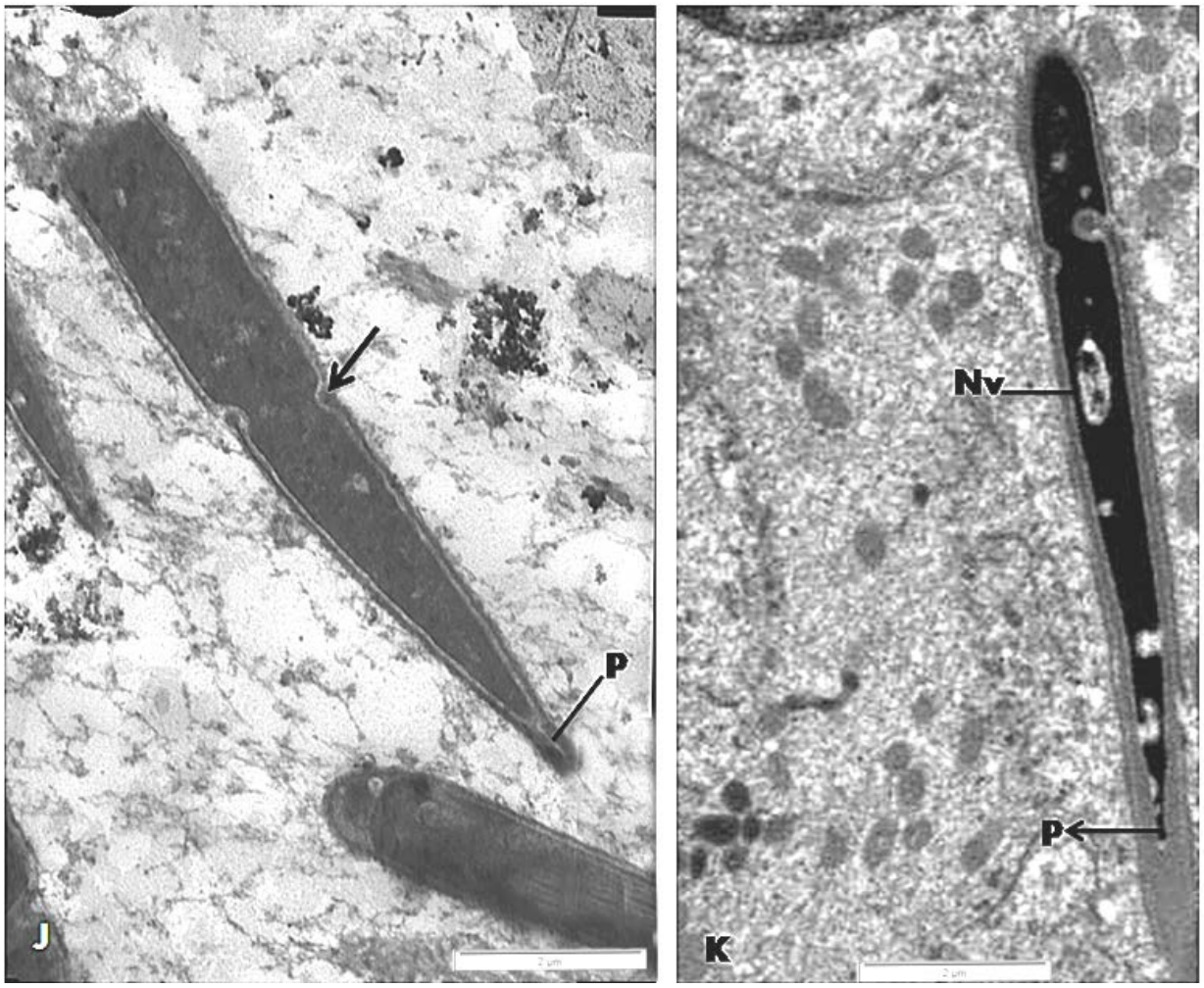

Figure 10j&k: Electron micrographs of steps 11 and 12 spermatids in the greater cane rat. In Step 11-spermatid **(j),** the perforatorium (P) develops. Note the marginal fossa (arrow). In **(k),** Step 12-spermatid shows the more conspicuous nuclear vacuole (Nv) and the perforatorium. Picture taken with Phillips CM10 TEM at 80 KV. Mag. X 20,000, **Scale bar = 2µm**.

In the 12 step spermatids, three distinct segments of the acrosomic cap can be well distinguished; the apical segment projecting beyond the anterior margin of the nucleus; a main segment extending back over and beyond the anterior half of the nucleus; and a differentiating equatorial segment comprising the caudal portion of the nucleus (Fig. 10k). The nuclear vacuole became more pronounced as this step marks the point of spermiation.

3.2.1.4 *Ultrastructure of the Sertoli Cell*

The ultrastructure of the Sertoli cell in the greater cane rat shows the typical irregularly-shaped cell with its basal portion attached to the basal lamina while its apical processes extend to the seminiferous tubular lumen (Fig. 11). The cell possesses typically large, indented, and irregularly shaped nucleus that is generally located at the basal portion of the cell. Prominent nucleolus with very dense nucleolonema that surround moderately dense internal part and heterochromatic clumps were seen scattered in the nucleus.

The supra-nuclear cytoplasm contains Golgi complexes, both lysosomes and phagolysosomes, as well as round and rod-shaped mitochondria that sometimes extend to the lateral and apical processes of the cells. Large lipid droplets were also seen in the cytoplasm of the cell with some small droplets present at the processes (Fig 11a). The infra-nuclear cytoplasm contained tubular form of the smooth endoplasmic reticulum and some rod shaped mitochondria (Fig. 11a & b).

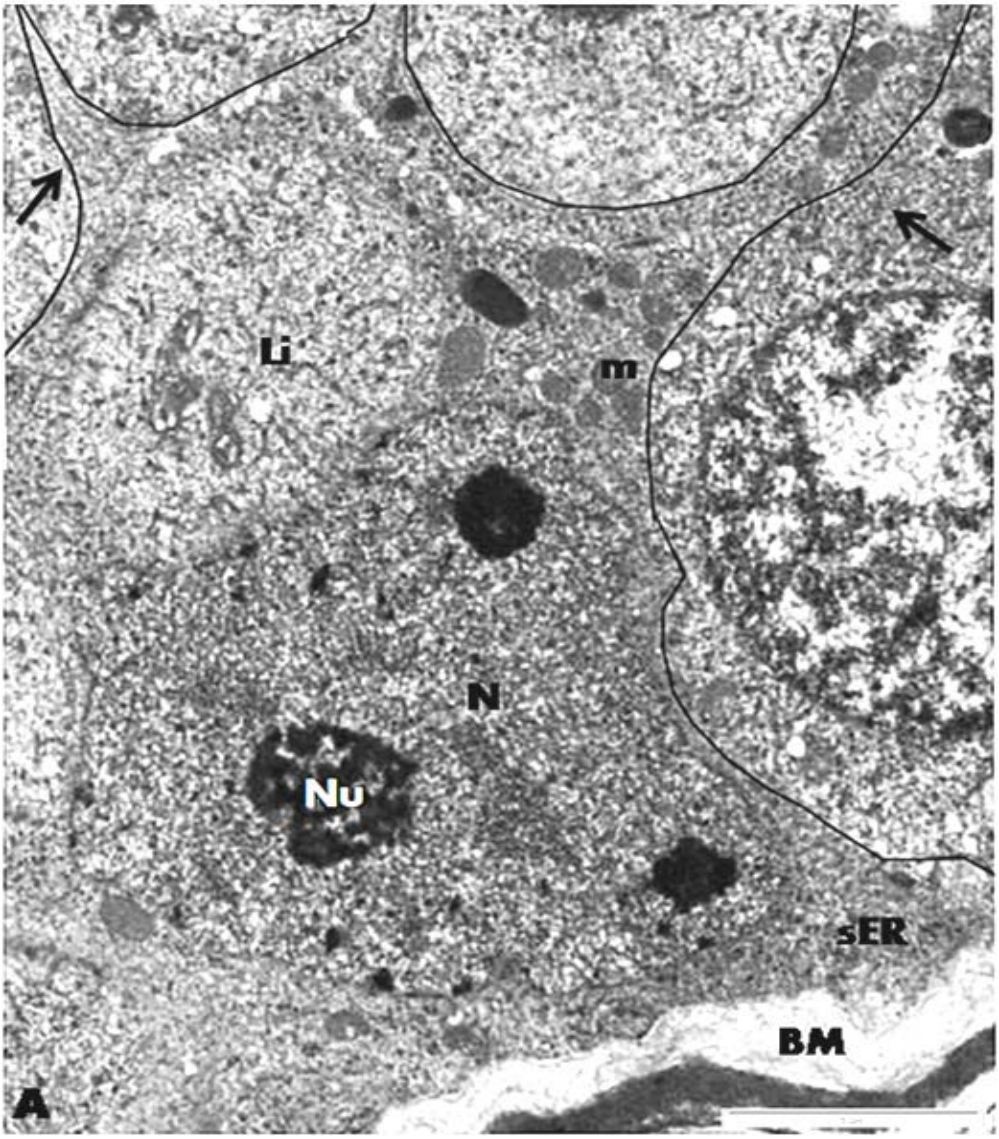

Figure 11A: Electron micrograph of the Sertoli cell in the testis of the greater cane rat. Note the cell processes (arrows), abundant mitochondria (m), irregularly shaped nucleus (N) with prominent multiple nucleoli (Nu), large lipid droplet (Li) and smooth endoplasmic reticulum. The basal cell membrane is attached to the basal lamina (BM). Picture taken with Phillips CM10 TEM at 80 KV. Mag. X 30,000, **Scale bar = 5µm**.

.

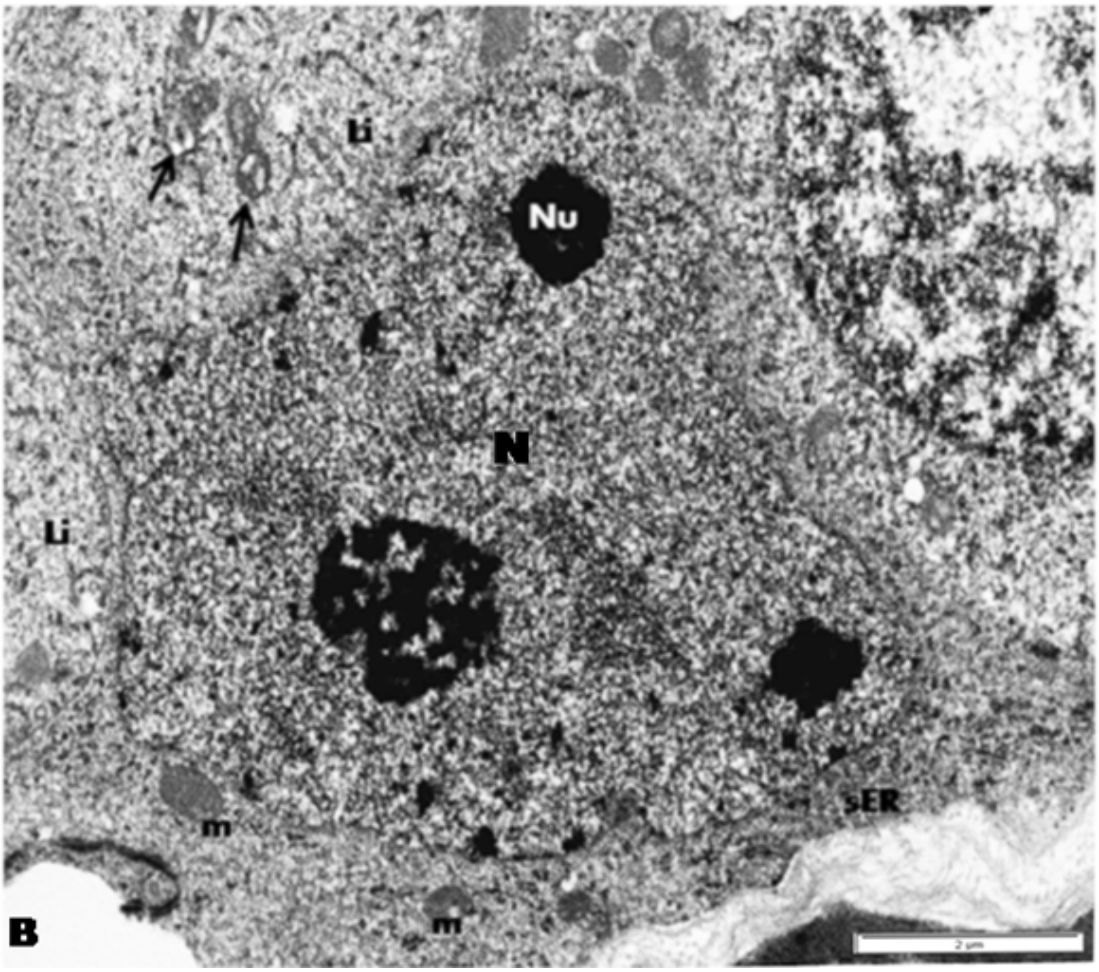

Figure 11B: Electron micrograph of the Sertoli cell in the testis of the greater cane rat showing the basal irregularly shaped nucleus (N) with prominent multiple nucleoli (Nu), large lipid droplet (Li) containing some electron dense granular structures (arrows) cisternae of smooth endoplasmic reticulum and abundant mitochondria (m). Picture taken with Phillips CM10 TEM at 80 KV. Mag. X 30,000, **Scale bar = 2µm**.

3.2.1.5 Ultrastructure of the Interstitial Endocrine (Leydig) Cell

The ultrastructure of a portion of the interstitium in the greater cane rat showed it contains the connective tissue matrix, characteristic Leydig cells arranged in clusters, macrophages and peritubular myoid cells covered by thin, flattened lymphatic epithelial cells that bound the intertubular lymphatic sinusoids (Fig. 12a). Though the shapes and sizes of Leydig cells vary within the cluster, they are mostly irregular or oval-shaped with short cytoplasmic processes that are associated with each other and the macrophages (Fig. 12a).

The largely elongated euchromatic nucleus of the Leydig cell possesses conspicuous nucleolus with few indentations of the nuclear membrane (Fig. 12b). The most prominent features of these interstitial endocrine cells were the presence of abundant round and elongated mitochondria containing both tubular and lamella cristae (Fig. 12b&c) as well as large dense network of interconnecting tubules of smooth endoplasmic reticulum (sER) to which spherical peroxisomes are closely associated (Fig. 12c). Also present are parallel cisternae of rough endoplasmic reticulum. The extracellular spaces in the cluster were seen to contain collagen fibrils (Fig. 12c).

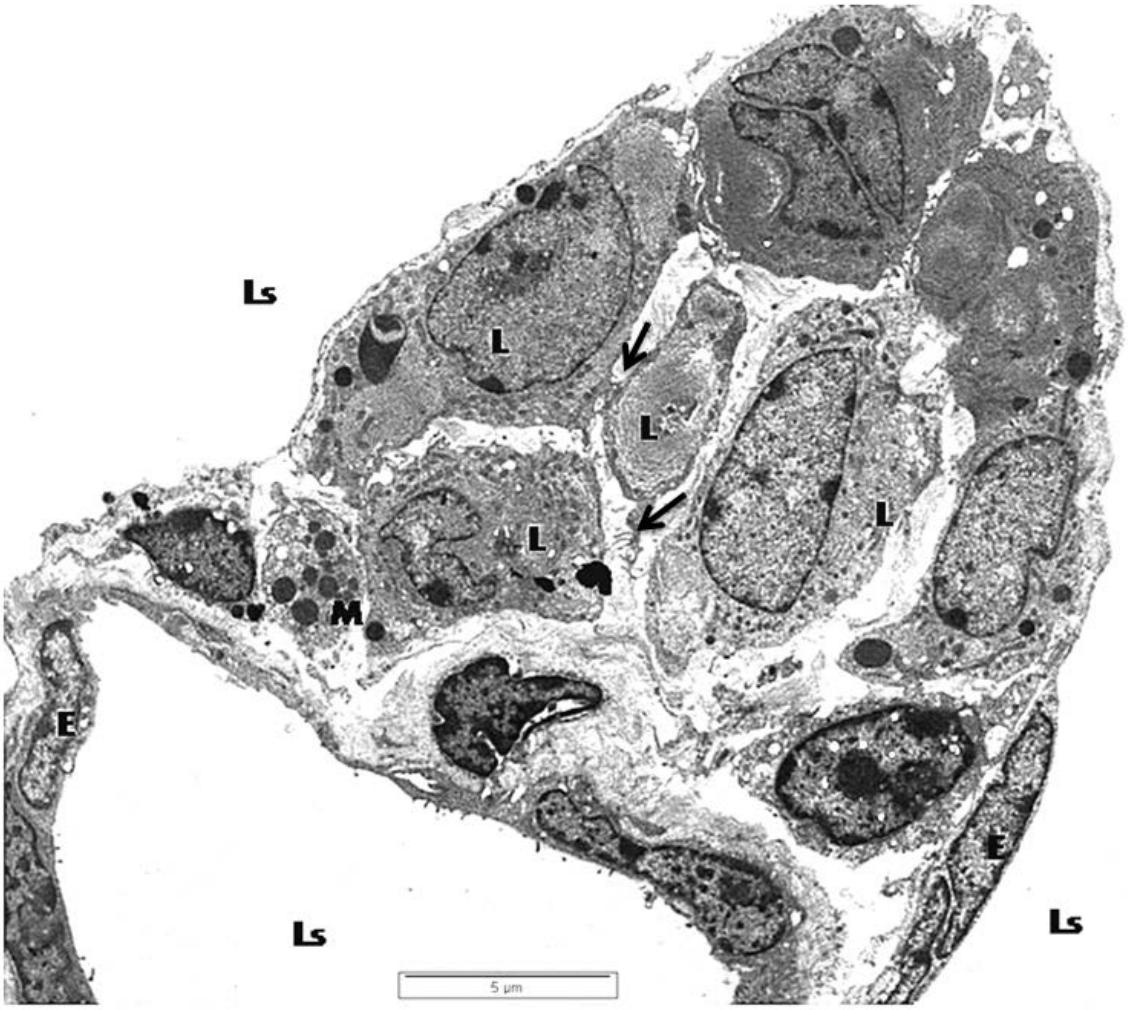

Figure 12a: Electron micrograph of the interstitium between the seminiferous tubules in the testis of the greater cane rat showing the Leydig cells (L) arranged in clusters with their processes (arrows), the lymphoid sinusoids (Ls) around and within the interstitium, macrophage (M) and lymphatic epithelial cells (E). Picture taken with Phillips CM10 TEM at 80 KV. Mag. X 30,000, **Scale bar = 5µm**.

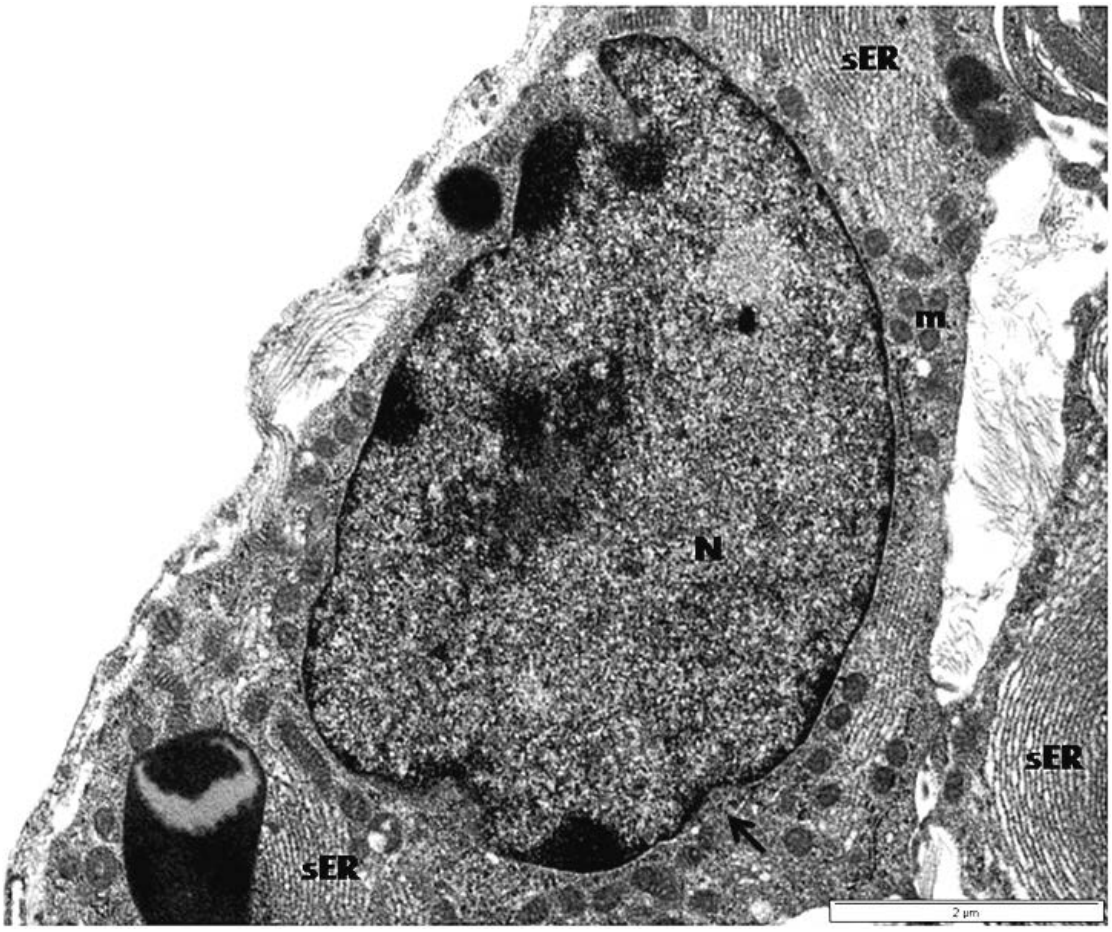

Figure 12b: Electron micrograph of the Leydig cell in the testicular interstitium of the greater cane rat. Note the indented nucleus (N), abundant mitochondria (m), parallel lamellae of smooth endoplasmic reticulum (sER) and flatten rough endoplasmic reticulum (arrow). Picture taken with Phillips CM10 TEM at 80 KV. Mag. X 30,000, **Scale bar = 2µm**.

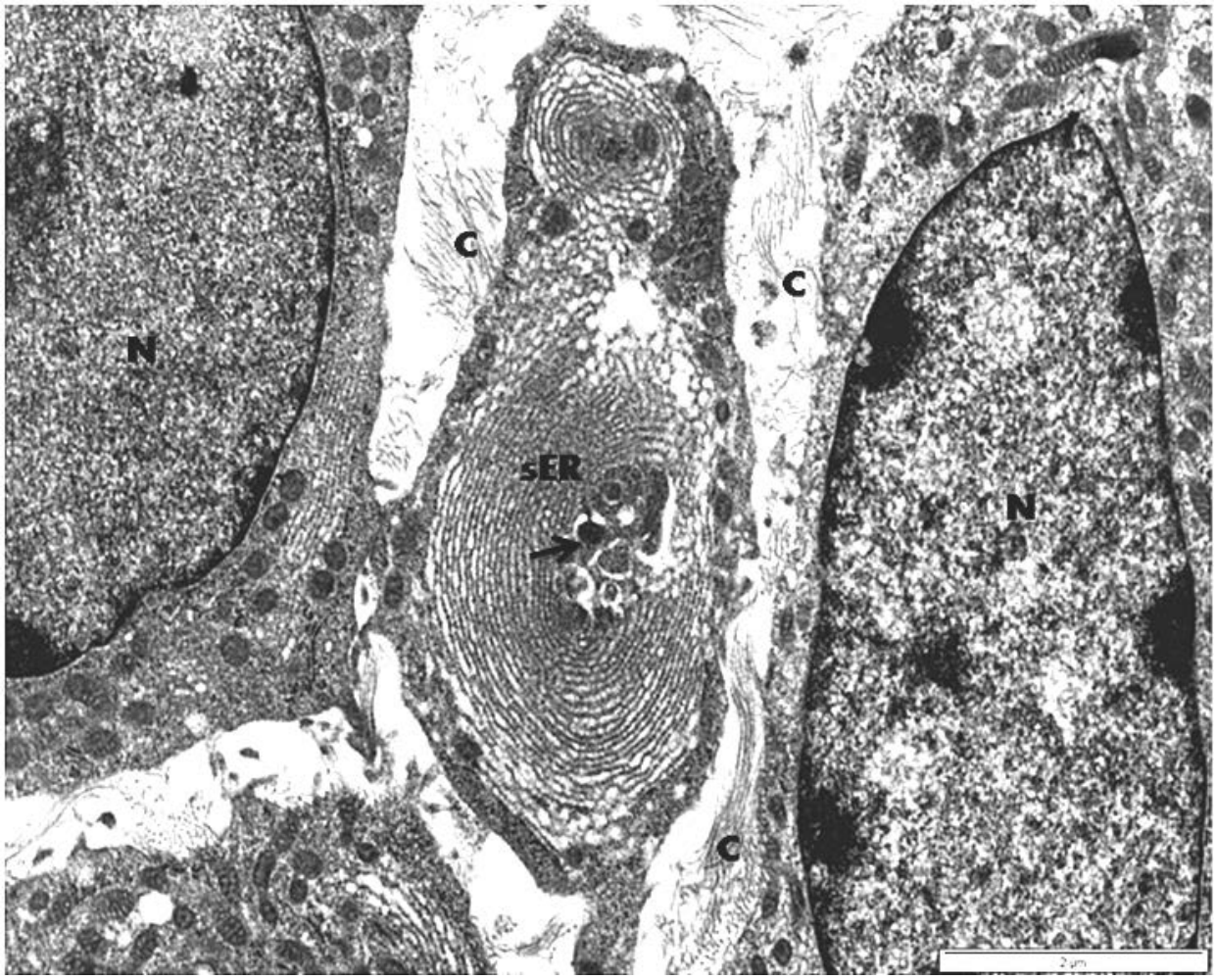

Figure 12c: Electron micrograph of the Leydig cell in the testicular interstitium showing the dense network or whorls of smooth endoplasmic reticulum (sER) with the closely associated peroxisomes (arrow) and the abundant extracellular collagen fibrils (C). (N) is the cell nucleus. Picture taken with Phillips CM10 TEM at 80 KV. Mag. X 30,000, **Scale bar = 2µm**.

3.2.1.6 *Cycle of the Seminiferous Epithelium*

In staging the seminiferous epithelium cycle in the greater cane rat, the higher resolution of the Toluidine-blue stained sections was combined with the electron microscopy of the spermatogenic cells. Based on the morphogenesis of the acrosomic system and degree of elongation and condensation of the head of the differentiating spermatids, there are nine (9) stages of the seminiferous epithelium in the cane rat. Each stage is characterized by different generations of germ cells, from spermatogonia to spermatids, arranged in a defined cellular association.

Stage 1: At this stage, there are A-type spermatogonia, pachytene spermatocytes, round and elongated spermatids in the epithelium. The newly formed spermatids have no distinct Golgi zone but display round nuclei with irregular patches of chromatin. The step 11 elongated spermatids present at this stage have central intranuclear vacuoles (Fig. 13a).

Stage 2: This stage has both A-type and In-type spermatogonia. Pachytene spermatocytes are also present. The nuclei of the round spermatids show acrosomal vesicle with proacrosomal granules as well as dense clumps of chromatin. The step 11 elongated spermatids complete the cellular association (Fig. 13b).

Stage 3: In this stage, the acrosomal vesicle starts to flatten on the nuclear surface of the round spermatid. Step 12 elongated spermatids present begin to move to the luminal aspect of the seminiferous epithelium to line the tubular lumen. Pachytene spermatocytes, intermediate and B spermatogonia are present (Fig. 13c).

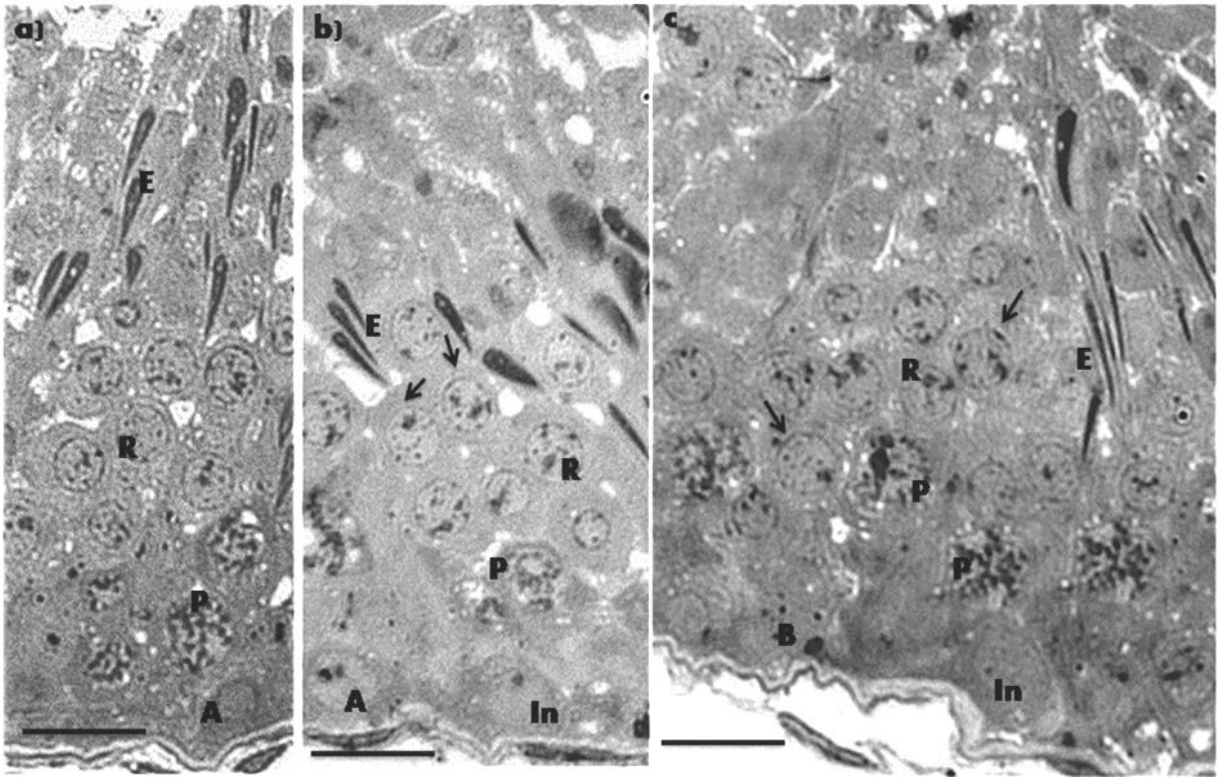

Figure 13a,b&c: Photomicrographs of stages 1, 2& 3 of the seminiferous epithelium cycle in the greater cane rat. **Fig. (a) Stage 1:** Presence of step 11-elongated (E) and step 1-round (R) spermatids; pachytene spermatocyte (P) and A-type spermatogonia. **Fig. (b) Stage 2:** Note the presence of acrosomal vesicle (arrow) on the round spermatids (R) and the presence of intermediate-type spermatogonia (In). **Fig. (c) Stage 3:** Presence of step 12 elongated spermatids (E) and the flattening of the acrosome on the round spermatid nuclei (arrows) as well as appearance of B-type spermatogonia (B) occurring together with In-type spermatogonia. **Toluidine blue,** Mag. X1000. **Scale bar = 10µm**.

Stage 4: In this stage, the acrosomal vesicle continues to flatten on the nuclear surface of the round spermatids with the absence of the elongated spermatids. Preleptotene and pachytene spermatocytes accompany the round spermatids followed by the B spermatogonia (Fig. 13d).

Stage 5: At stage 5, the spermatids nuclei appear round or oval with the prominence of acrosome over the nuclear surface. Elongated spermatids are also absent at this stage. Also present in the seminiferous epithelium at this stage are basally placed Leptotene spermatocytes with pachytene spermatocytes above them (Fig. 13e).

Stage 6: This stage is characterized by round spermatids in step 6 with the cap over the nuclei growing further in size and expanding laterally. The acrosomes are all beginning to be oriented toward the base of the seminiferous tubule. Leptotene and pachytene spermatocytes accompany the spermatids. Also present are residual bodies from the already spermiated step 12 spermatids (Fig. 13f).

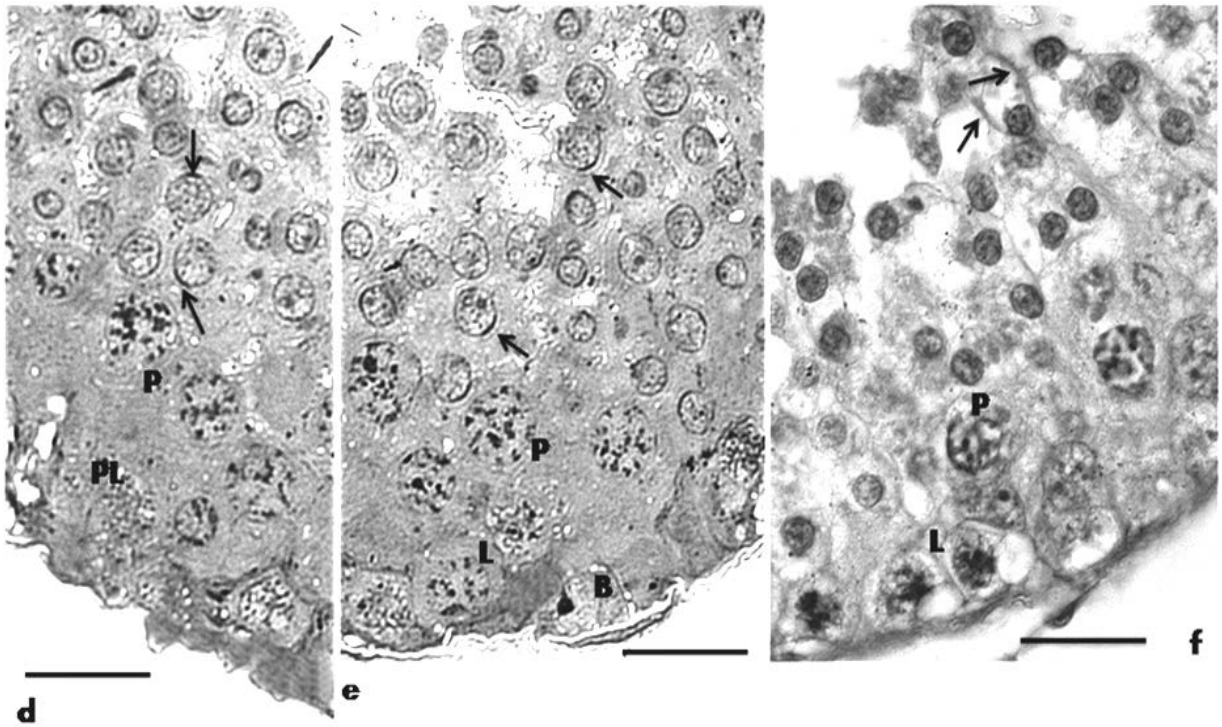

Figure 13d, e & f: Photomicrographs of stages 4, 5& 6 of the seminiferous epithelium cycle in the greater cane rat. **Fig. (d) Stage 4:** The flattening of the acrosome on the round spermatid nuclei (arrows) continues and Preleptotene spermatocyte (PL) appears together with pachytene spermatocyte (P) and B spermatogonia. **Fig. (e) Stage 5:** Note the spreading of acrosomal vesicle on the round spermatids (arrow) and the leptotene spermatocyte (L) and pachytene (P) and B-spermatogonium. **Fig. (f) Stage 6:** The nucleus of the round spermatids are beginning to condense. There are residual bodies of spermiated step 12 spermatids (arrow). **Toluidine blue,** Mag. X1000. **Scale bar = 10µm**.

Stage 7: This stage is characterized by the seventh step spermatids in which the nuclear elongation and condensation continued with the acrosomes completely oriented towards the base of the tubules. Distinct bilateral flattening of the nucleus can be observed. Pachytene and zygotene spermatocytes can be found with the zygotene closer to the tubular base. B spermatogonia persist at this stage (Fig. 13g)

Stage 8: This stage is characterized with step 8 to 9 spermatids with increasing elongation and condensation of the spermatid head. The pachytene spermatocytes at this stage also advance to become diplotene spermatocytes while there was increase in the number of zygotene spermatocytes (Fig. 13h).

Stage 9: There are step-10 elongated spermatids at this stage. The diplotene spermatocytes develop into secondary spermatocytes that form the new generation of round spermatids seen at this stage. A-type spermatogonia are present at this stage (Fig. 13i).

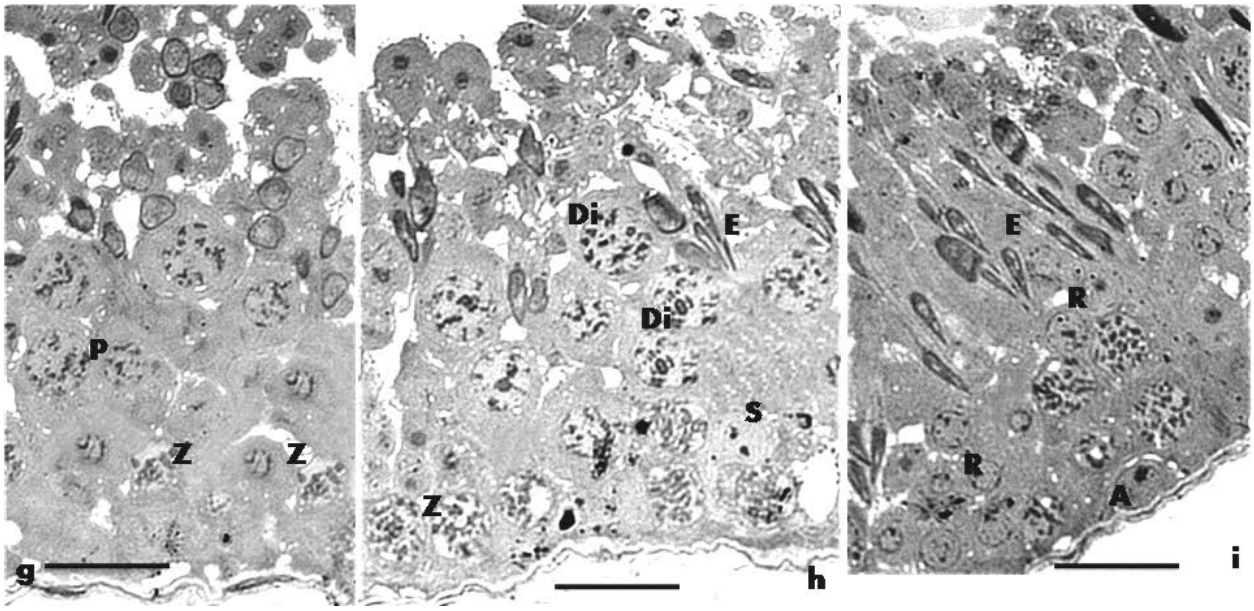

Figure 13g, h&i: Photomicrographs of stages 7, 8& 9 of the seminiferous epithelium cycle in the greater cane rat. **Fig. (g) Stage 7:** Elongation and condensation of round spermatid nuclei continues and leptotene spermatocytes become zygotene (Z) with pachytene spermatocyte (P) still present. **Fig. (h) Stage 8:** Consist 8 to 9-step spermatids (E) and diplotene spermatocyte (Di) while zygotene persists. Sertoli cell (S) can be seen. **Fig. (i) Stage 9:** Step 10 spermatids are present while the new round spermatids (R) begin to develop from secondary spermatocyte. A-type spermatogonia are present. **Toluidine blue,** Mag. X1000. **Scale bar = 10µm**.

3.2.2. EFFERENT DUCT

3.2.2. 1. Morphometry

Table 1: Histometric values of the three segments of Efferent duct in the greater cane rat.

	Tubular Diameter (µm)	Epithelial height (µm)
Proximal Efferent Duct	82.1 ±13.1	20.6 ±2.7
Middle Efferent Duct	107.2 ±11.9	18.1 ±1.7
Distal Efferent Duct	124.4 ±14.5	14.5 ±2.5

3.2.2.2. Gross Appearance

In the greater cane rat, the efferent ducts emerge from the rete channels at the craniomedial aspect of the testes. About six efferent ductules initially run relatively straight courses from the rete and then become wavy and highly convoluted as they approach the epididymis. Each duct subsequently opens individually into the initial segment of the epididymis in a pattern that can be schematically represented below (Fig. 14).

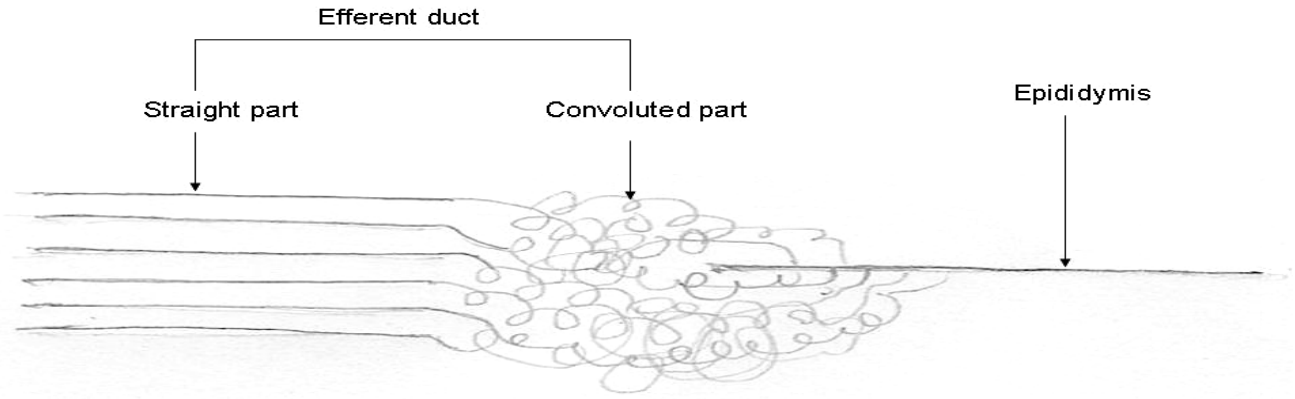

Figure 14: Schematic diagram to represent the pattern of arrangement of how the efferent ducts attach to the epididymis. Note the high convolution of the efferent ducts before attaching to the epididymis at multiple points.

3.2.2.3. Histological Appearance

The efferent duct in the greater cane rat is lined by simple columnar epithelium made up of both ciliated and non ciliated cell types. Three different segments with varying epithelial heights and ciliated to non ciliated cell ratio were observed along the length of the duct (Fig. 15).

The proximal segment, which connects directly to the rete testis, has epithelial height of 20.6 ±2.7µm and tubular diameter of 82.1 ±13.1µm (Table 1) with uneven luminal outline (Fig. 15a). There were relatively more non-ciliated cells than the ciliated cells in this segment (Fig 15b). The non-ciliated cells had oval nuclei located close to the base of the cells while the ciliated cells beared both microvilli and cilia The elongated nuclei of the ciliated cells were generally more towards the apical region of the cell and heterochromatic than those of the non ciliated cells (Fig. 15b). At higher magnification, few vacuoles were observed at the supranuclear region of non-ciliated cells (Fig. 15c)

In the middle efferent duct, the epithelial height was 18.1 ± 1.7µm and the tubular diameter was 107.2 ± 11.9µm. There was an increase in the number of non-ciliated cells relative to ciliated cells. While the ciliated cells are similar to that in the proximal part, the non-ciliated cells in this region showed increase in the size and number of the supranuclear vacuoles (Fig. 16). In addition aggregate of dense granules were also present at the subapical region of the cells (Fig. 16).

The distal efferent ducts, with the epithelial height of 14.5 ± 2.5µm (Table 1) and tubular diameter of 124.4 ± 14.5µm, were predominantly compose of numerous ciliated cells with few non-ciliated cells (Fig. 17). The characteristics of the ciliated cells in this segment were similar to that in the previous segments. However, the non-ciliated cells of this segment had few dense granules and vacuoles in their cytoplasm (Fig. 17).

Figure 15a: Photomicrograph of the proximal efferent duct in the greater cane rat showing the uneven outline of the ducts (D) and the surrounding connective tissues (Ct). **H&E,** Mag. X100. **Scale bar = 50µm**.

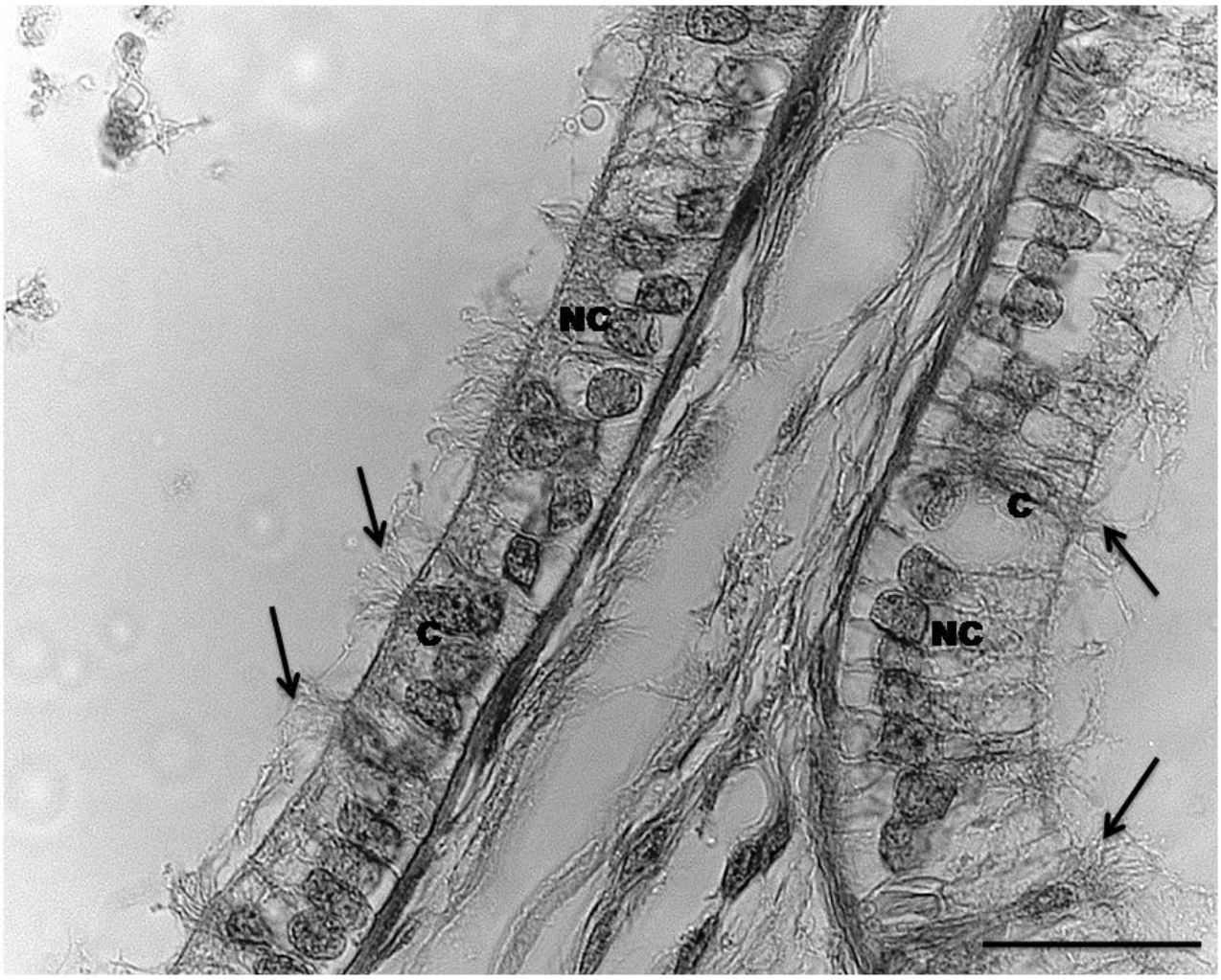

Figure 15b: Photomicrograph of the proximal efferent duct in the greater cane rat showing the ciliated (C) and the non-ciliated cells. The arrows indicate the cilia on the ciliated cells (C). **H&E on grayscale,** Mag. X1000. **Scale bar = 50µm**

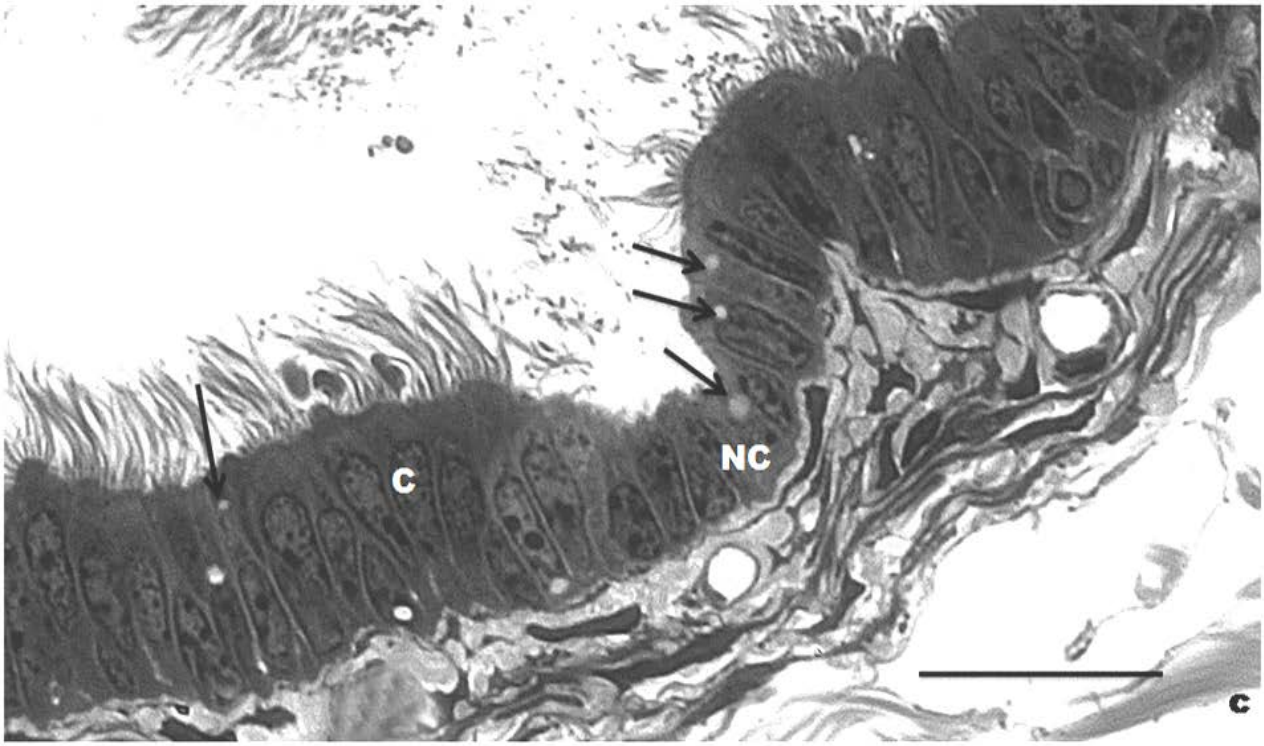

Figure 15c: Photomicrograph of the proximal efferent duct in the greater cane rat at higher magnification showing the supranuclear vacuoles (arrows) in the non- ciliated cells (NC). C is the ciliated cell. **Toluidine blue on grayscale,** Mag. X1000. **Scale bar = 20µm**

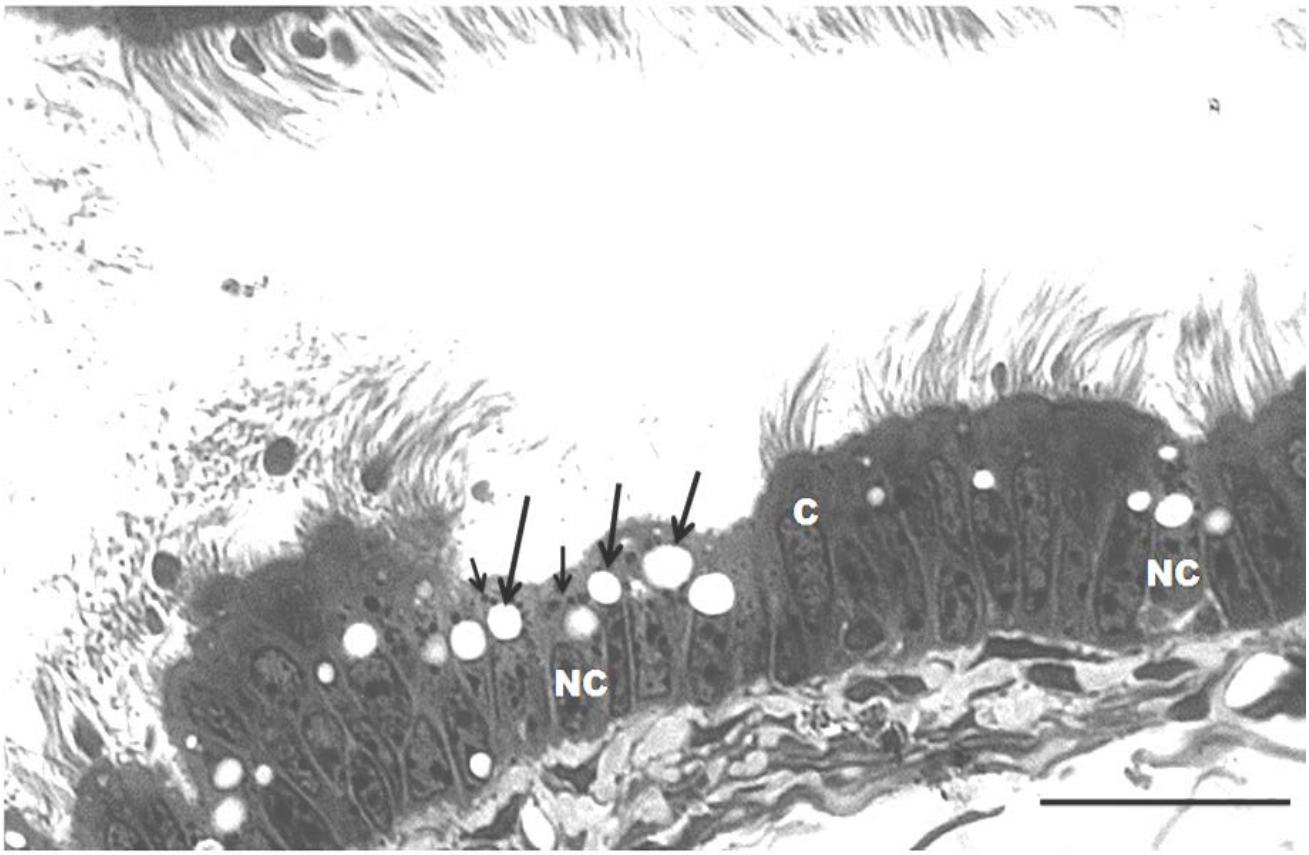

Figure 16: Photomicrograph of the middle efferent duct in the greater cane rat at higher magnification. Note the increase in the size and number of the supranuclear vacuoles (long arrows) as well as the aggregate of dense bodies (short arrows) in the non- ciliated cells (NC). C is the ciliated cell. **Toluidine blue on grayscale,** Mag. X1000. **Scale bar = 20µm**

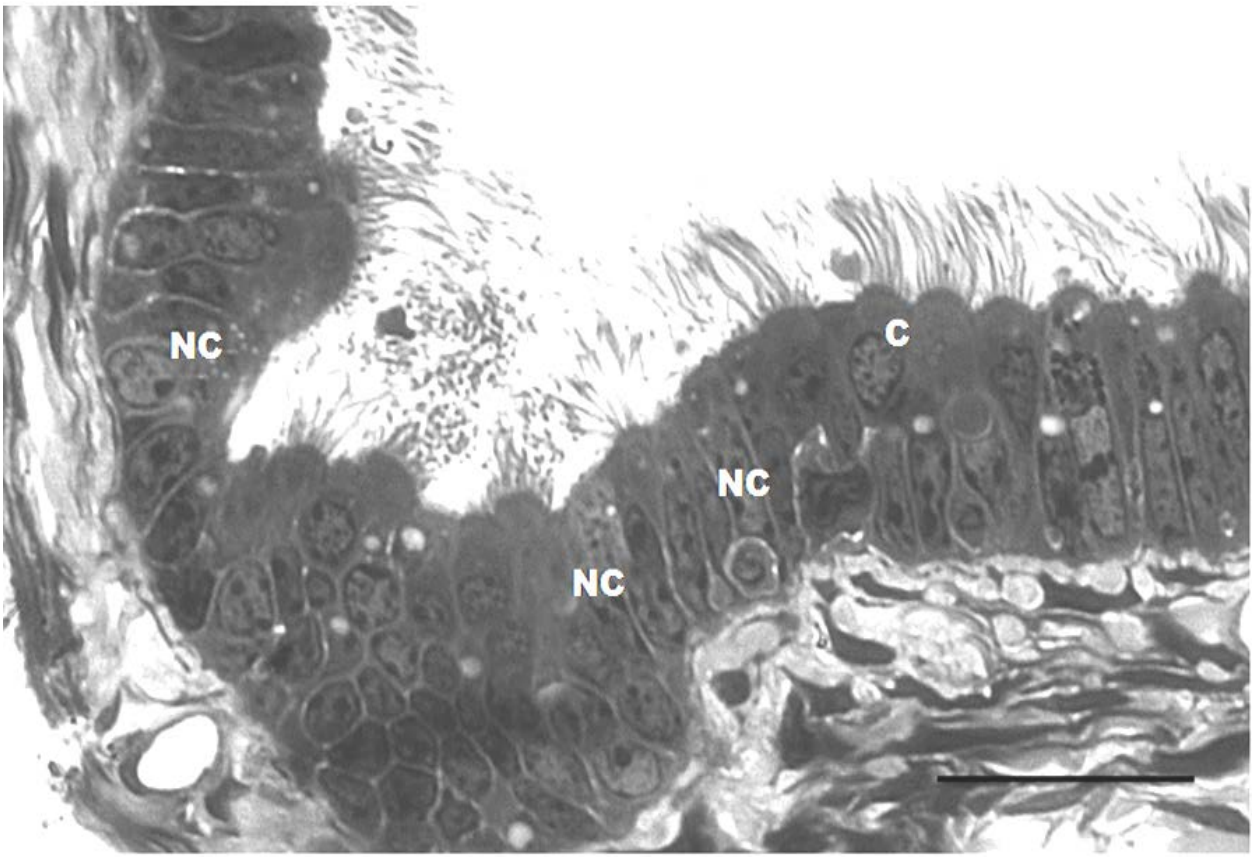

Figure 17: Photomicrograph of the distal efferent duct in the greater cane rat at higher magnification. Note the increase in the number of ciliated cells (C) relative to the non- ciliated cells (NC). **Toluidine blue grayscale,** Mag. X1000. **Scale bar = 20µm**

3.2.3 EPIDIDYMIS

3.2.3.1 Morphometry of Epididymis

***Table 2*:** The gross morphometric values of the epididymis in the greater cane rat.

	Body weight (g)	Epididymal weight (g)	Epididymal length (cm)	Epididymal volume (cm^3)
Mean	2490	0.33	2.69	0.38
Standard deviation	±0.24	±0.02	±0.68	±0.02

***P*=0.05**

***Table 3*:** The histometric values of the four epididymal segments in the greater cane rat.

	Tubular Diameter (µm)	Epithelial height (µm)	Epithelial height : Tubular diameter ratio
Initial Segment	214.34 ±17.27	58.10 ±5.68	3.7
Caput epididymis	229.18 ±17.88	47.62 ±5.98	4.8
Corpus epididymis	246.85 ±16.33	38.12 ±7.38	6.7
Cauda epididymis	500.11 ±105.27	17.01 ±1.41	29.4

***P*= 0.05**

The morphometric analysis showed that the epididymal weight was low relative to the body weight in the greater cane rat (Table 2). The epithelial height and the tubular diameter which combined the muscular thickness and luminal diameter vary along the different regions of the epididymis. While the difference in the ratio of tubular diameter : epithelial height was not so remarkable in the initial segment, caput and corpus, it was in the corpus and the cauda epididymis. These indicate a gradual decrease in epithelial heights from initial segment to the corpus but a sharp fall between the corpus and cauda (Table 3).

3.2.3.2 Gross Appearance

The epididymis in the greater cane rat was 2.69 ±0.68cm long. It is a highly coiled duct that extends from the efferent duct to the deferent duct (Fig. 18). The inverted S-shaped duct has average weight of 0.33 ±0.02g and average volume of 0.38 ±0.02ml. It is loosely attached to the medial border of the testes by a thin but well vascularised mesorchium. Grossly, two distinct segments can be identified namely – the cranial and the caudal parts (Fig. 18A).

The pinkish coloured cranial part that communicates directly with the efferent duct comprises of the initial segment, the caput and the corpus epididymis. This part is about two-third of the entire epididymal length and extends to about one-third of the length of the testes. It has relatively higher degree of the convolution and vasculature than the caudal part (Fig. 18b). The cream-coloured caudal part which corresponds to the cauda epididymis is relatively less convoluted, wider and lighter in colour. The degree of convolution gradually decreases towards the distal end of the caudal part as the coiled epididymal duct straightens out and continues as the deferent duct (Fig. 18b). The cauda epididymis does not extend to the caudal pole of the testis in the cane rat.

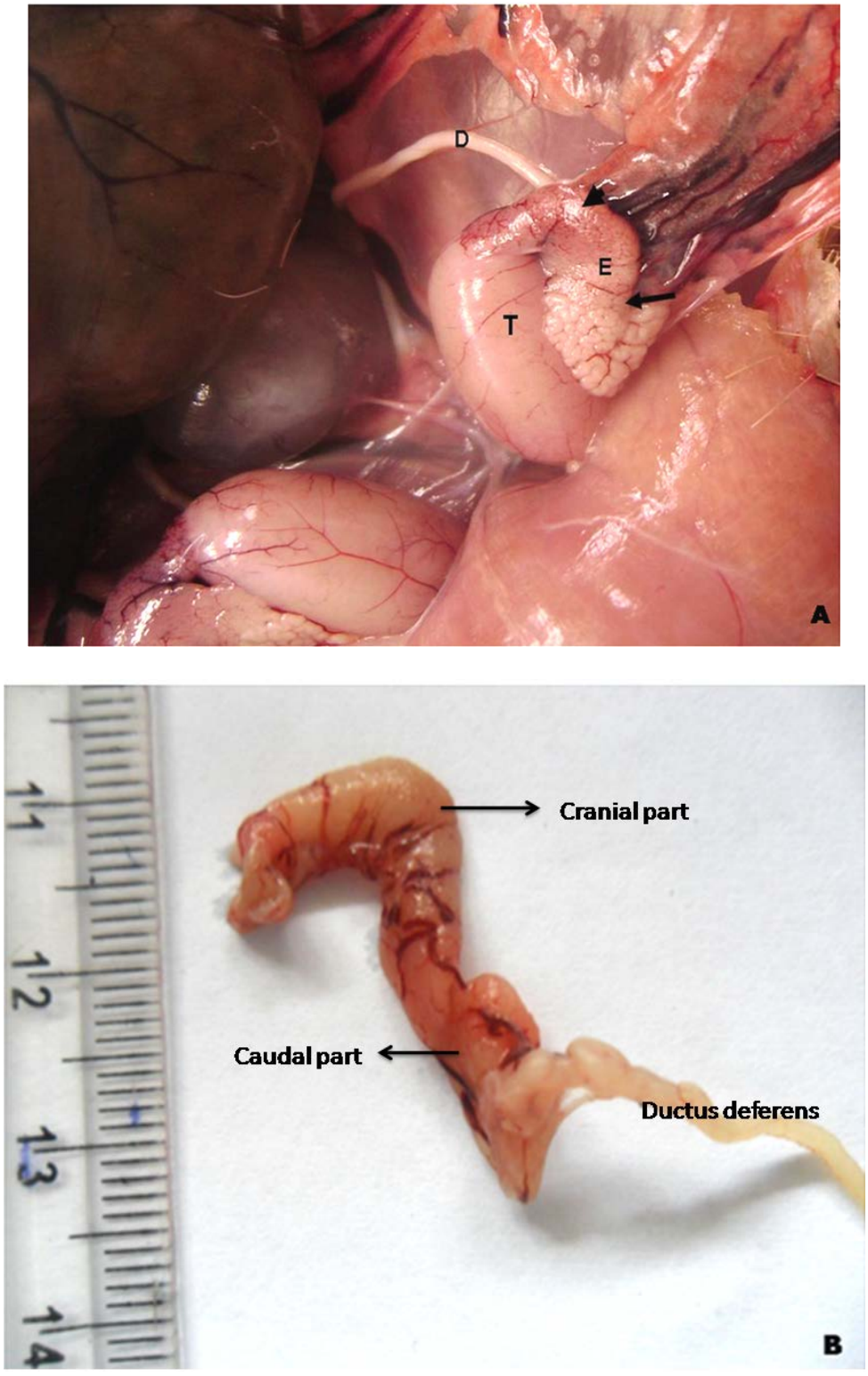

Figure 18: Photograph of epididymis of the greater cane rat. In (**A**) Note the cranial part (arrow head) and the caudal part (arrow). The inverted S-shaped epididymis is loosely attached to the testis (T), while the cauda epididymis continues as the deferent duct (D). (**B**) is the isolated epididymis

3.2.3.3 Histological Appearance

The cross sectional profile of the epididymal duct showed a round outline lined by pseudostratified columnar epithelium, surrounded by connective tissue lamina, circular smooth muscle fibres, the number of which increases progressively towards the cauda epididymis and embedded in loose connective tissue stroma (Fig. 19).

Based on the epithelial cell types, epithelial height, tubular diameter and luminal shapes, the epididymis of the greater cane rat has been divided into four regions – initial segment, caput, corpus and cauda epididymides. These regions are further subdivided into discrete intraregional zones on the basis of the differences in cytological characteristics of the epithelial cells in each region. Transition between regions was however observed to be gradual with overlapping of morphological characteristics between two adjacent regions.

Region 1 – Initial Segment

The luminal shape of this region was stellate with tubular diameter of 214.34 ±17.27µm and epithelial height of 58.10 ±5.68µm (Table 3). The epithelial lining is composed mainly of tall principal cells and basal cells as well as apical and narrow cells (Fig. 20a).

This segment shows three zones – proximal initial segment (PIS), middle initial segment (MIS) and distal initial segment (DIS) with each zone differing in the structural and ultrastructural features as well as the amount of the narrow and apical cells relative to the principal and basal cells. The zones are separated by connective tissue septae (Fig. 20b).

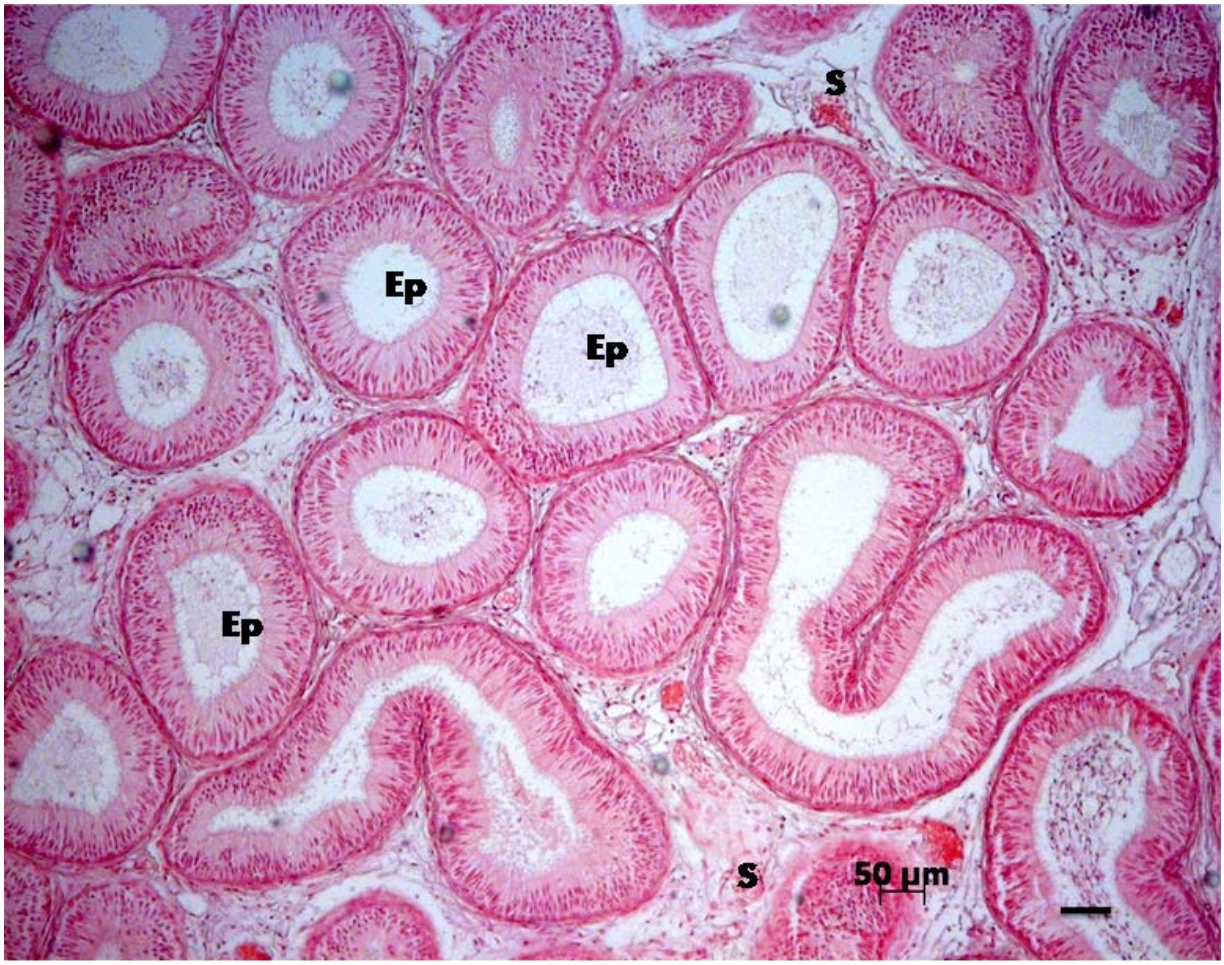

Figure 19: Photomicrograph of epididymal cross section in the greater cane rat. Note the circularly outlined epididymal ducts (Ep) embedded in connective tissue stroma (S). **H&E,** Mag. X400. **Scale bar = 50µm**.

Figure 20a: Photomicrograph of the initial segment of epididymis in the greater cane rat showing the pseudostratified epithelium with the principal (P) and basal (BC) cells. Note the stellate outlined lumen (L) and the stroma (S). **H&E,** Mag. X400. **Scale bar = 50µm**.

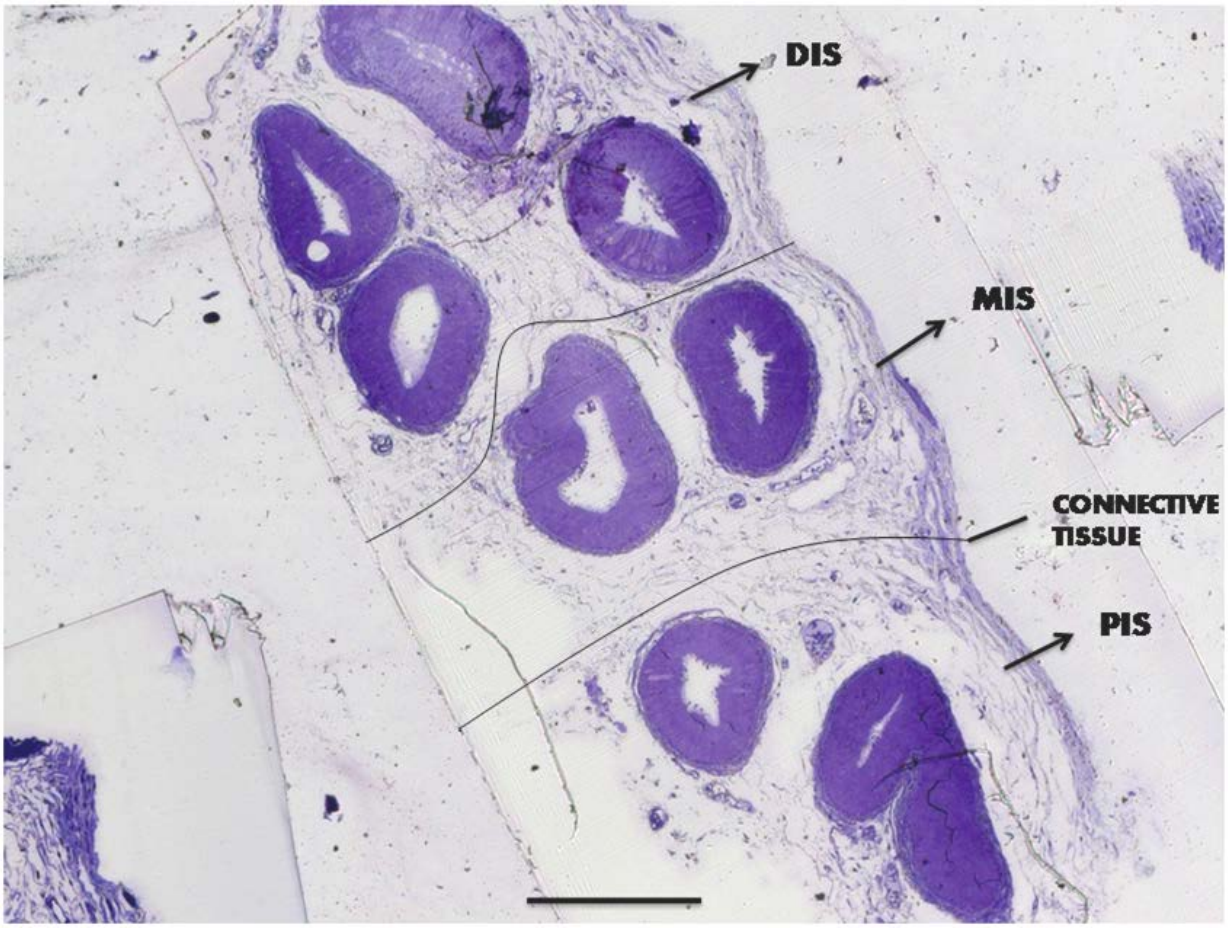

Figure 20b: Photomicrograph of the three zones; proximal initial segment (PIS), middle initial segment (MIS) and distal initial segment (DIS) of the initial segment of the epididymis in the greater cane rat each separated by connective tissue septae. **Toluidine blue,** Mag. X100. **Scale bar = 50µm**.

Histologically, the epithelium of PIS has predominantly principal cells and basal cells with little or no narrow and apical cells – less than 1% (Fig. 20c). The principal cells extend from the basal lamina to the tubular lumen and have oval, basally located nuclei with prominent nucleoli. Their apical surfaces are covered by microvilli. The basal cells are small and numerous with irregularly shaped nuclei. The apical and narrow cells are wedged in between the principal cells. While the nucleus of the apical cell was located at the basal half, that of the narrow cell was in the apical end of the cell (Fig 20c).

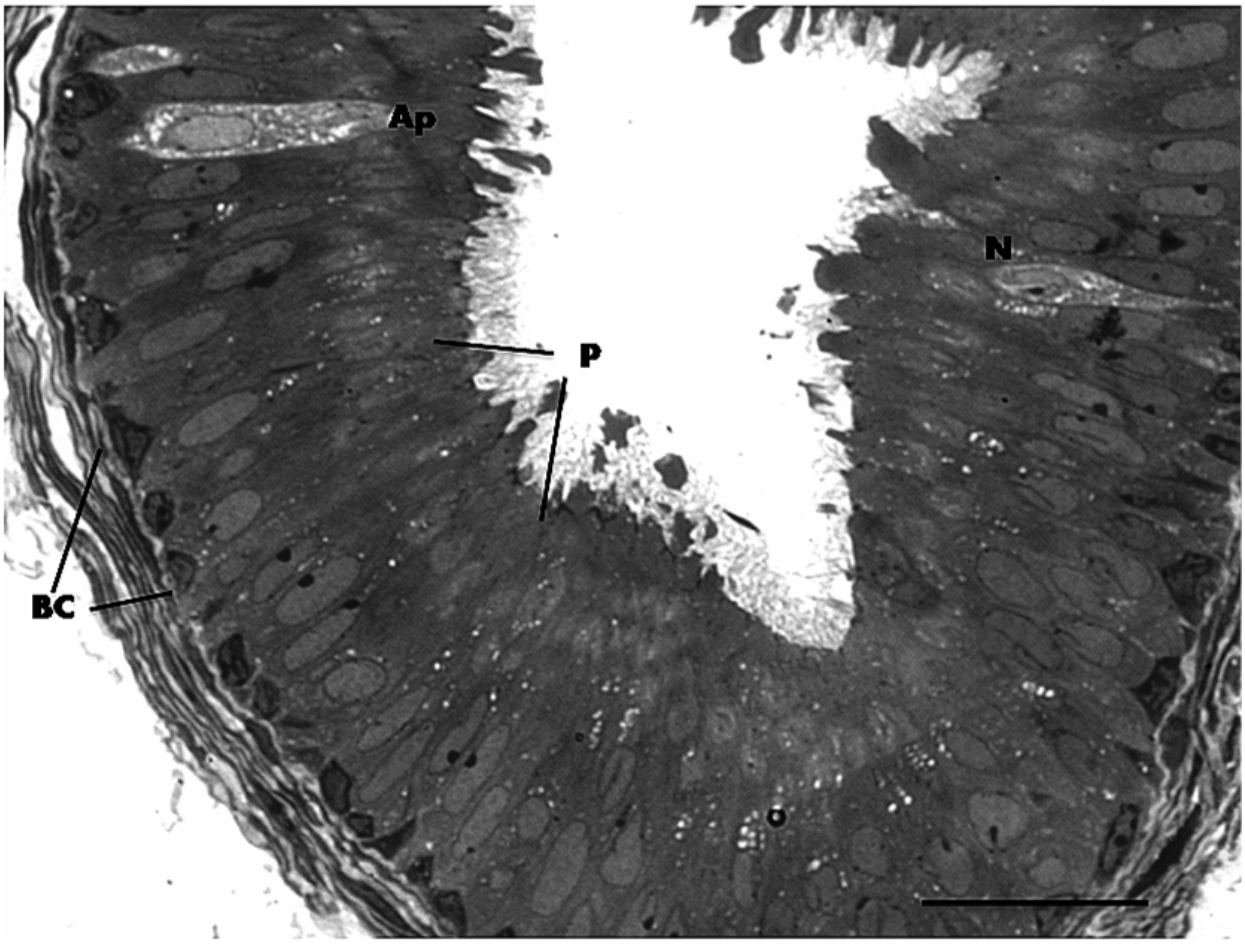

Figure 20c: Photomicrograph of the epithelium of proximal initial segment (PIS) of the epididymis in the greater cane rat. Note the few apical (Ap) and narrow (N) cells wedged in between the principal cells (P) with the basal cells (BC) attached to the epithelial basement membrane. **Toluidine blue,** Mag. X1000. **Scale bar = 20µm**.

The ultrastructure of the principal cell in the PIS revealed characteristic presence of abundant rough endoplasmic reticulum and extensive Golgi apparatus arranged in a peculiar whorl shape predominantly in the apical cytoplasm (Fig. 20d) with small vesicles, dense granules and multivesicular bodies scattered in and around the whorls. While the inner Golgi cisternae are dilated with pale materials, the outer cisternae are flat and surrounded by endoplasmic reticulum (Fig. 20e). Large sized multivesicular bodies were seen at the supranuclear area below the whorl (Fig. 20e). Some of the cells have branched and irregular shaped microvilli on their apical surfaces, while others have apical blebs. Small vacuoles were however present at either the subapical cytoplasm or blebs of the cells (Fig 20d&e). Numerous mitochondria, some of which appear in clumps were seen scattered more at the apical cytoplasm. Tight junctional complexes hold the apical ends of the cells together (Fig. 20e). The euchromatic nuclei of the principal cells are indented and contained multiple nucleoli (Fig. 20d). The infranuclear cytoplasm contained cisternae of rough endoplasmic reticulum and some round-to-rod shaped mitochondria (Fig. 20f). The fine structure of the basal cells in PIS showed well indented nucleus that is surrounded by cytoplasm which encloses mitochondria, few cisternae of endoplasmic reticulum and some vesicles (Fig. 20f)

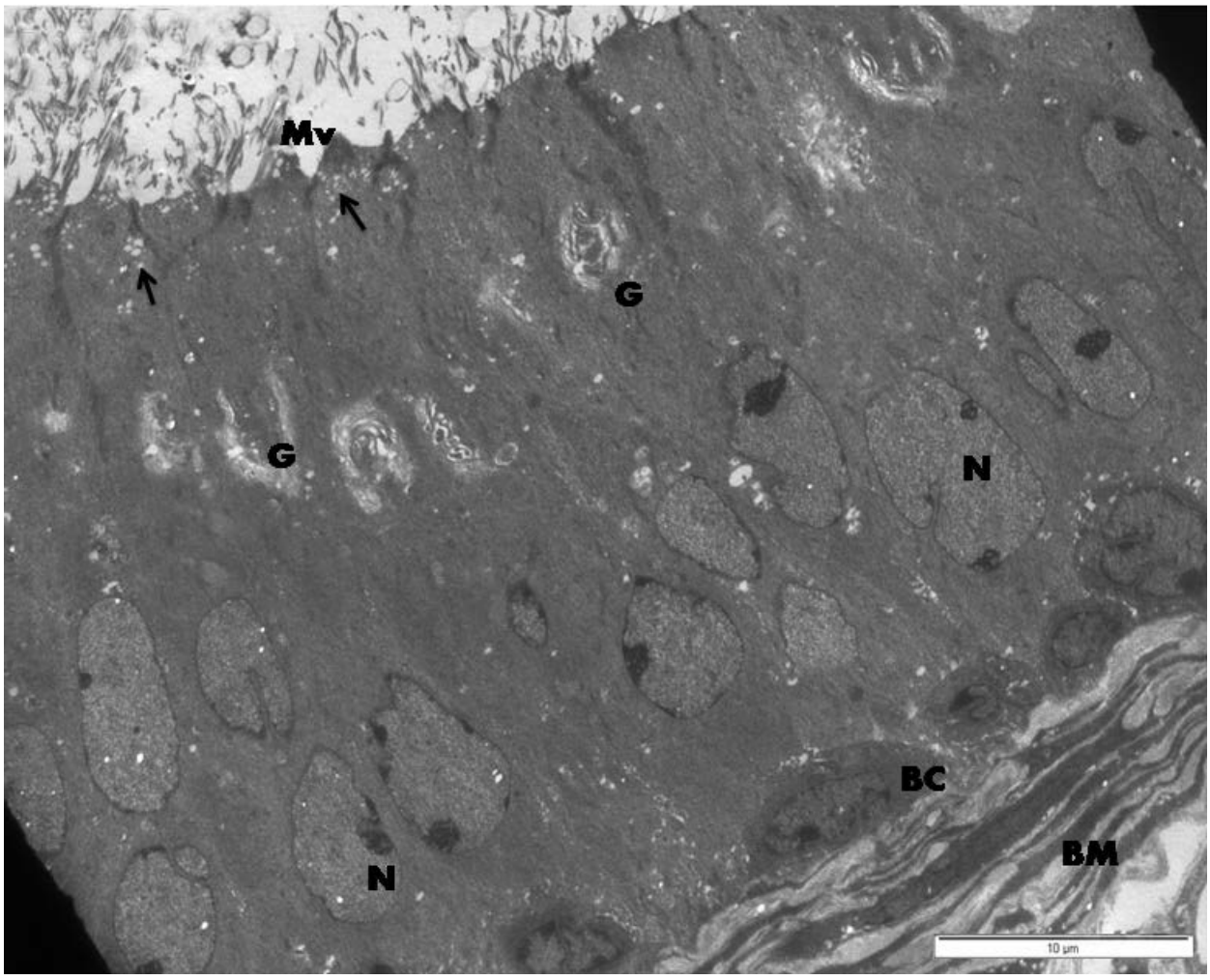

Figure 20d: Ultrastructure of the epithelium of proximal initial segment (PIS) of the epididymis in the greater cane rat. Note the presence of microvilli (Mv), prominent Golgi complexes (G), subapical vacuoles (arrows) and euchromatic nucleus (N) in the principal cell. The basal cells (BC) are anchored to the basement membrane (BM). Picture taken with Phillips CM10 TEM at 80 KV. Mag. X 12,000, **Scale bar = 10µm**.

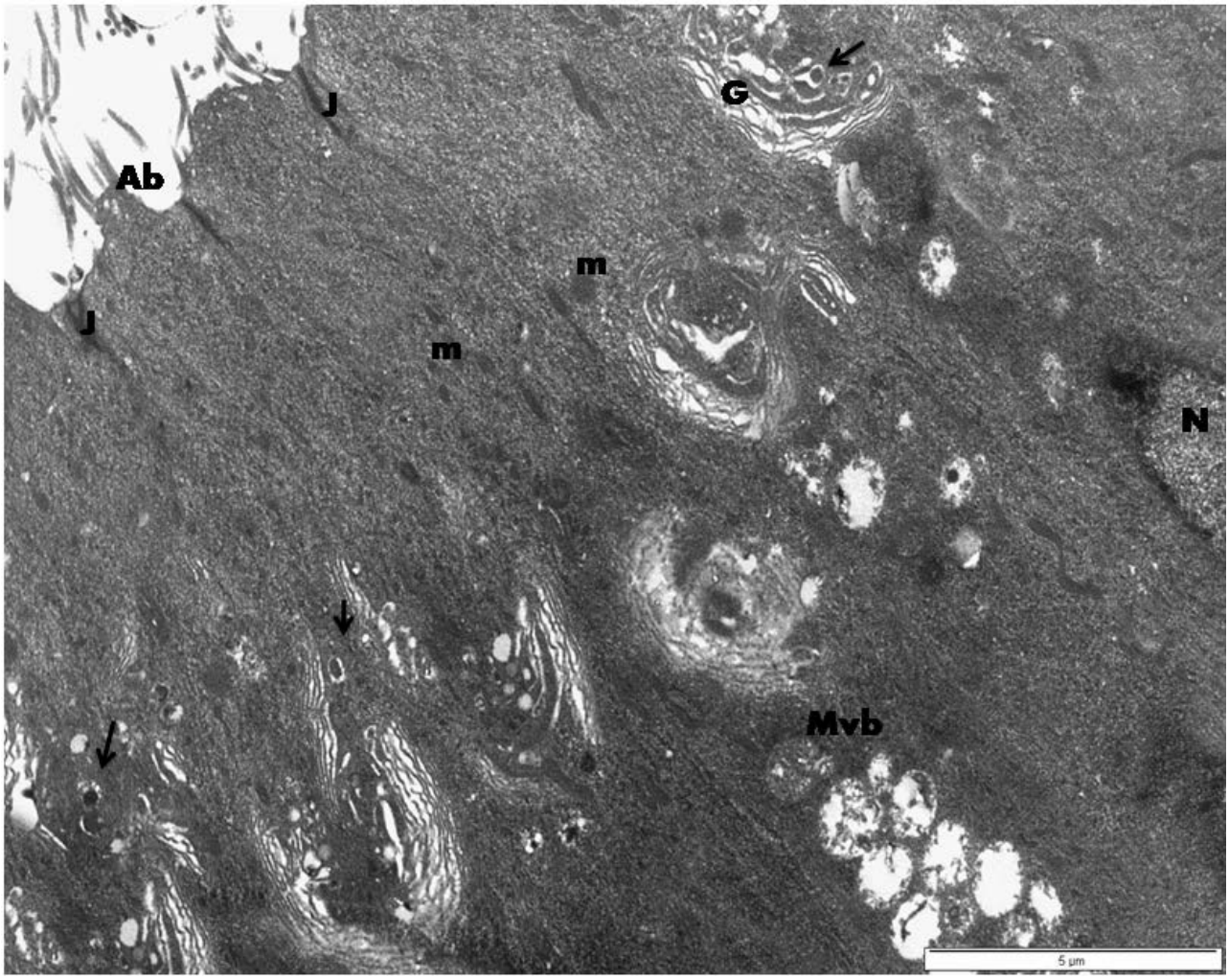

Figure 20e: Ultrastructure of the apical part of the principal cells of the proximal initial segment (PIS) of the epididymis of the greater cane rat. Note the apical bleb (Ab), tight junctional complexes (J), dilated cisternae of Golgi complexes (G) with small coated vesicles and dense granules (arrows) emanating from it, abundant mitochondria (m) of various shapes and presence of multivesicular bodies (Mvb) as well as euchromatic nucleus (N) of the principal cell. Picture taken with Phillips CM10 TEM at 80 KV. Mag. X 15,000, **Scale bar = 5µm**.

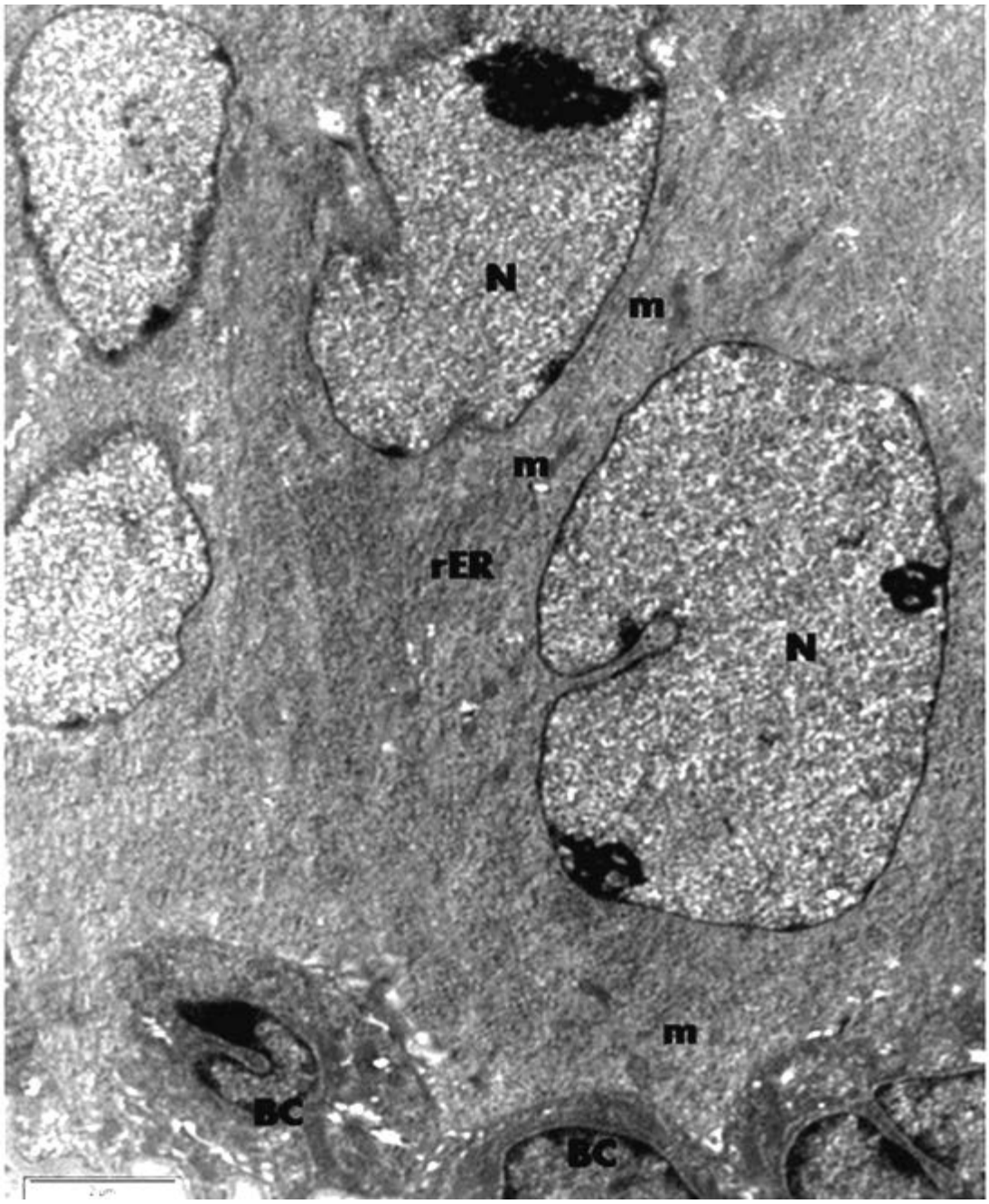

Figure 20f: Ultrastructure of the basal part of principal cells of proximal initial segment (PIS) of epididymis in the greater cane rat showing cisternae of rough endoplasmic reticulum (rER) and mitochondria (m). The basal cells (BC) with its indented nucleus and few organelles were also shown. Picture taken with Phillips CM10 TEM at 80 KV. Mag. X 20,000, **Scale bar = 2µm**.

The middle initial segment (MIS) showed an increase in the number of apical and narrow cells with the structural appearance of the principal and the basal cells being similar to that in the PIS. The apical and narrow cells stain lighter than the principal cells and display apical blebs, highly indented nucleus and a lot of secretory vacuoles (Fig. 20g). The apical cell which is more in number in this zone has a wide apical portion and a narrow stem that extend to the basal lamina. The nucleus is often seen at the basal half of the cell (Fig 20g).

Ultrastructurally, the principal cell in this zone is similar to that in PIS but the apical cell is characterized by the presence of blebs rather that microvilli on the luminal surface. The prominent feature of the apical cell is the presence of vacuoles of various sizes in both the apical and basal cytoplasm as well as the abundance of dense bodies, mitochondria and lysosomes (Fig 20h&i). While the supranuclear area contains dilated cisternae of Golgi complex, rough endoplasmic reticulum and endocytic vesicles, all surrounded by moderate-sized vacuoles, the infranuclear area has large vacuoles surrounded by mitochondria. The heterochromatic nucleus is highly indented (Fig 20i).

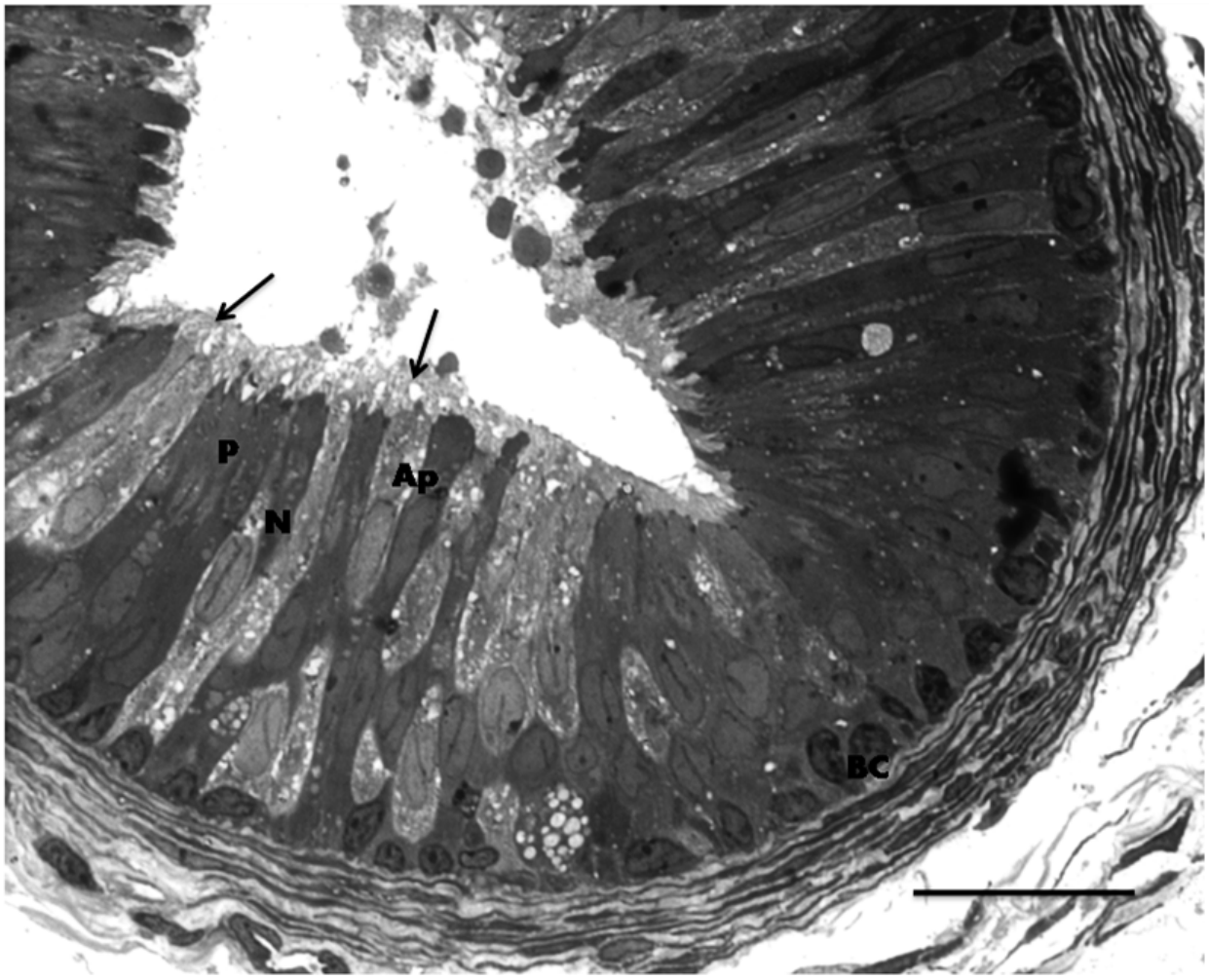

Figure 20g: Photomicrograph of the epithelium of middle initial segment (MIS) of the epididymis of the greater cane rat. Note the increase in the number of apical (Ap) and narrow (N) cells wedged in-between principal cells (P). Secretory blebs from these cells are also shown with the basal cells (BC) abutting the epithelial basement membrane. **Toluidine blue,** Mag. X1000. **Scale bar = 20µm**.

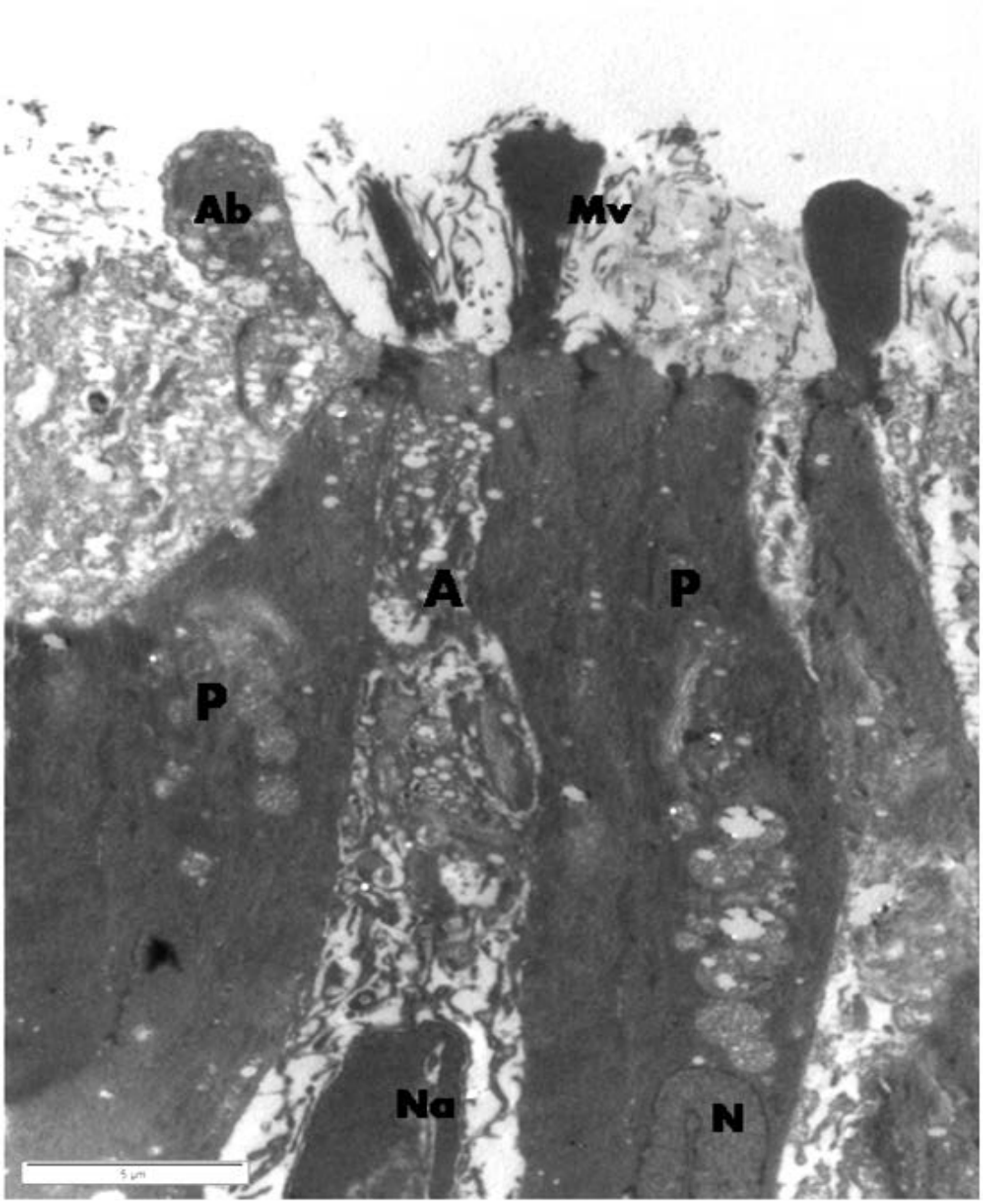

Figure 20h: Ultrastructure of the apical part of apical cell (A) wedged between principal cells (P) in MIS of epididymis in the cane rat. Note the apical bleb (Ab) and nucleus (Na) of the apical cell as well as the microvilli (Mv) and nucleus (N) of the principal cell. Picture taken with Phillips CM10 TEM at 80 KV. Mag. X 20,000, **Scale bar = 5µm**.

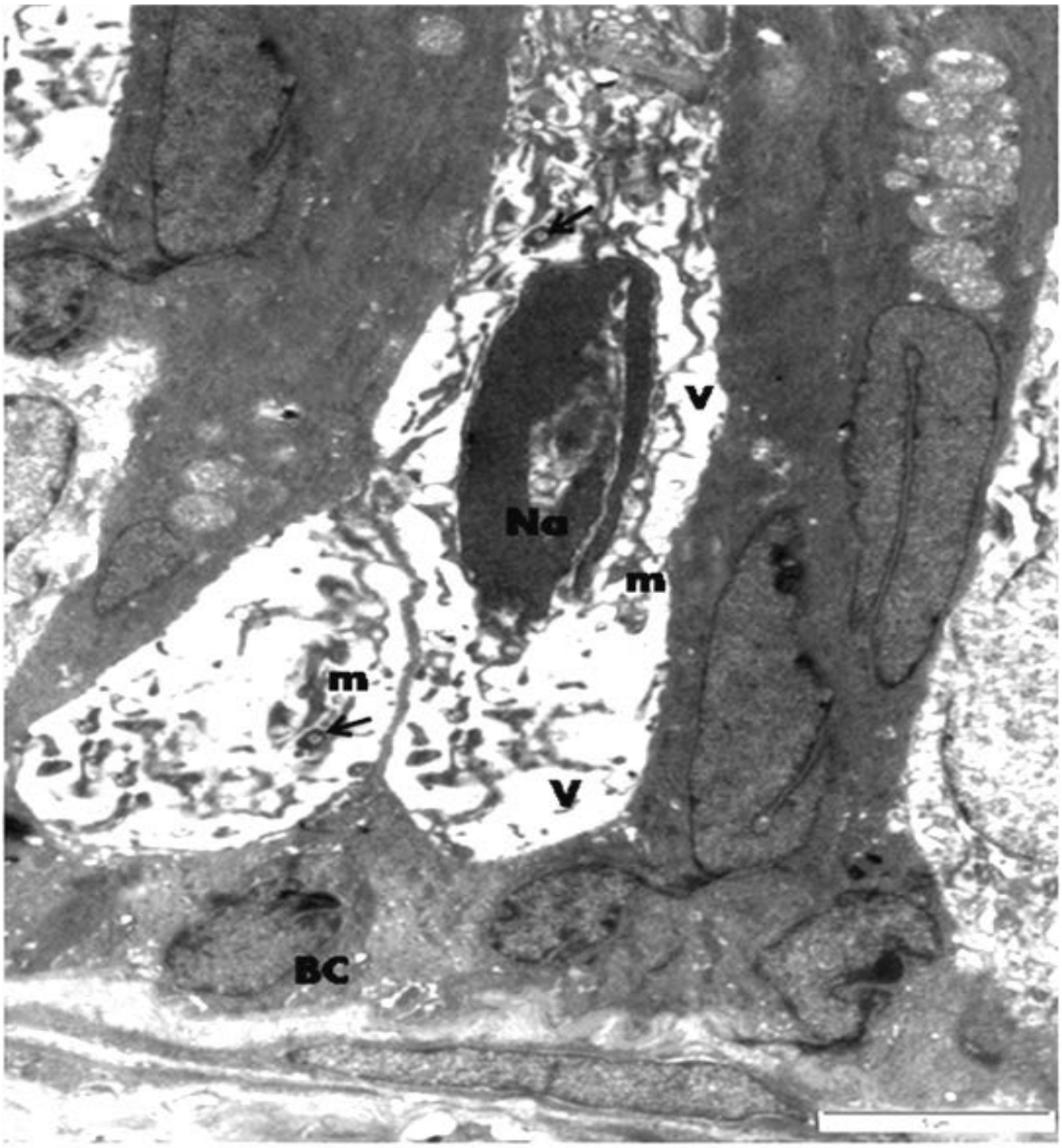

Figure 20i: Ultrastructure of the basal part of apical cell in MIS of epididymis in the cane rat. Note the vacuoles (V) surrounded by mitochondria (m), highly indented heterochromatic nucleus (Na) and the lysosomes (arrows) of the apical cell. The basal cell was also shown. Picture taken with Phillips CM10 TEM at 80 KV. Mag. X 20,000, **Scale bar = 5µm**.

The histological appearance of the distal initial segment (DIS) revealed further increase in the amount of apical and narrow cells as well as changes in the morphology of the principal cell. While the structures of the apical and narrow cells remain the same, a lot of the principal cells in this zone were packed with both pale and dark vacuoles (Fig. 20j). The released blebs from the apical and narrow cells were also observed in the lumen.

The fine structure of the principal cells in the DIS showed that, the apical surfaces are covered by numerous unbranched microvilli and the apical cytoplasm are laden with pale vacuoles of different sizes. At the supranuclear region, multivesicular bodies, small and coated vesicles as well as flat cisternae of Golgi apparatus and abundant tubular mitochondria were observed (Fig 20k). The infranuclear cytoplasm was packed with numerous flat and whorl-shaped cisternae of rough endoplasmic reticulum and dense-core mitochondria. Dense vacuoles that are suggestive of lysosomes are also present at this part of the cell (Fig. 20l). The basal cells found in all the zones in this region showed the same structural characteristic as already described.

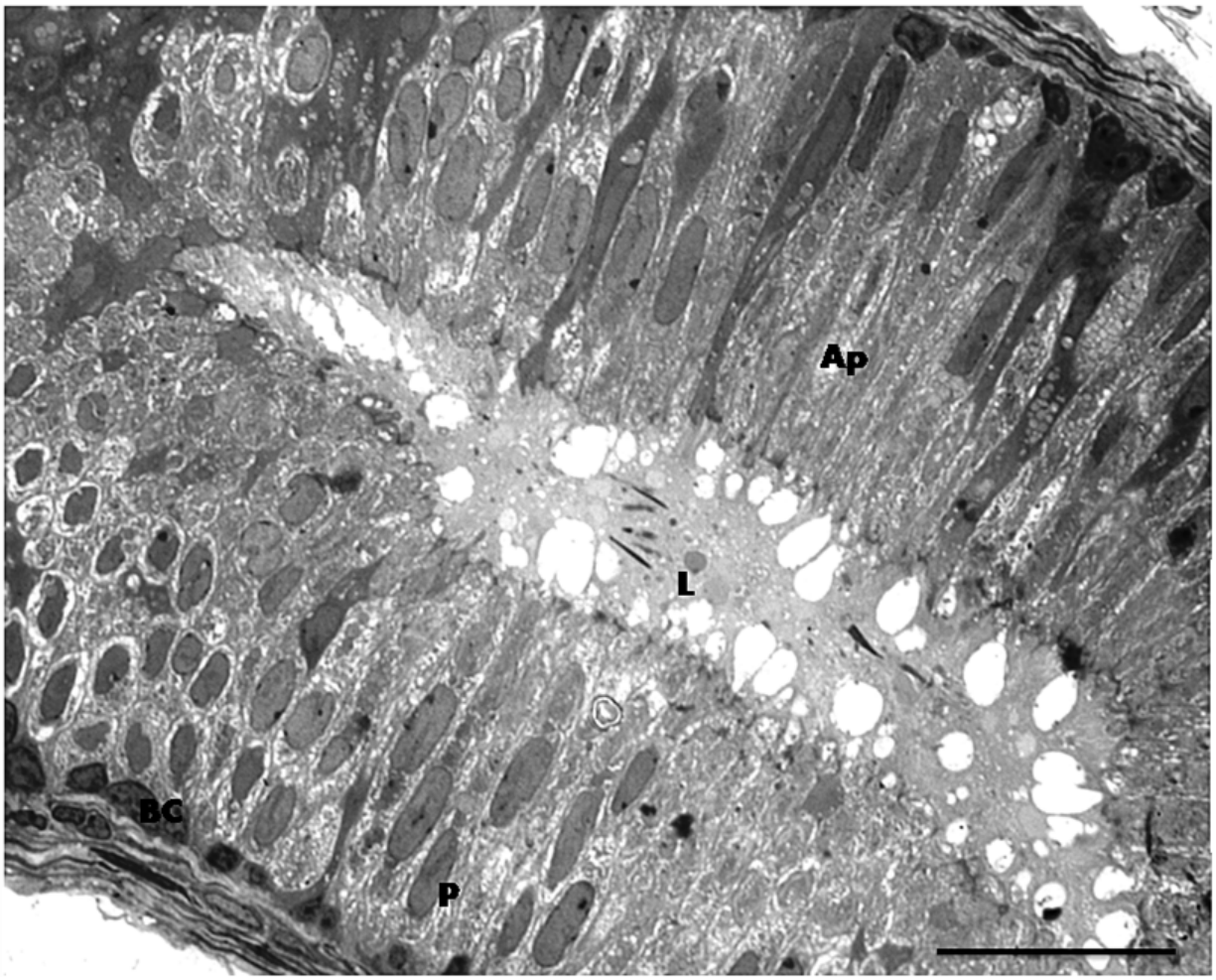

Figure 20j: Photomicrograph of the epithelium of distal initial segment (DIS) of epididymis in the greater cane rat. Note the increase in the number of apical (Ap) cells and changes in the structure of principal cells (P). Secretory blebs released into the lumen (L) were conspicuously shown with the basal cells (BC) attached to the epithelial basement membrane. **Toluidine blue,** Mag. X1000. **Scale bar = 20µm**.

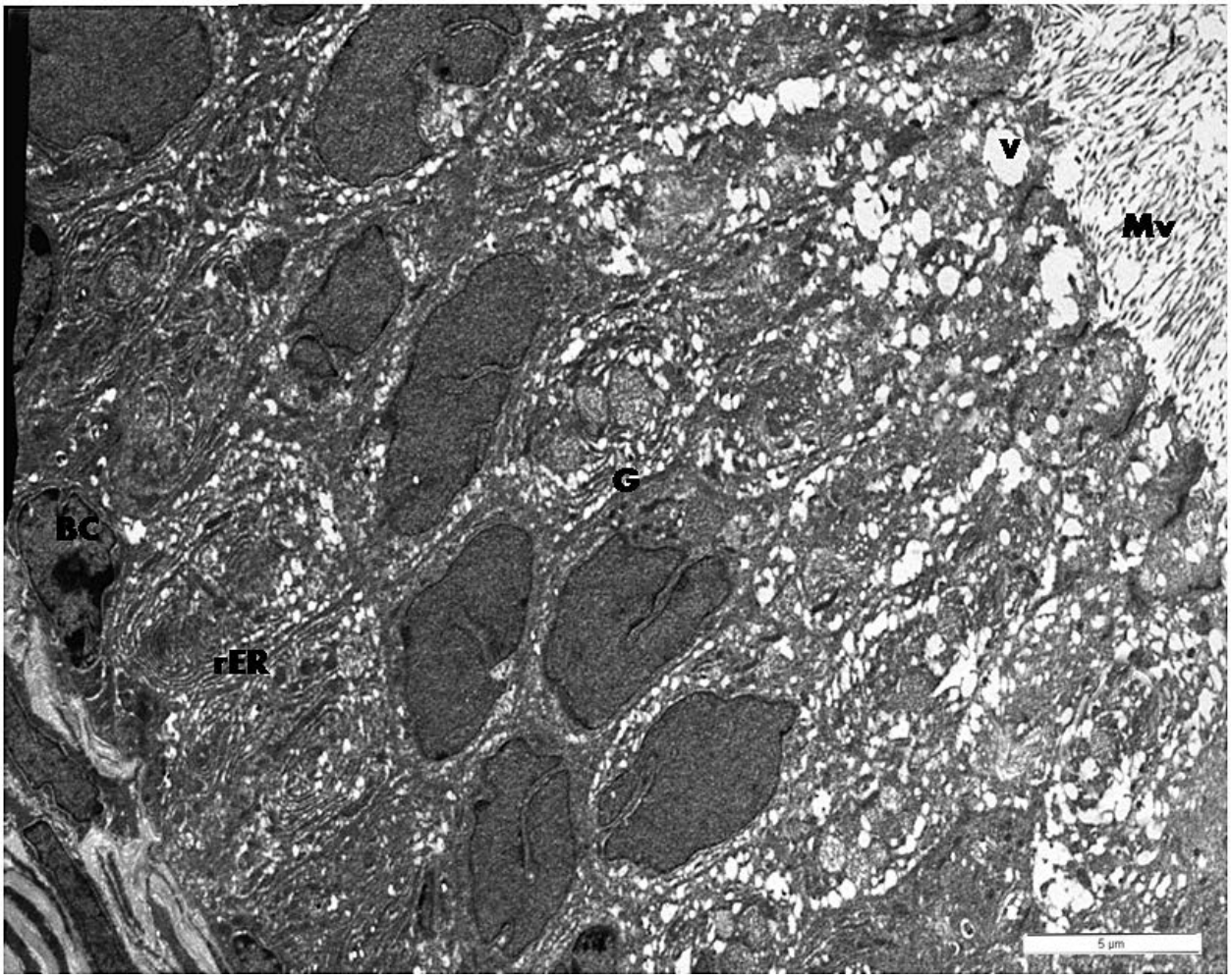

Figure 20k: Ultrastructure of the epithelium of distal initial segment (DIS) of epididymis in the greater cane rat. Note the unbranched microvilli (Mv), prominent Golgi complexes (G) and apical vacuoles (V) in the principal cell. The basal cells (BC) are also shown. Picture taken with Phillips CM10 TEM at 80 KV. Mag. X 12,000, **Scale bar = 5µm**.

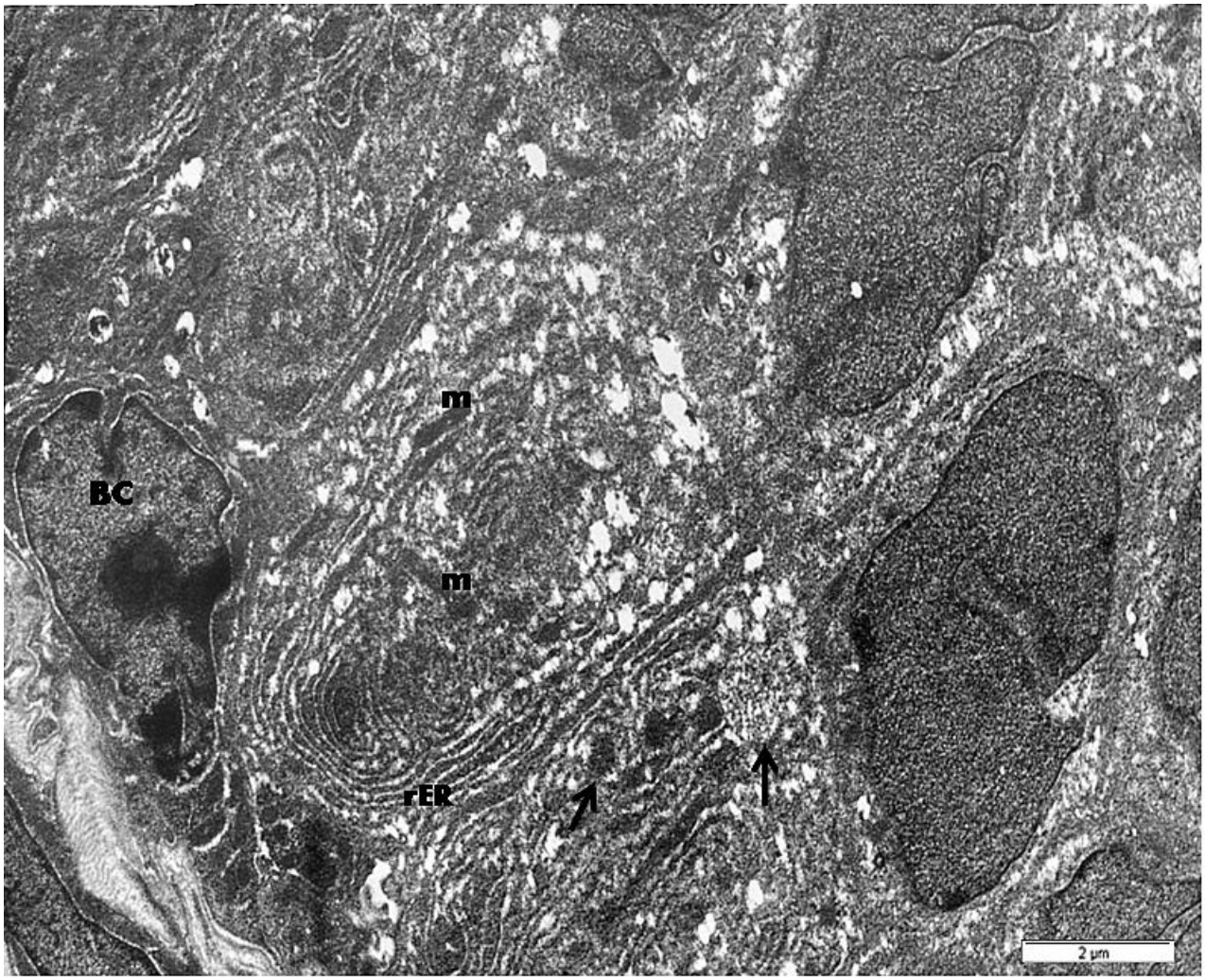

Figure 20l: Ultrastructure of the basal part of principal cells of distal initial segment (DIS) of epididymis in the greater cane rat showing cisternae of rough endoplasmic reticulum (rER) and abundant mitochondria (m) as well as dense vacuoles that look like lysosomes (arrows). The basal cells (BC) with its indented nucleus and few organelles were also shown. Picture taken with Phillips CM10 TEM at 80 KV. Mag. X 12,000, **Scale bar = 2µm**.

Region 2 – Caput Epididymis

The caput epididymis in the cane rat constitutes a zone as it showed the same histo-cytological architecture throughout its length. In this region the luminal outline had gradually changed from stellate to oval shape with a fairly uniform average epithelial height of 47.62 ±5.98µm and average ductular diameter of 229.18 ±17.88µm (Fig. 21a, Table 3). Principal, basal, apical and to a less extent, narrow cells make up the epithelial lining in this region (Fig. 21a&b).

The apical and principal cells in this region showed different structural features from that of region 1. Here the principal cells which are relatively less tall, have their nuclei pushed closer to the basal lamina by vacuoles of various sizes that fill the supranuclear and the apical cytoplasm (Fig. 21b). Whereas some had blebs on their apical surfaces, others are covered by microvilli. The apical cells also contain large vacuoles with blebs on their surfaces. The basal cells are similar in structure to those of the previous zones (Fig. 21b).

The electron micrograph of the principal cells reveals that the apical and supranuclear parts not only contain vacuoles but also multivesicular bodies, secretory vesicles, coated vesicles and lipid-like vacuoles with Golgi cisternae at the Golgi zone. While the nucleus showed several deep indentations and contained nucleolus, the microvilli were branched and several secreted vesicles and granules were seen in the lumen (Fig. 21c). The apical cell contained larger multivesicular bodies, secretory vesicles but with no distinct Golgi zone. The dome-shaped luminal surface was free of microvilli (Fig. 21c).

Figure 21a: Photomicrograph of the caput epididymis in the greater cane rat showing the pseudostratified epithelium with the principal (P), apical (Ap) and basal (BC) cells. Note the regular outline of the lumen (L). **H&E,** Mag. X400. **Scale bar = 50µm**.

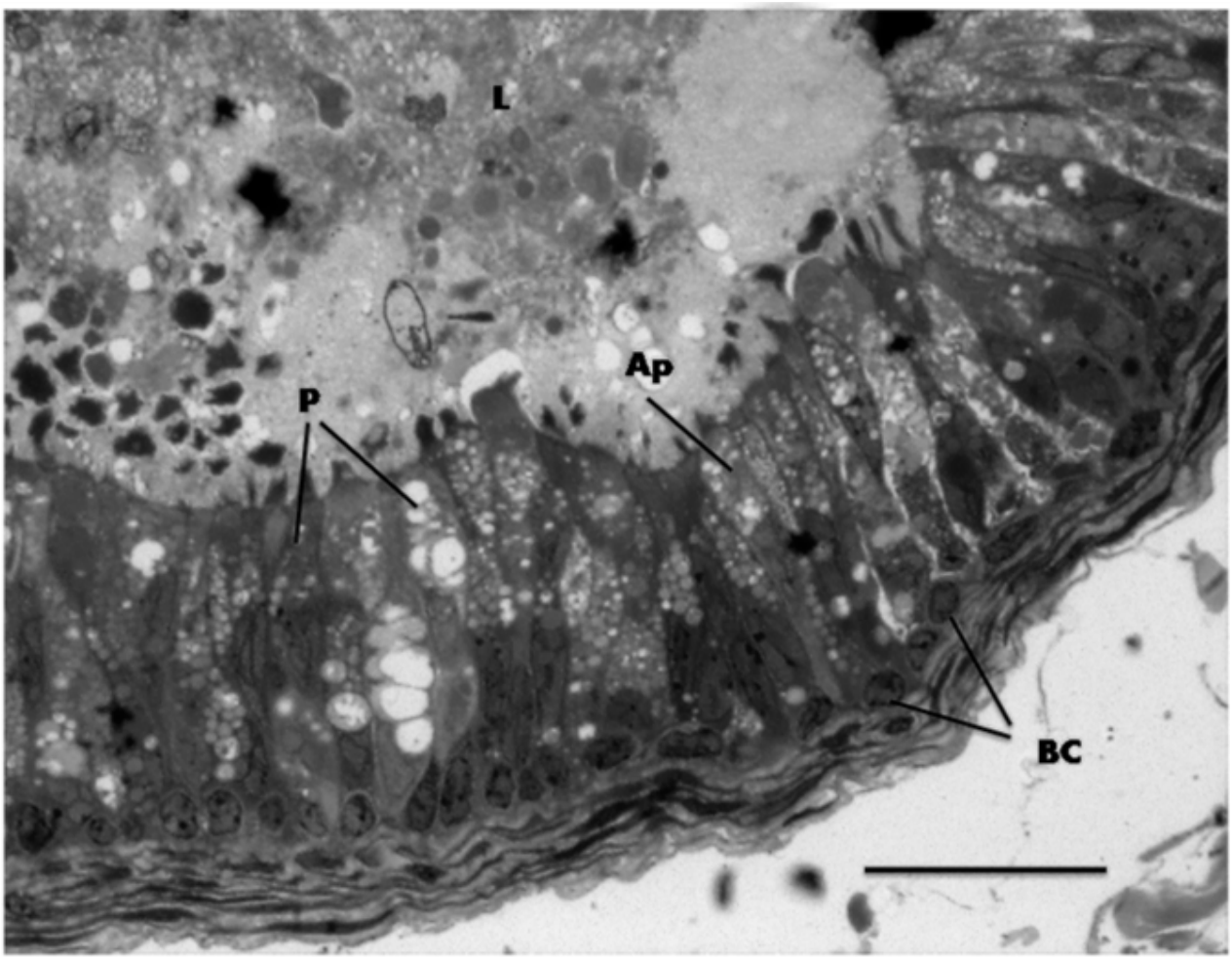

Figure 21b: A semi-thin section of the caput epididymal epithelium in the greater cane rat. Note the presence of the vacuoles of various sizes in the apical (Ap) and principal (P) cells. Secretory blebs from these cells also occupy the lumen (L) and the basal cells (BC) abutting the epithelial basement membrane. **Toluidine blue.** Mag. 1000. **Scale bar = 20µm**.

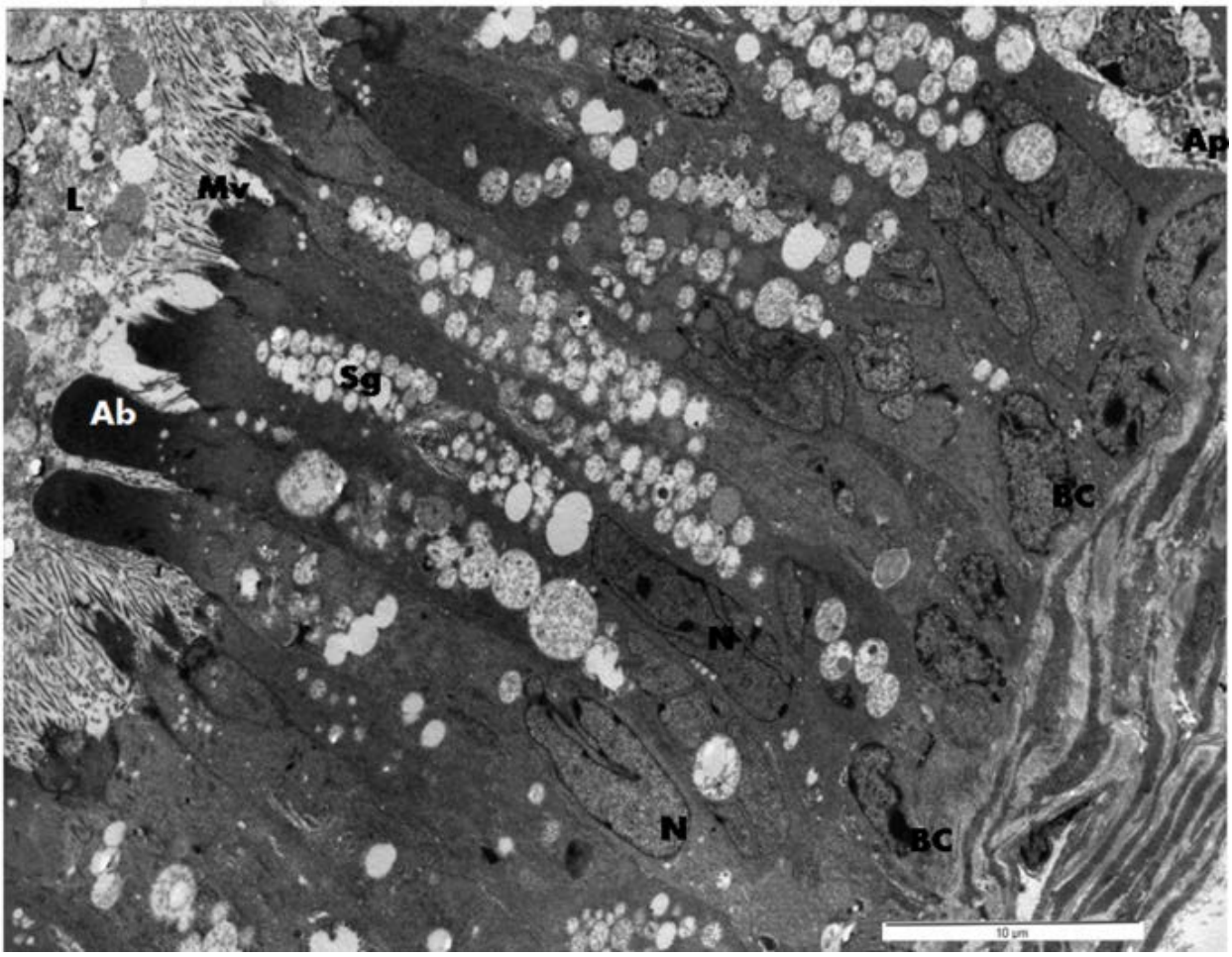

Figure 21c: Ultrastructure of the epithelium of the caput epididymis in the greater cane rat showing the principal cells with microvilli (Mv) and apical blebs (Ab), secretory vacuoles and granules (Sg) at the apical cytoplasm and some in the lumen (L) and euchromatic nucleus (N).The apical (Ap) and basal (BC) cells are also present. Picture taken with Phillips CM10 TEM at 80 KV. Mag. X 12,000. **Scale bar = 10µm**.

At higher magnification, the infranuclear parts of the principal and apical cells are packed with long flattened rough endoplasmic reticulum (Fig. 21d). However, the presence of both dilated and flat cisternae of the Golgi apparatus surrounded by secretory and coated vesicles, lipid-like vacuoles in the apical part of the principal cell (Fig. 21e) differentiate it from that of the apical cell that contains more of closely packed secretory granules (Fig. 21f). The ultrastructure of the basal cell in this region was not different from that in the initial segment.

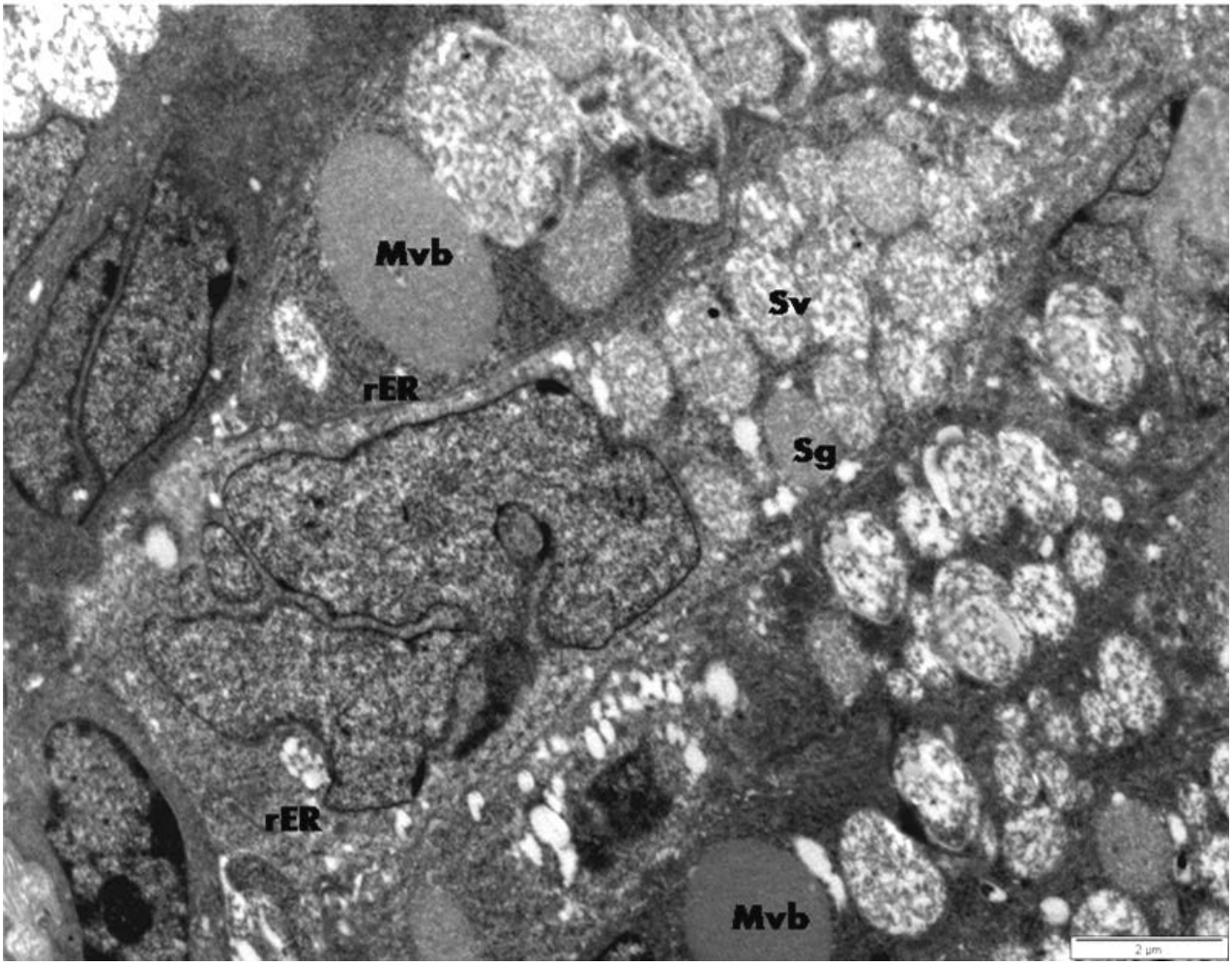

Figure 21d: Ultrastructure of the principal cells of the caput epididymis in the greater cane rat revealing the secretory vacuoles (Sv) and granules (Sg) at the apical cytoplasm and multivesicular bodies and rough endoplasmic reticulum at the infranuclear cytoplasm. Picture taken with Phillips CM10 TEM at 80 KV. Mag. X 20,000. **Scale bar = 2µm**.

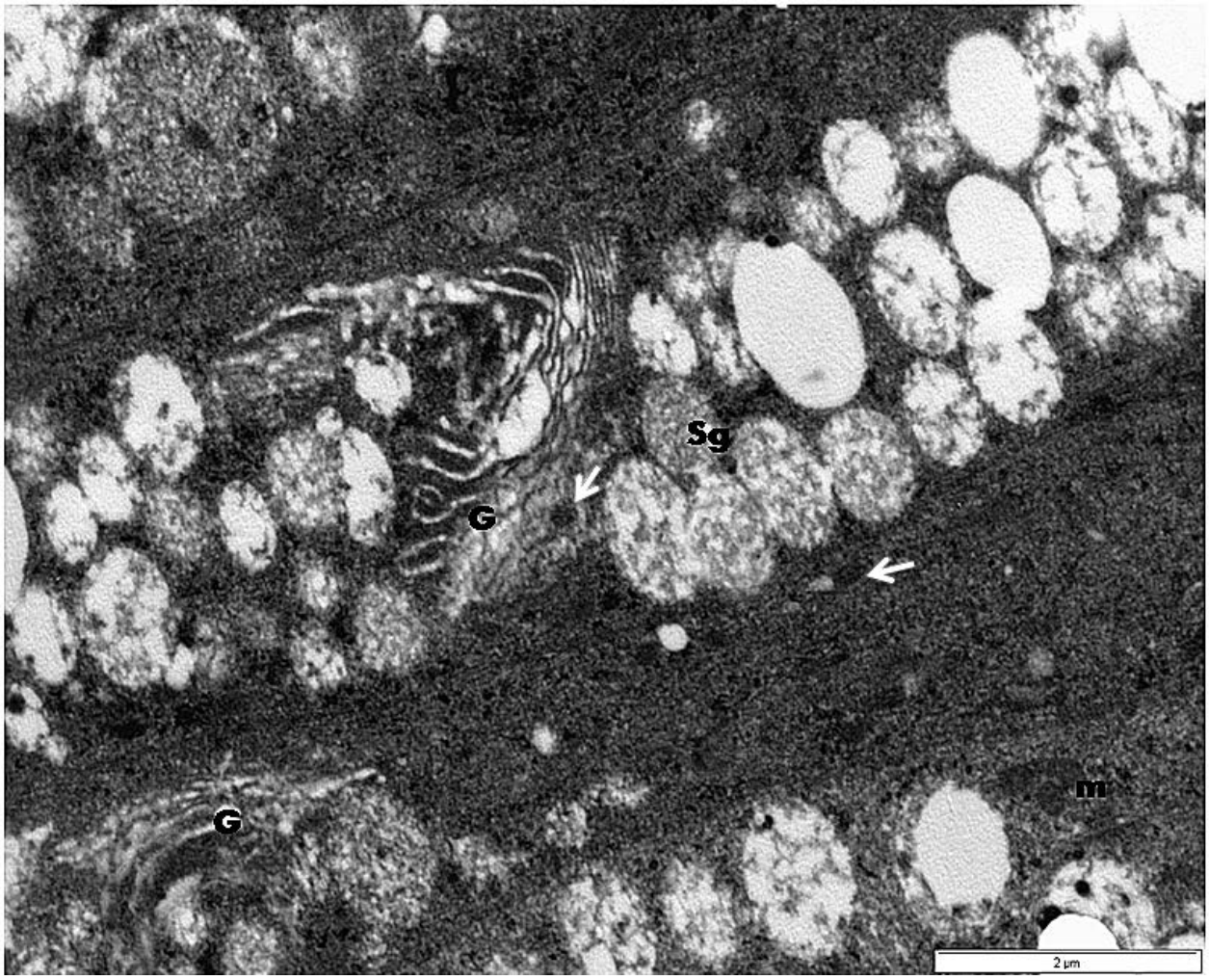

Figure 21e: Ultrastructure of the supranuclear cytoplasm of the principal cells in the caput epididymis showing the dilated cisternae of the Golgi complex (G), secretory granules (Sg) and coated vesicles (arrows) as well as mitochondria (m). Picture taken with Phillips CM10 TEM at 80 KV. Mag. X 20,000. **Scale bar = 2µm**.

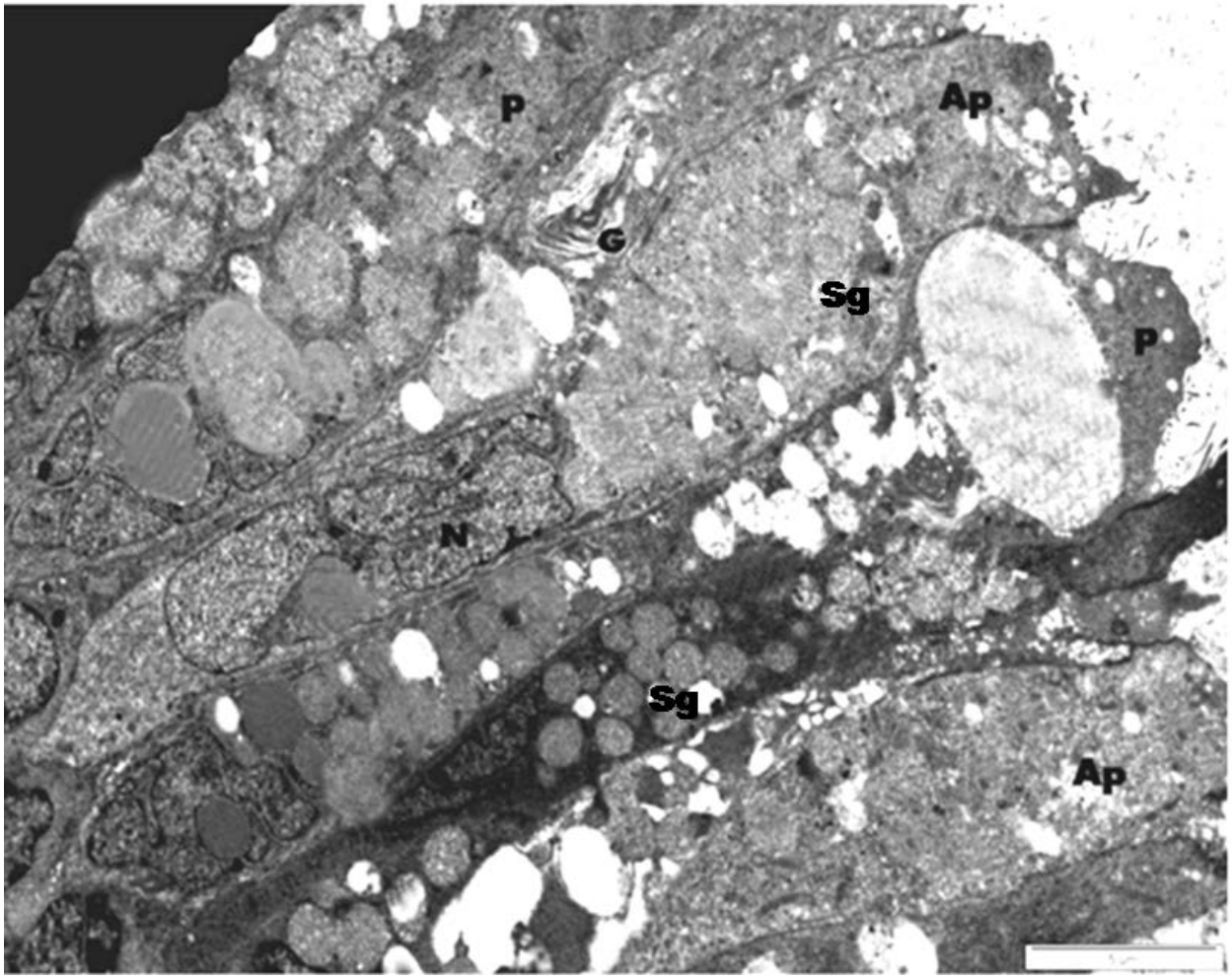

Figure 21f: Ultrastructure of the apical cell (Ap) in between of the principal cells (P) in the caput epididymis of the greater cane rat. Note the absence of microvilli and Golgi bodies in the apical cell relative to the principal cells. Also note the difference in the electron densities of the secretory granules (Sg) in both cells. Picture taken with Phillips CM10 TEM at 80 KV. Mag. X 20,000. **Scale bar = 2µm**.

Region 3 – Corpus Epididymis

The corpus epididymal region which indistinctly followed the caput, also constitute another zone as it showed similar structural and ultrastructural features all through its length. This region, which has average tubular diameter of 246.85 ±16.33µm, exhibit roundish luminal shape and the epithelium which is 38.12 ±7.38µm high, was composed of more principal, basal and clear cells but less apical and no narrow cells (Fig. 22a, Table 3).

Apart from the reduced height, the major histological feature of the principal cells in this region is the presence of prominent dense bodies of various sizes at the supranuclear part of the cells (Fig. 22b). Also present at this zone are clear cells which are flask-shaped cells of less density to the principal cells. While the principal and clear cells contain some dense bodies, the basal cell had similar features with the previous zones (Fig. 22b)

Ultrastructurally, the principal cell nucleus in this region is euchromatic, highly indented and irregular in outline. The supranuclear dense bodies are of various shapes, sizes and electron densities and extend to the apical areas where some flat and curved Golgi cisternae are present (Fig. 22c &d). Vacuoles of various sizes were also present at the subapical part while the luminal surfaces of the cells are covered by short microvilli (Fig 22d).

The clear cells are wider but less electron dense than the principal cells. The cells were filled with flocculent vacuoles of various sizes scattered all over (Fig 22c). The euchromatic nucleus, located at the cell centre, is highly indented. The infranuclear area, together with the vacuoles contained dense bodies (Fig. 22c). Whereas the basal cytoplasm of the principal cells contained rough endoplasmic reticulum, that of the clear cells have inconspicuous endoplasmic cisternae (Fig. 22c). The ultrastructure of the basal cells is not different from that observed in the previous zones.

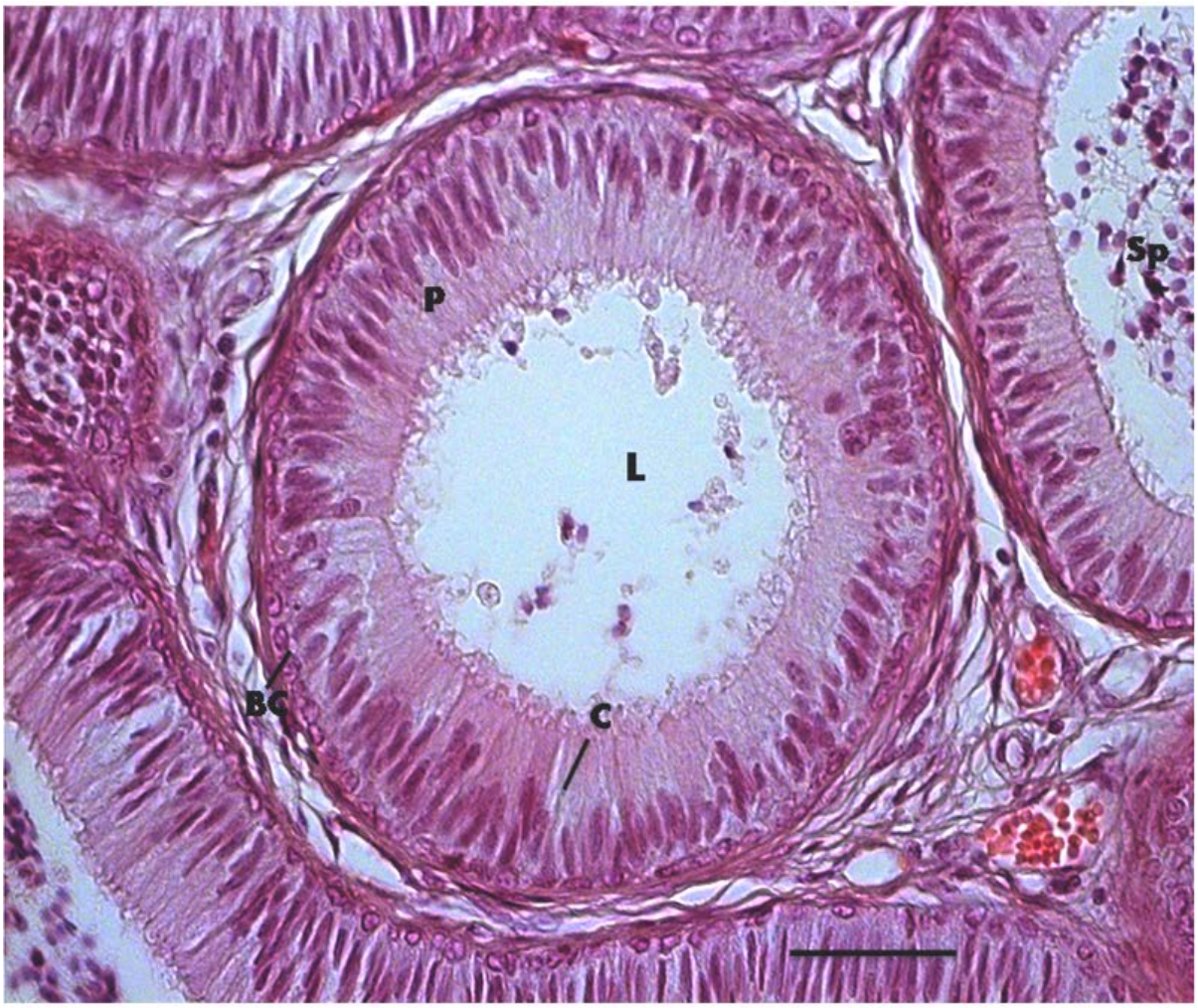

Figure 22a: Photomicrograph of the corpus epididymis in the greater cane rat. Note the pseudostratified epithelium with more of principal (P), clear (C) and basal (BC) cells. Note the round outline and the presence of large number of sperm cells (Sp) in the lumen (L). **H&E,** Mag. X400. **Scale bar = 50µm**.

Figure 22b: Photomicrograph of the corpus epididymal epithelium in the greater cane rat. Note the presence of the clear (C) and principal (P) cells containing dense bodies. The basal cells (BC) are attached to the epithelial basement membrane. **Toluidine blue,** Mag. X1000. **Scale bar = 20µm**.

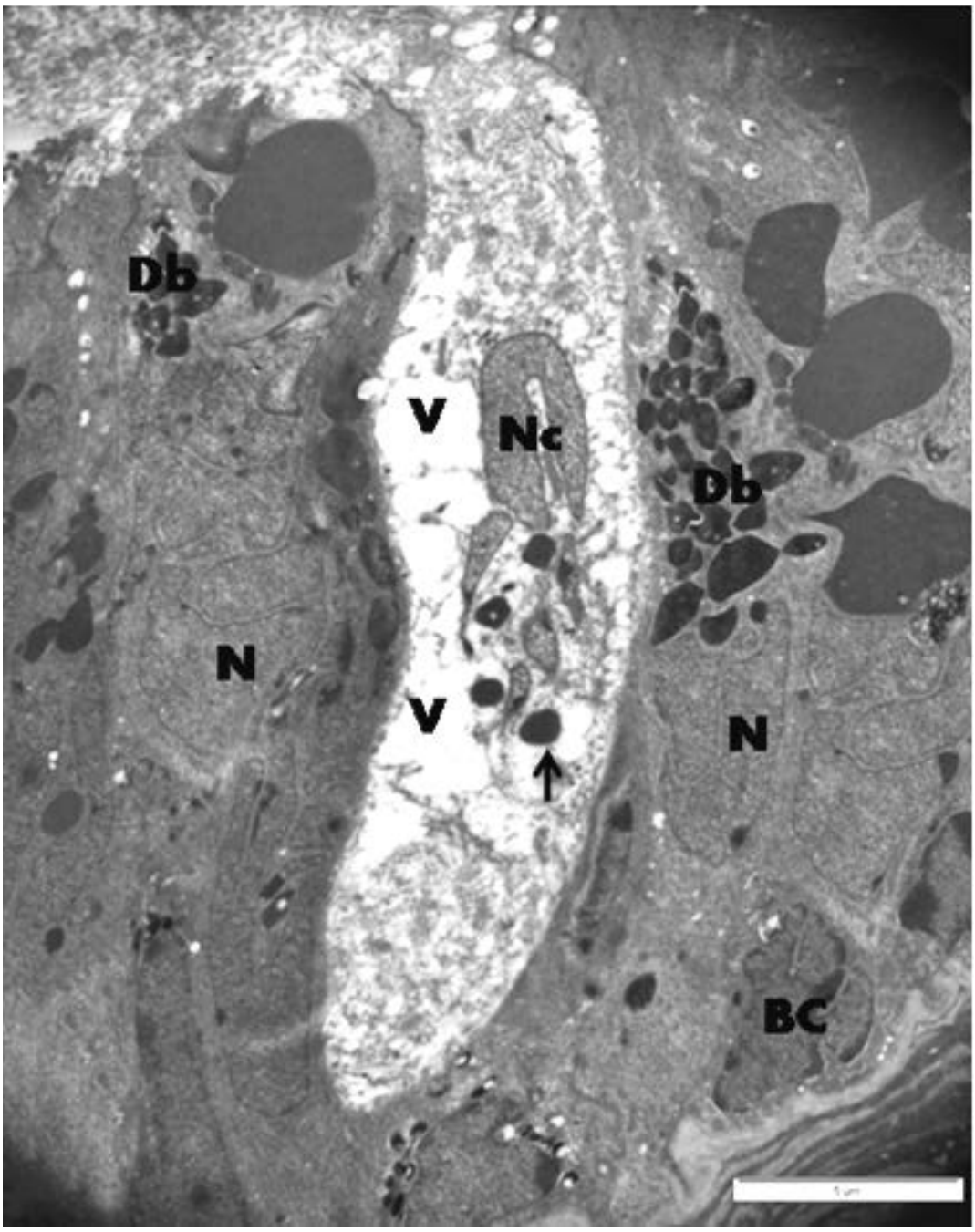

Figure 22c: Electron micrograph showing the principal, clear and basal cells in the corpus epididymis of the greater cane rat. Note the presence of irregularly shaped nucleus (N) and the dense bodies (Db) in the principal cells), as well as the presence of indented nucleus (Nc), large vacuoles (V) and round dense bodies similar to lysosome in the clear cell (arrow). The basal cells (BC) are also present. Picture taken with Phillips CM10 TEM at 80 KV. Mag. X 20,000. **Scale bar = 5µm**.

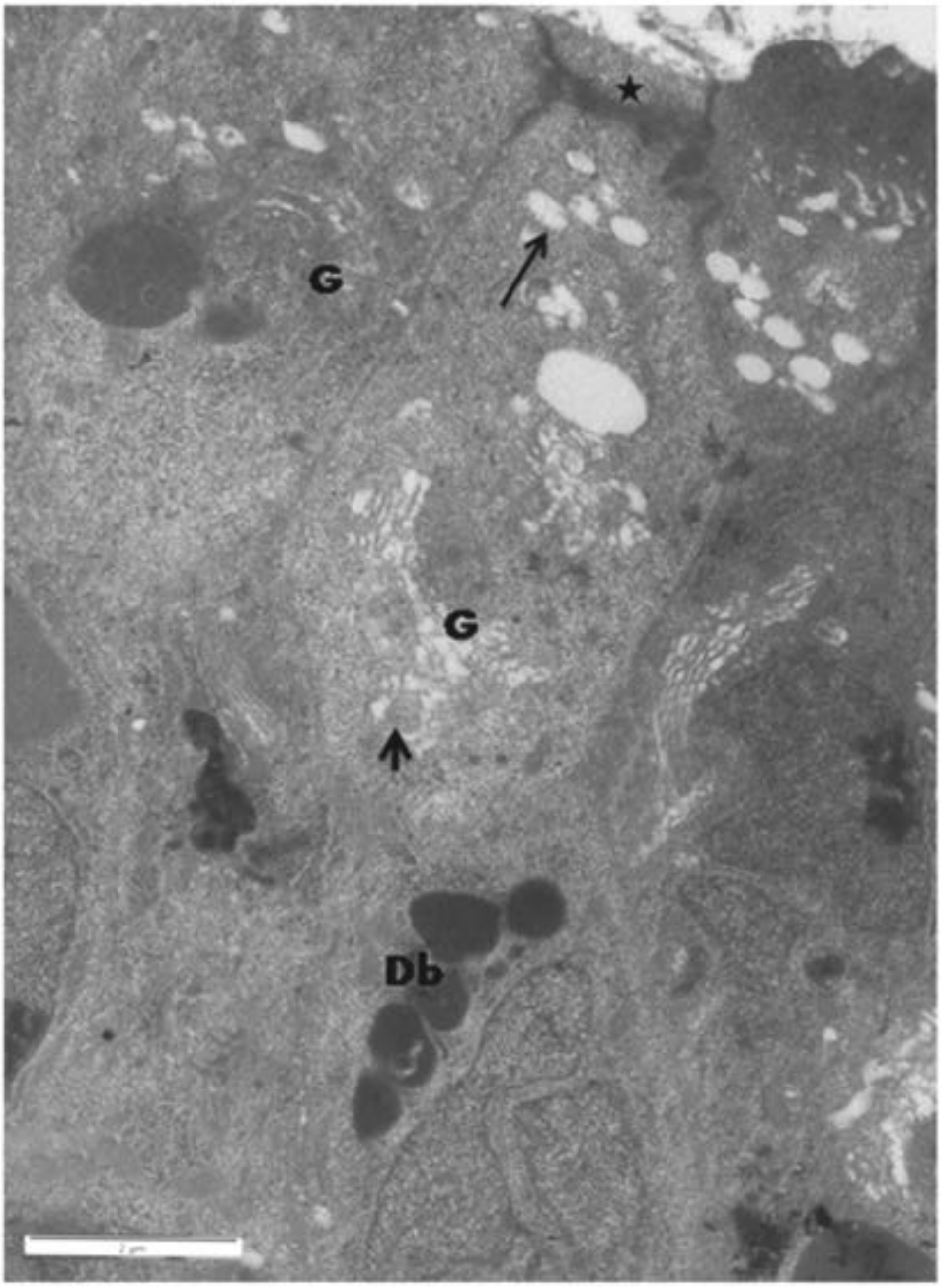

Figure 22d: Electromicrograph of the apical cytoplasm of the principal cell in the corpus epididymis of the greater cane rat. Note the flat Golgi cisternae (G), secretory granules suggestive of lysosomes (arrow head), subapical vacuoles (arrow), coated pit (asterick) and the dense bodies at the spranuclear area. Picture taken with Phillips CM10 TEM at 80 KV. Mag. X 20,000. **Scale bar = 2µm**.

Region 4 – Cauda Epididymis

The entire cauda epididymis region was lined by low cuboidal epithelium with uniform average height of 17.01 ±1.41µm and average tubular diameter of 500.11 ±105.27µm. The lumen is filled with sperm cells and there was an obvious increase in the thickness of the muscular coat that surrounded the tubules (Fig. 23a, Table 3).

The epithelium of the cauda epididymis consisted predominantly of principal and basal cells with few clear cells that showed similar features with that seen in the corpus epididymis. Although shorter than that in the previous zone, it also contained a lot of dense bodies (Fig 23b) with nuclei of about the same size with that of the basal cells. The basal cells were similar to that of the previous zones (Fig. 23b).

The major ultrastructural differences between of the principal cells in this zone and that of the corpus epididymis were increase in the amount of dense bodies at the supranuclear and apical cytoplasm as well as presence of less dense vesicles of various sizes around the rough endoplasmic reticulum at the infranuclear cytoplasm of the cells of this zone (Fig. 23c). This cell also had Golgi apparatus at the apical cytoplasm and microvilli were present on the luminal surface (Fig 23d). Fine structure of the basal cell was typical in this zone

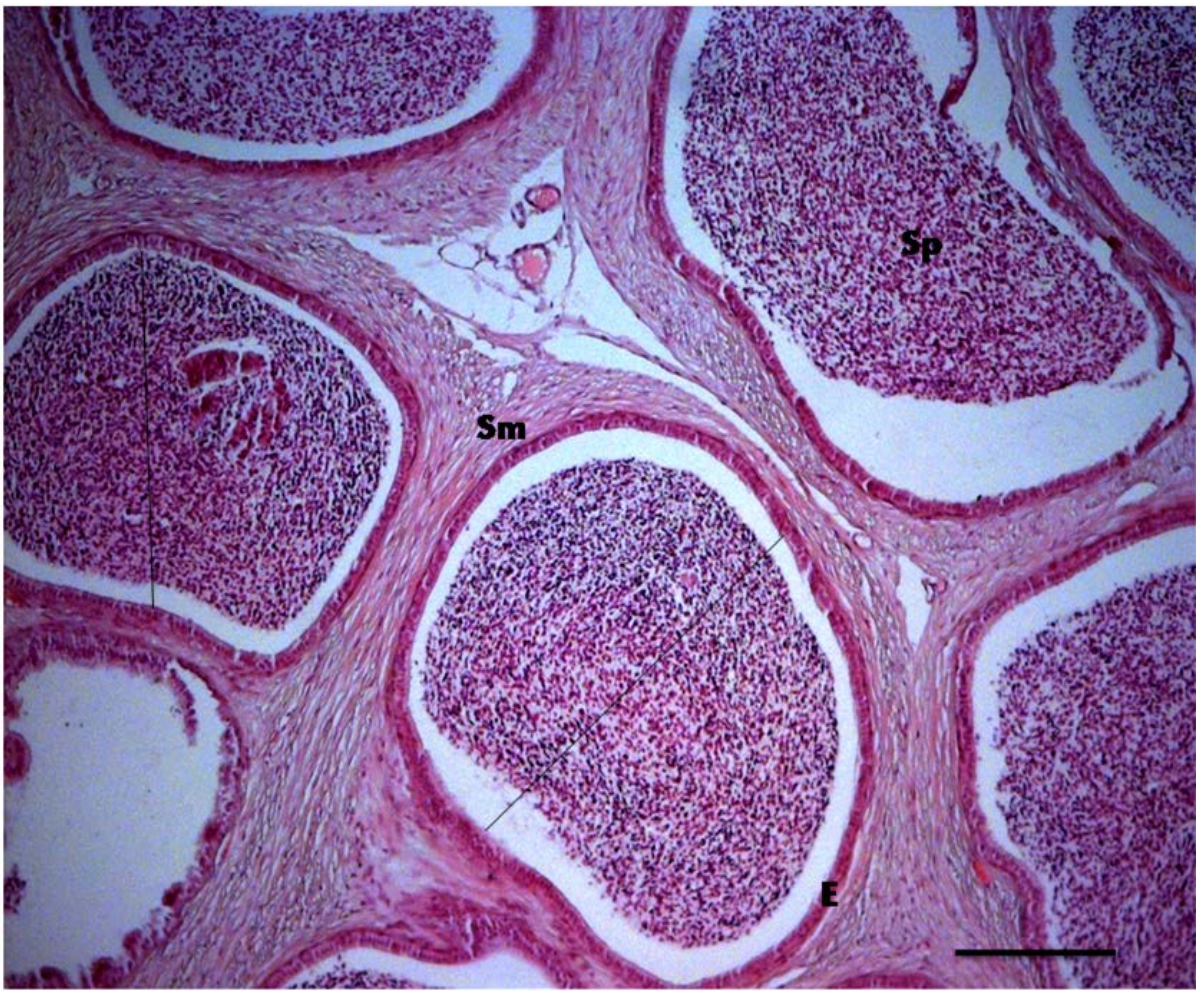

Figure 23a: Photomicrograph of the cauda epididymis in the greater cane rat. Note the low epithelium (E), the wide lumen filled with sperm cells (Sp) and the increase in the thickness of the smooth muscle layer (Sm). **H&E,** Mag. X100. **Scale bar = 50µm**.

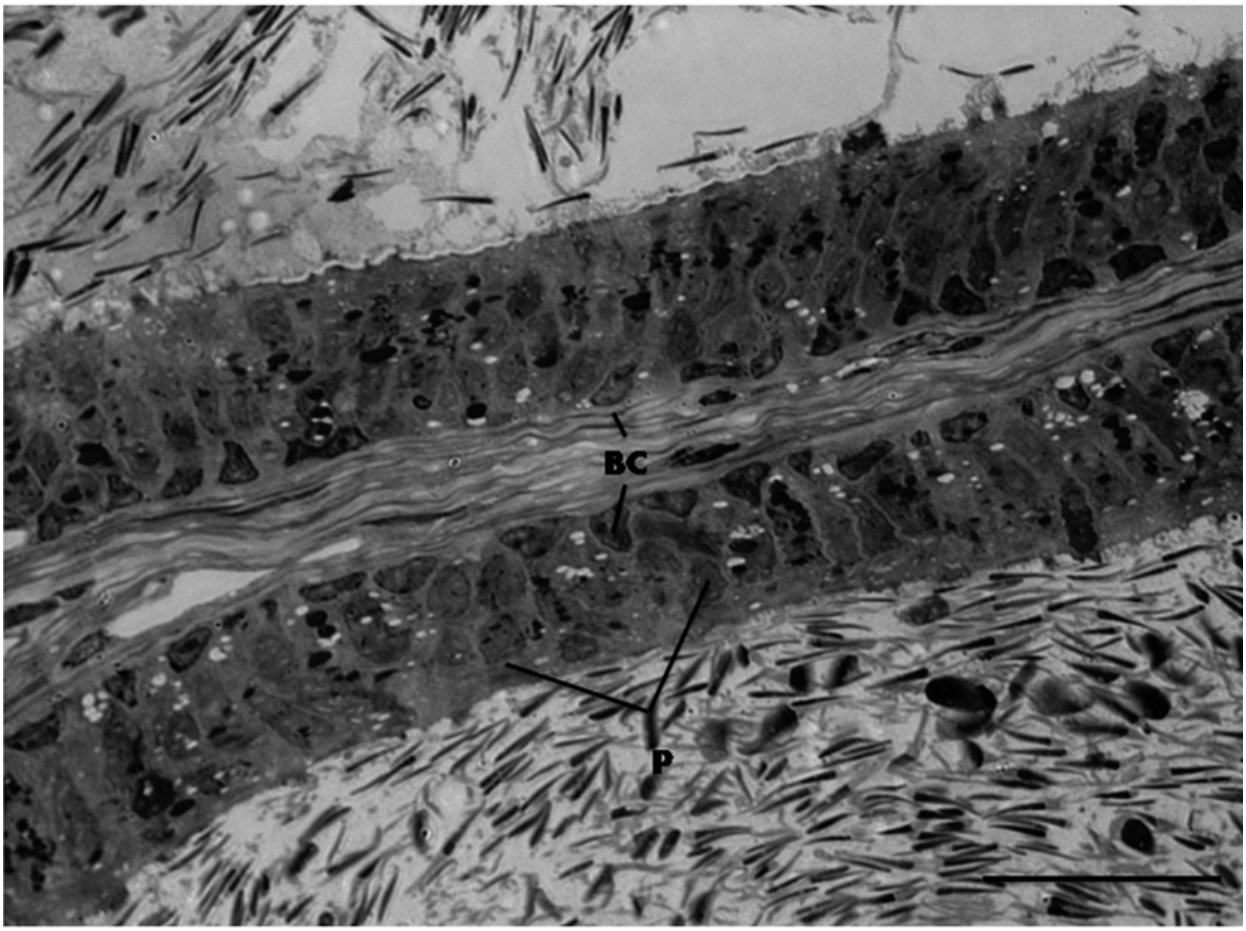

Figure 23b: Photomicrograph of the epithelium in the cauda epididymis of the greater cane rat. Note the low cuboidal principal (P) cells containing dense bodies. The basal cells (BC) are attached to the epithelial basement membrane and sperm cells (Sc) fill the tubular lumen. **Toluidine blue,** Mag. X1000. **Scale bar = 20µm**.

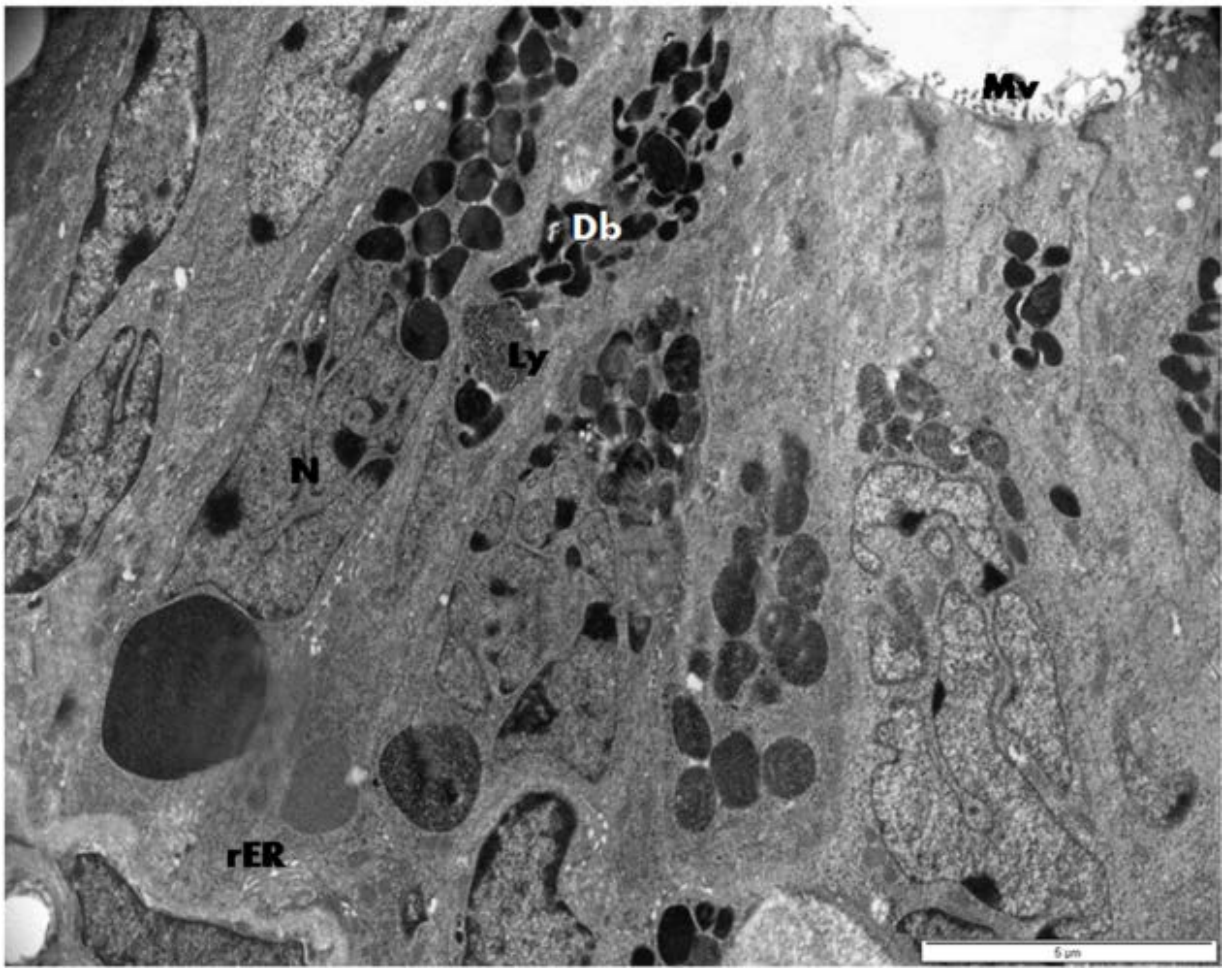

Figure 23c: Ultrastructure of the epithelium of the cauda epididymis in the greater cane rat showing the principal cells with microvilli (Mv), and numerous dense bodies (Db), lysosomes (Ly) at the supranuclear cytoplasm as well as irregularly shaped nucleus (N) and rER cisternae at the basal cytoplasm. Picture taken with Phillips CM10 TEM at 80 KV. Mag. X 20,000. **Scale bar = 5µm**.

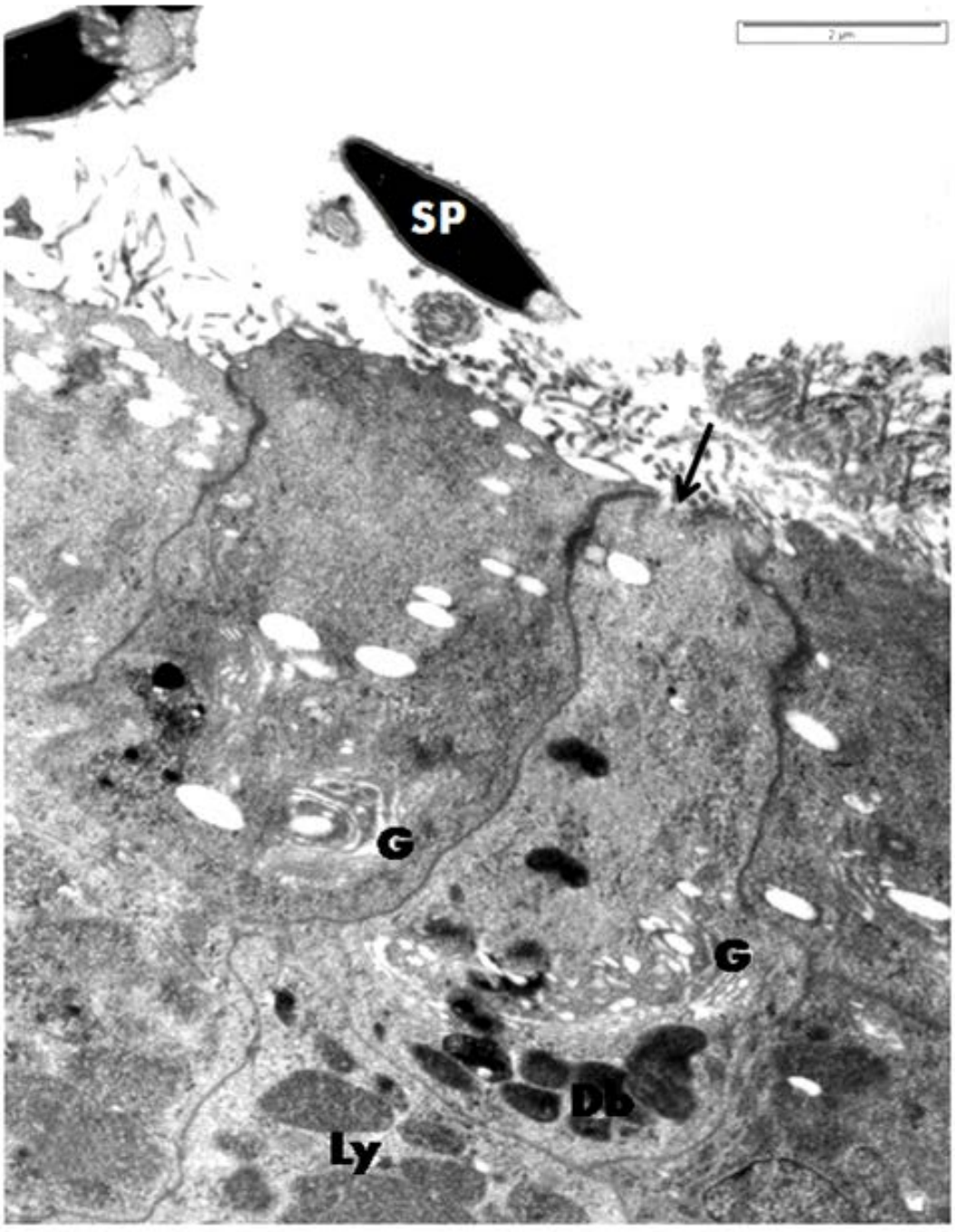

Figure 23d: Ultrastructure of the apical cytoplasm of the principal cell in the cauda epididymis of the greater cane rat. Note the damaged sperm cell (Sp) and residual bodies in the lumen, evidence of endocytosis (arrow), Golgi cisternae (G), dense bodies (Db) and lysosomes (Ly). Picture taken with Phillips CM10 TEM at 80 KV. Mag. X 20,000. **Scale bar = 2µm**.

3.2.4 VAS DEFERENS

3.2.4.1 Morphometry

Table 4: The gross morphometric values of the vas deferens with the body and testicular weights in the greater cane rat.

	Mean ±Standard Deviation
Body weight (g)	2230 ±0.24
Testicular weight (g)	1.42 ±0.4
Vas deferens weight (g)	0.09 ±0.02
Vas deferens length (cm)	7.75 ±1.44
Vas deferens volume (cm^3)	0.197 ±0.01

Table 5: Histometric values of the different regions of the vas deferens in the greater cane rat.

	Epithelial height (µm)	***Luminal diameter (µm)***	***Muscular thickness (µm)***
Proximal vas deferens	27.81 ±6.3	641.11 ±158.23*	207.49 ±65.75*
Middle vas deferens	22.13 ±5.21	386.65 ±112.91*	283.42 ±65.27*
Distal vas deferens	27.22 ±5.72	297.54 ±44.59*	357.78 ±96.27*

***p < 0.01

In the greater cane rat, there was a correlation between the vas deferens length and the testicular weight ($r^2 = 0.15$). While there was no statistically significant difference between the epithelial heights in all the three regions, there were significant differences in the luminal diameter and the muscular thickness among the different regions of the vas deferens (Table 5).

3.2.4.2 Gross Appearance

The vas deferens in the greater cane rat is a muscular tube lined by low cuboidal epithelium that gradually originates as a straight tube from the coiled cauda epididymis in the scrotum and ends in the ejaculatory duct in the pelvis (Fig. 24). The cream coloured tube which is 7.75 ±1.44cm long, with 0.197 ±0.01cm^3 in volume and weighing 0.09 ±0.02g, appears even in size throughout its length (Fig. 25; Table 4).

3.2.4.3 Histological Appearance

Based on the luminal diameter, degree of epithelial folding, muscular thickness and the blood supply, the cane rat vas deferens can be divided into three regions namely: the proximal region which is the part next to the cauda epididymis; the distal region, the part towards the ejaculatory duct; the middle region which lies between the proximal and distal regions (Fig 26). The proximal region has the greatest luminal diameter with circular profile of the mucosa but the thinnest muscular wall (Fig. 26a). While the luminal diameter decreases along the vas length, the muscular thickness, the mucosa folding and the number of the blood vessels increase with the distal part having the least luminal diameter, largest number of blood vessels, thickest muscles and completely folded mucosa (Fig. 26c). The middle region shares features of both the proximal and distal regions of the vas deferens (Fig. 26b).

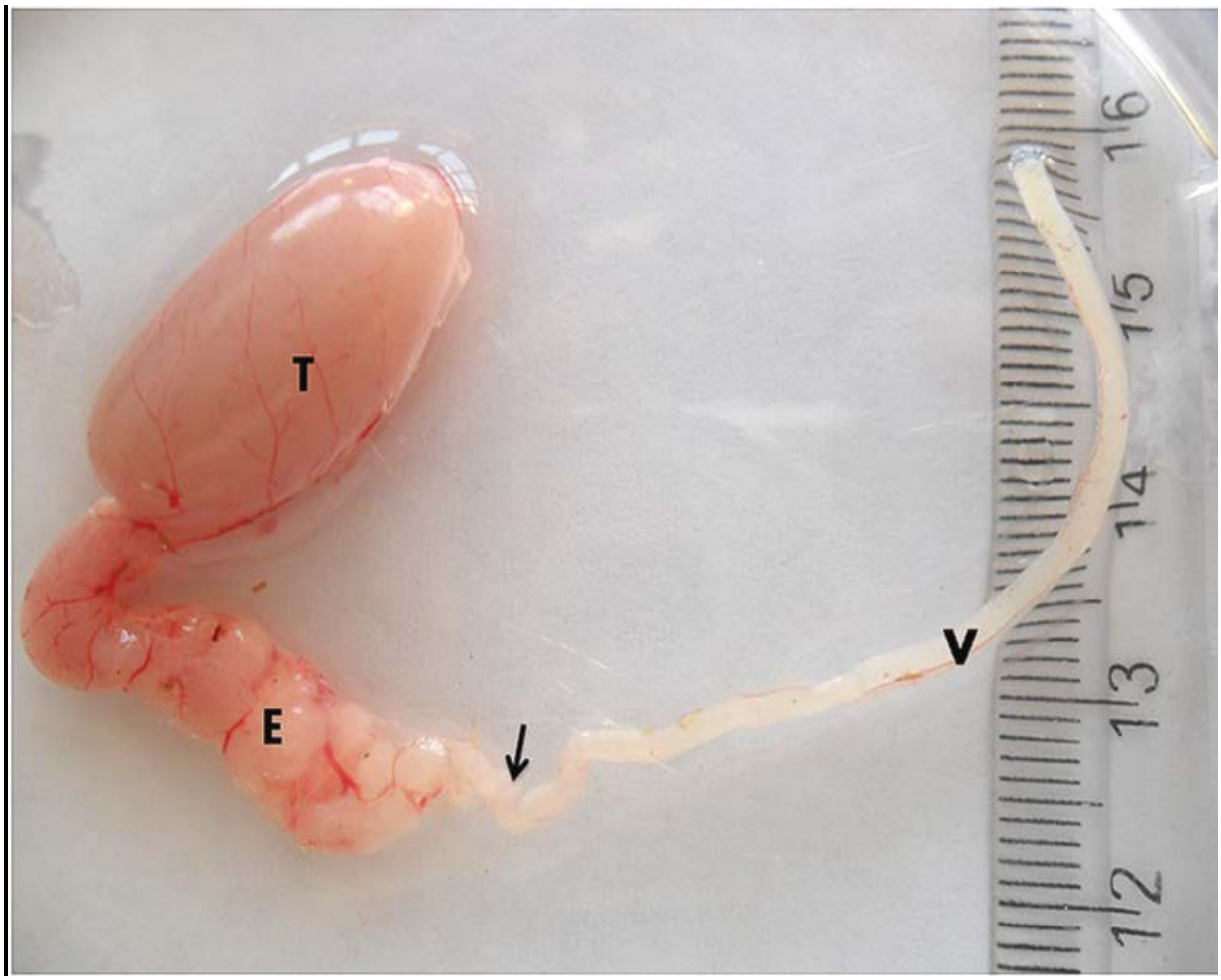

Figure 24: Photograph showing isolated testis (T), the epididymis (E) and the vas deferens (V) of the greater cane rat. Note the gradual straightening out (arrow) of the proximal region of the vas deferens from the highly coiled cauda epididymis. Mag. X5

Figure 25: Photograph of isolated vas deferens in the cane rat showing the evenness along its length.

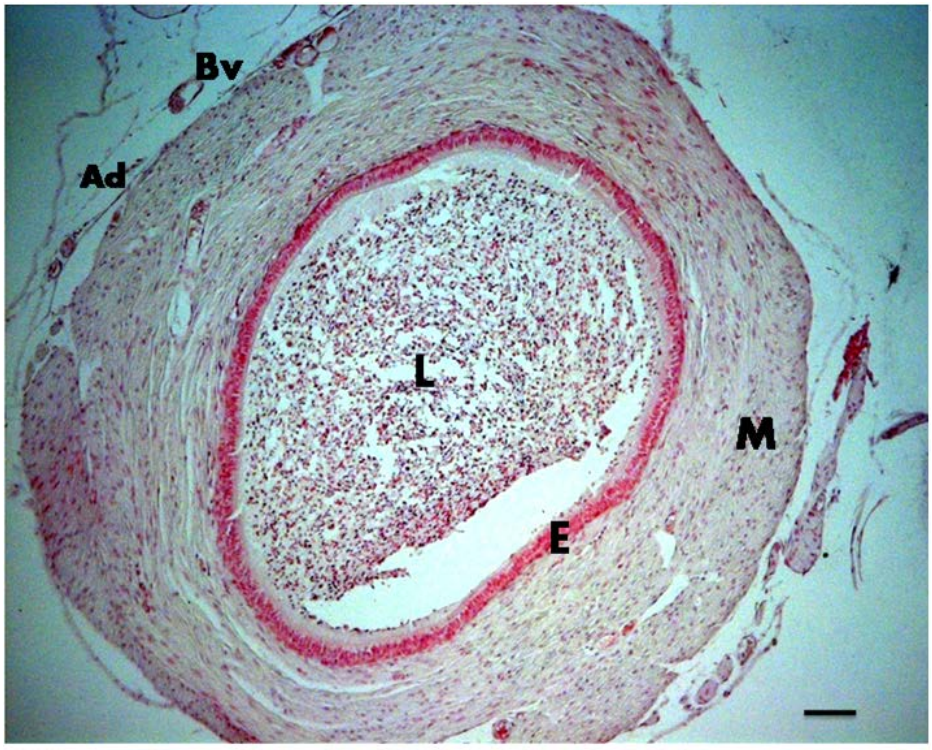

Figure 26a: Photomicrograph of the proximal region of the vas deferens in the cane rat. Note the three concentric layers – the adventitia (Ad) with blood vessels (Bv), the muscular layer (M) and epithelium (E) with circular profile that surroud the lumen (L) laden with sperm cells. Mag. X100. **Scale bar =50µm**

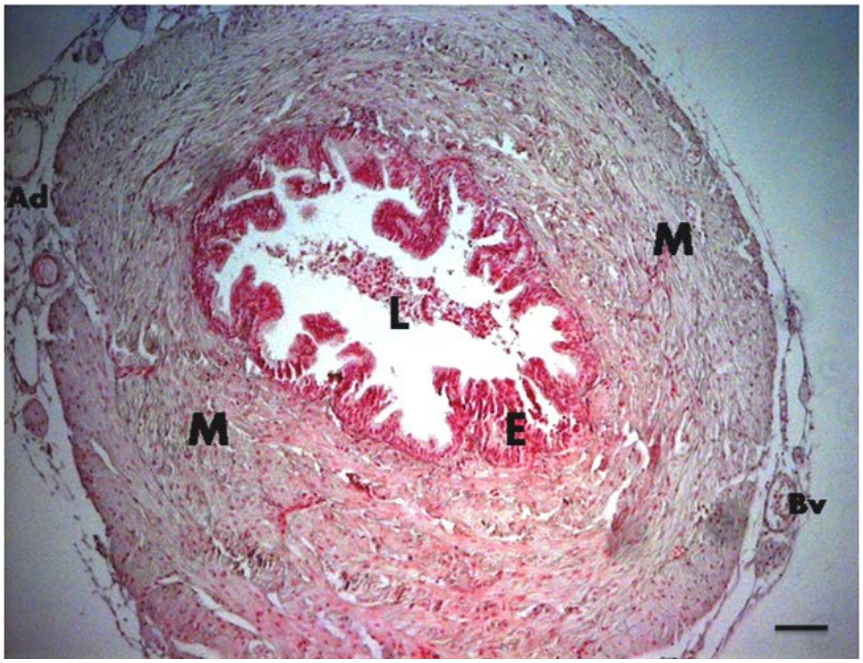

Figure 26b: Photomicrograph of the middle region of the vas deferens in the greater cane rat. Note the increase in the adventitia (Ad) blood vessels (Bv) and muscular layer (M) as well as the folding of the epithelium (E) that bound the lumen (L). H&E, Mag. X100. **Scale bar =50µm**

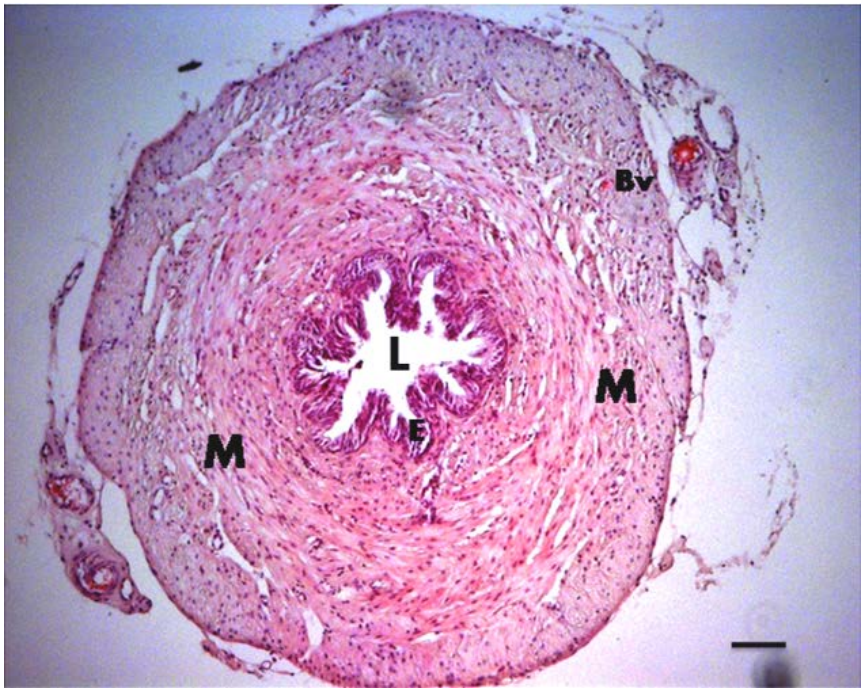

Figure 26c: Photomicrograph of the distal region of the vas deferens in the cane rat showing the presence of blood vessels (Bv) within the muscular layer (M) and increased folding of the epithelium (E) bounding a highly reduced lumen (L). H&E, Mag. X100. **Scale bar =50µm**

The pseudostratified epithelium of the vas deferens was composed of low principal cells, which were cuboidal at the proximal region but more columnar at the middle and distal regions; basal cells and some narrow cells at the distal region (Fig. 27). The nuclei of the principal cells are centrally located in the proximal region but in the basal half at the distal region with the apical surfaces of the cells covered with microvilli. The basal cells were flat and attached to the basement membrane that separate the epithelium from the loose lamina propriae that contains blood vessels. In the distal region, capillaries of the lamina propria formed a subepithelial network that extended underneath the infoldings (Fig 27). The muscular coat of the vas deferens is made up of inner and outer layers of smooth muscle with a third middle layer at the distal region (Fig. 26 &27).

3.2.4.4 *Ultrastructural Appearance*

The fine structure of the principal cells in the vas deferens of the greater cane rat revealed the presence of both bleb-like protrusion and numerous unbranched microvilli on the apical surface. The apical cytoplasm contained subapical vacuoles while the supranuclear area had Golgi apparatus and different sizes of multivesicular bodies and coated vesicles (Fig. 28). The nuclei of the cells were highly lobulated with prominent nucleolus (Fig. 28).

The basal cell contained lobulated nucleus surrounded by small cytoplasm that contained few organelles like mitochondria (Fig. 29). A prominent ultrastructural feature at the base of the vas epithelium is the presence of intraepithelial macrophages with cytoplasm that contains residual materials (Fig 28 & 29).

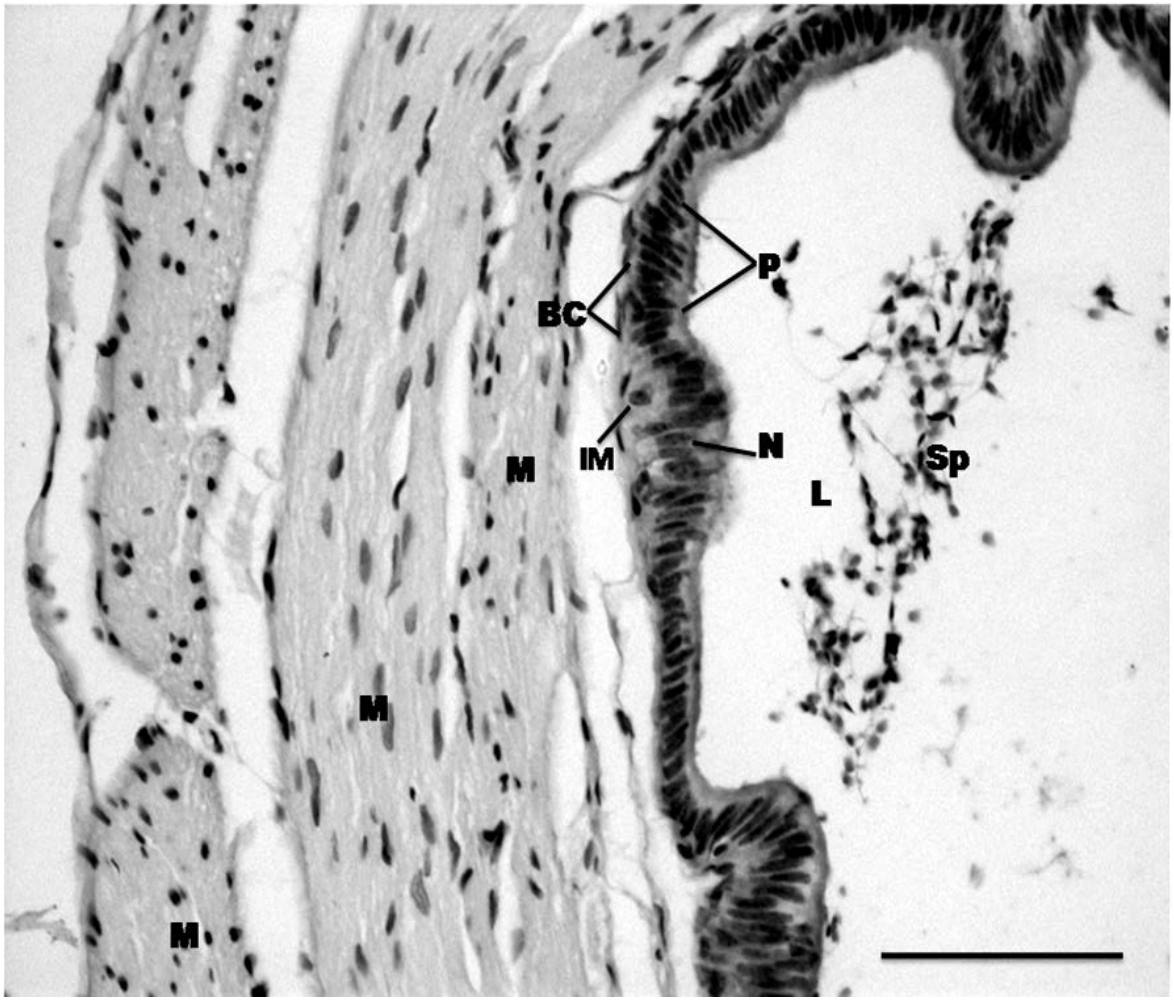

Figure 27: Photomicrograph of the epithelium of the vas deferens (middle region) in the cane rat. Note the columnar principal cells (P), the basal cells (BC), narrow cells (N), intraepithelial macrophage (IM) and the muscle layers (M) as well as the lumen (L) laden with sperm cells (Sp). **Toluidine blue,** Mag. X1000. **Scale bar =20µm**

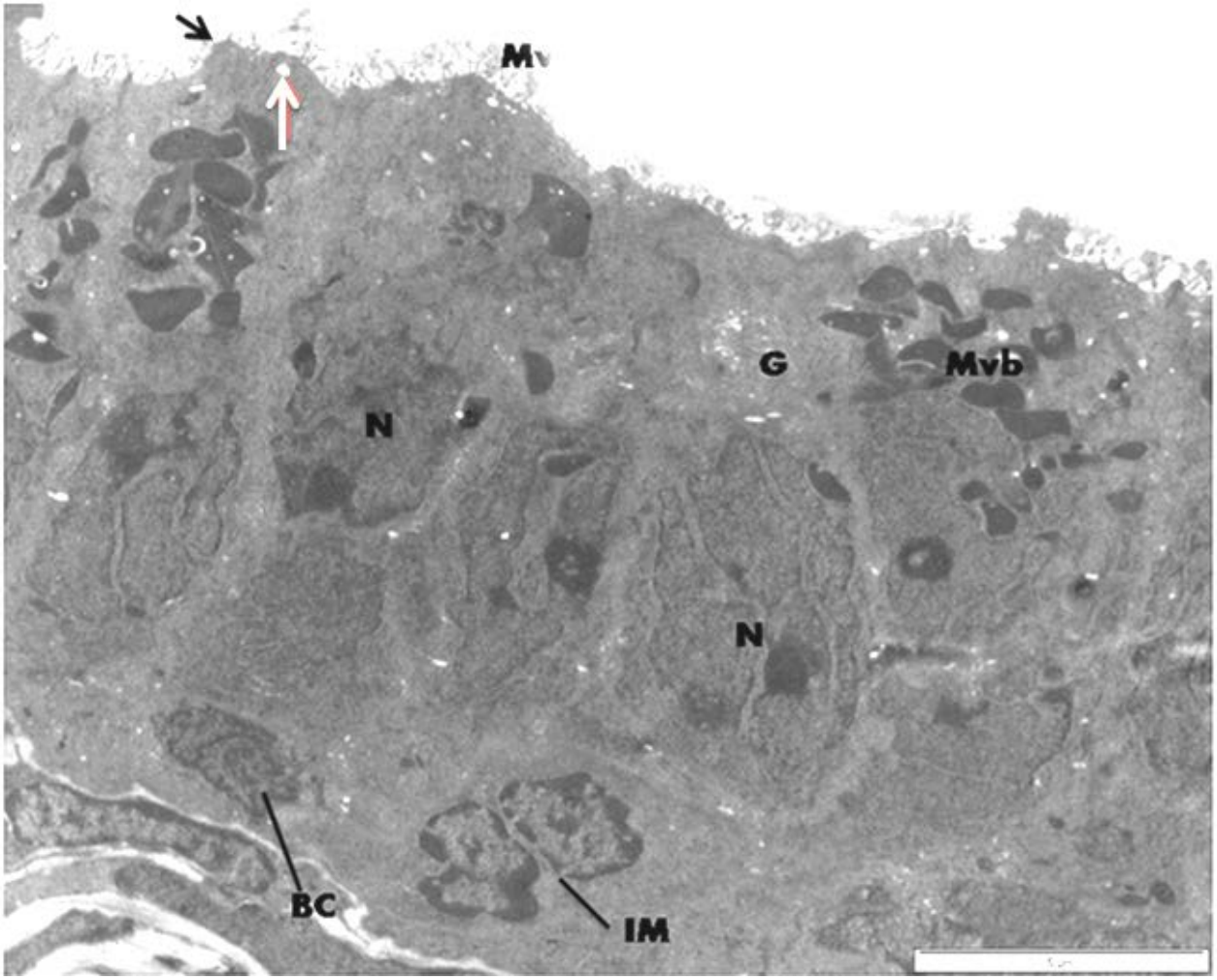

Figure 28: Ultrastructure of the epithelium in the vas deferens of the cane rat. Note the microvilli (Mv), the apical bleb (black arrow) and the subapical vacuoles (white arrow) as well as the Golgi complex (G), multivesicular and coated vesicles (Mvb) at the supranuclear area of the principal cells. The lobulated nuclei of principal cells (N), basal cells (BC) and intraepithelial macrophage (IM) are also present. Picture taken with Phillips CM10 TEM at 80 KV. Mag. X 20,000. **Scale bar =5µm**

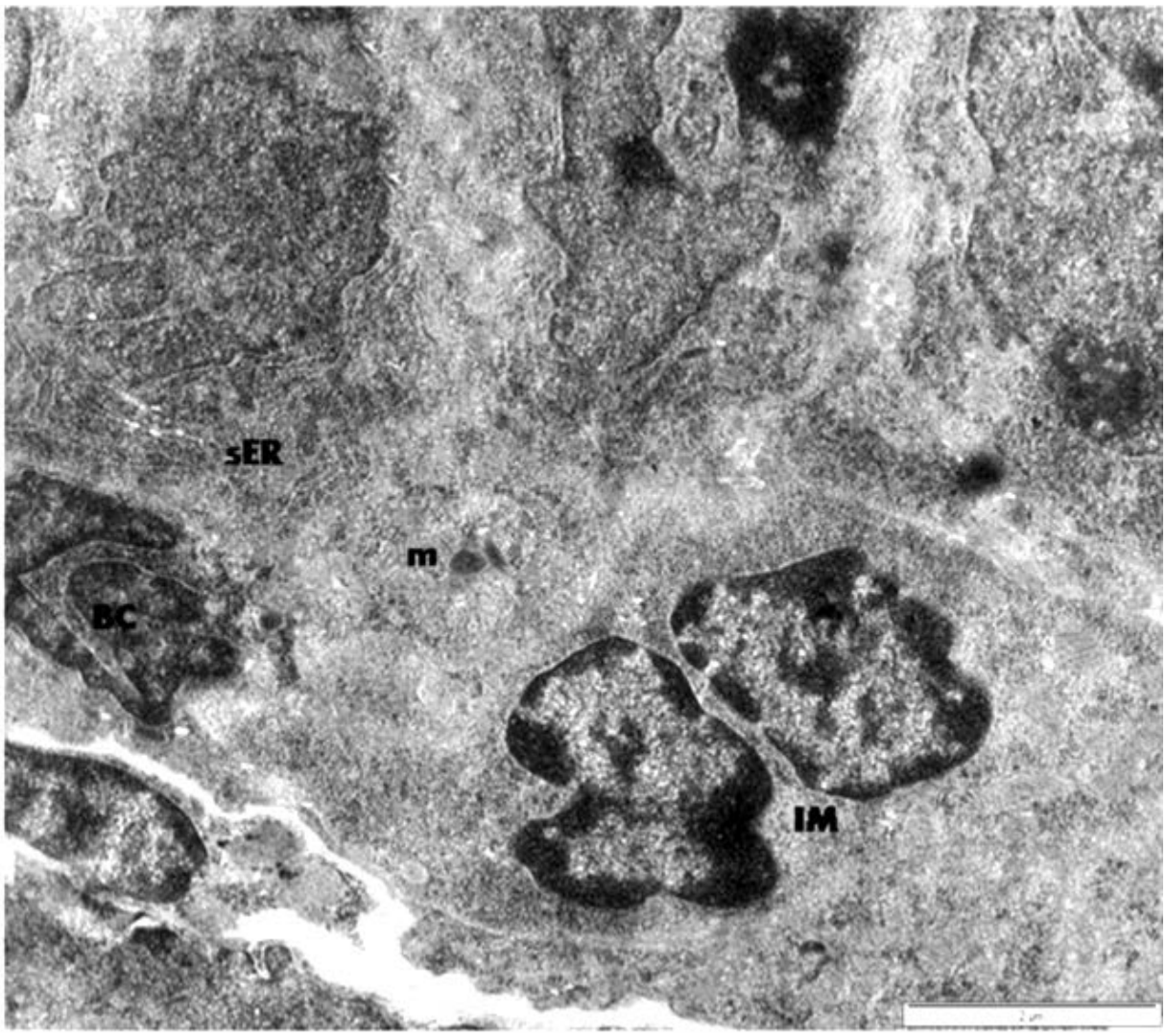

Figure 29: Ultrastructure of the basal epithelium of the vas deferens of the cane rat. Note the presence of smooth endoplasmic reticulum (sER) and mitochondria (m) at the infranuclear area of the principal cells. The basal cell (BC) and intraepithelial macrophage (IM) are also present. Picture taken with Phillips CM10 TEM at 80 KV. Mag. X 20,000. **Scale bar =2µm**

3.2.5 ACCESSORY SEX GLANDS

3.2.5.1. PROSTATE

3.2.5.1.1 Morphometry

Table 6: The Gross morphometry of the prostate gland in the greater cane rat

	Mean± Standard Deviation
Body weight (g)	2230 ±40
Prostate gland weight (g)	0.75 ±0.21*
Prostate gland relative weight (%)	0.034%
Prostate gland volume (cm^3)	0.76 ±0.21*

*The value represents the average of both left and right prostate glands

Table 7: Histo-morphometric parameters of the central and peripheral zones of the prostate gland in the greater cane rat

	Central zone (µm)	***Peripheral zone (µm)***
Epithelial height (µm)	11.67 ±1.23	11.79 ±1.30*
Epithelial fold height (µm)	190.97 ±52.77	58.85 ±13.27**
Luminal diameter (µm)	51.85 ±22.27	407. 74 ±85.80**
Fibromuscular thickness (µm)	13.82 ±3.24	12.34 ±2.32**

*$p > 0.01$; there is no significant difference between the central and peripheral zones

**$p < 0.01$; there is significant difference in these parameters between the central and the peripheral zones

3.2.5.1.2 Gross Appearance

The prostate gland in the greater cane rat weighed 0.75 ±0.21g with a volume of 0.76 ±0.21cm^3 (Table 6). It was a paired, tarry-brown coloured, lobulated gland located on either side of the bladder neck partly covering the internal orifice of the pelvic urethra (Fig. 30A& B). The right prostate revealed four distinct lobes; cranial, dorsal, lateral and ventral lobes relative to the urinary bladder while the left prostate had three indistinct lobes (Fig 30B & C). The right cranial lobe, which appeared as the smallest, related with the vesicular gland, the coagulating gland and urinary bladder whereas the lateral lobe touched the vesicular and coagulating glands. While the dorsal lobe partly covered the pelvic urethra, the ventral lobe related to the bladder and urethra (Fig. 30B &C). The left prostate lobes; dorsal, ventral and lateral also relate with the bladder, pelvic urethra, vesicular and coagulating glands (Fig. 30B& D). Each lobe opened with its distinct duct into the main excretory duct which subsequently opened into the internal orifice of the pelvic urethra (Fig 30B, C&D).

3.2.5.1.3. Histology

Histologically, each lobes of the prostate gland in the cane rat was covered by thin dense irregular connective tissues that send trabeculae into gland tissue dividing it into lobules. Each lobule consisted of secretory epithelium thrown into folds and surrounded by fibromuscular stroma from the trabeculae that housed blood vessels, nerves and lymphatics (Fig. 31A&B). Two histologically distinct types of lobules, corresponding to the two zones of the glands were recognized. The central zone, which was the gland part closer to the pelvic urethra, had lobules with almost round outline, abundant epithelial folding that nearly occlude the lumen and fibromuscular tissues of 13. 82 ±3.24µm thick, surrounding them (Fig 31A).The peripheral zone,

which was the part of the gland distant to the urethra, had lobules with wide lumen and relatively slightly less fibromuscular tissues of 12. 34 ±2.32µm thick, surrounding it (Fig 31B, Table 7). The secretory epithelia, which were the same for both zones except for their arrangement, were lined predominantly by simple cuboidal cells and scarce basal cells. The cuboidal cell which was approximately 11.73 ±1.25µm high had round fairly eccentric nucleus with prominent nucleolus (Fig 31C & D, Table 7).

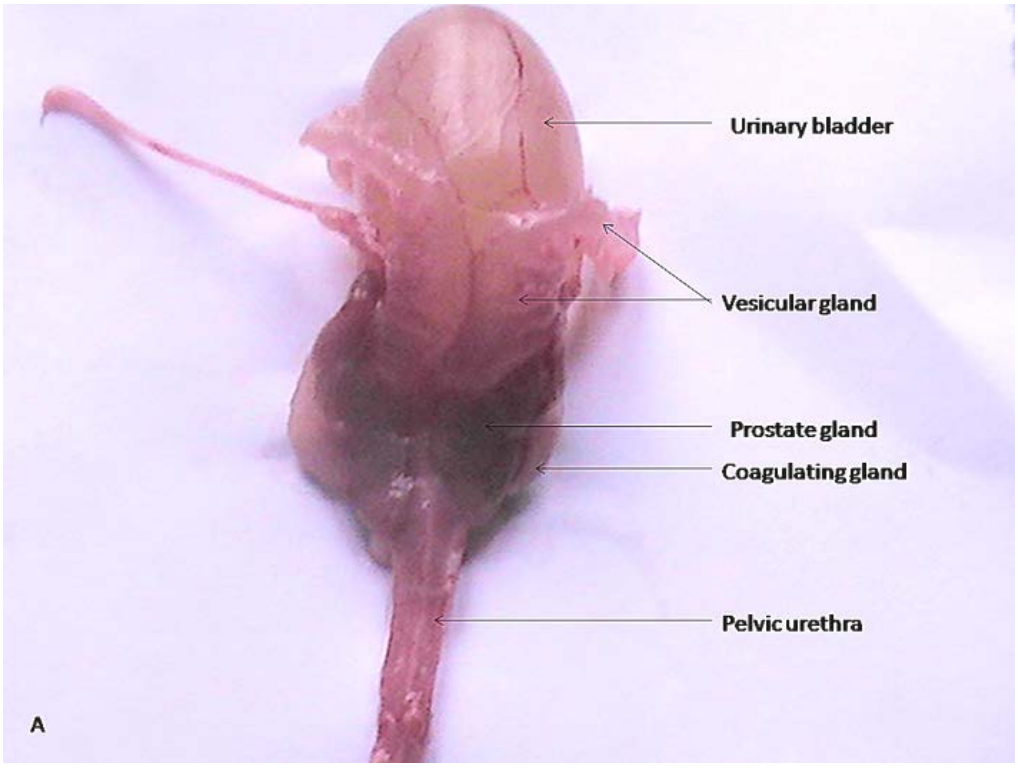
Urinary bladder
Vesicular gland
Prostate gland
Coagulating gland
Pelvic urethra
A

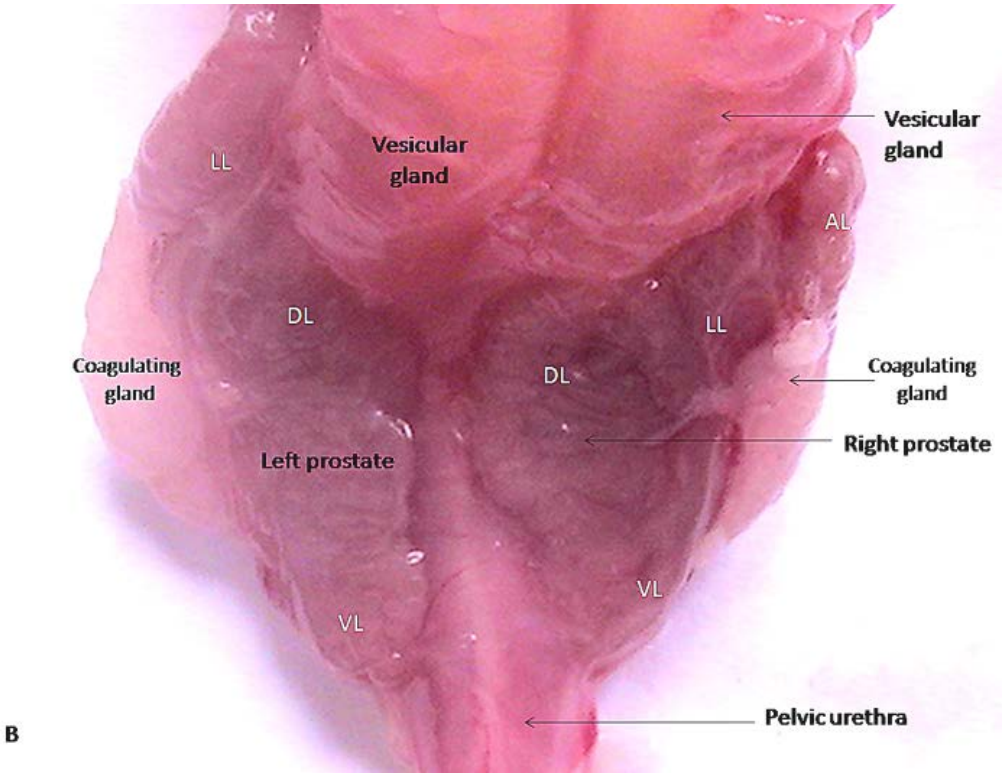
Vesicular gland
LL
Vesicular gland
AL
DL
LL
Coagulating gland
DL
Coagulating gland
Right prostate
Left prostate
VL
VL
Pelvic urethra
B

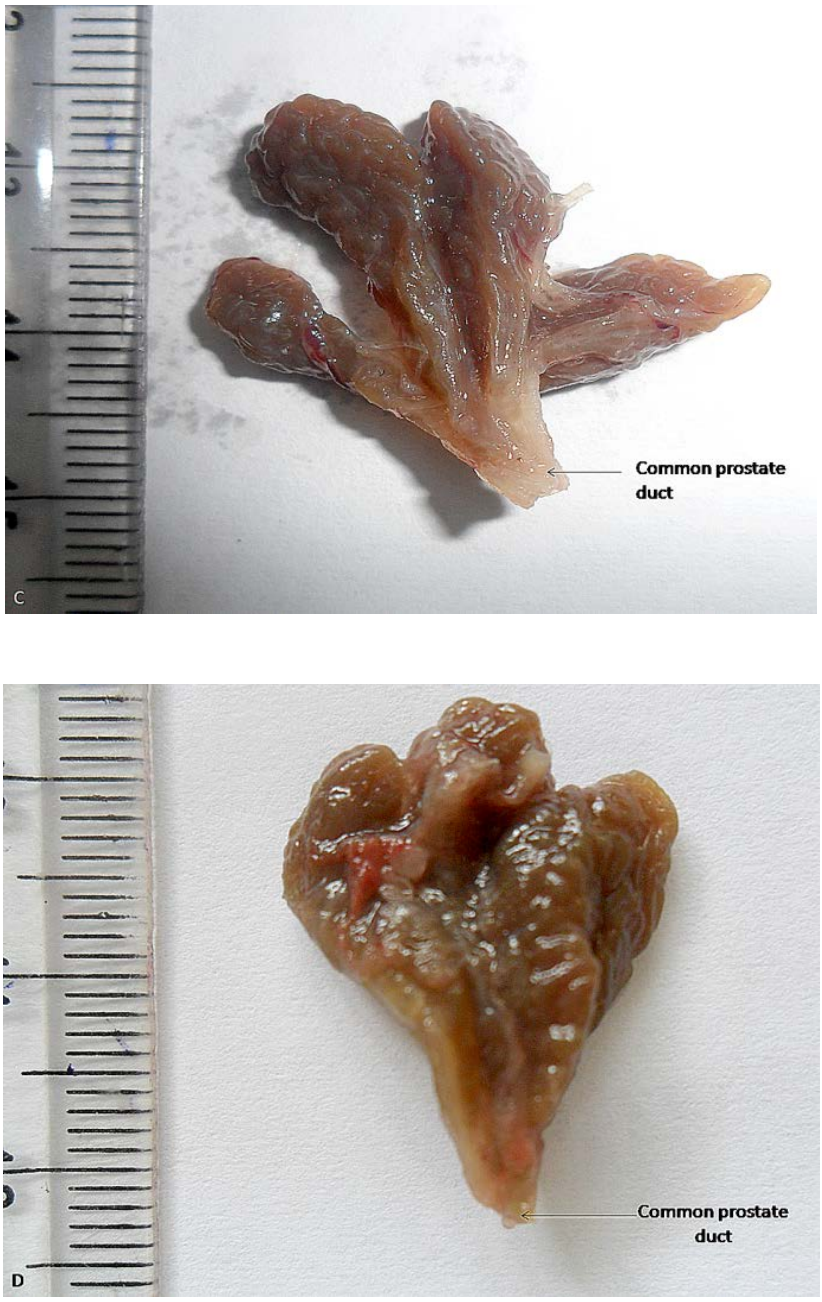

Figure 30: Photographs of the gross appearances of the prostate gland in the greater cane rat. Figure A showed the dorsal view of the prostate position relative to vesicular and coagulating glands and the urinary bladder. Figure B shows the dorsal view of the different positions of lateral (LL), dorsal (DL) and ventral (VL) lobes on the left and right prostate as well as the accessory lobe (AL) on the right prostate. Figure C was the isolated right prostate with the four distinct lobes while Figure D was the isolated left prostate with its three indistinct lobes and both showing common duct that opens into the pelvic urethra. Mag. **X5**

Figure 31A&B: Photomicrograph of the prostate gland in the greater cane rat. Figure A showed the secretory lobules (L) of the central zones. Note the epithelial foldings that almost occlude the lumen and the fibromuscular stroma (Fs) as well as blood and lymphatic vessels (arrows) in the stroma. Figure B is the secretory tubules (L) of the peripheral zones showing the less folded epithelium and the fibromuscular stroma (Fs) as well as the blood and lymphatic vessels (arrows) that pervade the stroma. **H&E.** Mag. X 100. **Scale bar: 50µm.**

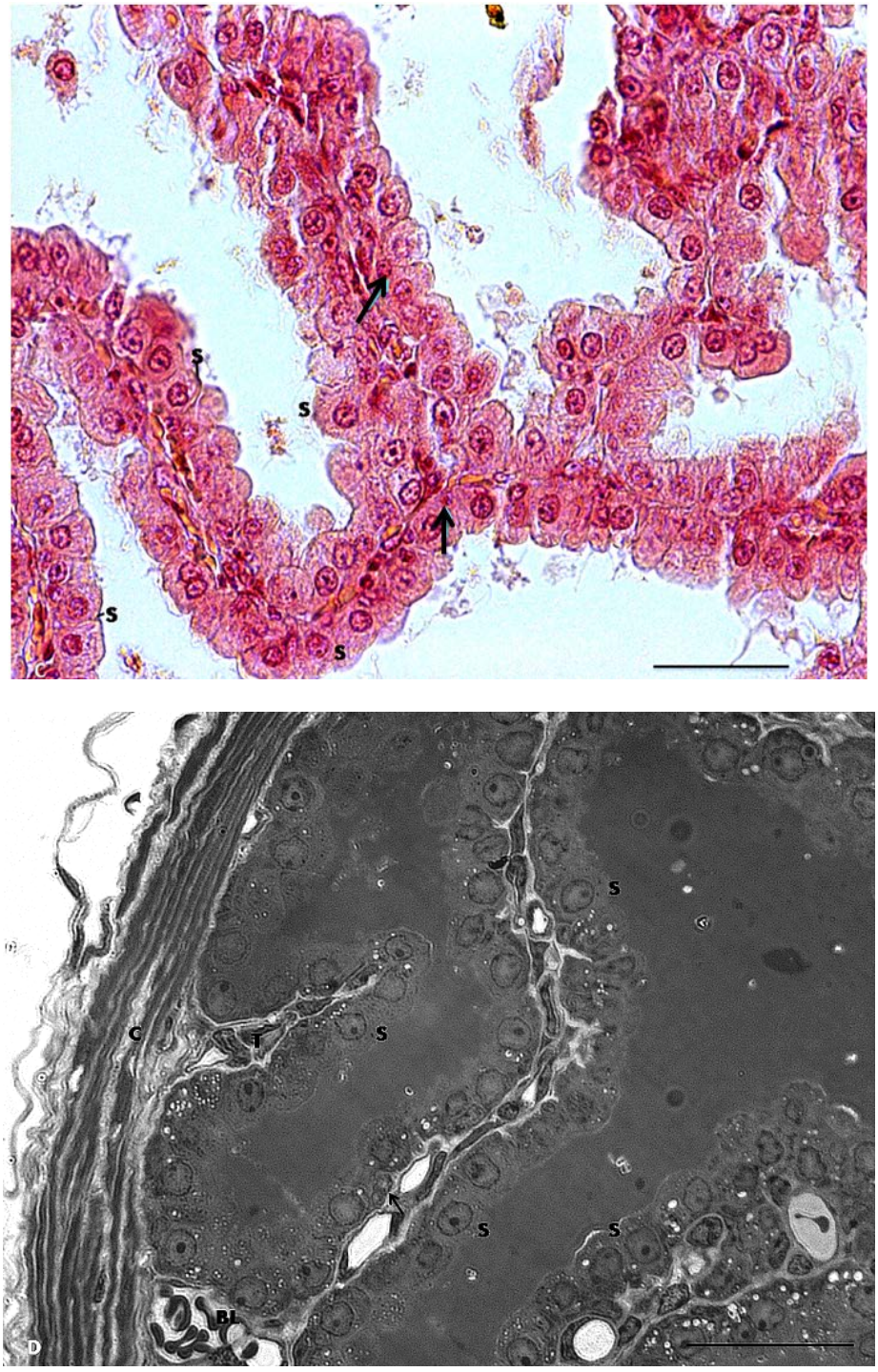

Figure 31C&D: Photomicrograph of the prostate gland in the greater cane rat. Figure C reveals the simple cuboidal (S) and the scarces basal (black arrows) cells that line the epithelium. **H&E,** Mag. X1000. **Scale bar: 20µm.** Figure D shows the epithelial folding made up of the simple cuboidal (S) and basal cells (arrows) and the thin lamina propriae (T) emanating from the fibromuscular stroma (C) containing blood vessels (BL). **Toluidine blue,** Mag. X1000. **Scale bar: 20µm.**

3.2.5.1.4. Ultrastructure

The predominant cuboidal cells of the prostate epithelium in the greater cane rat has a round centrally located euchromatic nucleus with prominent nuclear pores, narrow peripheral rims of heterochromatin and very conspicuous nucleolus (Fig. 32A).The supranuclear cytoplasm of these cells contains endoplasmic reticulum and numerous round-to-oval mitochondria as well as Golgi apparatus with some secretory vacuoles around it (Fig. 32A&B). There was also the presence of densely-packed secretory vacuoles close to the apical plasmallema of these cells while the apical surface was covered by moderately well developed coat of short microvilli and some bleb-like apical projections (Fig. 32A&B). The basal part of the cells has scanty cytoplasm and few mitochondria. While these cells were joined laterally by tight junctional complexes and desmosomes, intercellular lacunae were seen between these cells and the basal cells (Fig. 32C).

The scarce round-to-polygonal shaped basal cells in the prostate epithelium have scanty cytoplasm containing poorly developed mitochondria, endoplasmic reticulum and Golgi apparatus. The indented nuclei of these cells are largely euchromatic with no nucleolus (Fig. 32A&B). Some intraepithelial autonomic nerve terminals were seen close to the basal lamina of the epithelium (Fig. 32A).

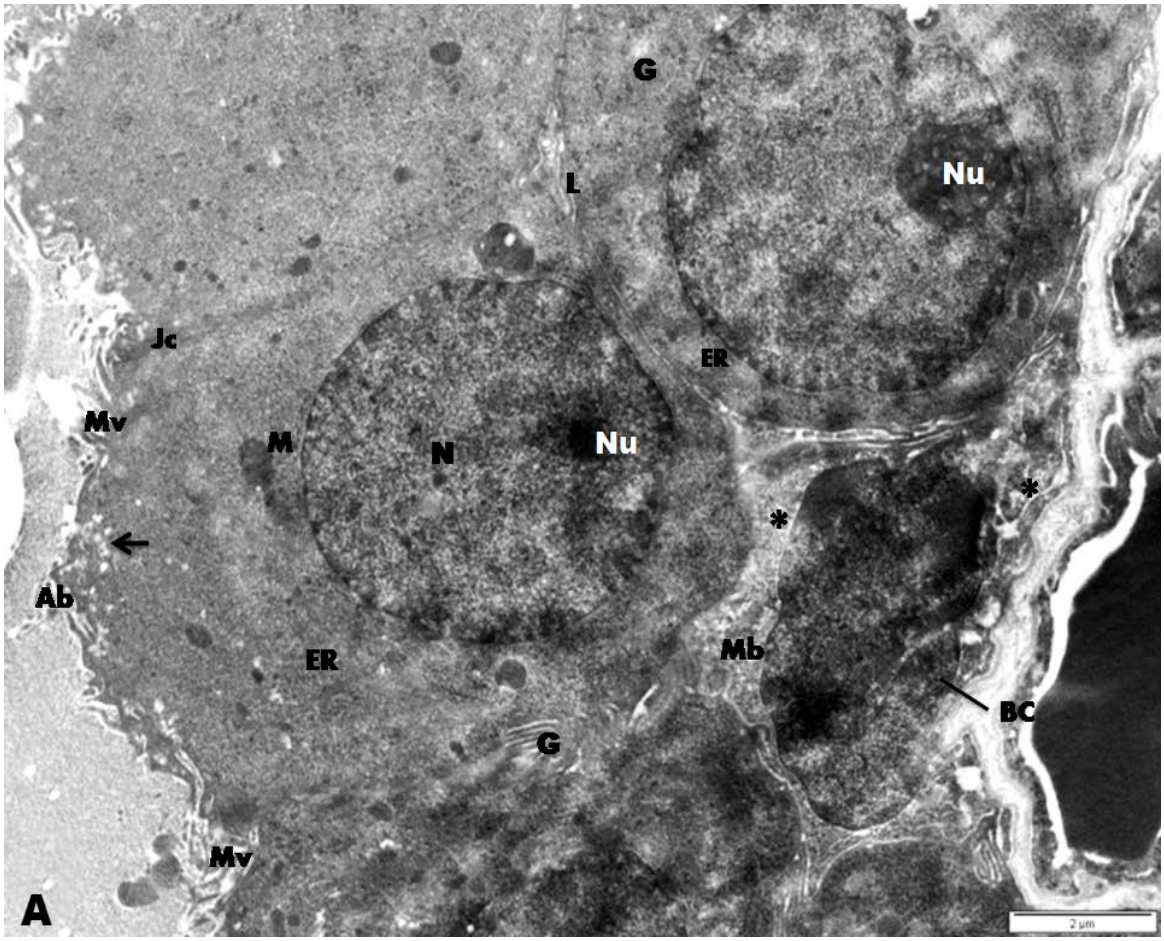

Figure 32A: The ultrastructure of the prostate gland epithelium in the greater cane rat showing cuboidal cells and basal cell (BC). In the cuboidal cell, note the apical bleb-like projection (Ab), the microvilli (Mv), junctional complex (Jc), the mitochondria (M), nucleus (N) with prominent nucleolus (Nu), endoplasmic reticulum (ER), Golgi apparatus (G) and the intercellular lacunae (L) between two cuboidal cells. In the basal cell, note the mitochondria (Mb) and poorly developed Golgi complex (Asterick). Also note the presence of intraepithelial autonomic nerve terminal (Ia) close to the basal lamina. . Picture taken with Phillips CM10 TEM at 80 KV. Mag. X 30,000. **Scale bar: 2µm**

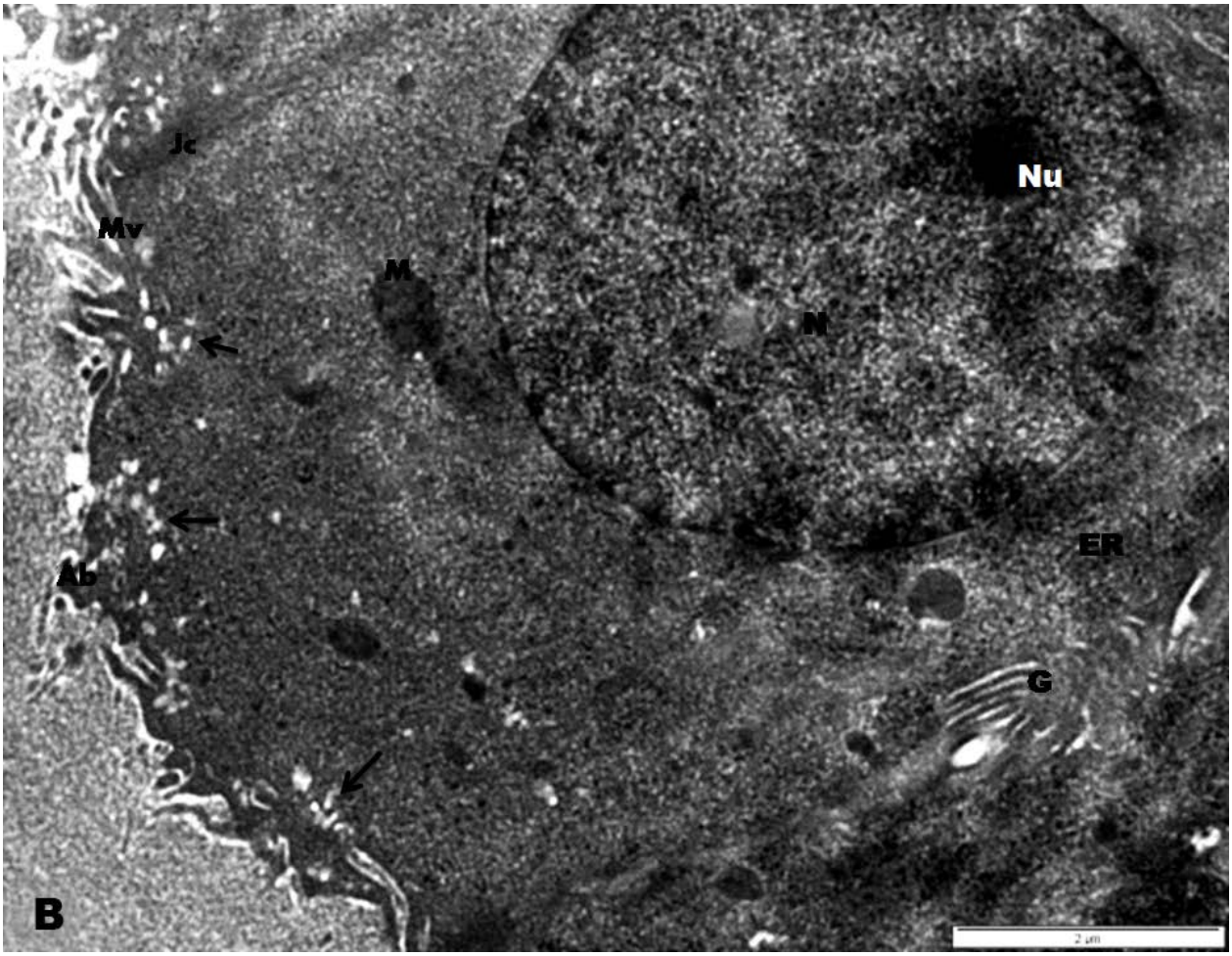

Figure 32B: Ultrastructure of the enlarged apical part of the simple cuboidal cell of the prostate gland epithelium of the greater cane rat. Note the secretory vacuoles cluster (arrows), prominent Golgi (G) and endoplasmic reticulum (ER). . Picture taken with Phillips CM10 TEM at 80 KV. Mag. X 30,000. **Scale bar: 2µm**

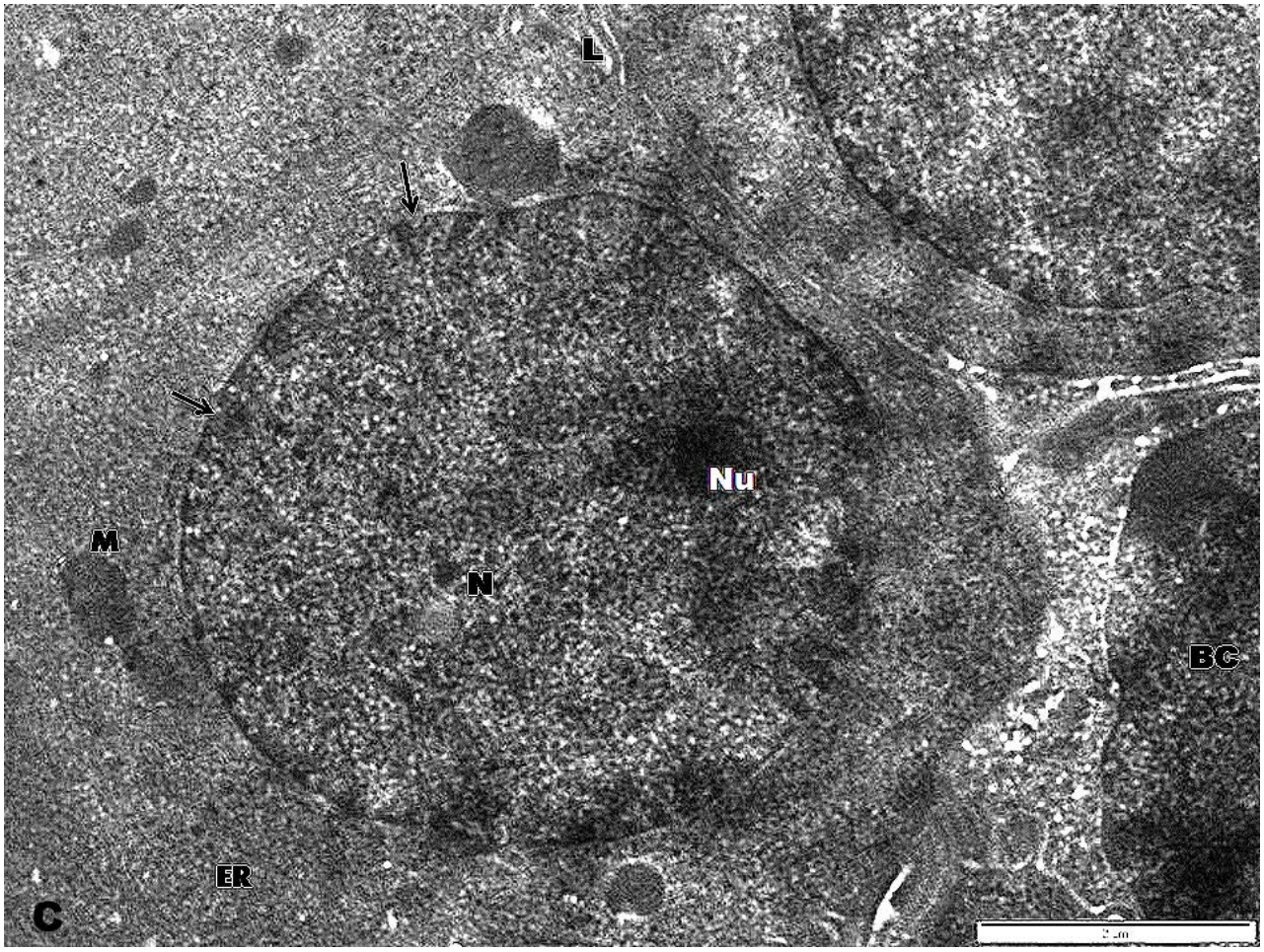

Figure 32C: Ultrastructure of the enlarged basal part of simple cuboidal cell and part of the basal cell (BC) of the prostate gland epithelium in the greater cane rat. Note the intercellular lacuna (L) and the pore (arrows) on the nucleus (N). Mitochondria (M) and Endoplasmic reticulum (ER) are also present. . Picture taken with Phillips CM10 TEM at 80 KV. Mag. X 30,000. **Scale bar: 2µm**

3.2.5.2. COAGULATING GLAND

3.2.5.2.1. Morphometry

Table 8: Morphometric values of the coagulating gland in the greater cane rat.

	Mean ± Standard Deviation
Body weight (g)	2230 ±40
Coagulating gland weight (g)	1.00 ±0.48
Coagulating gland relative weight (%)	0.045%
Coagulating gland volume (cm^3)	0.92 ±0.30
Coagulating gland epithelial height (µm)	12.20 ±2.8
Coagulating gland luminal diameter (µm)	287.02 ±95.2
Coagulating gland nuclear diameter (µm)	5.50 ±0.72
Coagulating gland stromal thickness (µm)	13.98 ±0.78
Coagulating gland fold height(µm)	95.75 ±3.50

3.2.5.2.2. Gross Appearance

In the greater cane rat, the coagulating gland is a paired, cream-coloured, transparent gland located at the angle between the vesicular and prostate glands (Fig. 33A). It is situated ventrolateral to the prostate, ventral to the vesicular gland but dorsolateral to the neck of the urinary bladder. Each triangularly-shaped gland, located at either side of the midline, weighed 1.0 ±0.48g, measured 0.92 ±0.30cm^3 in volume (Fig. 33B, Table 8)

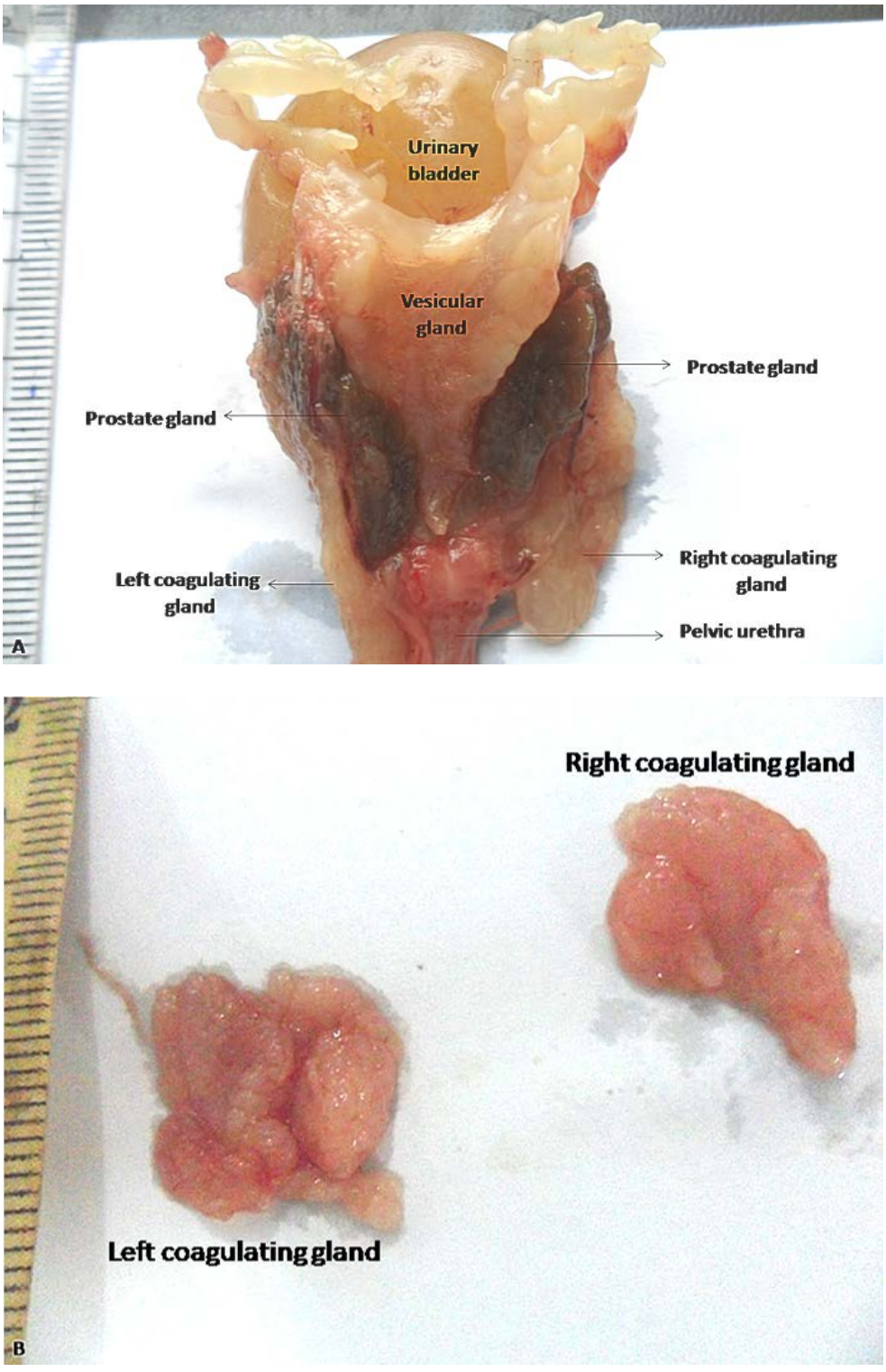

Figure 33: Photographs of the coagulating gland in the greater cane rat. (***A***): Gland relative to prostate gland, vesicular gland, urinary bladder and the pelvic urethra (Dorsal view). (***B***): Isolated coagulating glands.

3.2.5.2.3. Histology

The gland was covered by dense irregular capsule which divides the gland into secretory lobes (Fig. 34a). Each lobe is made up of folded mucosa surrounded by connective tissue stroma that is 13.98 ±0.78µm in thickness and contains smooth muscles and blood vessels (Fig. 34a & c). The glandular mucosal fold with average height of 95.75 ±3.50µm was composed of epithelial cells underlied by thin stromal septa that originate from the stroma (Fig. 34b & c). The simple cuboidal epithelium with the height of 12.2 ±2.8µm, was made up predominantly of principal cells at different stages of secretion intermingled with occasional basal cells (Fig. 34b & c). The apical surfaces of the non-secreting cells were studded with microvilli while the secreting cells have prominent apical blebs of various heights. Each cell nucleus was usually located at the basal half but often displaced to the centre or apical half by the secretions of the cell. This nucleus also measures 5.5 ±0.72µm in diameter and contained conspicuous nucleolus (Fig 34c& d, Table 8).

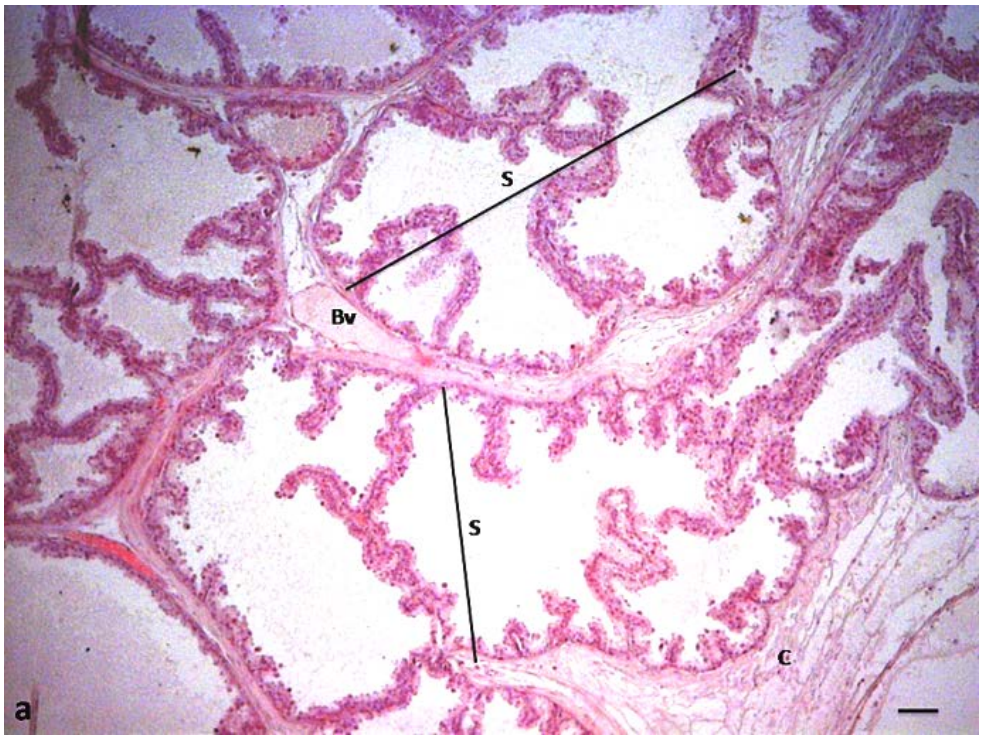

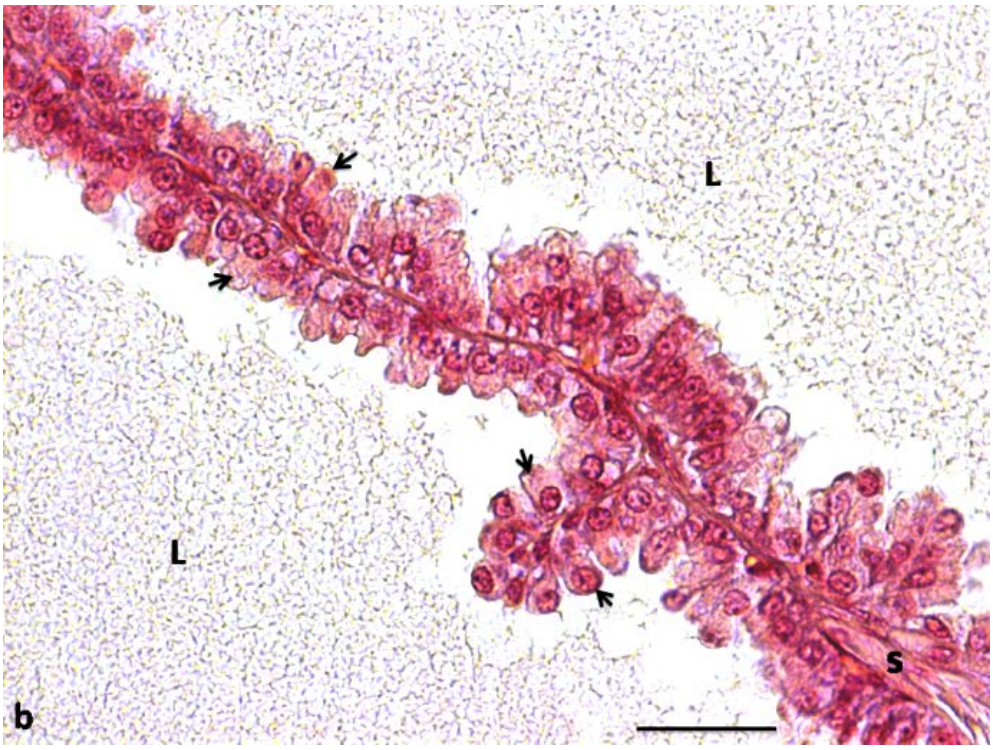

Figure 34a &b: Histology of the coagulating gland of the greater cane rat. ***(a)*** shows secretory lobes (S), the stromal blood vessels (Bv) and the capsule (C) that surrounds each lobe. H&E, **Scale bar: 50µm.** ***(b)*** Mucosal fold that projects into the secretory lumen (L) consisting of the principal cells (arrows) underlain by stromal septum (S). H&E, Mag. X1000. **Scale bar: 20µm**.

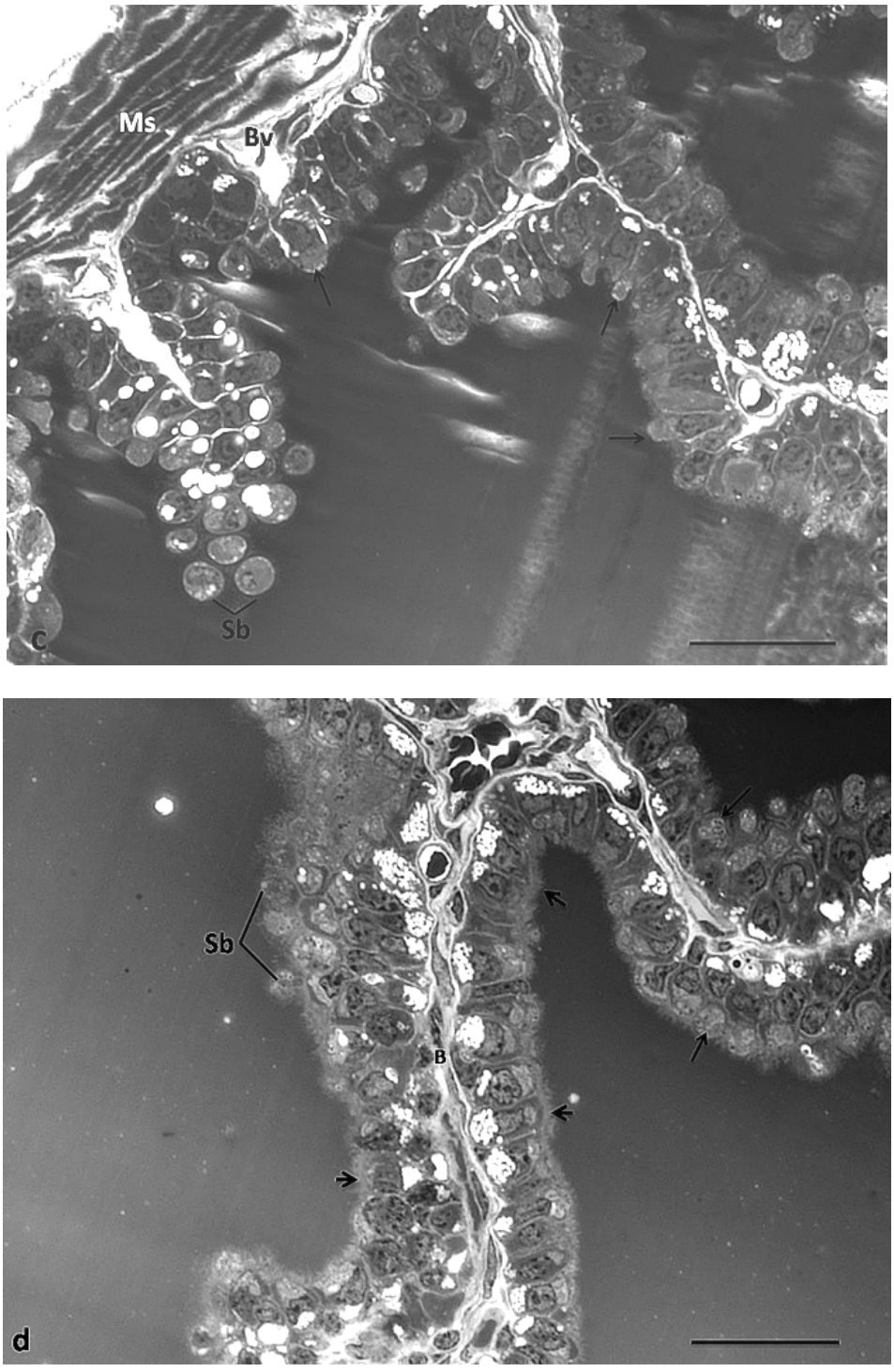

Figure 34c &d: Histology of the coagulating gland of the greater cane rat. ***(c)*** Secretory cells with their apical blebs (arrows) and some of the secreted blebs (Sb) released in the lumen and the stroma muscular layers (Ms) ***(d)*** Non-secreting cells (short arrows) with microvilli, some secreting cells (long arrows) with their apical blebs and released blebs (Sb) as well as basal cells (B). **Toluidine blue**,**grayscale.** Mag. X1000. **Scale bar: 20µm**

3.2.2.5.3. Ultrastructure

The secretory cells of the coagulating gland in the greater cane rat exhibited some peculiar variation in their fine structural appearances and the blebbing of the apical part. Generally, the apical surfaces of the cells were covered with abundant microvilli but cells forming blebs had relatively scanty microvilli depending on the stage of their bleb formation (Fig 35a & b). However, once the bleb was released into the glandular lumen, the microvilli were fully restored (Fig. 35a). The apical bleb contains numerous secretory granules and secretory vesicles. While some of the secretory granules showed electro-lucent matrix with granular and homogenous contents, others were seen to have dense inclusions of varying sizes (Fig. 35b & c). The secretory vesicles were smaller than the granules and the entire bleb cytoplasm appears granular (Fig. 34c). At secretion the bleb together with its contents and membrane pinches off from the cell into the lumen (Fig. 35a & b).

The apical cytoplasm of the cells before the formation of the bleb contains abundant Golgi apparatus with both dilated and flattened profiles some of which are arranged in straight or curved pattern. Secretory granules at different stages of development were also observed close to the Golgi cisternae (Fig. 35b &c). The supranuclear cytoplasmic matrix, which contains few mitochondria, is relatively more than that at the basal part (Fig. 35c).The irregularly shaped nuclei of the secretory cells are euchromatic with heterochromatic patches attached to the nuclear membrane and centrally placed prominent nucleolus (Fig 35b&d). The basal part of the cell is almost completely filled with cisternae of the rough endoplasmic reticulum and numerous secretory vesicles and scanty cytoplasm. The cisternal cavities are dilated with homogenous electron-lucent content (Fig. 35d).

The basal cells were flat with flattened elongated nuclei and scarce cytoplasm. Their notched nuclei were predominantly euchromatic with patches of heterochromatic clumps but completely lacking nucleolus (Fig 35a & d). Few organelles were also observed in the scanty cytoplasm.

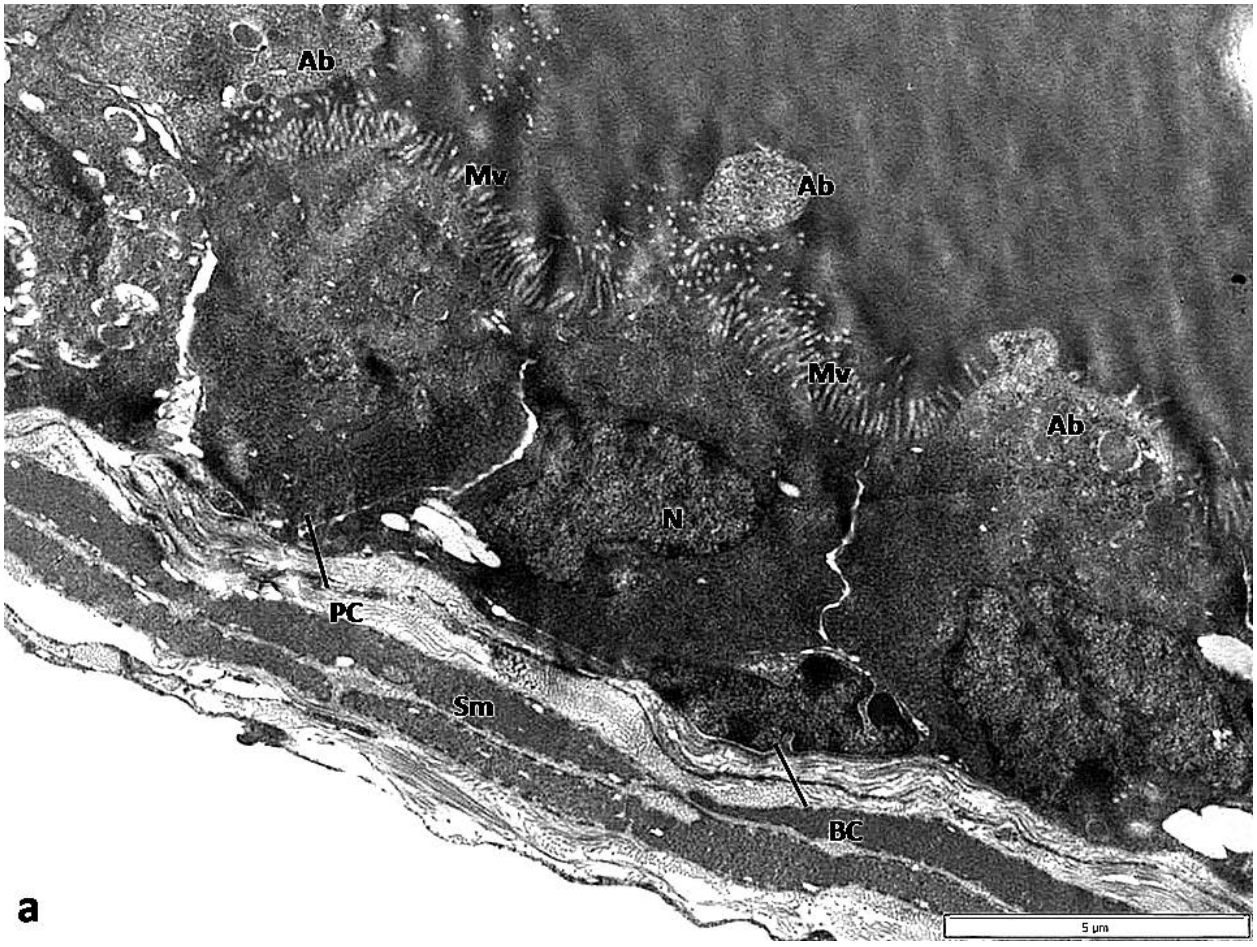

Figure 35a: Ultrastructure of the coagulating gland in the greater cane rat showing the principal (PC) and basal (BC) cells as well as the stromal smooth muscles (Sm). Note the nucleus (N), apical bleb (Ab) at different levels of formation and the microvilli (Mv) on the apical surface of the principal cells. Picture taken with Phillips CM10 TEM at 80 KV. Mag. X 20,000. **Scale bar: 5µm**.

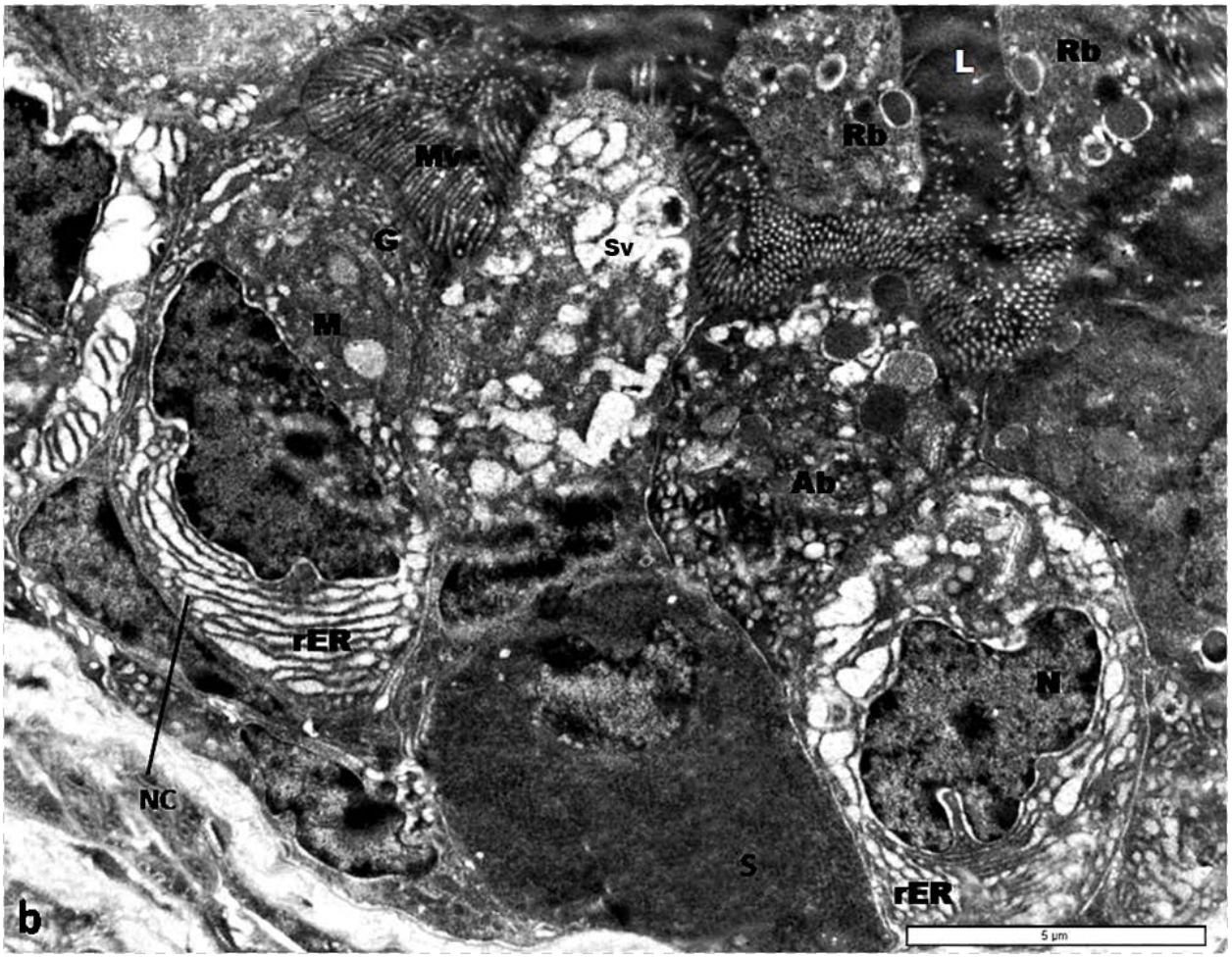

Figure 35b: Ultrastructure of secreting (S) and non-secreting (NC) principal cells in the coagulating gland of greater cane rat. Note the prominent microvilli (Mv), Golgi apparatus (G), secretory granules (M), secretory vacuoles (Sv) and the rough endoplasmic reticulum (rER) in the non secreting cells as well as apical bleb (Ab) on the secreting cells and released blebs (Rb) in the glandular lumen (L). . Picture taken with Phillips CM10 TEM at 80 KV. Mag. X 20,000. **Scale bar: 5µm**.

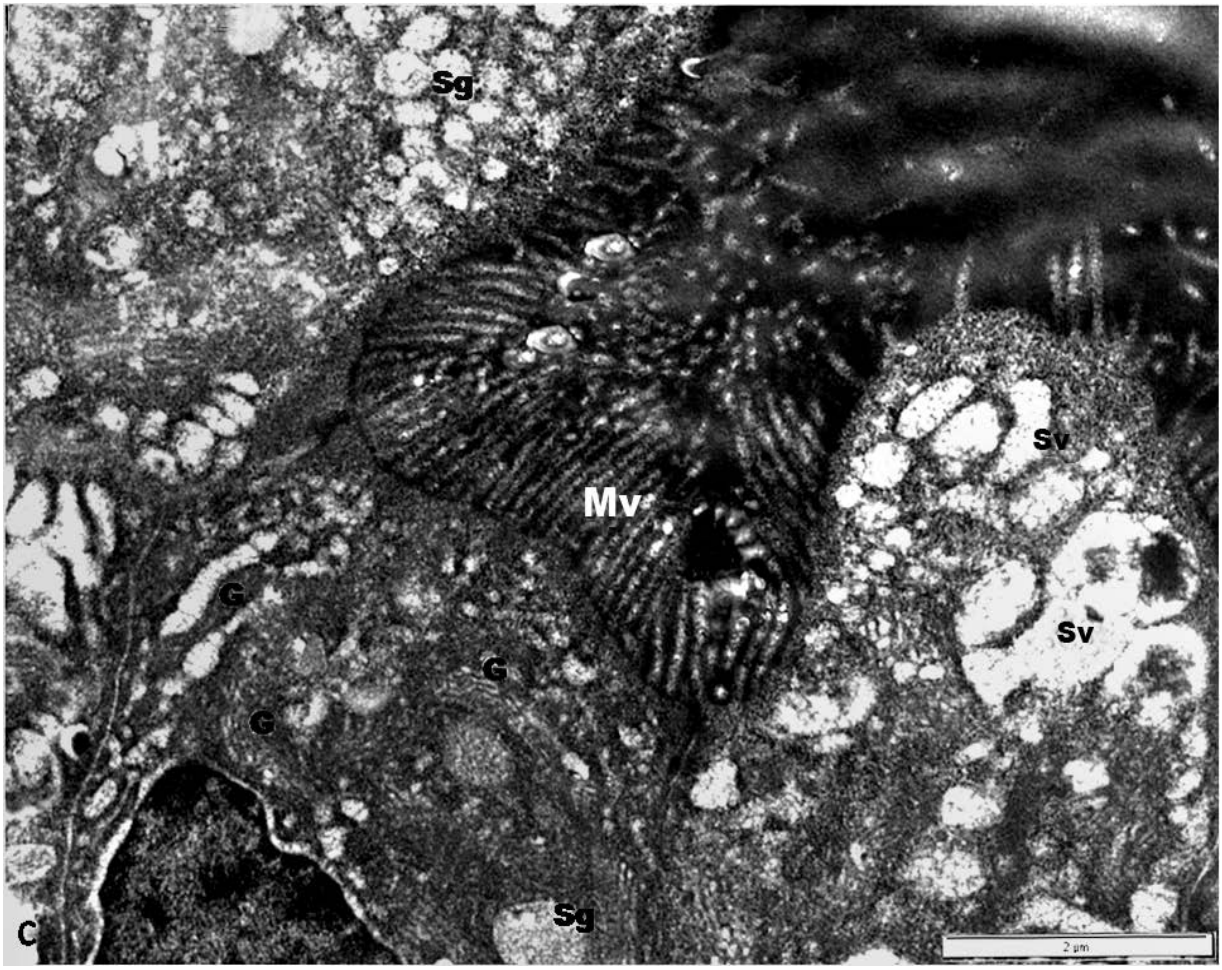

Figure 35c: Ultrastructure of the apical cytoplasm of non secreting principal cell of the coagulating glandof the greater cane rat showing the golgi complexes (G), secretory granules (Sg) and microvilli (Mv) as well as the presence of secretory vacuoles of varying electron-density in the apical bleb of secreting cell. . Picture taken with Phillips CM10 TEM at 80 KV. Mag. X 20,000. **Scale bar: 2µm**

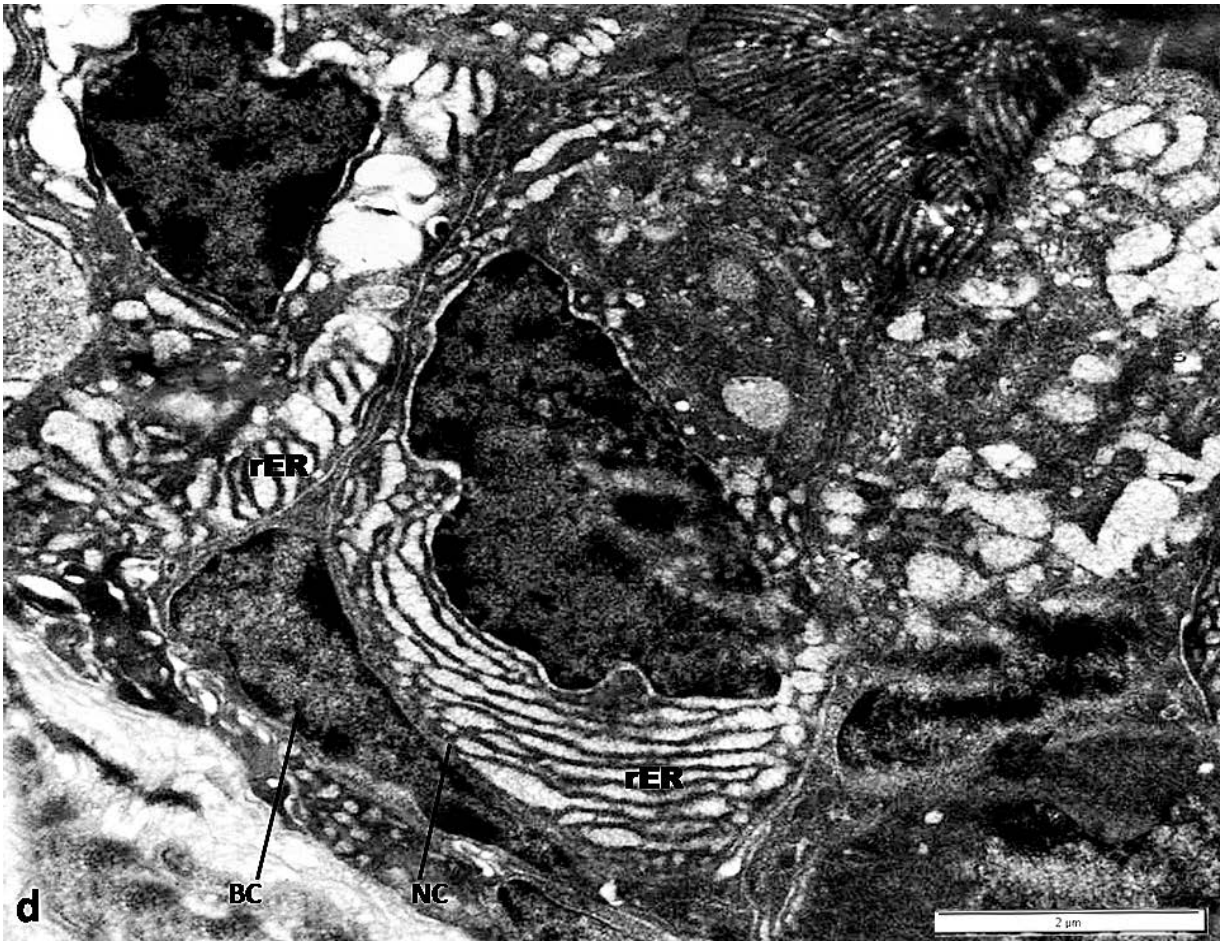

Figure 35d: Ultrastructure of the basal cytoplasm of the principal cells showing the dilated cisternae of rER at the basal part of the non secreting cells (NC). The basal cells (BC) have scanty organelles. Picture taken with Phillips CM10 TEM at 80 KV. Mag. X 20,000. **Scale bar: 2µm**

3.2.5.3 VESICULAR GLAND

3.2.5.3.1 Morphometry

Table 9*: The gross and histometric values of the Vesicular gland in the greater cane rat.*

	Mean ± Standard Deviation
Body weight (kg)	2.23 ±0.40
Vesicular gland weight (g)	1.15 ±0.67
Vesicular gland relative weight (%)	0.05%
Vesicular gland volume (cm^3)	1.03 ±0.50
Vesiculargland length (cm)	5.30 ±1.16
Vesicular gland epithelial height (µm)	12.64 ±1.94
Vesicular gland luminal diameter (µm)	919.47 ±125.13
Vesicular gland nuclear diameter (µm)	5.43 ±0.57
Vesicular gland muscular diameter (µm)	287.40 ±62.32
Vesicular gland epithelial fold height(µm)	321 ±70.26

3.2.5.3.2 Gross Appearance

The vesicular gland in the greater cane rat was a paired transparent and elongated tube, 5.3 ±1.16cm long, 1.03 ±0.5cm^3 in volume and weighing 1.15 ±0.67g constituting 0.05% of the body weight (Table 9). It was located dorsal to the urinary bladder and anterior to the prostate and coagulating glands on either side of the midline (Fig. 36A). Each gland, which anteriorly deviated from the midline, had short finger-like branches but posteriorly converged with the other gland at about the midline to give a Y-shaped outline (Fig. 36B).The branches on each anterior part was 0.5cm in length with pointed extremities while the unbranched posterior part of

the glands tapers into duct that open separately into the pelvic urethra (Fig. 36B &C). The colourless secretions contained within the gland became viscous to gel-like or even solid when exposed.

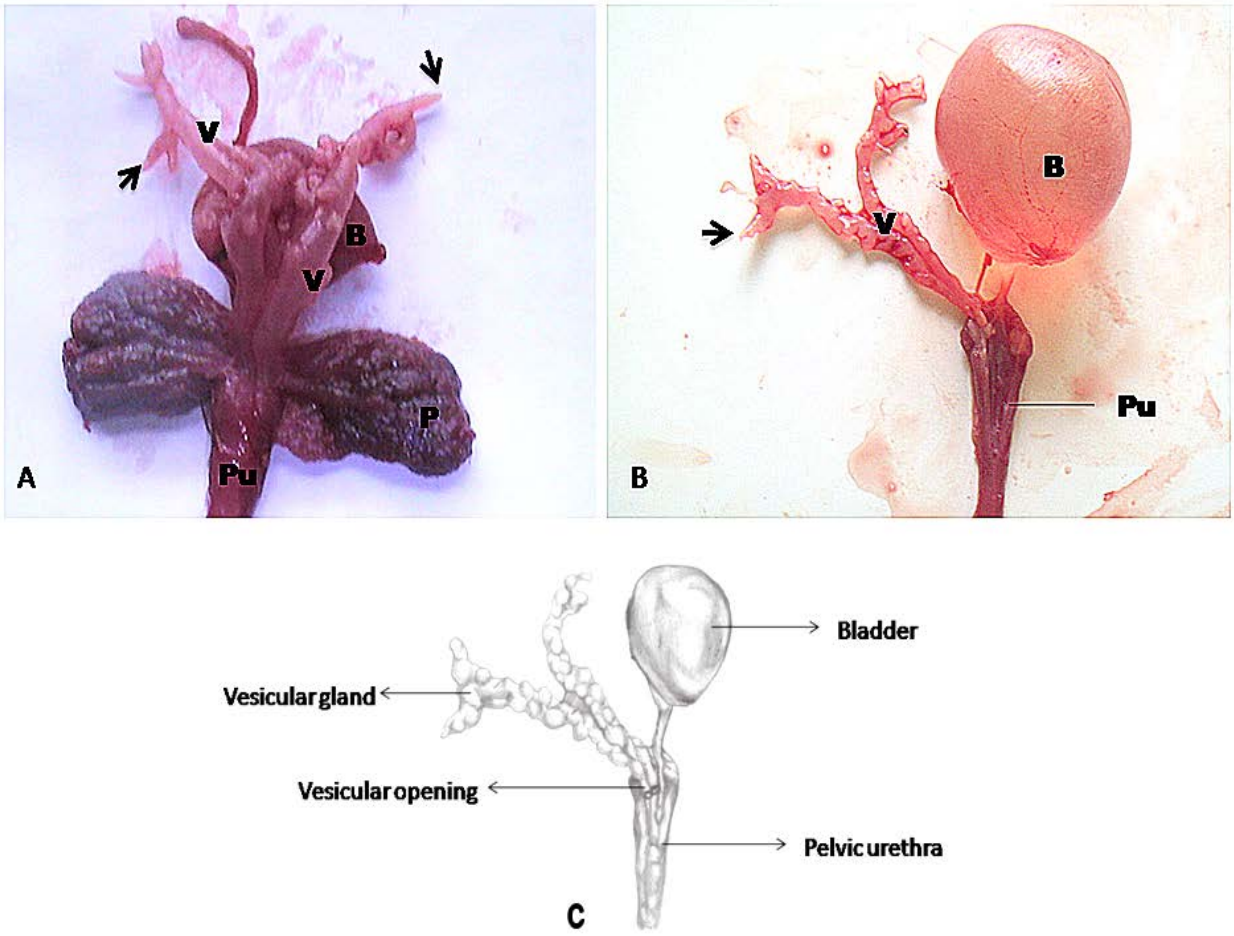

Figure 36: Photographs of the vesicular gland in the greater cane rat. In (***A***) (Dorsal view) note the gland (V) lying dorsal to the urinary bladder (B) and anterior to the reflected prostate gland (P) as they all open into the pelvic urethra (Pu). In (***B***) note the opening of the elongated tubular vesicular gland (V) into the pelvic urethra (Pu) and the urinary bladder (B) with the other glands removed. The branches of the cranial part of the gland are also shown (arrows). (***C***) is the schematic diagram of the vesicular gland. Mag. **X5**

3.2.5.3.3 Histology

The glandular tissues of the vesicular gland in the cane rat were composed of three radially arranged layers: mucosa, muscularis, and adventitia (Fig. 37A). The mucosa was thrown into branching and anastomosing folds resulting in the formation of cavities and recesses with the mucosa (Fig. 37A & C). The fold, with a mean height of 321.53 ±70.26µm, consisted of a secretory epithelium and a thin underlying lamina propria, appearing more abundant in the anterior branched part almost completely occluding the lumen, than the posterior (Fig. 37C). The simple columnar epithelium was about 12.64 ±1.90µm high and contained predominantly principal cells with scarce basal cells (Fig. 37B & D). These principal cells had their nuclei located at the base perpendicular to the lamina propriae, with moderately condensed chromatin and a conspicuous nucleolus (Fig. 37B & D). Each nucleus measures 5.43 ±0.57µm in diameter (Table 7). Under the light microscope, all these cells appear almost similar including the Toluidine-stained sections (Fig. 37C &D). The few basal cells that rest on the epithelial basal lamina had eccentric nuclei with no nucleolus (Fig. 37D). The lamina propria composed mainly of loose connective tissue with fibroblasts, collagen and elastic fibers. The muscular layers which was averagely 287.40 ±62.38µm thick were made up of circular and longitudinally arranged smooth muscle fibres, collagen and elastic fibres as well as blood vessels surrounded by connective tissue adventitia (Fig. 37A & C)

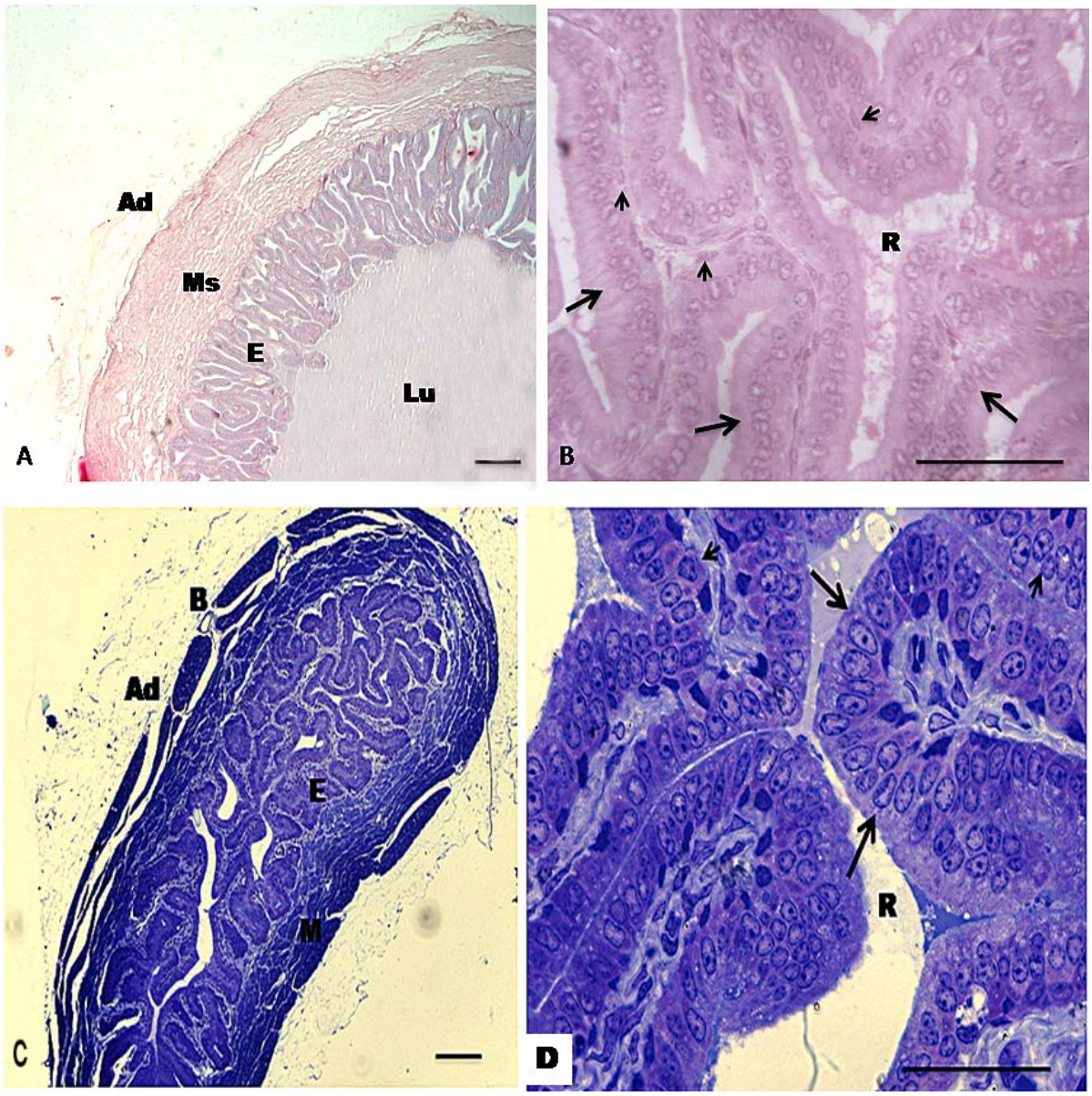

Figure 37: Histology of the walls of the vesicular gland (***A***) and the glandular epithelium (***B***) of the greater cane rat. Note the adventitia (Ad) with some blood vessels; the muscle layers (Ms) and the folded epithelium (E) with the recesses as well as the glandular lumen (Lu). The glandular epithelium (Figure B) with the principal cells (large arrows) and the scarce basal cells (small arrows) as well as the recess (R) formed by the mucosa folding. **Figure C** is the cranial branch of the vesicular gland showing similar layers and the folded epithelium (E) that almost completely occluded the glandular lumen. **Figure D** shows the glandular epithelium with the columnar principal cells (large arrows) and the scarce basal cells (small arrows) as well as the recess (R) formed by the mucosa folding. **H & E** (A & B), **Toluidine Blue** (C & D). **Scale bar**: A & C = 50 µm, B & D = 25 µm. Mag. (A & C) X100; (B & D) X1000.

3.2.5.3.4 Ultrastructure

Two variants of principal cells can be distinguished according to their electron density and cytoplasmic characteristics; the light principal cells (LPC) and the dense principal cells (DPC) (Fig. 38). Both cell types extend from the basement membrane to the glandular lumen and their luminal surfaces were studded with microvilli (Fig. 39A &B). At the lateral plasma membrane beneath the luminal surface, the cells are joined by junctional complexes (Figs. 38& 39A). The light principal cell (LPC), which was predominant, was columnar and relatively less dense containing coated granules and apical blebs. While the apical cytoplasm contained a lot of secretory vacuoles and vesicles, the apical to supranuclear cytoplasm contains well developed Golgi complexes appearing as stacks of parallel elongated saccules with dilated edges (Fig. 39B). The round, indented nucleus of the LPC contains large conspicuous nucleoli and fine euchromatin with some heterochromatic areas usually associated with the nuclear envelope (Fig. 38& 39A&B). One prominent feature of these cells was the presence of abundant mitochondria with some surrounded by the well-developed cisternae of rough endoplasmic reticulum (rER) (Fig. 38& 39B).

The dense principal cell (DPC) was more pyramidal and electron dense than the LPC. They had abundant well developed Golgi complexes located at the mid-apical cytoplasm with less secretory vesicles and vacuoles at the apical cytoplasm (Fig. 38). The rER was also well developed but restricted more to the basal cytoplasm and surrounded by secretory vesicles and mitochondria (Fig. 38&40A). The fairly indented nucleus of the DPC was round and encloses granular dense euchromatin with heterochromatin areas that were either free or associated with the nuclear envelope. Just like the LPC, interdigitations also connected its basal plasma membrane to the basal cells and the underlying basal lamina as well as maintained close contact with the neighbouring cells (Fig. 40A).

The basal cells were flat, wedged between the bases of two or more principal cells with flattened nuclei and scarce cytoplasm (Fig. 38& 40A). The invaginated nucleus enclosed a granular uniformly distributed euchromatin with heterochromatic areas usually associated with the nuclear envelope with no prominent nucleolus (Fig. 40A).The cytoplasm had few cisternae of rough endoplasmic reticulum and mitochondria. Its apical and basal plasma membrane was related to the principal cells and basal lamina by interdigitations (Fig. 40A)

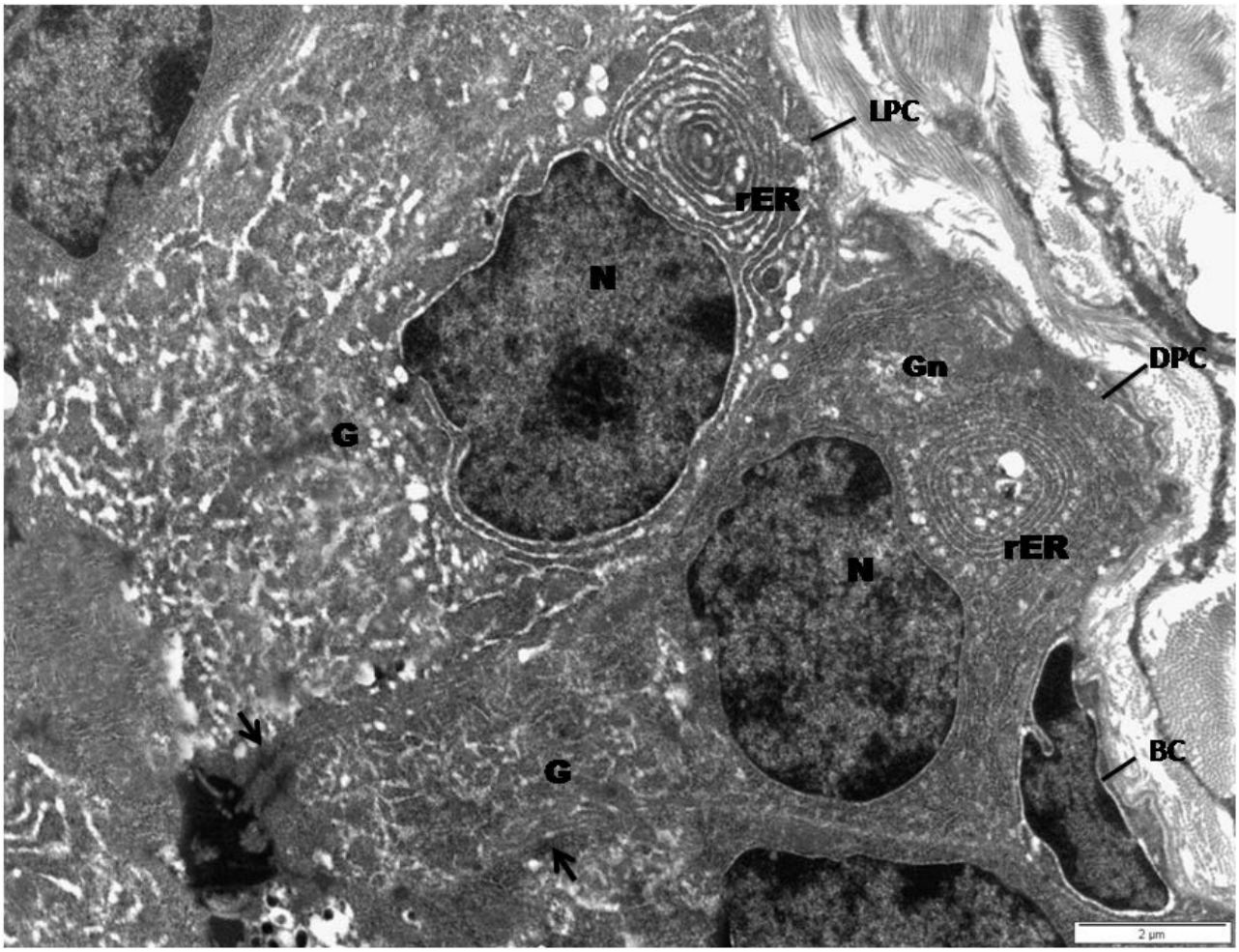

Figure 38: Ultrastructure of the two principal cells in the vesicular gland of the greater cane rat. The light principal cell (LPC) and the dense principal cell (DPC) as well as the basal cell (BC) of the vesicular gland. Note the elaborate rough endoplasmic reticulum (rER), the Golgi complex (G), glycogen (Gn) the nucleus (N) and the junctional complexes (arrows) holding the cells. Picture taken with Phillips CM10 TEM at 80 KV. Mag. X 20,000. **Scale bar**: 2 µm

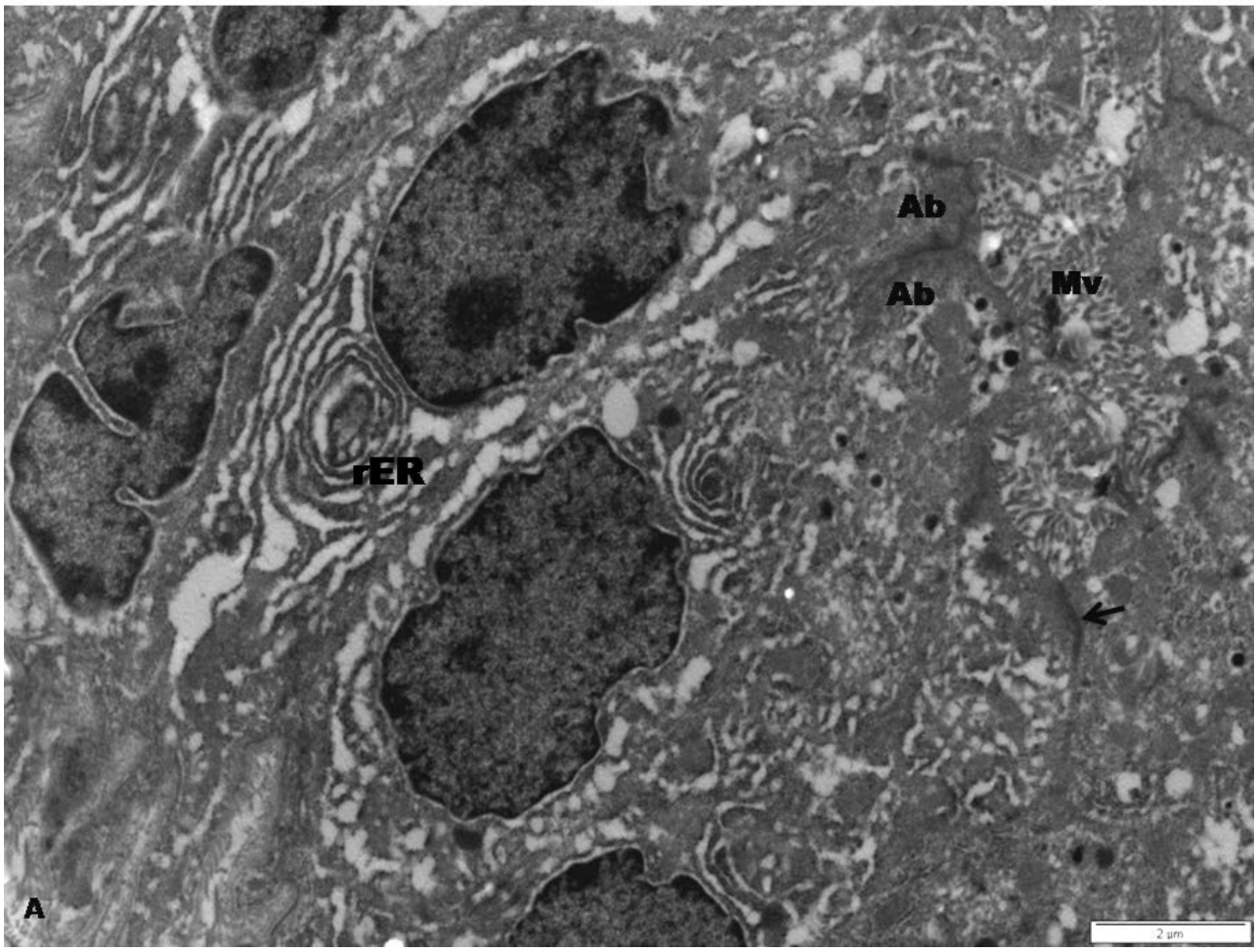

Figure 39A: Ultrastructure of light principal cells (LPC) of the vesicular gland in the greater cane rat. Note the apical bleb (Ab) the abundant microvilli (Mv), rough endoplasmic reticulum (rER) and the Junctional complex (arrow). Picture taken with Phillips CM10 TEM at 80 KV. Mag. X 20,000. **Scale bar**: 2 µm.

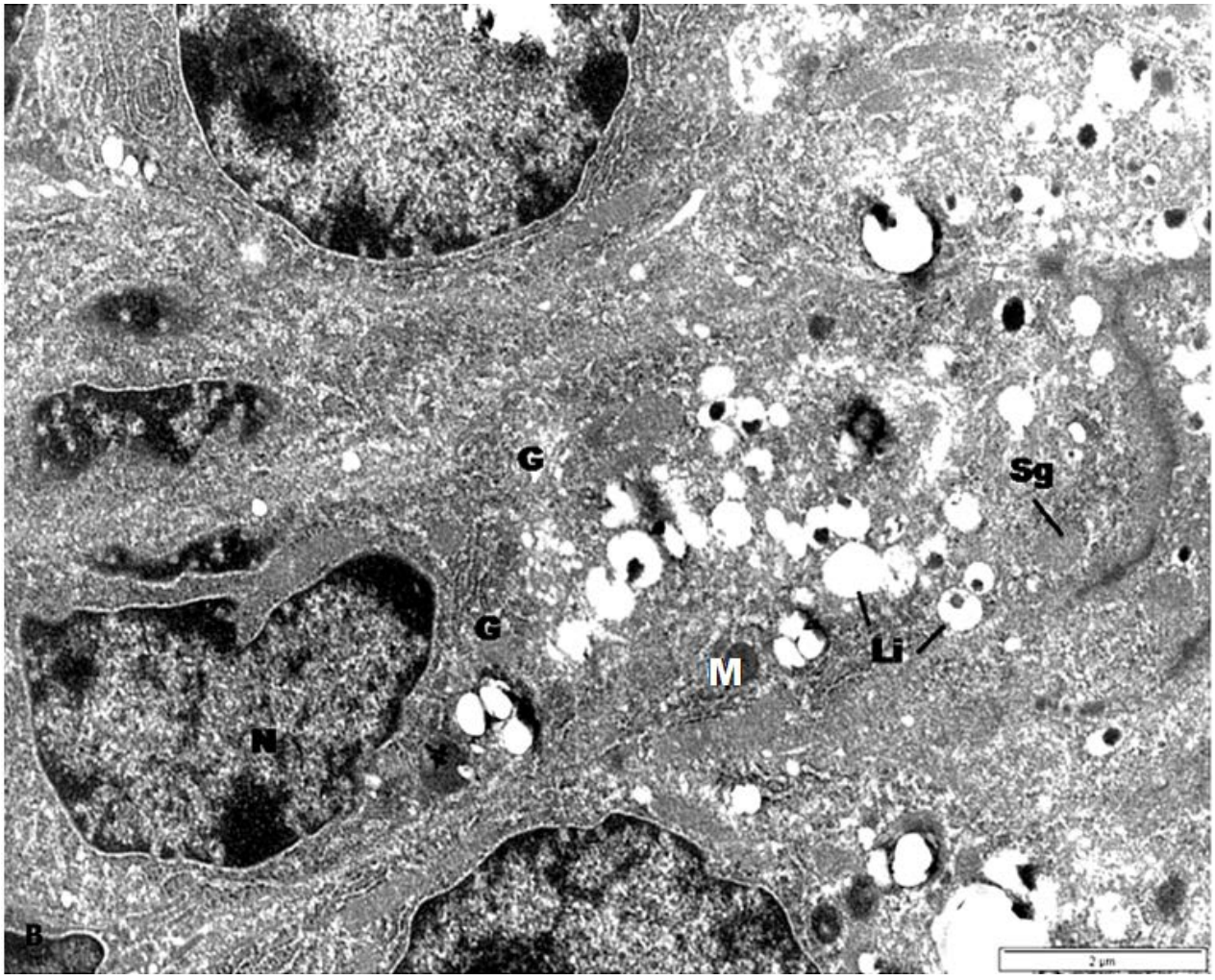

Figure 39B: Ultrastructure of light principal cells (LPC) of the vesicular gland in the greater cane rat showing the apical part of the LPC with the presence of Golgi (G) around the nucleus (N), mitochondria (M), the secretory vesicle (Sg) and abundant Secretory vacuoles (Li). Picture taken with Phillips CM10 TEM at 80 KV. Mag. X 20,000.**Scale bar**: 2 µm.

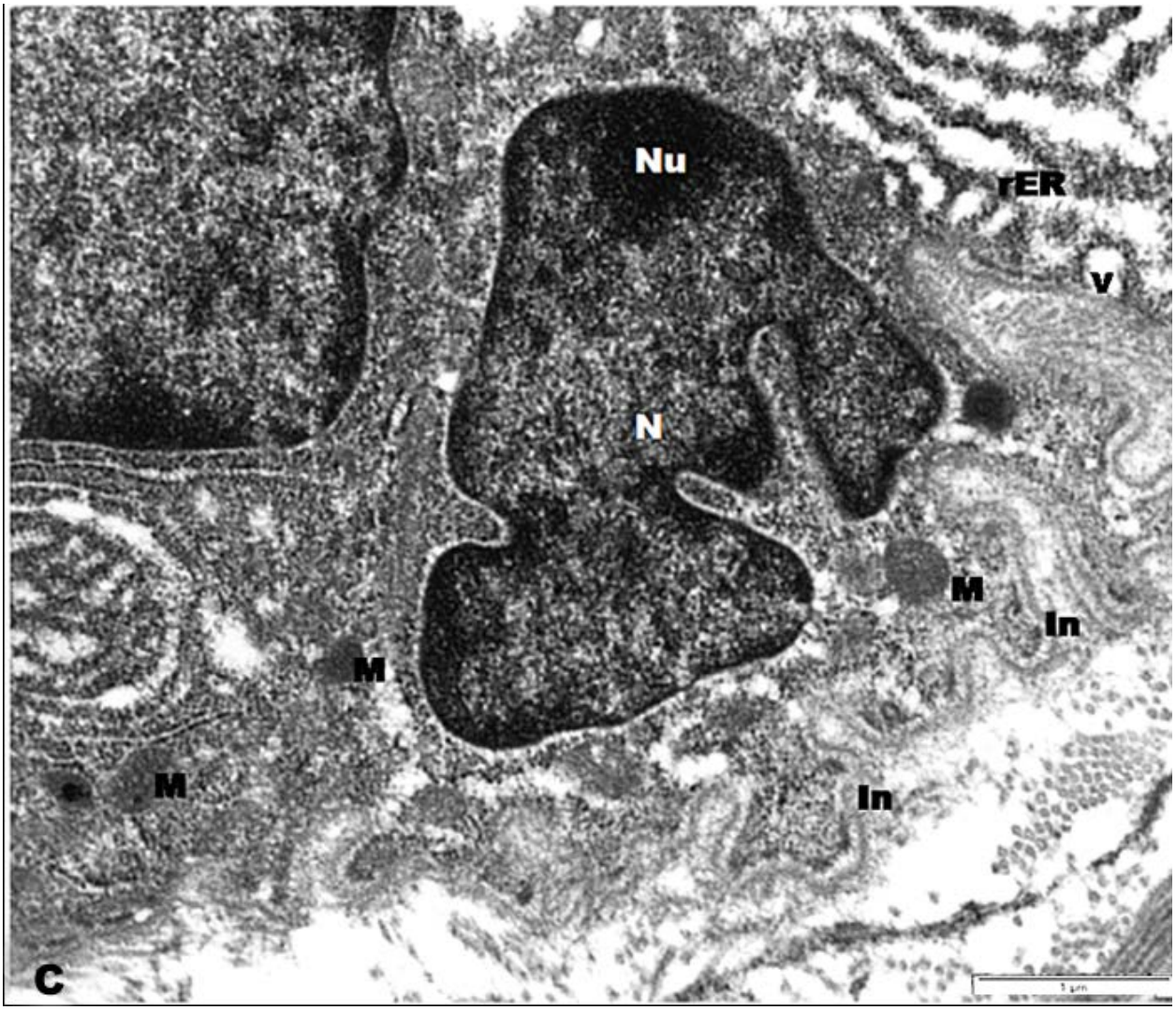

Figure 39C: Ultrastructure of basal part of light principal cells (LPC) further showing the cisternae of the rER with dilated edges and small vesicles (V), abundant mitochondria (M), the interdigitations (In) as well as the nucleus (N) with prominent nucleolus (Nu). Picture taken with Phillips CM10 TEM at 80 KV. Mag. X 30,000. **Scale bar**: 1 µm

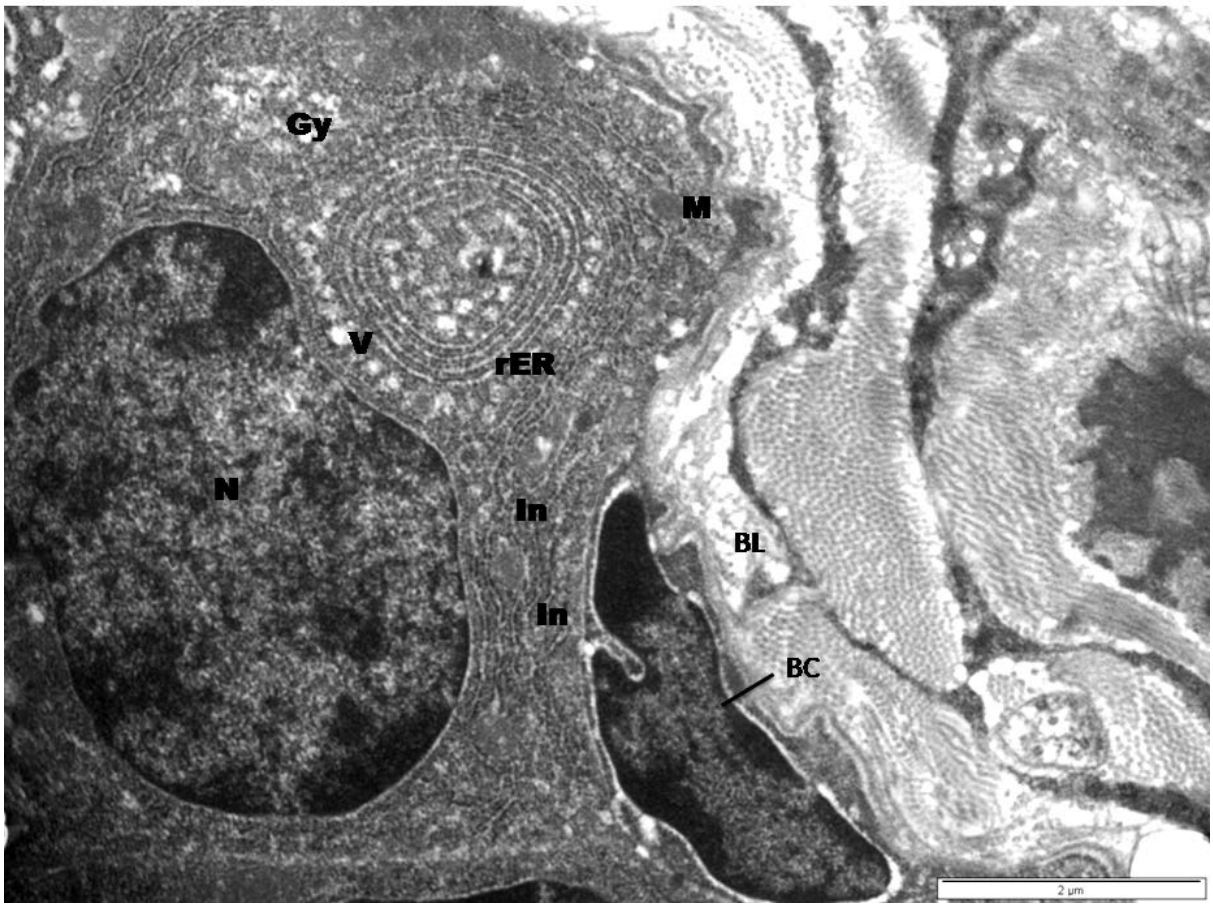

Figure 40A: Ultrastructure of the basal part of dense principal cell (DPC) and basal cell of the vesicular gland in the greater cane rat. Note the mitochondria (M), the cisternae of rough endoplasmic reticulum (rER) with small vesicles (V), the interdigitations (In) between the DPC, basal cells (BC) and basal lamina (BL). Also note the fairly indented nucleus (N) and glycogen (Gn). Picture taken with Phillips CM10 TEM at 80 KV. Mag. X 20,000. **Scale bar**: 2 µm

3.2.5.4 BULBOURETHRAL GLAND

3.2.5.4.1 Morphometry

Table 10: The gross and histo-morphometric values of the bulbourethral gland of the greater cane rat.

	Mean	Standard deviation
Total Body weight (g)	2230	±0.40
Bulbourethral weight (g)	0.19	±0.06
Bulbourethral relative weight (%)	0.008	
Bulbourethral volume (ml)	0.24	±0.08
Bulbourethral diameter (cm)	0.63	±0.17
Secretory epithelial height (µm)	14.15	±0.92
Secretory unit diameter (µm)	39.98	±3.86

Table 11: The coefficient of correlation among animal age, weights of the testis bulbourethral, vesicular, prostate and coagulating glands of the greater cane rat.

	Age(month)	*Testis weight (g)*	*Vesicular weight (g)*	*Prostate weight (g)*	*Coagulating weight (g)*	*Bulbourethral weight (g)*
Age (month)	1					
Testis (g)	0.17	1				
Vesicular weight (g)	0.20	0.27	1			
Prostate weight (g)	0.37	0.29	0.76	1		
Coagulating weight (g)	0.37	0.40	0.60	0.73	1	
Bulbourethral weight (g)	0.08	0.44	0.44	0.53	0.73	1

3.2.5.4.2 Gross Appearance

The bulbourethral gland in the greater cane rat was a paired gourd-shaped gland located dorsolaterally, one on each side of the pelvic urethra (Fig. 41A & B). The gland was surrounded by the bulbocavernosus muscles in the region of the cruz of the penis. Each gland, with an average volume of 0.24ml ±0.08µm and an average diameter of 0.63 ±0.17µm, weighed 0.199 ±0.06g, forming about 0.008% of the body weight (Table 10). While the weight of this gland correlated positively with the weights of the vesicular (r = 0.44) and the prostate glands (r = 0.53), it showed a strong positive correlation with the coagulating gland (r = 0.73) (Table 11). The glands projected caudolaterally from the point of its opening into the urethra through a relatively long excretory duct that pierced the wall of the pelvic urethra at the crux of the penis where it opened. It was yellowish in colour in the fresh state with a smooth shining surface (Fig. 41A & C).

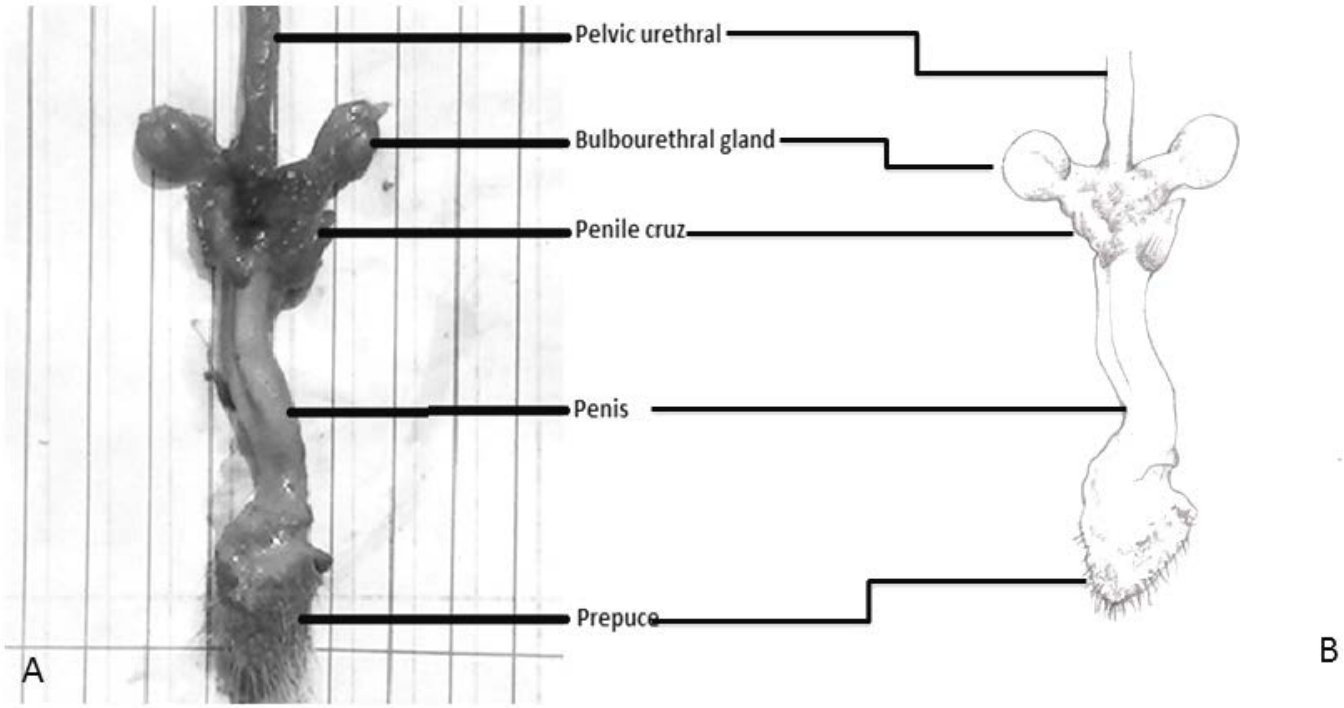

Figure 41: A) showed dissected part of the male reproductive tract of the greater cane rat. **B** is the schematic representation. Note the position of the bulbourethral gland relative to the pelvic urethra and the cruz of the penis. **C** is the photograph of the isolated gourd or pea-shaped paired bulbourethral gland in the greater cane rat. Mag. **X5**

3.2.5.4.3 Histology

Histologically, the bulbourethral gland in the greater cane rat was divided into lobes by both thin connective tissue capsules and striated skeletal muscles (Fig. 42) while the lobes were further divided into lobules by the capsules. Each lobule contains variable number of round secretory units or endpieces which were compact tubuloalveolar glands radiating from a central excretory ductule lined by pseudostratified epithelium (Fig. 43A). The ductules opened into ducts that subsequently open into the main excretory duct. The round secretory units consisted of 8-10 pyramidal to columnar epithelial cells with flattened, basally located nuclei and granule-filled cytoplasm that surrounded a narrow lumen (Fig. 43B). These secretory units had an average diameter of 39.98 ±3.86µm and a mean epithelial height of 14.15 ±0.92µm (Table 10). Surrounding the endpieces and excretory ducts were interstitial tissues that contain abundant smooth muscles and blood vessels (Fig. 42& 43B).

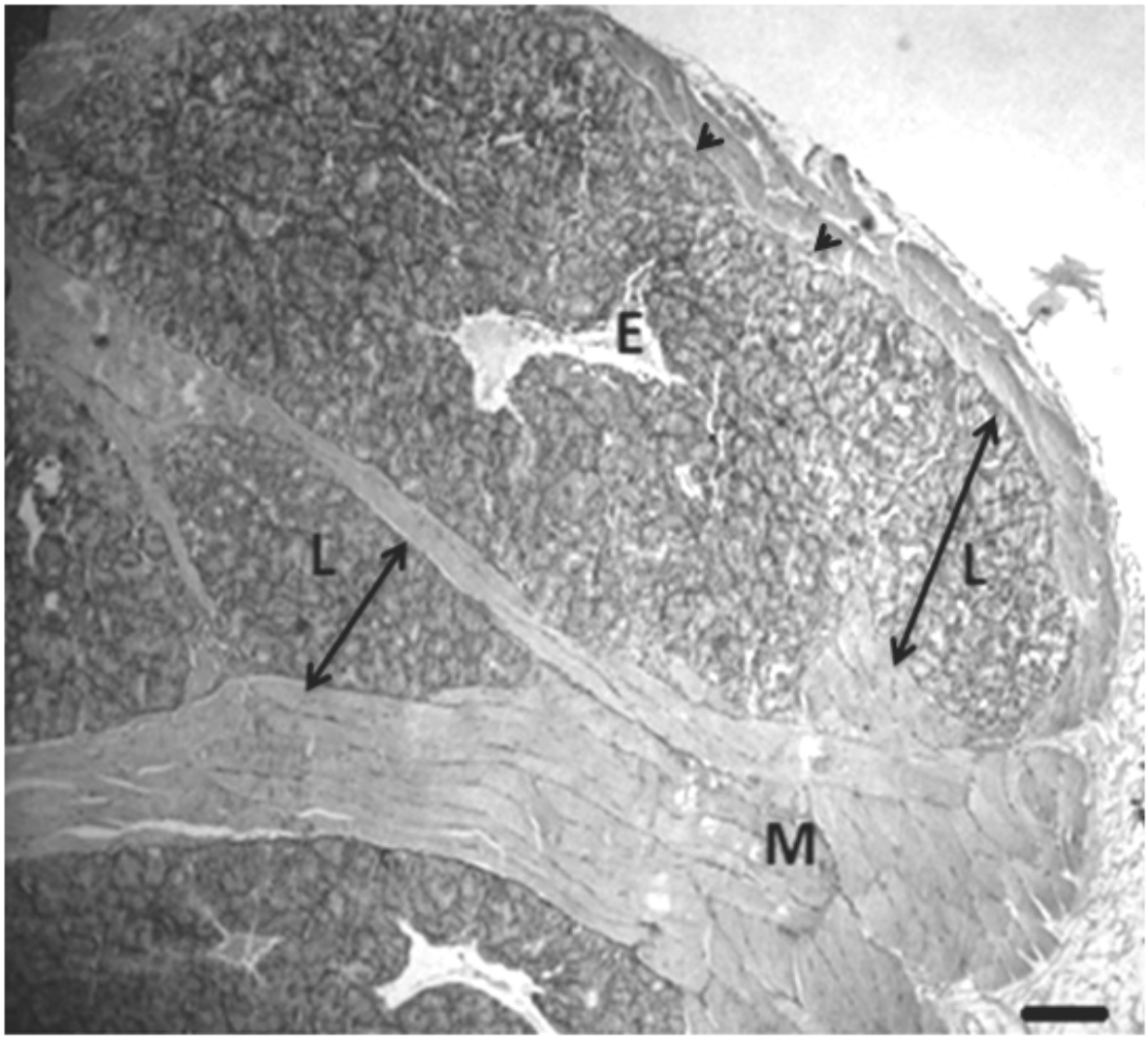

Figure 42: Photomicrograph of a section of the bulbourethral gland in the greater cane rat. Note the division of the gland into lobes and lobules (L) by thin connective tissue capsule (arrow heads) and the striated muscle (M). The excretory ducts (E) drain the secretory products of the gland. H&E, Mag. X100. **Scale bar: 50µm**

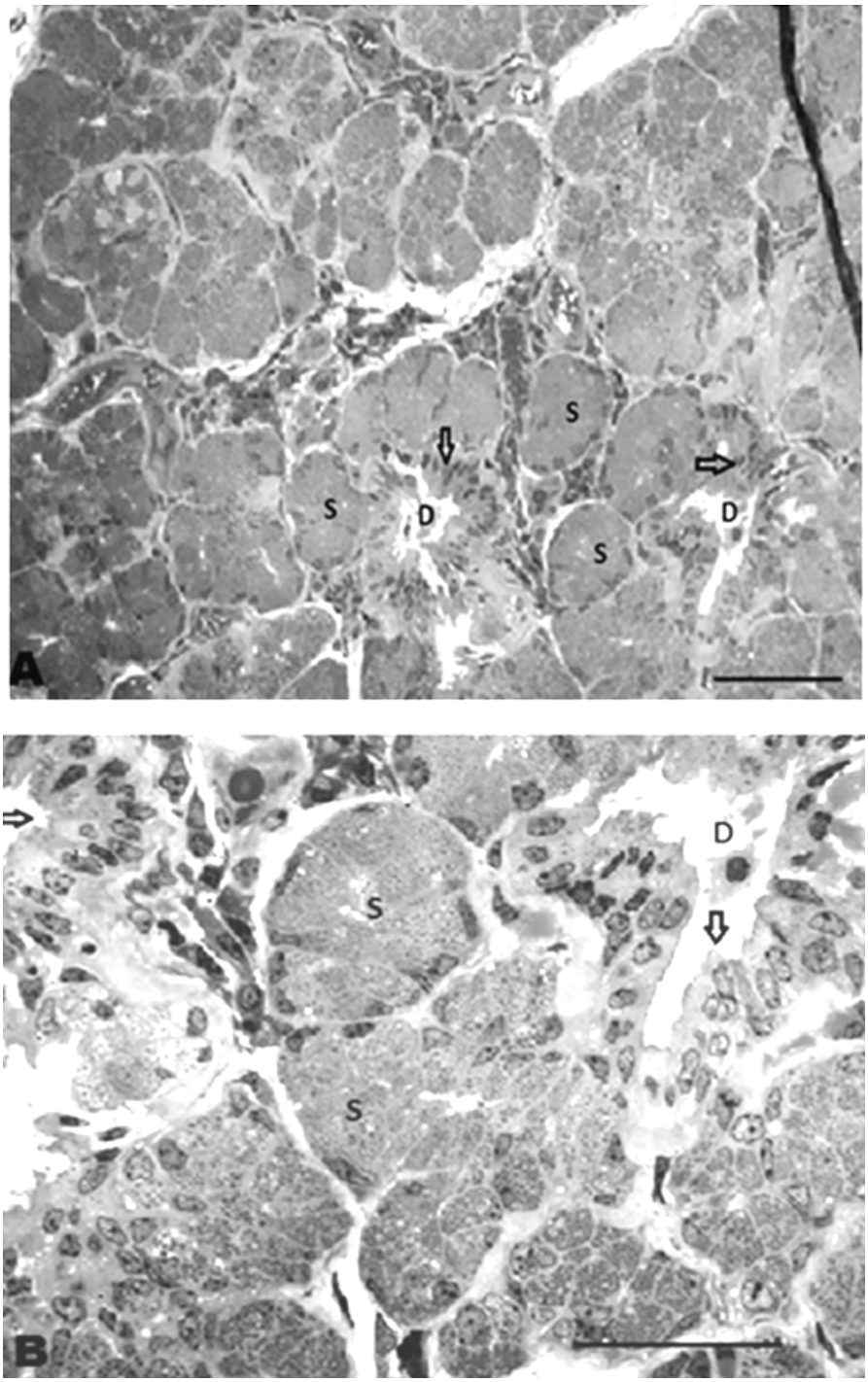

Figure 43 shows semithin sections of the bulbourethral gland in the greater cane rat. In (**A)** note the secretory unit/endpiece (S) and the excretory ducts (D) lined by pseudostratified epithelium (arrows). **Toluidine blue**, , Mag. X100, **Scale bar: 50µm. (B**) shows the glandular epithelium of Cowper's glands. Note the secretory units (S) with the pyramidal to columnar cells surrounding narrow lumen. The excretory ducts (D) and the epithelial lining (arrows) were also shown. **Toluidine blue grayscale**, Mag. X100, **Scale bar: 20µm**

3.2.5.4.4 Ultrastructure

The glandular epithelial cells that line the endpieces had basally located nuclei that contain predominantly granular euchromatin with small areas of heterochromatin which were mainly connected to the nuclear membrane (Fig. 44A & B).The ground cytoplasm at the base of the cells contained elongated mitochondria, rough endoplasmic reticulum with dilated cisternae and Golgi apparatus (Fig. 44B).

One of the striking features of these glandular cells was the presence of large number of round to oblong shaped, electron dense, membrane-bound secretory granules (Fig. 44B).These secretory granules, in the columnar cells, virtually filled the entire cytoplasm thereby compressing the nucleus and cytoplasmic organelles, while in the pyramidal cells it was observed that the perinuclear areas were not completely filled by secretory granules (Fig. 44A & B). Some of the granules showed uniform electron-density and others had regions of lesser density (Fig. 45A). Although few of the secretory granules did not show membrane boundary, no secretory vacuoles was observed in these epithelial cells. However, the electron-lucent cytoplasmic area surrounded the granule with dense strands radiating from each granule (Fig. 44B & 45A).

At the apical region of the epithelium, some of the granules were seen to bulge into the glandular lumen with no union between their membranes and the apical plasma membrane. Rather, the apical surfaces were studded with microvilli (Fig. 45B). Also, junctional complexes with digitations and narrow intercellular spaces joined the cells to each other (Fig 44B & 45B).

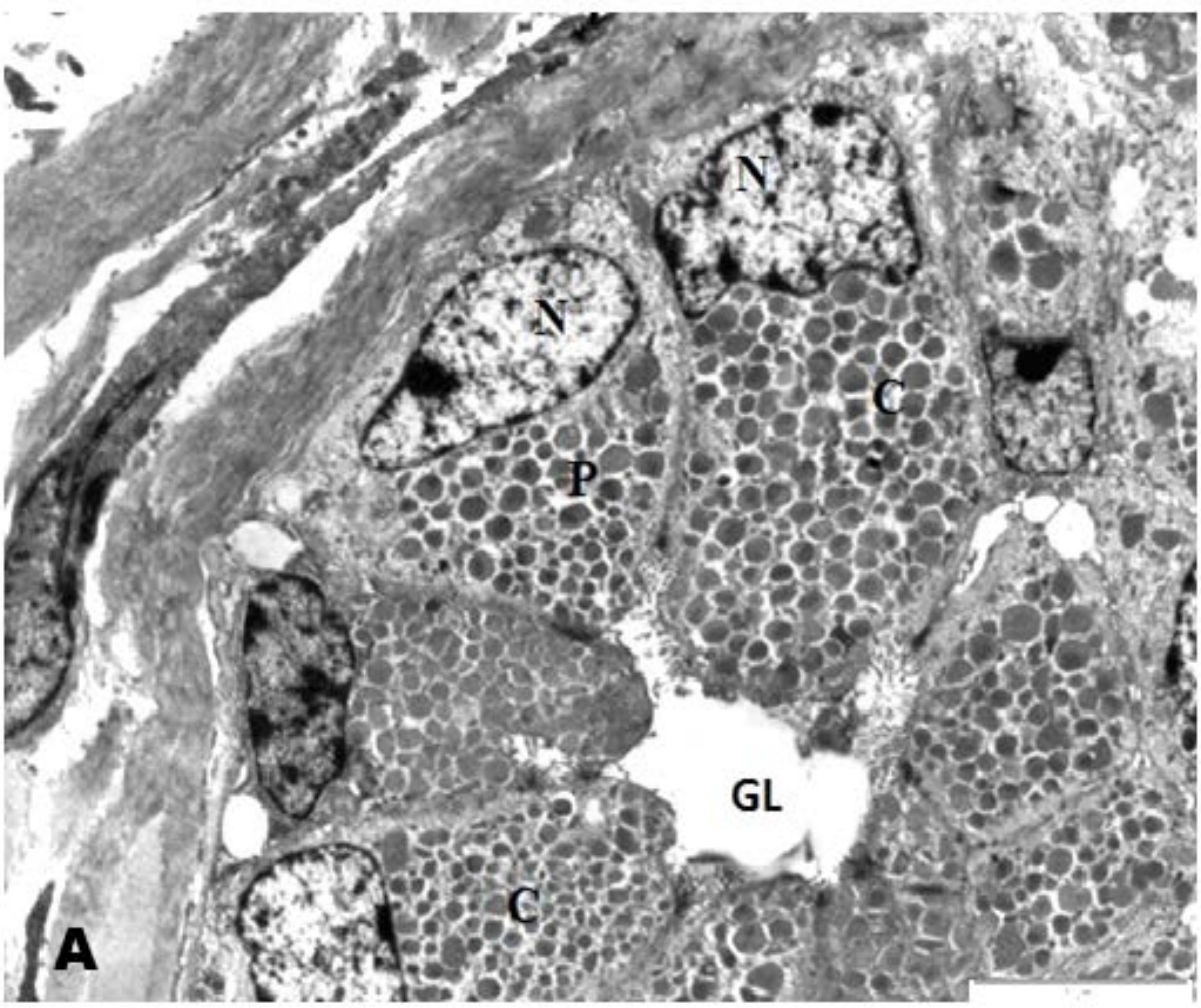

Figure 44A: Ultrastructure of the secretory epithelium of the bulbourethral gland of the greater cane rat. Note the euchromatic nucleus (N), pyramidal (P) and columnar cells (C) surrounding a narrow glandular lumen (GL). Picture taken with Phillips CM10 TEM at 80 KV. Mag. X 20,000. **Scale bar: 5µm**.

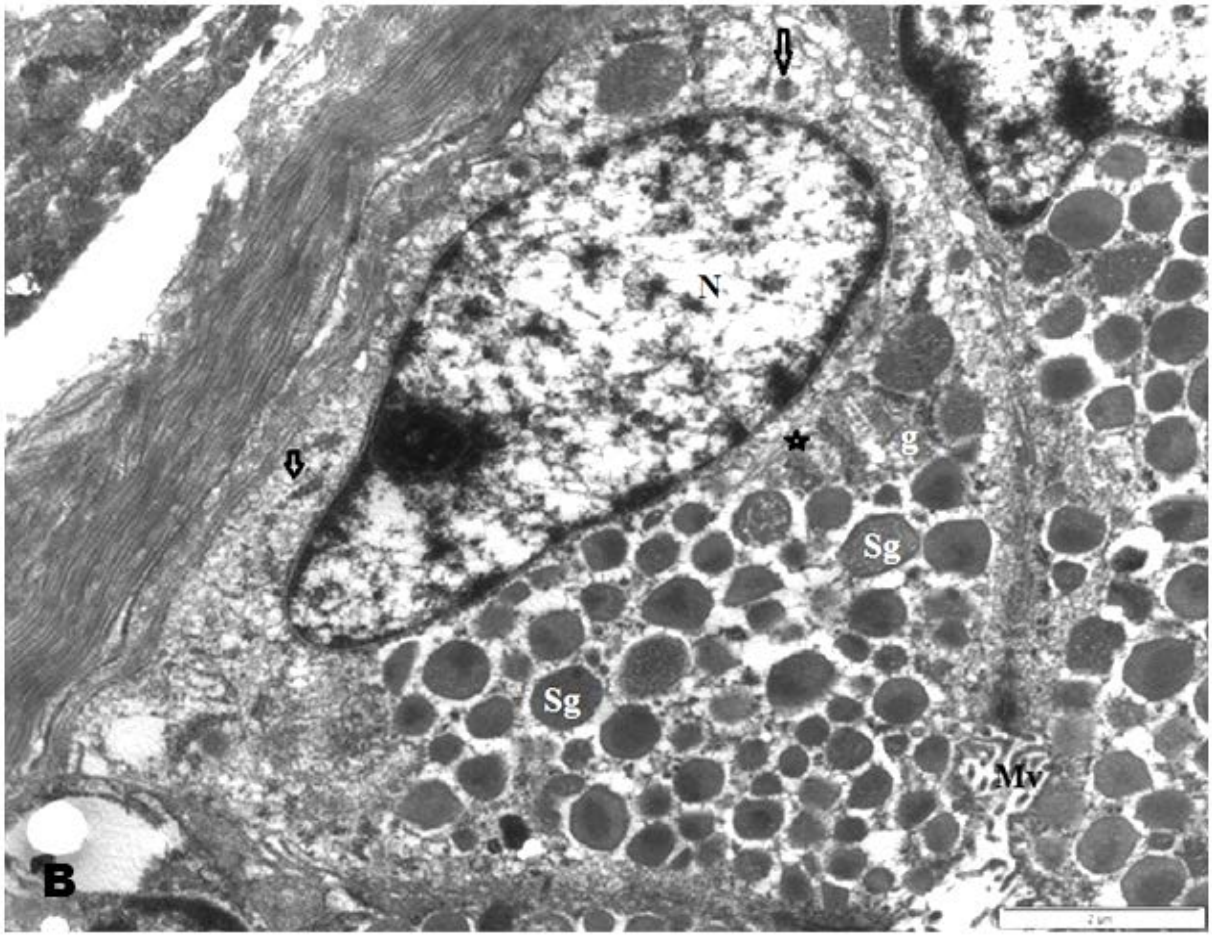

Figure 44B: Ultrastructure of the pyramidal cell of secretory epithelium of the bulbourethral gland of the greater cane rat. Note the organelles; Golgi apparatus (g), rough endoplasmic reticulum (asterisk), round to elongated mitochondria (arrows) confined to the basal part of the cell by the secretory granules (Sg) and the microvilli (Mv) on the apical surface. Picture taken with Phillips CM10 TEM at 80 KV. Mag. X 30,000. **Scale bar: 2µm**

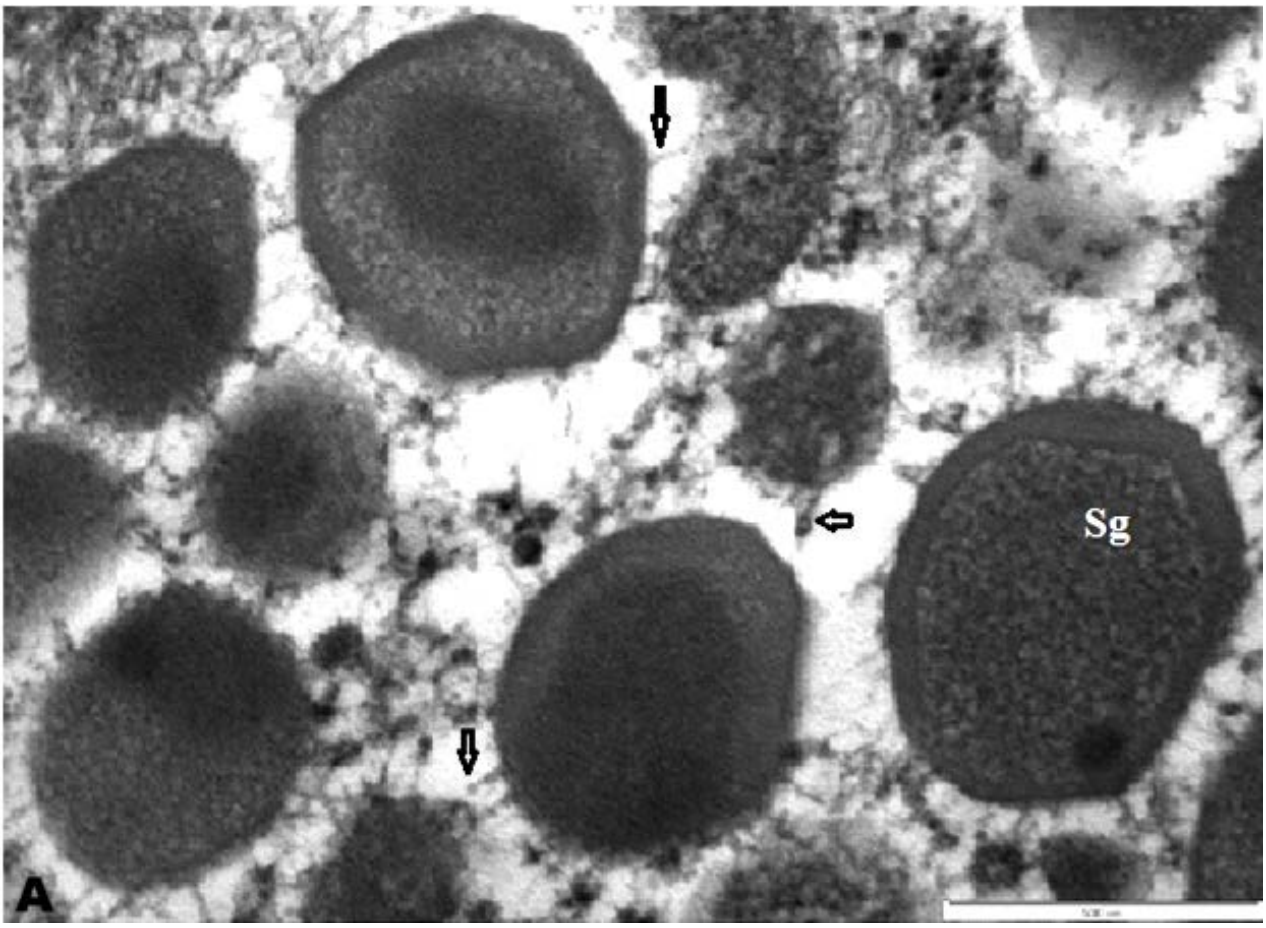

Figure 45A: The secretory granules in the supranuclearand part of the glandular cells of the Cowper's gland of the greater cane rat. Note the secretory granules with and without membrane as well as varying electron densities. Electron dense strands (arrows) radiating from each granule is also shown. Picture taken with Phillips CM10 TEM at 80 KV. Mag. X 50,000. **Scale bar: 500nm.**

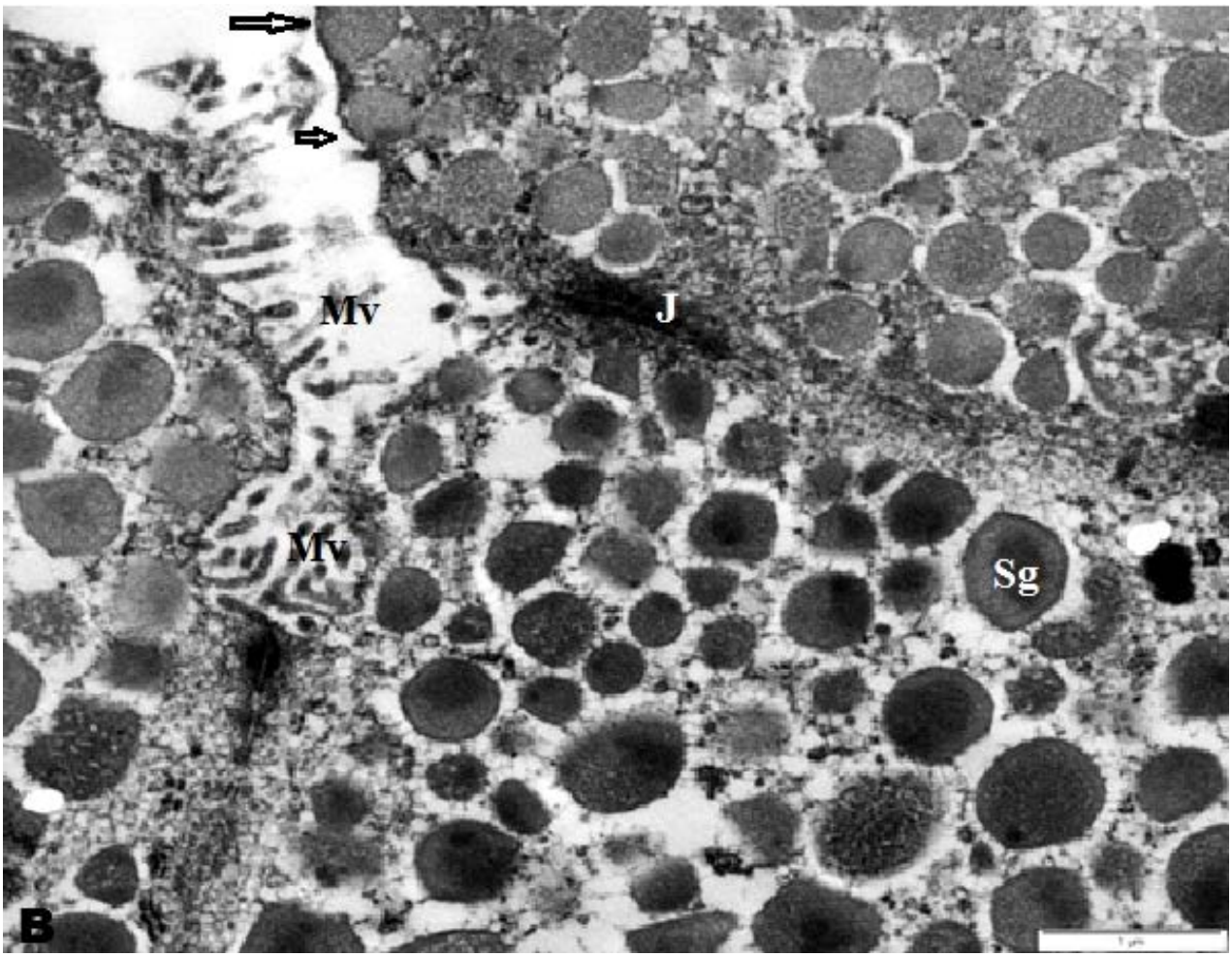

Figure 45B: The ultrastructure of the apical part of the glandular cells of the Cowper's gland of the greater cane rat. Note the microvilli (Mv), junctional complex (J) between the cells and the secretory granules (Sg). The arrows indicate the apocrine mechanism of granular release in this gland. Picture taken with Phillips CM10 TEM at 80 KV. Mag. X 30,000. **Scale bar: 1µm**.

3.3. DISCUSSION

The testis of the greater cane rat is suspended in a fold of skin that is brownish stained in sexually matured males. In most species, the scrotum had a well-defined structure but with varying locations and conformation (Hutson *et al*, 1997). According to Machado-Junior *et al*, (2011) variations in scrotal structure, such as the presence and degree of scrotal bipartition, affect testicular structure and spermatogenic efficiency especially in mammals with well defined scrotum like goat. The finding of this study is in contrast with the reports of Addo *et al*, (2003) and Opara (2010) who found that the cane rat had no scrotum as the testes were abdominally situated. However, the presence of brownish skin-fold and the possible location of the testis in both the abdominal and inguinal regions in the cane rat suggest that the skin pouch simply enclosed the testis without any major impact on its functions.

In understanding the process of spermatogenesis in various mammalian species, histological and ultrastructural analysis of the spermatogenic cells; spermatogonia, spermatocytes and spermatids have been carried out in several mammals especially rodents (Van Haaster and De Rooij, 1993). While the fine structures of the spermatogonia, dividing spermatocytes and the differentiating spermatids follow a general trend in most mammals, differences in cytological details are observed from one species to another resulting in a rich variety of forms (Bustos-Obregon, 1975; Segatelli *et al*, 2000). Although the observed histological architecture of the seminiferous tubules in the greater cane rat had close semblance to that of other rodents already studied (Oakberg, 1956; Hess, 1990; Van Haaster and De Rooij, 1993; Munoz *et al*, 1998; Segatelli *et al*, 2000), it was unique in the cellular association and the ultrastructure of the spermatogenic cells especially in the formation of acrosome.

The histological organization in the cane rat seminiferous epithelium revealed the spermatogenic process as a highly organized and well synchronized cyclic event evidenced by the presence of well defined germ cell associations. In the transformation of spermatogonia to spermatozoa, older germ cells became associated with younger ones in a specific cyclic manner (Hess, 1990). A cycle of seminiferous epithelium occurred from the point of disappearance of a given cellular association to its reappearance in a given area of the seminiferous epithelium (Clermont, 1972; Segatelli *et al*, 2004). These cellular associations, commonly referred to as stages of the seminiferous epithelium cycle, vary in number and duration among mammalian species (Weinbauer *et al*, 2001).

The characterized nine stages of the cycle of the seminiferous epithelium in the cane rat were based on the development of the acrosomal system and changes in the nuclear morphology of the spermatids which occurred in twelve (12) steps. The number of stages in the spermatogenic cycle does not only vary with species but also with the criteria used to characterize them. A simpler and less arbitrary method for stage characterization is using the criteria of tubular morphology which usually yield 8 stages in all species (Franca *et al.*, 1999; Paula *et al.*, 1999). However, the recognition of stages based on the morphologic changes in the spermatids provided the most excellent stage classification that can serve as foundation for biochemical and physiological studies of spermatogenesis as well as provide standard to which testicular histopathology can be compared (Hess, 1990; Segatelli *et al*, 2004). Using these same criteria, Leblond and Clermont (1952) and Hess (1990) characterized 14 stages in rat, Oakburg (1956) defined 12 stages in mouse and Russells *et al* (1990) reported 8 stages in Dog. While Segatelli *et al*, (2001) reported 12 stages in gerbil, Munoz *et al*, (1998) designated 9 stages to Viscacha. The observed 9-stages of the spermatogenic cycle in the cane rat is similar to that

observed in rodents particularly the viscacha which is another hystricomorphic rodent (Munoz *et al*, 1998; Busso *et al*, 2005).

In this work, three types of spermatogonia, A-type, Intermediate (In) type and B-type were observed based on their shape, size and nuclear morphology. According to Samuelson (2007), the A-type divides to give rise to the In-type which subsequently forms the B-type spermatogonia with evident progressive chromatin condensation from the A-type to B-type. Using the whole mount of the seminiferous tubules, Van Haasters and De Rooij, (1993) reported six generations of spermatogonia in Djungarian hamster with the A and B-types having three subtypes. On the basis of shape and progression of the nuclear chromatin condensation, the generations of spermatogonia observed in the cane rat were consistent with that reported in rat (Clermont, 1972), mouse (De Rooij, 1973), gerbil (Segatelli *et al*, 2002) and ram (Loks *et al*, 1982). Also, the ultrastructural appearance of each spermatogonium type in terms of cellular organelles, shape and chromatin condensation, in the cane rat was similar to what was reported in the gerbil (Segatelli *et al*, 2000; 2002).

From the ultrastructural analysis, the spermatid differentiation and acrosomal formation occurred in twelve (12) steps in the greater cane rat. The number of spermiogenic steps varies among mammals and had been found to be species-specific (Clermont, 1972; Russel *et al*, 1990). There are nineteen (19) steps in the rat (Leblonds and Clermont, 1952), eighteen (18) in Squirrel (*Funabulus palmarum*) (Patil and Saidapur, 1991), sixteen (16) in both mouse (Oakberg, 1956) and hamster (Oud and De Rooij, 1977; Van Haaster and De Rooij, 1993), fifteen (15) in both Mongolian and desert gerbils (Saidapur and Kamath, 1994; Segatelli *et al*, 2001), fourteen (14) in monkey (*Macaca arctoides*) (Clermont and Antar, 1973) and twelve (12) in dog (Foote *et al*, 1972) and Viscacha (*Lagostomus maximus maximus*) (Munoz *et al.*, 1998). According to

Segatelli *et al*, (2000; 2002), the difference in the number of spermiogenic steps in different mammalian species was as a result of the difference in fine details of the acrosomal formation which consequently determined the final shape of the acrosome over the sperm head.

While the general events of the formation and development of the acrosomal system in the greater cane rat is similar to those described in other rodents, it however, had its species-specific characteristics. Whereas in most rodents (Hess, 1990; Van Haaster and De Rooij, 1993; Munoz *et al*, 1998; Segatelli *et al*, 2000), the head of the early spermatids was covered by the acrosomal vesicle and not by the acrosomal granules, in the cane rat the entire acrosomal system comprising the vesicle and granule covered the head of the early spermatids. This was comparable only to that described in the golden hamster (Leblond and Clermont, 1952). In the same vein, after the attachment of the acrosomal granules to the nucleus, the nuclear surface may become flattened or indented with the degree of indentation varying from one species to another (Segatelli *et al*, 2000). The observed flattening of the nuclear surface by the acrosome with no clear indentation in the cane rat was contrary to that obtained in rat (Leblond and Clermont, 1952), Viscacha (Munoz *et al*, 1998) and gerbil (Segatelli *et al*, 2000) but consistent with that in the monkey (Bedford and Nicander, 1971).

Another species-specific characteristic in the spermatid differentiation in the greater cane rat is the abundance of nuclear vacuoles at nuclear elongation and condensation phases. In most rodents, it is either absent as in gerbil (Segatelli *et al*, 2000), or where present, it was small and occasional as in rat, rabbit and monkey (Bedford and Nicander, 1971). The presence of large amount of nuclear vacuoles during the nuclear condensation phase similar to that observed in the cane rat had, however, been reported only in the human spermatids (Gordon, 1969).

The cytoarchitecture of the Sertoli cell in the greater cane rat was consistent with that observed in the rat (Fawcett, 1975; Kianifard *et al*, 2012). It has been established that at different stages of the spermatogenic cycle, there are quantitative and qualitative alterations in the shape, distribution and arrangement of the organelles in the Sertoli cell (Fawcett, 1975; Ueno and Mori, 1990; Wrobel and Bergmann, 2006, Ichihara and Pelliniemi, 2007). Although the ultrastructure of Sertoli cell was studied at a particular stage in this work, from the histological stand point, stage variations in the morphology of this cell also exist in the cane rat.

The testicular interstitial tissue presented a unique cyto-organization in the greater cane rat. Generally, the arrangement of interstitial tissue showed marked species variations in terms of abundance of Leydig cells, amount of interlobular connective tissues and the location as well as the degree of development of the lymphatic system. It equally played vital role in the interpretation of the physiology of the testis in any given mammalian species (Fawcett *et al*, 1973; Wrobel and Bergmann, 2006). While the interstitial arrangement in the cane rat is similar to that of guinea pig and Chincilla (Fawcett *et al*, 1973; Busso *et al*, 2012) in terms of the presence of large fluid-filled lymphatic sinusoids surrounding all the seminiferous tubules and large amount of intertubular connective tissue, it differs from these two species in having large amount of collagen fibrils in the intertubular connective tissues like that of the ram (Fawcett *et al*, 1973). The amount and arrangement of the Leydig cell in the interstitium was also comparable only to that of the pig (Wrobel and Bergmann, 2006). Therefore, this peculiar arrangement will have an impact on the physiology of the testis in the greater cane rat.

The ultrastructure of the Leydig cell in the greater cane rat was consistent with that of other rodents (Mori *et al*, 1980; 1982; Mendis-Handagama *et al*, 1990, Ichihara *et al*, 1993). The observed intimate association of the Leydig cells with macrophage and the presence of Leydig

cytoplasmic processes at the site of adhesion had also been reported in the rat (Ichihara *et al.*, 1993). This association might equally suggest functional coupling between the two cells as it is in the rat (Ichihara *et al.*, 1993).

The mediastinum testis which has been described as the intracellular reflection of the tunica albuginea by Dhingra (1977) varies widely in different species of mammals. According to Wrobel and Bergmann (2006), the mediastinum of the stallion and many rodents is relatively small and located in a marginal position whereas in ruminants, pigs, cats and dogs, it occupies a central position along the longitudinal axis of the gonad. There is little fibrous mediastinum testis in the rat (Setchell, 1977), rabbit, hamster (Dhingra, 1977) and the giant rat (Oke, 1988). The mediastinum testis of the greater cane rat, located at the margin, had very little or no fibrous component, extending about 10mm from the cranial pole and was about one-fifth of the length of the testis. These characteristics made it similar to that of other rodents like rat, rabbit, hamster and giant rat (Oke, 1988).

The rete testis can be divided into intratesticular, intratunical and extratesticular as observed by Roosen-Runge (1961). It has also been shown that the intratesticular portion of the rete is minor in both birds and mammals (Budras and Meier, 1981). The rete testis in the cane rat, located in the mediastinum, can be described as intratesticular and intracapsular which is similar to what has been observed in the African giant rat (Oke, 1988).

The structure of the efferent ducts varied among species and between segments of the ducts in the same species (Aire and van der Merwe, 2003). In rodents the ducts converge into a common duct that feeds into the initial segment of the epididymis while in large mammals including man, parallel efferent ducts form multiple entries into the head of the epididymis

(Joseph, *et al.*, 2009). The pattern in the greater cane rat is similar to that of man and confirms the observation of Aire and van der Merwe (2003) that the efferent ducts, after emerging from the testis, run in a relatively straight course from the rete testis and become wavy and highly convoluted as they approach the epididymis where they subsequently open individually into the initial segment of the epididymis.. However, according to Joseph *et al.* (2009), the enormous variation between species still leaves many questions about the ways in which efferent duct connect with rete testis and the epididymis.

As reported by Clulow *et al.* (1998) and Joseph *et al.* (2011) the efferent ducts are the only excurrent ducts whose epithelium normally contain ciliated cells in addition to non-ciliated cells, both of which function in modifying their flow-through in many ways. However, the non-ciliated cell component showed cytological variations, principally in the absence or presence of vacuoles and dense granules as well as their relative proportions where present, along the length of the efferent ducts in the different mammalian species (Aire and van der Merwe, 2003). There are three non-ciliated cell types in man (Morita, 1966), bull (Goyal and Hrudka, 1981) and goat (Goyal *et al.*, 1992; Gray *et al.*, 1983). While four cell types were reported in dog (Hess and Bassily, 1988), Aire (1980) reported two cell types in birds. In man, bull and goat, unlike in the rat, the proximal non-ciliated cell type (type 1) contained no granules or vacuoles, the middle non-ciliated type (type II) contained numerous dense granules, while the distal cell type (type III) exhibits no granules, but contained numerous vacuoles (Morita 1966; Goyal and Hrudka 1981; Goyal *et al.* 1992). The three non-ciliated cell types observed in the cane rat were similar to that reported in man, bull and goat and consistent with the earlier account of Aire and van der Merwe (2003) on the efferent ducts of the cane rat.

While the presence, number and size of the vacuoles in the different non-ciliated cell types were associated with fluid absorption , the significance of the dense granular bodies found in both type 1and type II but only occasionally in type III was not clearly understood. Vincentini *et al*, (1990) opined that, in the hamster, they are absorbed, concentrated and transformed luminal macromolecules, but Aire and van der Merwe (2003) simply considered them to be cell secretions with roles connected with sperm maturation, since they contain glycoproteins.

Because of the need to understand the role of the epididymis, the study of its morphology at gross, histological and ultrastructural levels has been extensively carried out in most domestic and laboratory species (Flickinger *et al*, 1978; Goyal, 1985; Robaire and Hermo, 1988; Goyal and Williams, 1991; Arrighi *et al*., 1993; Schimming and Vincentini, 2001). However, only few reports are available on wild species especially those undergoing domestication in West Africa (Oke *et al*, 1988; Aguilera-Merlo *et al*, 2005). This work presented, for the first time, the detailed structural and ultrastructural features of the epididymis in the greater cane rat.

Grossly, based on its position relative to the testis, the epididymis of the cane rat could not be distinctly divided into head, body and tail. In most mammals, the gross appearance of the epididymis allows a visual identification of the different segments which comprise the proximal region (the initial segment and the caput), the corpus and the distal cauda (Robaire *et al*., 2006; Turner, 2008). According to Goyal and Williams (1991), though these divisions may provide useful landmarks at the gross level, they do not correspond to the structural and functional diversities exhibited by the epididymis along its length. Therefore, the epididymal gross appearance in this animal might simply be a species peculiarity that has no direct functional implication.

The histological, morphometrical and ultrastructural analysis of the cane rat epididymis confirmed the presence of the four anatomical regions – initial segment, caput, corpus and cauda epididymis. On the basis of differences in the type, amount, height and cytological characteristics of the epithelial cells, the cane rat epididymis had been subdivided into six functional zones. The precise numbers of epididymal zones are species-specific and may also vary within the same species depending on the criteria of classification (Goyal and Williams, 1991; Arroteia *et al*, 2012). Four zones had been recognized in the rat (Hamilton, 1975), five in mouse, hamster, African giant rat and goat (Flickinger *et al.*, 1978; Takano, 1980 ; Oke *et al*, 1988; Goyal and Williams, 1991), seven and eight in guinea pig (Hoffer and Greenberg, 1978) and the rabbit (Jones *et al.,* 1979), respectively. The six zones in the cane rat can therefore be said to be characteristic of this species of animals. As reported by Goyal and Williams, (1991) and corroborated by Joseph *et al*, (2011), irrespective of the number of zones within any species, there is always an overlapping of morphological and functional characteristics between two adjacent zones and there are more structural diversities along the length of the proximal segment than along the length of the body and tail segments. The observed presence of three of the six zones in the initial segment alone and the close semblance in the ultrastructure of the epithelial cells in the body and tail segments confirmed this report in the greater cane rat.

The observed variation in the epithelial height and tubular diameter along the cane rat epididymal length is consistent with that of most mammals (Nicander, 1957; Goyal, 1985; Goyal and Williams, 1991; Joseph, *et al.*, 2011). However in some species like goat (Goyal and Williams, 1991), the epithelial height does not decrease gradually along the length of the epididymis but falls sharply from the initial segment to the caput and more so from the proximal

to distal cauda epididymis. The sharp fall in the epithelial height was only noticed from the corpus to the cauda epididymis in this study.

In all segments of the cane rat epididymis, the epithelium was mainly composed of principal and basal cells with apical, narrow and clear cells present in segment-specific manner. The epididymal epithelium in all mammalian species consists of principal, basal and other cells such as apical, narrow, clear and halo cells as well as intraepithelial lymphocytes and macrophages (Calvo *et al.*, 1999). However, the presence, distribution, frequency and structural characteristics of these other cells vary particularly among rodents (Aguilera-Merlo *et al*, 2005; Arroteia *et al.*, 2012). While the apical cells were found in the initial segment in rat, mouse and hamster (Hamilton, 1975; Flickinger *et al.*, 1978; Soranzo *et al.*, 1982), it extended to the caput and corpus epidydimis in the guinea pig and monkey (Ramos and Dym, 1977; Hoffer and Greenberg, 1978). It was however absent in the initial segment in the African giant rat (Oke *et al.*, 1988). The observation in the cane rat was consistent with that in the guinea pig and monkey. Conversely, the clear cells which were present in the corpus and cauda epididymis in rat, hamster, mouse and opossum (Orsi *et al.*, 1980), were absent in all other species including guinea pig, monkey, ruminants (Goyal and Williams, 1991) and man (Holstein, 1969). The distribution of the clear cell in the greater cane rat, this time, follows the trend in rat, hamster and mouse.

In the same vein, narrow and halo cells had been reported in the initial segment in rat (Sun and Flickinger, 1982; Robaire *et al.*, 2006) but not in African giant rat (Oke *et al*., 1988). Also, intraepithelial lymphocytes and macrophages that were abundant in all segments of the epididymis of the African giant rat have not been reported in rat. The cane rat stands in-between, having narrow cells with neither halo cells nor intraepithelial lymphocytes and macrophages.

The accounts of Dacheux *et al*, (2005) and Robaire *et al*, (2006), showed structural and functional similarities between the halo cells and intraepithelial lymphocytes/macrophages which suggested that in species where one was absent, the other cell took up the function. With the absence of both cells in the epididymal epithelium of the cane rat, it is yet unclear how their functions are handled in this animal.

The morphological differences observed in the regions and zones of the greater cane rat epididymis was consistent with that of laboratory, wild and domesticated animals and man (Oke *et al,* 1988; Robaire and Hermo, 1988; Goyal and Williams, 1991; Lasserre *et al.*, 2001) in terms of the distinctness of the initial segment from other regions, the decreasing principal cell heights, changing luminal shapes and increasing concentration of luminal sperm cells from the initial segment to the cauda epididymis. It was however different from these rodents in terms of the numbers of zones found in the initial segment and the ultrastructural peculiarities of the epithelial cells in the cane rat. The presence of three zones within the initial segment of the epididymis in the cane rat is unique and has not been reported in any of the studied animals.

In all mammalian species, the uniqueness of each zone stems from the fine structural features of the principal cells primarily and that of other cells in the epithelium (Goyal and Williams, 1991; Joseph *et al*, 2011). The ultrastructural appearance of the principal cells in the initial segment in the greater cane rat was comparable to that observed in other rodents (Hoffer and Karnovsky, 1981; Robaire and Hermo, 1988; Oke *et al*, 1988) in having prominent branched microvilli with the presence of large stacks of Golgi saccules, mitochondria and multivesicular bodies at the supranuclear area. The infranuclear area was also packed with rough endoplasmic reticulum. However the whorled pattern of arrangement of the dilated Golgi apparatus and the presence of clumps of mitochondria at the supranuclear area were peculiar features in the first

zone of the initial segment in the cane rat. It is not impossible that these might affect the type of protein and steroid secreted by these cells. While the functional significance of these features are yet unknown, Oke *et al*, (1988) had reported the presence of mitochondria clumps in the same area in the giant rat.

In rat and man, (Robaire *et al*, 2006; Cornwall, 2009), the tight junctions between adjacent epithelial cells were said to form blood-epididymis-barrier which restricted passage of a number of ions, solutes, and macromolecules through the epididymal epithelium as well as served as an extension of the blood-testis-barrier in these species. The observed tight junctional complexes found between adjacent principal cells and other cells might also serve the same purpose in the greater cane rat.

According to Robaire *et al*, (2006) and Joseph *et al.* (2011), the presence of endocytotic features such as microvilli, coated vesicles and pits and subapical vacuoles were sure evidences of absorptive function in the principal cells. In the same vein, while the presence of highly developed Golgi complexes and numerous cisternae of rough endoplasmic reticulum in the supranuclear and infranuclear areas are morphological correlates of protein synthesis, whorls of smooth endoplasmic reticulum, mitochondria with tubular cristae and lipid droplets are morphological correlates of steroid synthesis. The presence of these organelles in the principal cells of the different zones in the cane rat epididymis confirms they are involved in both absorptive and secretory functions with zone 1 being involved in more of absorptive functions; zones 2-4 in "net secretion" than "net absorption" and zones 5-6 being involved in "net absorption" rather than "net secretion". This trend had also been observed in ram, bull and goat (Amann *et al*, 1982; Pholpramool *et al*, 1985; Goyal, 1989). Moreover, since different kinds of epididymal secretory proteins and glycoproteins have been characterized in different species

(Goyal and Williams, 1991), the different kinds of proteins secreted by the principal cells of different epididymal zones in the greater cane rat is still a subject for research.

The characteristic presence of abundant vacuoles of various sizes and densities in the principal cells of zones 2 and 3 in the cane rat had been observed in mouse, hamster and guinea pig (Takano, 1980; Hoffer and Karnovsky, 1981) with the large vacuoles particularly similar to the lipid droplets found in the guinea pig. These lipid droplets together with whorls of smooth endoplasmic reticulum and the mitochondria with tubular cristae in the principal cells of these zones in the cane rat suggested the possibility of steroid synthesis in this cell. While the possibility of *de novo* synthesis of testosterone in some mammalian species like mouse, rat, rabbit and ram had long been indicated by Hamilton (1971), morphological evidence of testosterone synthesis has only been shown in the principal cells of zone 2 in guinea pig epididymis (Hoffer and Karnovsky, 1981). There is therefore the need for further proof of testosterone synthesis in the principal cells of these zones in the cane rat.

Apart from the principal cells, the distribution and structural features of other cells: apical, narrow, clear and basal cells equally showed zonal characteristics. The distribution of the apical, narrow and clear cells along the epididymal duct in the greater cane rat followed the same pattern as in the rat (Adamali and Hermo, 1996) where the apical and narrow cells were found more in the initial segment and caput but were replaced by clear cells in the corpus and cauda epididymis (Joseph *et al*, 2011). However, with regards to structural features, whilst the narrow cell in the cane rat was similar to that in the rat, the apical cells differed from that in the rat only in having its nucleus at the basal half of the cell which was similar to what was reported in the ovine species (Marengo and Amann, 1990). Since the structural features of both apical and narrow cells in all species suggested they were involved in intracellular transport between the

lumen and the epithelial cells; in degradation of specific proteins and carbohydrates within their lysosomes; and in protecting spermatozoa from a changing environment of harmful electrophiles (Adamali and Hermo, 1996; Robaire *et al*., 2006), the slight structural variation observed in the apical cells in the cane rat epididymis may have no functional significance.

In most mammalian species, the clear cells are endocytic cells endowed with coated pits, vesicles, endosomes, multivesicular bodies, lysosomes as well as lipid droplets (Hermo *et al*., 1994, 2005; Robaire *et al*., 2006). These structural features are similar to what was observed in the greater cane rat. According to Joseph *et al*, 2011, the endocytic activity of the clear cells, which involves taking up the contents of the cytoplasmic droplets released by the spermatozoa as they transit through the duct, is greatest where the clear cells are most concentrated. While clear cells were more in cauda epididymis in rat (Hermo *et al*, 1988), they were observed to be more in the corpus epididymis in the greater cane rat.

In the greater cane rat, the basal cells which resided in the epithelial base, had poorly developed organelles and were structurally similar in all the epididymal zones. By the reason of their contact with the basement membrane, basal cells formed an extensive cellular sheet surrounding the epididymal epithelium and shared extensive interdigitations with the plasma membrane of adjacent principal cells (Robaire *et al*., 2006; Cornwall, 2009). These were equally observed of the basal cells in the epididymal epithelium of the cane rat. According to Joseph *et al*, (2011) several functions have been proposed for the epididymal basal cells based on their location in the epididymal epithelium. Aside from mechanical support for principal cells, it is believed that basal cells can endocytose factors derived from the blood or principal cells (Hermo and Papp, 1996) and may help to regulate principal and clear cell functions (Cheung *et al*, 2005; Shum *et al*, 2009). Although the structural similarities of epididymal basal cells among

mammalian species can imply functional similarity, further proof of these functions by cane rat basal cells is imperative.

The structure of the vas deferens in the greater cane rat was generally similar to that of most mammalian species (Flickinger, 1975; Hamilton & Cooper, 1978; Kennedy & Heidger, 1979; Clermont & Hermo,1988; Nistal, *et al*, 1992) being a straight muscular tube that extended from the cauda epididymis to the ejaculatory duct in the pelvis. However the length, the degree of muscular thickness, epithelial folding and luminal diameter vary in different species and were dictated by the type of sexual mating system adapted by each species (Anderson *et al*, 2004). According to Anderson (1994), female mammals might mate with either a single partner (monogamous and polygynous mating systems) or multiple partners (multimale–multifemale and dispersed mating systems) during the periovulatory phase of the ovarian cycle. Multiple partner matings had been reported to result in the potential for competition to occur between the ejaculates of rival males, within the female's reproductive tract, for access to her ova (Birkhead, 2000). Sperm competition determined the evolutionary selection for either relatively large or small testes; long or short vas deferens length as well as the relative muscular thickness of the vas deferens (Anderson *et al*, 2004). The observed vas deferens length and muscular thickness relative to the body and testicular weights in the greater cane rat was comparable to that reported for porcupine, opossum and lemur (Smith, 1984; Anderson and Dixson, 2002; Anderson *et al*, 2004) which maintained monogamous and polygynous mating system. In the same vein, the morphology and morphometry of the cane rat vas deferens, combined with the relatively low gonadosomatic index which had earlier been established (Adebayo *et al*, 2009b), implied monogamous and polygynous mating system with lack of sperm competition in this species.

The observed presence of prominent Golgi profiles, subapical vacuoles, multivesicular bodies, mitochondria and both rough and smooth endoplasmic reticulum in the principal cells of the cane rat vas deferens suggested both absorptive and secretory abilities of these cells. In rat (Hermo, 1995), monkey (Leong and Singh, 1990) and man (Nistal *et al*, 1992), the principal cells, which contained similar organelles were involved in fluid absoption from and secretion of synthesized steroids into the vas lumen. Also, the presence of intraepithelial macrophage in the cane vas deferens which had equally been reported in rat, monkey and man suggested possible involvement in spermiophagy. From these structural and ultrastructural stand points, it can be said that the vas deferens in the cane rat are involved in both sperm concentration and sperm phagocytosis apart from the known function of sperm transport.

The gross pattern of lobulation of the cane rat prostate was unique in that, while it resembles the prostate glands in species like rat (Hayashi *et al*., 1991), viscacha (Chaves *et al*., 2011), chinchilla (Cepeda *et al*., 2006), dog (Niu *et al*., 2003) and cat (Wrobel and Bergmann, 2006) in being paired, lobulated and not completely covering the pelvic urethra, it is however different from that of rat which has two lateral, dorsal and ventral lobes or others that have two undivided lobes.

In the rat prostate, based on their relative positions to the urethra, four histological zones; anterior, central, peripheral and transitional had been reported (McNeal, 1981; Wendell, 2000). According to Sluczanowska-Glabowska *et al*, (2010) these zones have lobules with different histological, histochemical and even histopathological features. This study showed only two zones, the central and peripheral zones in the prostate gland of the greater cane rat. Similar zones had also been reported in mice (Harmelin *et al.*, 2005) and viscacha (Chaves *et al*., 2011) prostates with the central zone lined by cylindrical pseudostratified cells and the peripheral zone

lined by cuboidal cells, but the epithelial lining in the two zones of the cane rat prostate were the same being predominantly simple cuboidal with occasional basal cells. The prostate epithelial lining in most rodents such as rat (Bartsch and Rohr, 1980), guinea pig (Wong and Tse, 1981), gerbil (Corradi *et al*., 2013) and in man (Sluczanowska-Glabowska *et al*., 2010) was mainly columnar cells. Also, while the thickness of the lobular fibromuscular stroma is more in the central zone relative to the peripheral zone in human (Hafez and Spring-Mills, 1979), rat (Bartsch and Rohr, 1980) and viscacha prostates (Chaves *et al*., 2011), the fibromuscular thickness in both zones were not significantly different in the cane rat prostate.

The general ultrastructural features of the predominant secretory cuboidal cells of the greater cane rat prostate gland were largely similar to that reported in rodent such as rat (Ghodesawar *et al.*, 2004), hamster (Toma and Buzzel, 1988), guinea pig (Wong and Tse, 1981) and mouse (Brandes and Portella, 1960) having prominent nucleus with nuclear pores, apical cytoplasm laden with mitochondria, secretory granules and vacuoles as well as supranuclear cytoplasm with Golgi complex and endoplasmic reticulum. However, in the cane rat, the round nucleus possessed a prominent nucleolus which was not commonly encountered in rat (Hafez, 1979; Ghodesawar, *et al.*, 2004). Also the presence of lacunae between secretory and basal cells had been observed in the rat and human prostate (Hafez, 1980), but not between two secretory cells as observed in the cane rat. With regards to secretion mechanism, the presence of apical bleb-like projections in the cane rat prostate suggested an apocrine mode of secretion which is similar to that reported in mice (Jesik, *et al.*, 1982), rat (Bartsch and Rohr, 1980; McNeal, 1981) and camel (Aly *et al*., 1991).

The fine structure of the basal cells in the prostate glands of the cane rat was consistent with that of the rat and humans (Bonkhoff *et al*., 1994). To a large extent, the basal cells in rat and

humans prostate had been proven to serve, under the influence of certain stimulus, as reserve or stem cells proliferating to replace secretory cells (Bonkhoff *et al*., 1994). With these structural similarities, the basal cells of the greater cane rat prostate are believed to be reserve cells for the secretory cells

The gross feature of the coagulating gland in the greater cane rat was unique, being different from that reported in other rodents. In the mouse (Carvalho *et al*, 2003), rat (Carballada and Esponda, 1992) and African giant rat (Oke and Aire, 1996), the gland is tubular and runs lateral to the entire length of the vesicular glands while in the Viscacha (Chaves *et al*, 2011), it was located at the upper part of the prostate.

Although the general histological architecture of the coagulating gland in the cane rat is similar to that of other rodents, the pattern of mucosal folding in its secretory acini was unique. The mucosal folding in most rodents (Oke & Aire, 1996; Harmelin *et al*, 2005; Chaves *et al*, 2011) did not traverse the entire lumen of the secretory acini as did occurred considerably in the acini of the coagulating gland in the greater cane rat. This structural arrangement might impact on the storage and secretory contributions of this gland to the semen and copulatory plug formation in the cane rat.

The observed presence of microvilli on the apical surfaces of the secretory cells was also reported in the mice (Calvalho *et al.,* 2003), rat (Melo *et al*, 1997) and African giant rat (Oke & Aire, 1996). While it is sparse and small in these rodents, it was large and abundant in the greater cane rat. According to Badia *et al*, (2006) the presence of abundant microvilli and coated vesicles had been associated with absorptive activity in the seminal vesicles. Although the significance of these well-developed microvilli in the coagulating gland of the cane rat was yet to be fully understood, the possibility of an absorptive role cannot be ruled out.

The presence of apical blebs with secretory materials suggested apocrine mode of secretion. According to Aumuller *et al,* (1999) apocrine secretory mechanism is another way of extruding soluble and membrane-bound proteins that are produced in the cytoplasm and intracellularly transported without the involvement of endoplasmic reticulum, Golgi apparatus or the secretory granules. Glands that secrete by apocrine mechanism will normally have cells with apical blebs that contain secretory products and at different stages; some pinching off from the cell and discharged into the lumen and others still attached to the cells with few and scattered microvilli (Wong and Tse, 1981). Although apocrine method of secretion had been described in the coagulating glands of most rodents (Wong and Tse, 1981; Oke and Aire, 1996; Groos *et al,* 1999) as well as in other glands in both animals and man (Satoh *et al*., 1992; Aumuller *et al*., 1999; Baccari *et al*., 2000, Badia *et al.,* 2006), this secretion method always coexist with merocrine secretory activities in these glands (Badia *et al.,* 2006). The observations in the present study suggested apocrine secretory activities predominate in the coagulating gland of the cane rat.

The observed well-developed Golgi apparatus and rough endoplasmic reticulum with dilated cisternae containing electron-lucent materials as well as the presence of secretory granules in the secretory epithelium of the coagulating gland in the cane rat were similar to that reported in most rodents. These features tended to suggest a robust protein synthesis with the packaged secretory products released through the merocrine mechanism (Aumuller *et al*, 1999; Zaviacic *et al*, 2000). Merocrine secretion is established when the secretory granules are seen bulging or fusing to the apical cell membrane or are present in the luminal content (Badia *et al.,* 2006; Słuczanowska-Głabowska *et al*., 2010). From this study however, no structural evidence of merocrine secretion was seen in the coagulating gland. The presence of basal cells had been reported in the

coagulating glands of rodents (Oke and Aire, 1996; Melo *et al*, 1997; Calvalho *et al*., 2003) but its functional significance is still not clear. In the mouse, where the coagulating gland was considered as the anterior prostate lobe, the basal cells were said to play essential role in the maintenance of normal differentiation of the secretory cells and the integrity of the prostatic ducts (Kurita *et al*., 2004). Research work is, however, needed to ascertain the possible roles of the basal cells in the coagulating gland of the greater cane rat.

In the rat and mouse, the anterior prostate lobe is considered to be the coagulating gland (Harmelin *et al*., 2005). However, in African giant rat and Viscacha, the gland presents distinct structural characteristics different from the prostate (Oke and Aire, 1996: Chaves *et al*, 2011) With the structural and ultrastructural peculiarities of the coagulating gland presented in this work, this gland differs from the prostate gland and can be taken as a distinct accessory sex gland in the greater cane rat.

The observed shape of the vesicular gland in the greater cane rat presented another variation in the morphology of this gland among the rodent species. Though branched tubular structure of the vesicular gland had been reported in two Neo-tropical hystricomorphic rodents, Agouti (Mollineau *et al*., 2009) and Paca (Ayres de Menezes *et al.*, 2010), it is unique in the greater cane rat in that the branches were short and restricted to the cranial part of the gland.

The two types of columnar principal cells found in the secretory epithelium of the vesicular gland of the greater cane rat had been previously reported in the seminal vesicles of humans (Riva and Aum¨uller, 1994) and several mammalian species like Brazilian zebus (Cardoso *et al.*, 1979), bulls (Amselgruber and Feder, 1986), buck and rams (Wrobel, 1970; Skinner *et al.*, 1968), guinea pigs (Veneziale *et al.*, 1974). According to Riva and Aum¨uller, (1994) the

difference in the histological appearances of the vesicular columnar cells could be attributable to the different stages of their secretory cycle. Therefore, while the light principal cells of cane rat vesicular gland might represent the functionally differentiated cells, the dense principal cells might be referred to as 'aged' cells showing signs of cellular degeneration which was similar to the dense columnar cells found in seminal vesicle of pig (Badia *et al*, 2006).

The presence of well-developed rough endoplasmic reticulum and golgi apparatus and the abundance of mitochondria seen in the principal cells of the vesicular glands in the greater cane rat was similar to that reported in the seminal vesicle of rats (Murakami and Yokoyama, 1989), African giant rat (Oke & Aire, 1997), pig (Badia *et al.*, 2006) and man (Riva and Aum¨uller, 1994). These suggested that principal cells of this gland are concerned with intense protein synthesis and secretions. As shown by Albert *et al*, (2002), large amount of ATP, at least four high-energy phosphate bonds are expended during protein synthesis. This enormous energy demand might explain the abundant presence of mitochondria in the cytoplasm of the principal cells. In addition, in the boar where eighty to ninety percent of the seminal plasma proteins are secreted by the seminal vesicles (Strzezek *et al*., 2000), some of the mitochondria were surrounded by the cisternae of the rough endoplasmic reticulum (Badia *et al.,* 2006) similar to what had been observed in this study. Although the seminal plasma protein contribution from the vesicular glands in the greater cane rat is yet to be elucidated, the vesicular glands might also be responsible for the bulk of the protein in the seminal plasma of the greater cane rat.

The observed microvilli and coated vesicles in the epithelial cells suggested the possibility of absorptive function in the principal cells of the vesicular gland in the greater cane rat. In rat (Murakami and Yokoyama, 1989), pig (Badia *et al*., 2006) and man (Aum¨uller and Riva, 1992), the seminal vesicle had been reported to be involved with absorptive functions and in

phagocytosis of spermatozoa. In pig seminal vesicle, the presence of microvilli and coated vesicles as well as presence of complex interdigitations between epithelial cells had been reported as evidences of their possible involvement in absorption and transcellular transport of materials stored in the gland lumen (Mata, 1995; Badia *et al*., 2006). The interdigitations observed between the epithelial cells and the stroma in the greater cane rat might suggest the existence of paracrine control between the stroma and the mucosa of the gland.

The structure and ultrastructure of the basal cell in the vesicular gland of the cane rat was consistent with that of most eutherine species. While the search for the exact function of the basal cells is still ongoing, different roles have been suggested for these cells. They could have structural role (Hayward *et al.*, 1996), serve as reserve or stem cells of the columnar cells (Verhagen *et al*., 1988; Riva and Aum¨uller, 1994) and could act as a potential mediator of luminal cell activity by regulating transport of material between secretory and stromal cells (El-Alfy *et al*., 2000). The presence of interdigitations between the principal cells, the basal cells and the stroma as well as the immunolocalization of the ERα in the basal cells (in the chapter 4 of this work) suggested regulatory and structural roles for basal cells in the vesicular gland of the cane rat.

The viscous, gel-like nature of the vesicular glands secretion observed in the cane rat suggests they are involved in the formation of copulatory plug. Semen coagulation at the time of mating and copulatory plug formation observed in some rodents were products of complex biochemical interaction that involved the coagulation of a specific protein secreted by the seminal vesicles (Notides and Williams-Ashman, 1967; Parr *et al.*, 1994). The nature and properties of the particular vesicular protein involved in this complex biochemical interaction in the cane rat awaits further study.

In almost all eutherian species, the Bulbourethral glands is a compound tubulo-alveolar gland that is covered by dense connective tissue capsule from which several septae penetrate and divide the gland into lobes and lobules (Cakir and Karatas, 2004; Badia *et al.,* 2006). However there appeared to be both striated and smooth muscles as well as connective tissue involvement in the separation of the lobes and lobules in the greater cane rat. Each lobule, separated by scanty interstitial tissues, is composed of endpieces/secretory units and excretory ducts both of which are lined by single layered cells. The appearance of these secretory cells varies with age and functional activity of the gland. In the pig, Badia *et al*, (2006) reported that secretory cells are columnar to pyramidal shaped cells with largely the same biochemical and cellular compositions. At the initial stages, the cells appeared columnar but as secretory activity progresses with more secretory granules produced, the cells became pyramidal with nuclei and cytoplasmic organelles compressed to the base and all perinuclear spaces occupied by granules. This was in contrast to what was observed in the greater cane rat where the cells become columnar as secretory activity increases. In the same vein, while the excretory ducts of Cowper's glands in most rodents were lined by simple cuboidal cells (Sirigu *et al.,* 1993) and simple columnar in pigs (Badia *et al.*, 2006), it was found to be pseudostratified in the cane rat. This was comparable to what obtained in the humans (Chughtai *et al.,* 2005).

According to Dunker and Aumuller (2002) a striking feature of bulbourethral glandular epithelium in most rodents is the presence of large amount of filamentous or reticulated secretory vacuoles alongside with the secretory granules. This feature was observed to be absent in the bulbourethral glandular epithelium of the greater cane rat. In pigs, although the presence of secretory vacuoles in glandular epithelium was not reported, two types of secretory granules were recognized based on the electron-density and organization of their composed materials

(Badia, *et al*, 2006).The presence of high content of membrane-bound secretory granules in the glandular epithelium of the Cowper's gland in the greater cane rat was similar that of other rodents and man (Parr *et al*, 1994; Testa-Riva *et al.*, 1994). Secretory granules of the glandular epithelium in the mice Cowper's gland were also either uniformly electron-dense or showed regions of lesser density which can be attributable to the heterogeneity of the granular compositions (Fawcett, 1981; Badia *et al*., 2006). The variation in the granular densities seen in the glandular epithelium of this gland in the cane rat might be due to the heterogeneity of the granular composition. In addition, the presence of electron dense strands radiating from the secretory granules seems to be a unique feature of the glandular epithelium in the cane rat bulbourethral glands. To the best of our knowledge, this has not been reported in the bulbourethral gland of any mammalian species. Further studies, however, are needed to fully elucidate the composition and functional interpretation of the secretions of this gland in the cane rat.

With respect to the mode of release, the observed presence of secretory granules bulging into the glandular lumen with no association between their membranes and that of the apical plasma membrane suggests an apocrine mode of release of the secretory granules. While only merocrine type of release mechanism was reported in pigs (Badia *et al.*, 2006), both apocrine and merocrine types were seen in humans (Testa-Riva *et al*., 1994). From this study, no evidence of merocrine secretion was found in the cane rat bulbourethral gland. The presence of abundant microvilli on the apical surfaces of the bulbourethral glandular epithelium observed in the cane rat had also been reported in the pig bulbourethral gland (Badia *et al.*, 2006). In the pig however, the microvilli were few, short and located at the lateral surface of the apical plasma membrane. In addition, with the presence of apical tight junctional complexes between the cells, the microvilli

were possibly involved in the absorption of material from the glandular lumen. Albeit, the roles they play in modifying the composition of the secretory products in the glandular epithelium and lumen, are yet to be fully clarified.

Our findings indicated that the shape of the bulbourethral glands in the greater cane rat is gourd-shaped, similar to that in the humans. The size of the gland relative to body weight was however, smaller compared to that of pigs, ruminants and cats but similar to that of rat. In the same vein, the strong positive correlations observed between the weights of the bulbourethral glands and that of coagulating, prostate and vesicular glands might be related to their combined roles in the formation of semen and copulatory plug. In rodents, it had been established that complex biochemical interactions exist among the secretions of coagulating, vesicular and Cowper's glands (with more between the coagulating and Cowper's gland) resulting in semen coagulation at the time of mating (Parr *et al.*, 1994; Beil and Hart, 1973).

In conclusion, the present study provided information on the structural and ultrastructural peculiarities of testis, excurrent duct and the accessory sex gland in the greater cane rat. The observed morphological peculiarities will naturally determine the functioning of these organs as well as composition and characteristics of the secretory products of the glands which were yet to be fully understood. These information, however, provide basis for further physiological, pathological and pharmacological analysis as well as the detailed functional interpretations of these organs and gland in the reproductive biology of the greater cane rat.

CHAPTER 4

IMMUNO-LOCALIZATION OF ESTROGEN (ERα AND ERβ) AND PROGESTERONE RECEPTORS (PR) ALONG THE REPRODUCTIVE TRACT AND IMMUNO-ASSAY OF SERUM LEVELS OF THE FIVE SEX HORMONES AND ESTIMATION OF ANTHROPOMETRICAL VALUES IN THE MALE GREATER CANE RAT (*Thryonomys swinderianus*).

4.1 INTRODUCTION

It is an established fact that hormones play vital roles in the development and functioning of the male reproductive system as well as regulate its responses to different environmental conditions (Min and Lee, 2010). While luteinizing hormone (LH) stimulates the production of testosterone from the Leydig cells in the testis, the follicle stimulating hormone (FSH) is important to sperm maturation in the epididymis (Emmanuella and Emmanuella, 2002). Testosterone is the primary hormone that regulates the process of spermatogenesis as well as the growth and secretory activities of the male gonads, the excurrent ducts and accessory sex glands (Kalra and Kalra, 1979; Robaire *et al.,* 2007). It has now been established that estrogen, which is produced from androgen by an irreversible reaction catalyzed by P450 aromatase (CYP19A1) enzyme (Carreau and Hess, 2010), plays key roles via intracellular estrogen receptors (ERs) in the development and maintenance of reproductive function and fertility (Carreau *et al.,* 2008) as well as in pathological processes observed in tissues of the reproductive system (Prins and Korach, 2008). In fact, in the recent work of Carreau *et al*, (2011), it was reported that the highly organized and coordinated spermatogenic processes are controlled by a well-regulated estrogen–androgen hormonal balance. The alteration of this endocrine balance, which can be caused by obesity, has equally been shown to disrupt or impair spermatogenesis and epithelial morphology of the epididymis in both man and rodents (Hess, 2003; MacDonald *et al*, 2010). According to Joseph *et al*, (2011) estrogen and its two receptors, ERα and ERβ, show a high degree of species

variability in their pattern of distribution along the genital tract and often reveal a different topography in the cell types of the male genital organs.

The role of progesterone in the male reproductive tract is largely unknown. However, progesterone receptors (PR) have been identified in some segments of the genital tract as well as in the epithelium and stroma of both the penis and prepuce of male sea lions, primates and man (Colegrove *et al.,* 2009). The import of this receptor in these organs is equally yet unknown simply because few studies have examined the expression, distribution and function of progesterone receptor in the mammalian males (Luetjens *et al*., 2006; Colegrove *et al*., 2009). In understanding the functions of estrogen and possibly progesterone in the physio-pathological mechanism of the male reproductive tract, it is important to first establish the pattern of distribution of their receptors along the reproductive tract as well as characterize anthropometrical indices like body mass index (BMI) and Lee index in order to set limits for obesity especially in wild rodents undergoing domestication.

Information on the male sex hormones and the distribution of their receptors along the reproductive tract as well as the BMI of the male greater cane rat are grossly lacking. Therefore, this part of the work describes the localization and distribution of estrogen (ERα and β) and progesterone receptors and characterizes the average serum levels of five sex hormones – testosterone, estrogen, progesterone, luteinizing and follicle stimulating hormones in sexually matured male greater cane rat. It also attempts to set obesity limits by characterizing optimal values for body mass (BMI) and Lee indices (LI) in the greater cane rat.

4.2. MATERIALS AND METHODS

4.2.1 Animals

A total of Seventy two (72) sexually matured adult male greater cane rats, obtained from Good health Farms Igbesa, Ogun State and Pavemgo Grasscutter Farm, Ibereko, Badagry, Lagos state, were used in this study. Six (6) males were used every month from March, 2012 – February, 2013. The animals were kidded and raised in captivity with known reproductive and medical records. Their ages ranged from 15 – 24 months and they weighed between 2kg – 3.5kg (2000 – 3500g). All the animals had brownish perineal staining which is usually used as index of sexual maturity in male cane rat (Adu and Yeboah, 2003). They were left to acclimatize for three weeks at the Grasscutter domestication unit, College of Veterinary Medicine, Federal University of Agriculture, Abeokuta and maintained on the combination of maize, cassava and ground nut cake with salt to taste. They were also provided with Elephant grass stems and water was given *ad libitum*.

4.2.2 Sample Collection and Tissue Processing

Blood Sample Collection, Body and Tissue Measurements

Each of the six animals for each month was lightly anaesthesized with chloroform in a closed container after which body measurements; weight, height, and nose-to-anus length of each cane rat was taken and recorded. The age of each animal for the month was also recorded. The weights were taken using the Mettler's weighing balance; the heights were measured from the scapular point to the ankle while the length was measured from the tip of the nose to the anus.

The body mass and Lee indices for each animal were calculated as recommended by Bernardis (1970) and adapted by Novelli *et al.*, (2007): BMI = body weight (g) divided by the square of the nose-to-anus length (cm). Lee index = cube root of body weight (g) divided by nose-to-anus length (cm).

Blood samples were collected from the six animals for the month through the left ventricle of the heart using sterile hypodermal needle and syringe. The blood samples, stored in plain sample bottles were allowed to clot and serum samples for the hormonal immunoassay separated after centrifuging the blood at 1000rpm in a centrifuge (Model 800, England). Each animal, after blood collection, was then opened-up through a mid-ventral abdominal incision. The ischiatic arch was completely disarticulated to expose the reproductive organs. The testes were carefully dissected out individually. The weight, linear measurements (length, width and diameter) and volume of the testes were taken for each of the six animals for each month using microwa analytical balance, vernier caliper and water displacement method respectively.Samples were then taken for histology.

Hormonal Assays

The serum levels for testosterone, estrogen, progesterone, luteinizing and follicle stimulating hormones were assayed for each of the six animals in each month of the year using the Microplate Immunoenzymometric assay kits specific for each hormone. For testosterone, the DS-EIA-STERIOD-TESTOSTERONE-RT kit (Interco Diagnostic Ltd, UK) was used while for estrogen, ESTRADIOL-ELISA test kit (Fortress Diagnostics Ltd, UK) was employed. The progesterone kit used was the DS-EIA-STEROID-PROGESTERONE-RT (Interco Diagnostic Ltd, UK) while DS-EIA-GONADOTROPIN-LH (Interco Diagnostic Ltd, UK) and DS-EIA-GONADOTROPIN-FSH (Interco Diagnostic Ltd, UK) were used for the luteinizing and follicle

stimulating hormones respectively.Each kit contains Calibrators (serum reference for the hormone at graded concentrations), Control serum, Conjugate (monoclonal anti-hormone-antibodies conjugated with horse radish peroxidase), Anti-hormone-coated microtiter wells, Washing solution (concentrated 25folds), TMB-Substrate (Tetramethylbenzidine in citric acid buffer and H_2O_2) and stopping reagent (0.2M sulphuric acid solution)

The test kit operates on the principle of delayed competitive enzyme immunoassay which implies that, the hormone present in the sample serum, for instance testosterone, competes with the enzyme-testosterone conjugate for binding with the anti-testosterone antibody coated on the microtitre plates to form antigen-antibody complex. While the unbounded conjugate is removed by washing, the enzyme on the bounded fraction digests the TMB-Substrate. This enzyme activity of the bounded fraction, revealed by the colour change in the TMB-Substrate solution, is what is measured by the microtitre plate reader at 450nm and 620nm wavelength absorbance. The measure of this enzyme activity is inversely proportional to the concentration of the testosterone present in the sample serum. The actual concentration of the particular hormone (in this example, testosterone) present in the assayed serum sample can therefore, be deduced from a dose-response curve generated by plotting the absorbance against the known standard/reference serum testosterone concentrations (calibrators)

The test procedure according to the user instruction for each kit, which is almost the same for all the five hormones, was duly followed in this work. 25µl of each of the calibrators, control serum and sample serum of each of the six cane rats for each month, were pipetted into appropriately labeled microtitre wells in duplicate. 10µl of the conjugate was added to each well, swirled for 20-30 seconds to mix, covered and incubated for 60minutes at room temperature. After 60minutes the content of the microtitre were decanted and blot-dried with absorbent tissue

paper. To each well, 300µl of reconstituted washing solution (prepared by mixing the concentrated Washing Solution and distilled water at ratio 1:25 in a separate jar) was then added, decanted and blot-dried. This washing was repeated four (4) additional times, after which 100µl of TMB-Substrate was pipetted into each well at timed intervals and incubated for 15-20minutes at room temperature in a dark cupboard. The reaction was then stopped by the addition of 150µl of the stopping reagent into each well at timed intervals and the microtitre wells read on an ELISA reader (Elx 800, BioTek, England).

A 4-parameter calibrator curve was plotted with the optic densities/Absorbance on the Y-axis and calibrator concentration on the X-axis. The serum concentration of the hormone in each sample was estimated by locating the average absorbance of the sample duplicates on the vertical axis of the graph, finding the intersection point on the curve and reading the concentration from the horizontal axis of the graph. All the test validation criteria for each of the assay were met in this work in accordance with the kit manufactures' instructions.

Immunohistochemistry Protocols for Estrogen (α and β) and Progesterone receptors

Preparation of Tissue sections

For the immunohistochemical study, serial sections were made from the paraffin embedded samples used for histological studies (in chapter three of this work). The 4µ-thick sections were mounted on clear gelatinized slides after floating on a warm water bath and dried overnight in a 37^0C incubator (FSim-S-P08, Laboratory Marketing Service, South Africa). The mounted tissue samples were deparaffinized using xylene and rehydrated in graded ethanol series of 100%, 90%, 70% and washed in running water for 5minutes prepared for antigen retrieval,

permeabilization, blocking and incubation with primary and secondary antibodies for each of the receptors.

Antigen Retrieval Techniques for Estrogen (α and β) and Progesterone receptors

The antigen retrieval is usually done on sections taken from formalin-fixed, paraffin-embedded tissues in order to enable those antigens that are blocked by the cross-linking of the formalin fixation to be uncovered for binding to the relevant antibody. Here, for both estrogen and progesterone receptors, the microwave oven method using Citrate buffer solution at pH 6 was employed for the antigen retrieval (in accordance with the antibody manufacturer's instruction). The Citrate buffer solution was prepared by dissolving 2.94g of Tri-sodium citrate (dihydrate) (Associated Chemical Enterprise, South Africa) in 1000ml distilled water and the pH adjusted to 6 after which 0.5ml of Tween- 20 (Merck, Germany) was added. The solution was thoroughly mixed and stored at 4^0C before use. The Tris buffer solution (TBS) used for all the washings was also prepared by dissolving 17.54g of NaCl and 12.12g of Tris base (Tris (hydroxymethyl) aminomethane) (Merck, Germany) in 2litres of distilled water with pH adjusted to 7.6 with 5M HCl.

To retrieve the Estrogen (α and β) and progesterone antigens, the sections were heated in the microwave oven (DMO 289 Model, Defy Appliances Ltd. South Africa) set at 720W for 10minutes. They were then allowed to cool for 30minutes before being washed in running water for another 5minutes. After washing, the area around the sections was wiped dry and delineated with Dako pen (Dako, Glostrup, Denmark). Endogenous peroxidase activity was neutralized by incubating the sections in prediluted 3% H_2O_2 (RE7101) obtained from Novocastra^{TM} kit (Peroxidase Detection System; Product number: RE 7110-K, Novocastra Laboratories Ltd, UK)

for 5-10minutes. The sections were then washed by stirring 3times for 10minutes each in TBS at pH 7.6 before being blocked in protein.

Protein blocking

After washing in TBS, the sections for the Estrogen (α and β) and progesterone receptors were then incubated in pre-constituted protein blocking solution (RE 7102) obtained from the Novocastra™ kit for 20minutes. The solution contained 0.4% Casein in phosphate-buffered saline with stabilizer, surfactants and 0.2% Bronidox L as preservative. After blocking, the sections were stir-washed 3times for 10minutes each in TBS ready for the primary antibodies.

Incubation with primary and secondary antibodies

To avoid freeze/thaw cycle, both antibodies were aliquoted into ependoff tubes and stored at -20^{0}C. Prior to its use on the tissue samples, the combination and dilutions of the primary antibodies together with the detection system were validated and optimized on a series of both known positive and negative controls.

The sections for the Estrogen receptors were incubated overnight at 4^{0}C in 1:100 dilution of 1µl rabbit polyclonal for Estrogen receptor alpha (ERα – Ab37438, abcam®, UK) and Estrogen receptor beta (ERβ – Ab3577, abcam®, UK) on separately labelled slides. The following day, the sections were rinsed 3times, 10minutes each in TBS and incubated, at room temperature for 30minutes, in 1:300 dilution of biotinylated goat-anti-rabbit secondary antibody (Vector Laboratories Inc. USA) made in TBS. The sections were again washed 3times, 10minutes each in TBS. This was then followed by incubation with Streptavidin-Horse Radish

Peroxidase mixture (RE 7104) obtained from the Novocastra™ kit, for 30minutes at room temperature. The mixture contained 1-1.4µg of Streptavidin-HRP in 1ml Tris-buffered saline with protein stabilizer and 0.35% Pro-Clin™ 950.

In the case of Progesterone receptor, the sections were also incubated overnight with 1:60 dilution of mouse monoclonal (PR-AT 4.14) to progesterone receptor – ChIP Grade (Ab2764, abcam®, UK) at 4^0C. The next day, the sections were stir- washed in TBS 3times for 10minutes each. The sections were then incubated for 30minutes, at room temperature, in 1:300 dilution of biotinylated polyclonal goat-anti-mouse secondary antibody (Dako Glostrup, Denmark) made-up in TBS, after which the sections were stir-washed 3times for 10minutes each in TBS. This was also followed by incubation with Streptavidin-Horse Radish Peroxidase mixture (RE 7104) obtained from the Novocastra™ kit, for 30minutes at room temperature.

All the sections (both for Estrogen and Progesterone receptors) were incubated for 5minutes at room temperature in 1:20 dilution of pre-diluted diaminobenzidine (DAB) chromogen (RE 7105) in DAB substrate buffer (RE 7106) both obtained from the Novocastra™ kit. The chromogen contained 1.74% w/v 3'3 diaminobenzidine in a stabilizer solution, while the substrate was made of 0.05% H_2O_2 and preservative. The sections were then washed in running water for 5minutes, counterstained in hematoxylin. After counterstaining, the sections were dehydrated, cleared in 70%, 95% and absolute alcohol twice for a minute each, xylene twice for 2minutes each and then mounted with coverslip in DPX mountant (Merck, Germany)

Control sections used for Immunohistochemistry

The positive control used for the Estrogen receptor alpha (ERα) was sections of the human breast cancer tissue, while sections of rat brain were used for the Estrogen receptor beta (ERβ). Sections of pregnant rat uterus were used as a positive control for progesterone receptor (PR). For the negative control, the primary antibodies were omitted and TBS used on an adjacent section for every treated section.

4.3 RESULTS

4.3.1 Serum Hormonal assay in the greater cane rat

Table 12: The mean, standard deviation and range of serum concentration of testosterone, estrogen, progesterone, luteinizing and follicle stimulating hormones in the male greater cane rat

	Testosterone (nmol/L)	*Estrogen (pg/mL)*	*Progesterone (nmol/L)*	*Luteinizing Hormone (mIU/ml)*	*Follicle stimulating Hormone (mIU/ml)*
Mean	**4.11**	**27.5**	**4.32**	**1.79**	**2.54**
±SD	**±2.57**	**±11.6**	**±2.04**	**±0.48**	**±0.55**
Range	**0.2-8**	**10-65**	**2-6.5**	**1.15-3.1**	**2-4**

Testosterone

The mean testosterone level in the greater cane rat was 4.11 ±2.57 nmol/L (1.18ng/ml) (Table 12). The values range from 0.2 – 8nmol/L (0.05 – 2.30ng/ml) in the sampled population (*n=72*) using a kit with 0.2nmol/L lower detection limit and intra- and inter assay co-efficient of variations at 5.6% and 6.5%, respectively.

Estrogen

The serum level of estrogen in the male greater cane rat was observed to be 27.5 ±11.6 pg/ml (Table 12). In the sampled population (n=72), the value range was 10-65 pg/ml with the kit having a sensitivity of 6.5pg/ml and within- and between assay co-efficient of variation of 7.8% and 9.7%, respectively.

Progesterone

Immunoassay revealed the presence of progesterone in the serum of the greater cane rat. The mean serum progesterone level was 4.32 ±2.04 nmol/L (Table 12). The values range from 2 – 6.5nmol/L in the sampled population (n=72) using kit with 0.5nmol/L sensitivity, 3.5% intra- and inter assay co-efficient of variations.

Luteinizing and Follicle stimulating hormones

The mean serum value for luteinizing hormone was 1.79 ±0.48mIU/ml with the values ranging from 1.15 – 3.1mIU/ml while that of follicle stimulating hormone (FSH) is 2.54 ±0.55 mIU/ml and value range of 2 -4 mIU/ml (Table 12) in the sampled population of greater cane rat (n=72). The values were obtained with luteinizing hormone kit whose intra- and inter-assay precision has co-efficient of variation of 4.06% and 4.36% respectively, as well as lower detection limit of 0.3mIU/ml. While the sensitivity of the FSH kit was also 0.3 mIU/ml, the intra- and inter-assay co-efficient of variation were both 7.9% apiece.

4.3.2. Anthropometrical Indices in the greater cane rat

Table 13: The mean, standard deviation and range of age, linear body measurements and anthropometric values in the male greater cane rat

	Age (Months)	*Body weight (kg)*	*Body length (cm)*	*Height (cm)*	*BMI (g/cm^2)*	*Lee index (g/cm)*
Mean	**12.8**	**2.23**	**43.6**	**16.36**	**1.18**	**0.30**
±SD	**±6.15**	**±0.40**	**±3.17**	**±1.04**	**±0.20**	**±0.02**
Range	**7-24**	**1.42-3.04**	**37-50.5**	**14.5-19**	**0.88-1.70**	**0.27-0.35**

Table 14: The mean, standard deviation and range of body weight, gross testicular morphometric data and anthropometric values in the male greater cane rat

	Body weight (kg)	*Testicular weight (g)*	*Testicular volume (cm^3)*	*Testicular diameter (cm)*	*BMI (g/cm^2)*	*Lee index (g/cm)*
Mean	**2.23**	**1.43**	**1.33**	**1.10**	**1.18**	**0.30**
±SD	**±0.40**	**±0.40**	**±0.26**	**±0.13**	**±0.20**	**±0.02**
Range	**1.42-3.04**	**0.84-2.57**	**1-2**	**0.9-1.5**	**0.88-1.70**	**0.27-0.35**

Table 15: Correlation co-efficients between age, body measurements, testicular morphometric and anthropometric parameters in the male greater cane rat

	Age (months)	*Body weight (g)*	*Body length (cm)*	*Height (cm)*	*Testicular weight (g)*	*Testicular Volume (cm^3)*	*BMI (g/cm^2)*	*Lee Index (g/cm)*
Age (months)	1							
Body weight (g)	0.57	1						
Body length (cm)	0.34	0.56	1					
Height (cm)	-0.09	0.33	0.17	1				
Testicular weight (g)	-0.18	0.01	-0.04	0.44	1			
Testicular Volume (cm^3)	-0.13	0.09	0.03	0.21	0.68	1		
BMI (g/cm^2)	0.34	0.61	-0.25	0.01	-0.04	0.01	1	
Lee index (g/cm)	0.09	0.27	-0.64	0.10	0.02	0.01	0.84	1

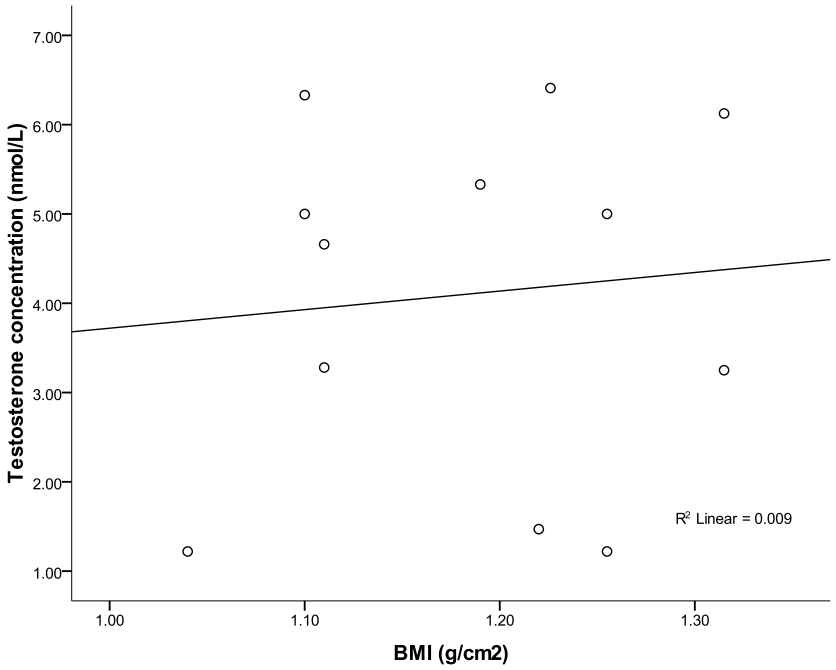

Figure 46: Scatter plot showing the relationship between the body mass index and the serum testosterone concentration in the greater cane rat. Each plot represents the mean of six samples and shows the linear correlation co-efficient (R^2).

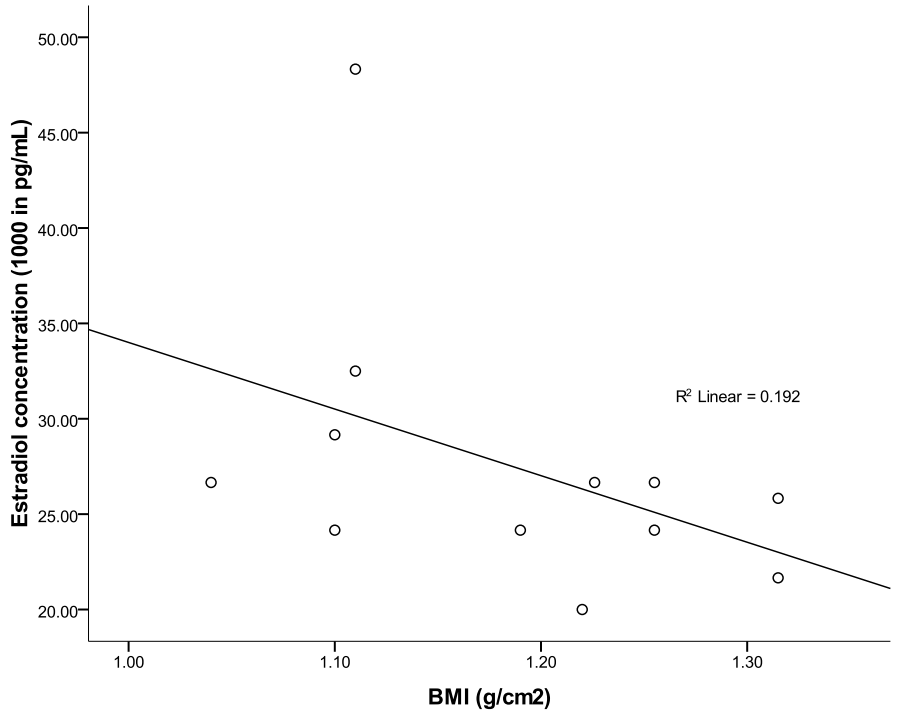

Figure 47: Scatter plot of the correlation between the body mass index and the serum estradiol concentration in the greater cane rat. Each plot represents the mean of six samples and shows the linear correlation co-efficient (R^2).

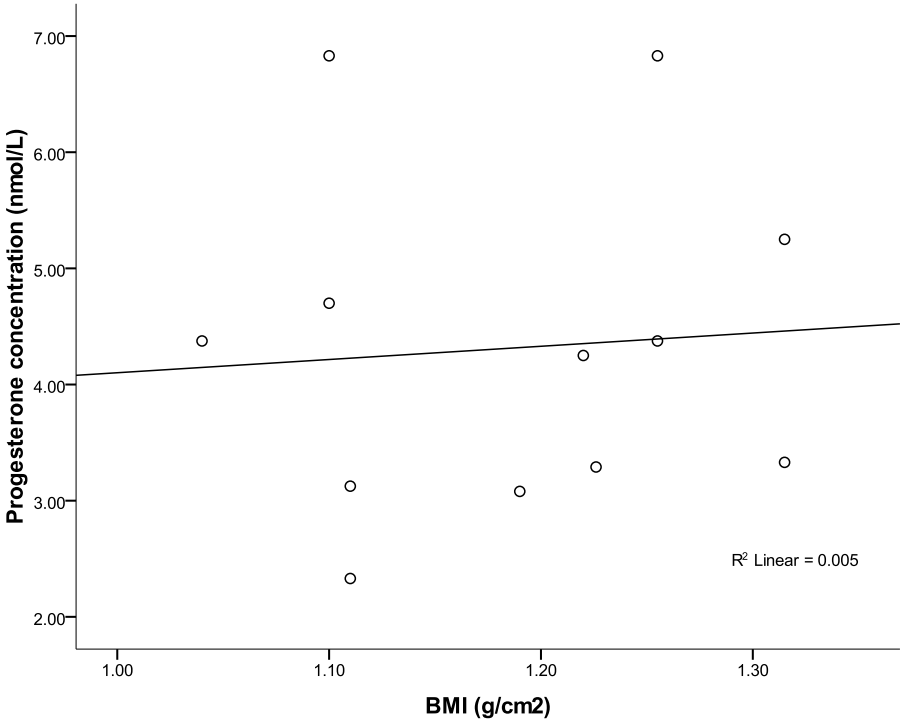

Figure 48: Scatter plot of the relationship between the body mass index and the serum progesterone concentration in the greater cane rat. Each plot represents the mean of six samples and shows the linear correlation co-efficient (R^2).

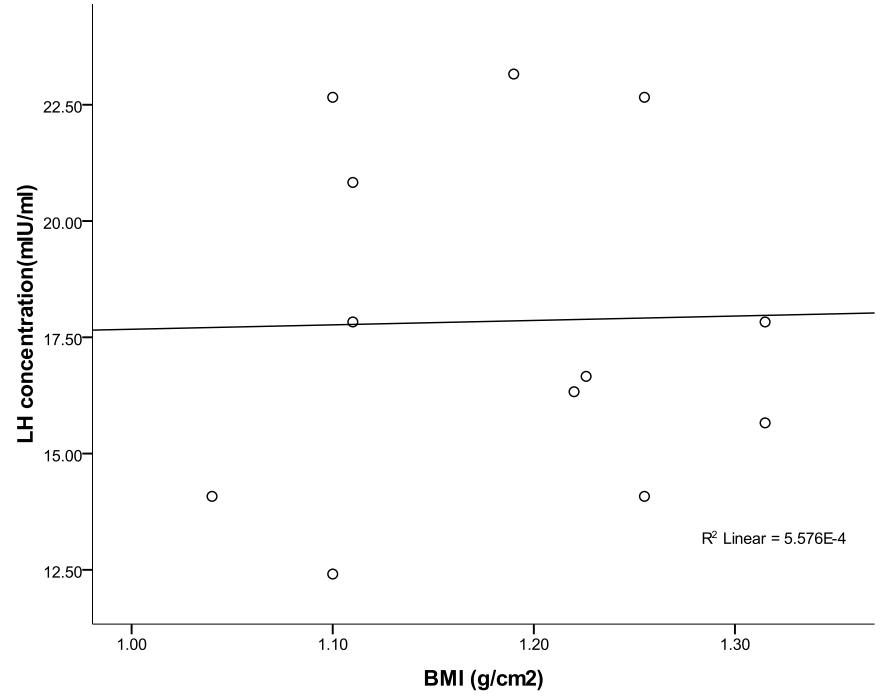

Figure 49: Scatter plot of the relationship between the body mass index and the serum LH concentration in the greater cane rat. Each plot represents the mean of six samples and shows the linear correlation co-efficient (R^2).

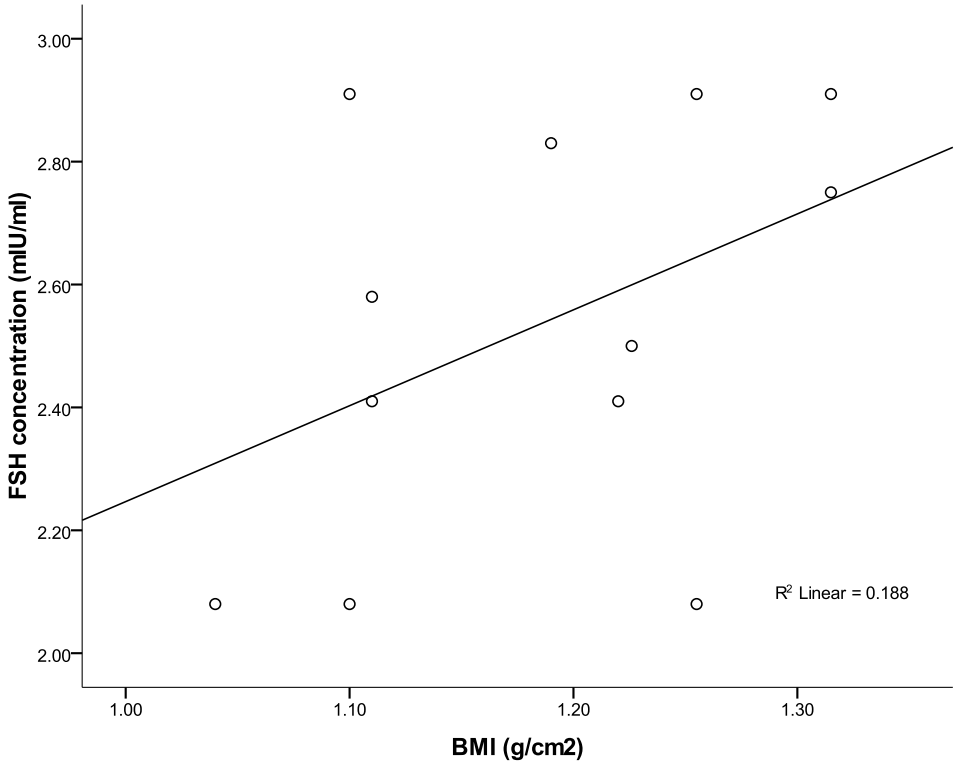

Figure 50: Scatter plot showing the relationship between the body mass index and the serum FSH concentration in the greater cane rat. Each plot represents the mean of six samples and shows the linear correlation co-efficient (R^2)

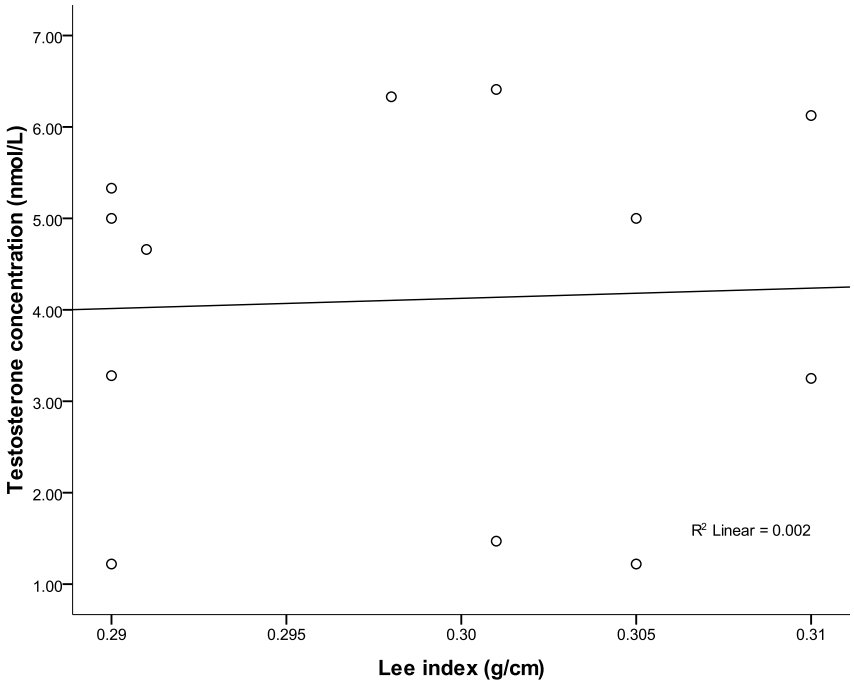

Figure 51: Scatter plot of the correlation between the Lee index and the serum testosterone concentration in the greater cane rat. Each plot represents the mean of six samples and shows the linear correlation co-efficient (R^2).

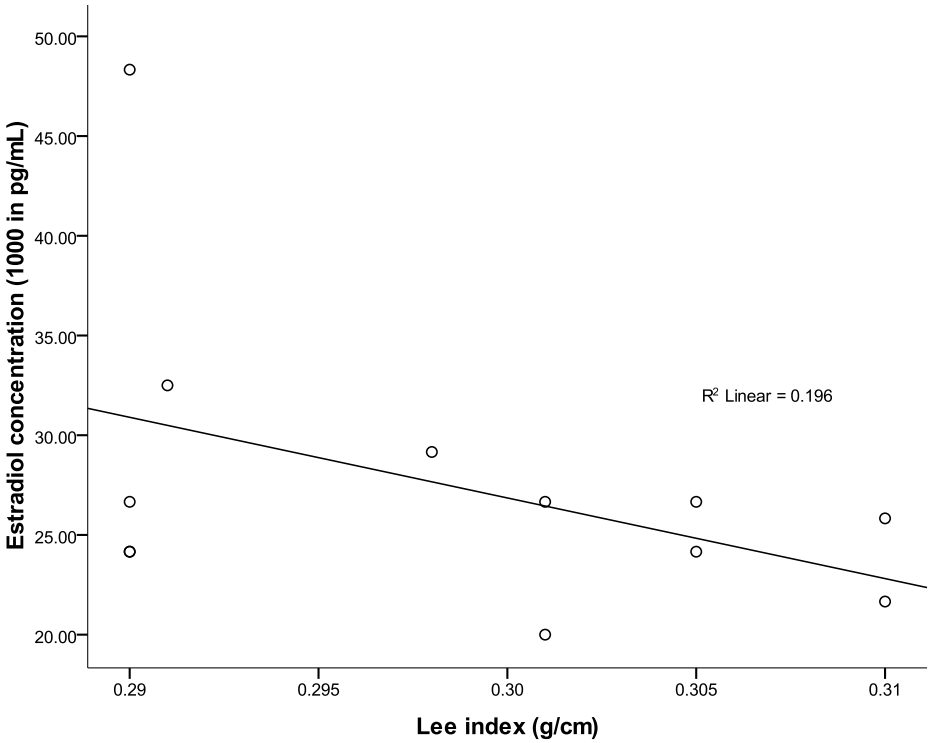

Figure 52: Scatter plot of the relationship between the Lee index and the serum estradiol concentration in the greater cane rat. Each plot represents the mean of six samples and shows the linear correlation co-efficient (R^2).

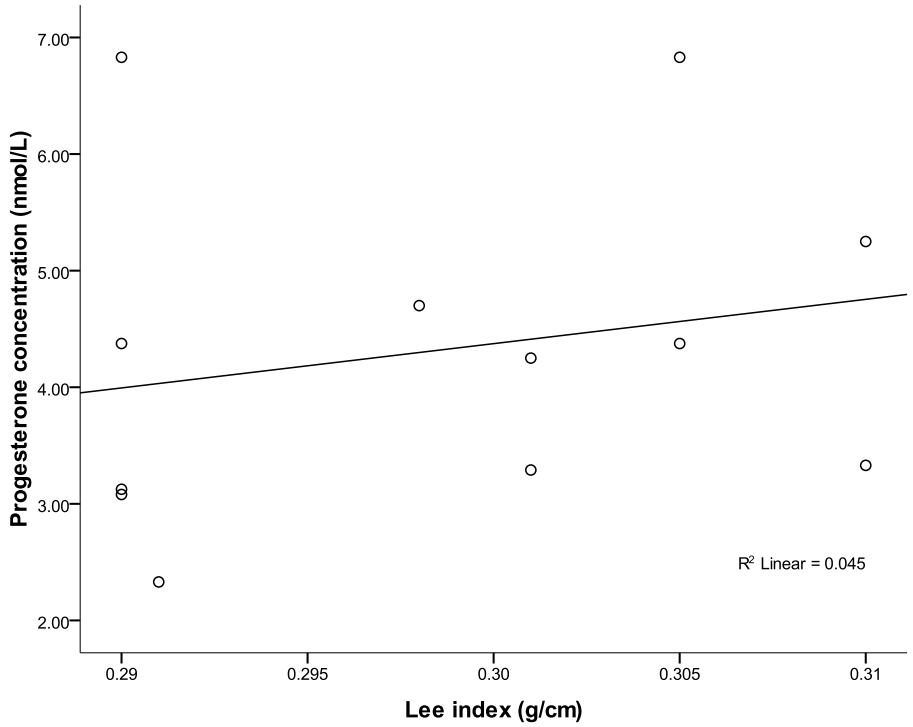

Figure 53: Scatter plot showing the relationship between Lee index and serum progesterone concentration in the greater cane rat. Each plot represents the mean of six samples and shows the linear correlation co-efficient (R^2)

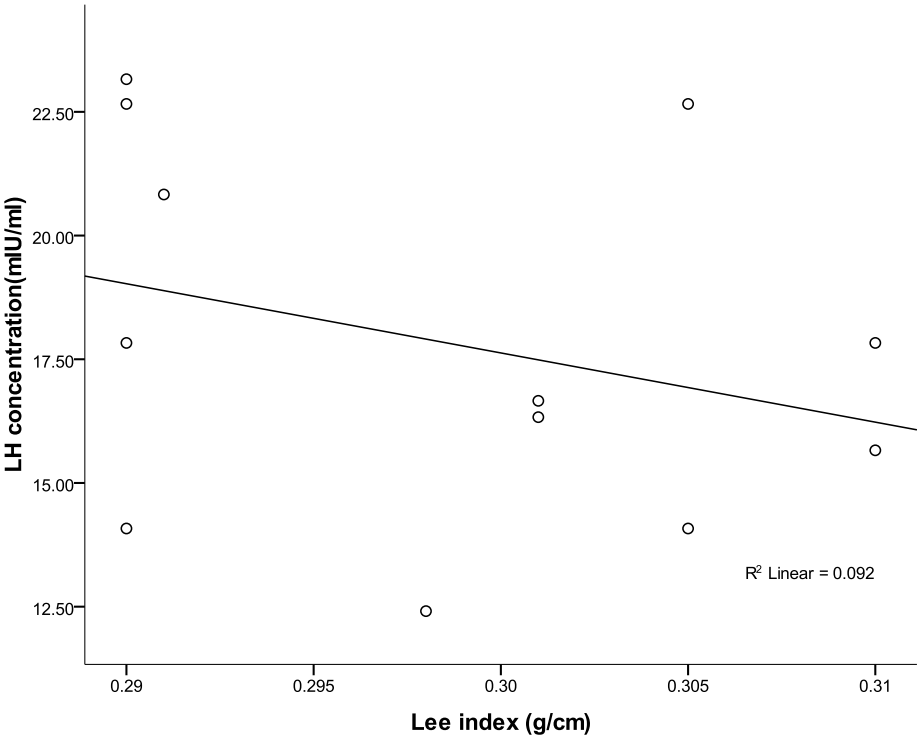

Figure 54: Scatter plot of the correlation between the Lee index and LH concentration in the greater cane rat. Each plot represents the mean of six samples and shows the linear correlation co-efficient (R^2).

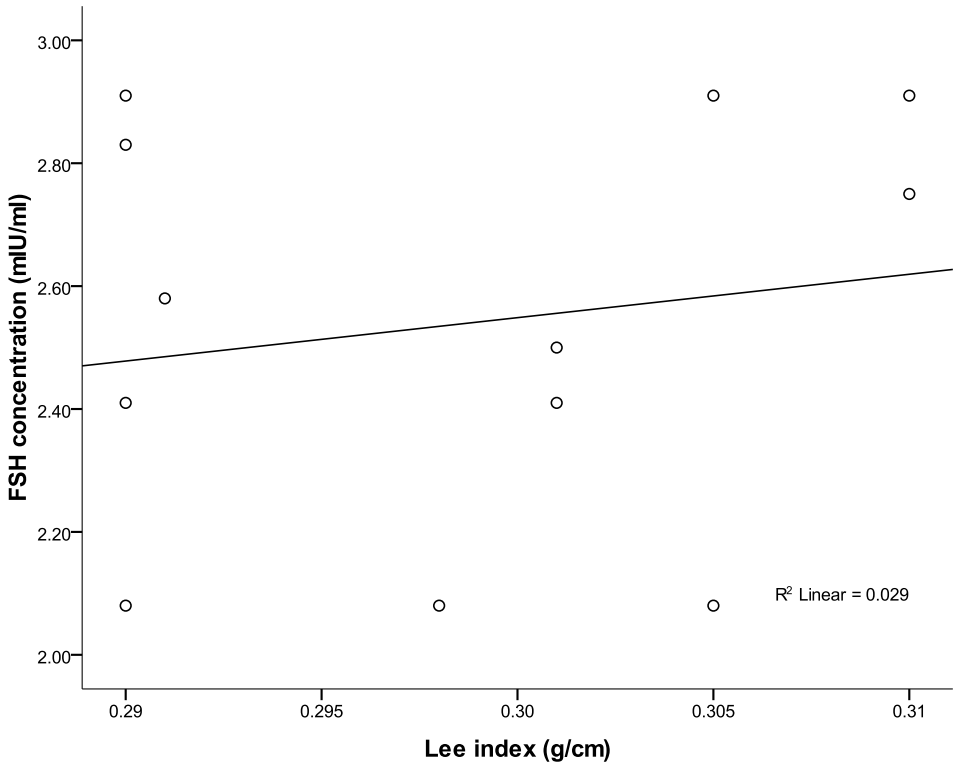

Figure 55: Scatter plot showing the relationship between Lee index and serum FSH concentration in the greater cane rat. Each plot represents the mean of six samples and shows the linear correlation co-efficient (R^2)

Table 13 showed the mean values of the linear body measurements as well as the mean values of two anthropometric indices, the body mass index (BMI) and the Lee index (LI) while table 14 revealed the mean values of the gross testicular morphometry in the greater cane rat. Table 15 showed how both the body linear measurements and the gross testicular morphometry correlate with the two anthropometric indices (BMI and LI). Each of the graphs represented the summary of the relationship between one of the hormones and each index.

From this work, it was observed that at the age range of 7-24 month, the BMI ranges from 0.88-1.70g/cm^2 with a mean value of 1.18 ±0.20g/cm^2 while LI at the same age ranges from 0.27-0.35g/cm with a mean value of 0.30 ±0.02g/cm (Table 13 & 14). There was a significantly

positive relationship between the animal height and the testicular weight and volume (r^2 = 0.44 and r^2 = 0.21 respectively) whereas no correlation was observed between length of the animals and the testicular weight and volume. In the same vein, neither the BMI nor LI showed any correlation with the testicular weight and volume in the greater cane rat (Table 15). The scatter-grams showed the BMI and LI followed almost the same pattern having no correlation with serum testosterone, progesterone, LH and FSH concentrations (Fig. 46,48,49,50,51,53,54 &55) but low correlations with serum estradiol concentration (r^2 = 0. 2 for both indices) (Fig. 47 &52)

4.3.3 Estrogen and Progesterone receptors Immunohistochemistry in the greater cane rat

Table 16: Summary of localization of the progesterone (PR), estrogen alpha and beta (ERα & ERβ) receptors along the entire reproductive tract and in the accessory sex glands of the greater cane rat.

	PR	ERα	ERβ
Testis	-	+	+
Eff. duct *	-	+	+
Epididymis			
-Init. Seg**	-	+	+
- caput	-	+	+
- corpus	-	+	+
- cauda	+	+	+
Vas deferens	-	+	+
Prostate	-	+	+
Coagulating	-	+	+
Vesicular	-	+	+
Bulbourethral	-	-	-

***** Efferent duct. ******Initial segment.

4.3.3.1 Testis

Estrogen and Progesterone receptors Immunostaining

The testes in the greater cane rat showed positive immunostaining for both estrogen receptors (ERα & ERβ) but negative for the progesterone receptor (PR). In the seminiferous tubules ERα was located on the nuclei of the Sertoli and peritubular myoid cells while in the interstitium it was found on the Leydig cell nucleus (Fig. 56). The ERβ was however localized in the cytoplasm and nuclei of seminiferous epithelial cells as well as the nuclei of the Leydig cells (Fig. 57).

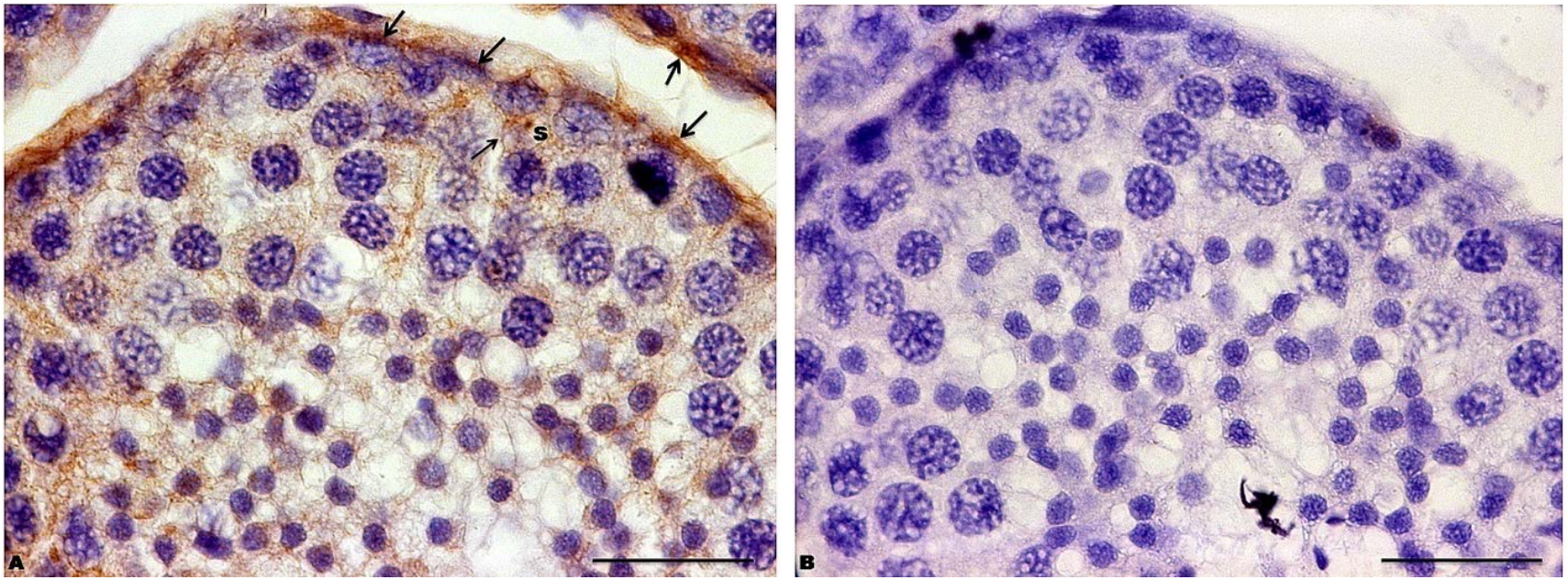

Figure 56A&B: Photomicrographs of the ERα immunohistochemistry in the testis of the greater cane rat. Figure A showed the ERα-positive staining of the Sertoli cell nuclei (S) and the peritubular myoid cells of the seminiferous epithelium (arrows) while Figure B was the negative control. Mag. X400

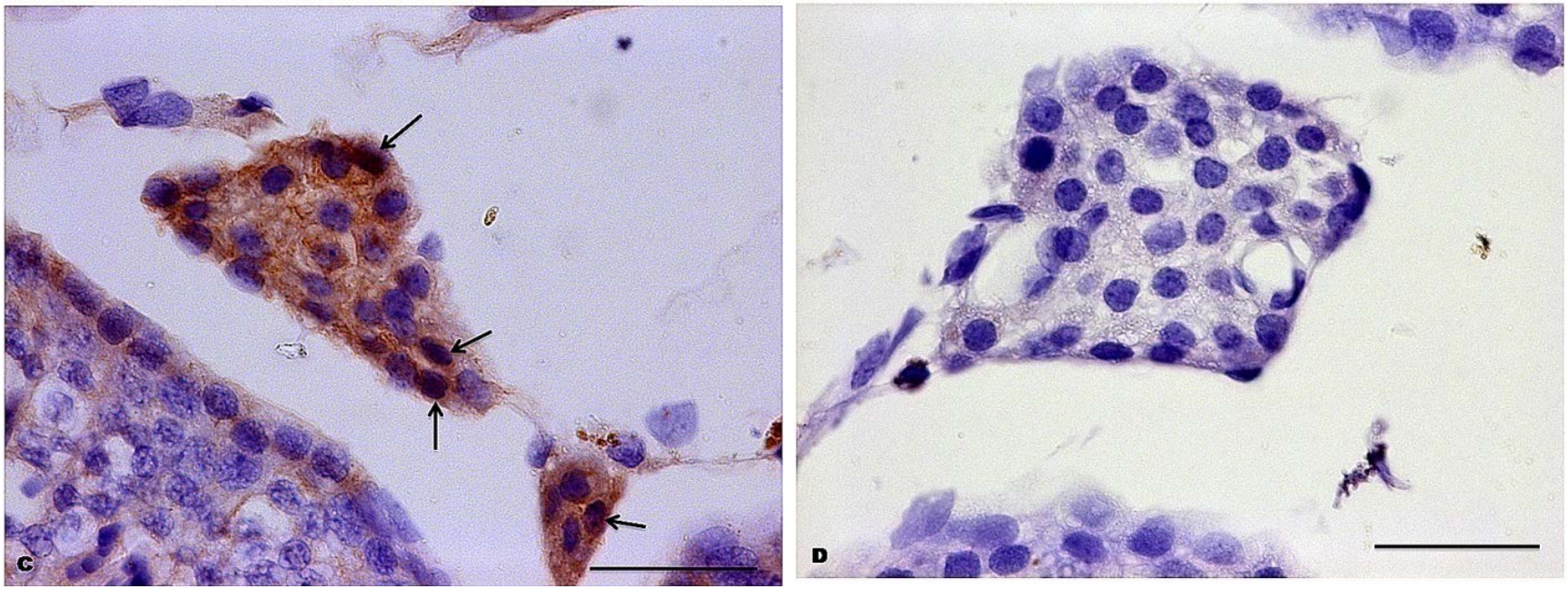

Figure 56C&D: Photomicrographs of the ERα immunohistochemistry in the testis of the greater cane rat. Figure C reveals the ERα-positive staining of Leydig cells in the interstitium (arrows) and Figure D was the negative control. Mag. X400, **Scale bar: 50µm**

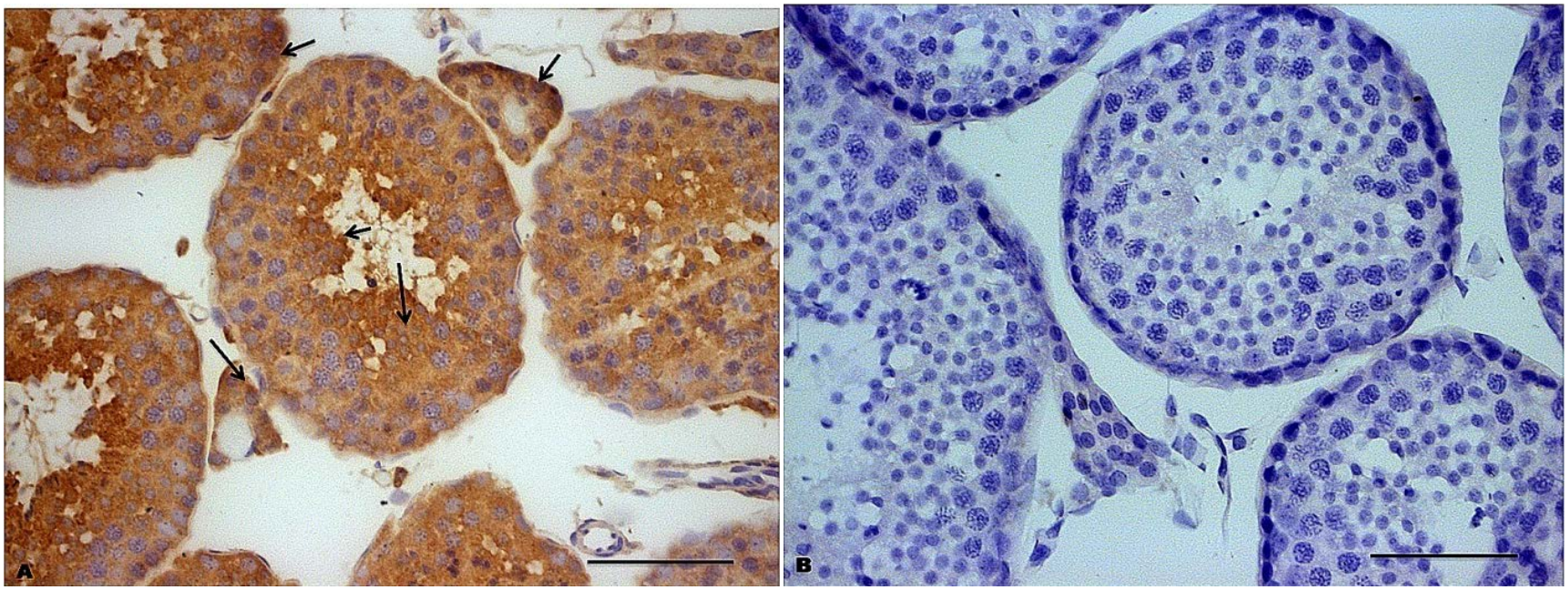

Figure 57: Photomicrographs of the ERβ immunohistochemistry in the testis of the greater cane rat. Figure A showed the ERβ-positive nuclear and cytoplasmic staining of the germinal cells and Leydig cells (arrows) while Figure B was the negative control. Mag. X400, **Scale bar: 50µm**

4.3.3.2 Efferent Duct

Estrogen and Progesterone receptors Immunostaining

The immunohistochemistry of the efferent duct in the greater cane rat showed positive staining for both ERα and ERβ with the intensity of staining increasing from proximal to distal efferent duct but no labeling for progesterone receptor (PR) (Fig. 58). While there are slight nuclear staining for ERα in both ciliated and the non ciliated cells, the cytoplasm of the ciliated cells showed intense staining for this receptor (Fig. 58A & B). Interestingly the ERα was also intensely expressed in the stroma of the efferent duct in the cane rat (Fig. 58A). There was strong immunostaining for ERβ in both the ciliated and non ciliated cells as well as the stroma of the efferent duct in the greater cane rat (Fig.59A&B).

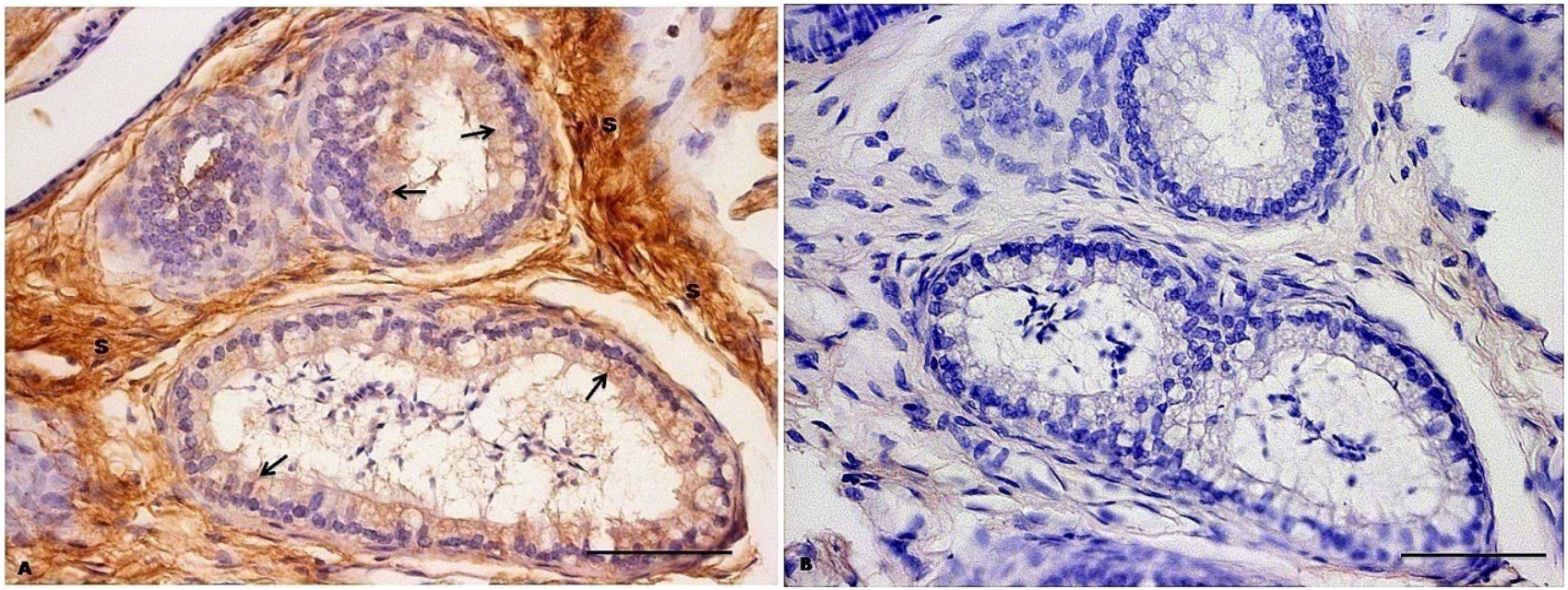

Figure 58: Photomicrographs of the ERα immunohistochemistry in the efferent duct of the greater cane rat. Figure A showed intense ERα-positive stainings of the ciliated cells (arrows) and the stroma (S) while Figure B was the negative control. Mag. X400, **Scale bar: 50µm**

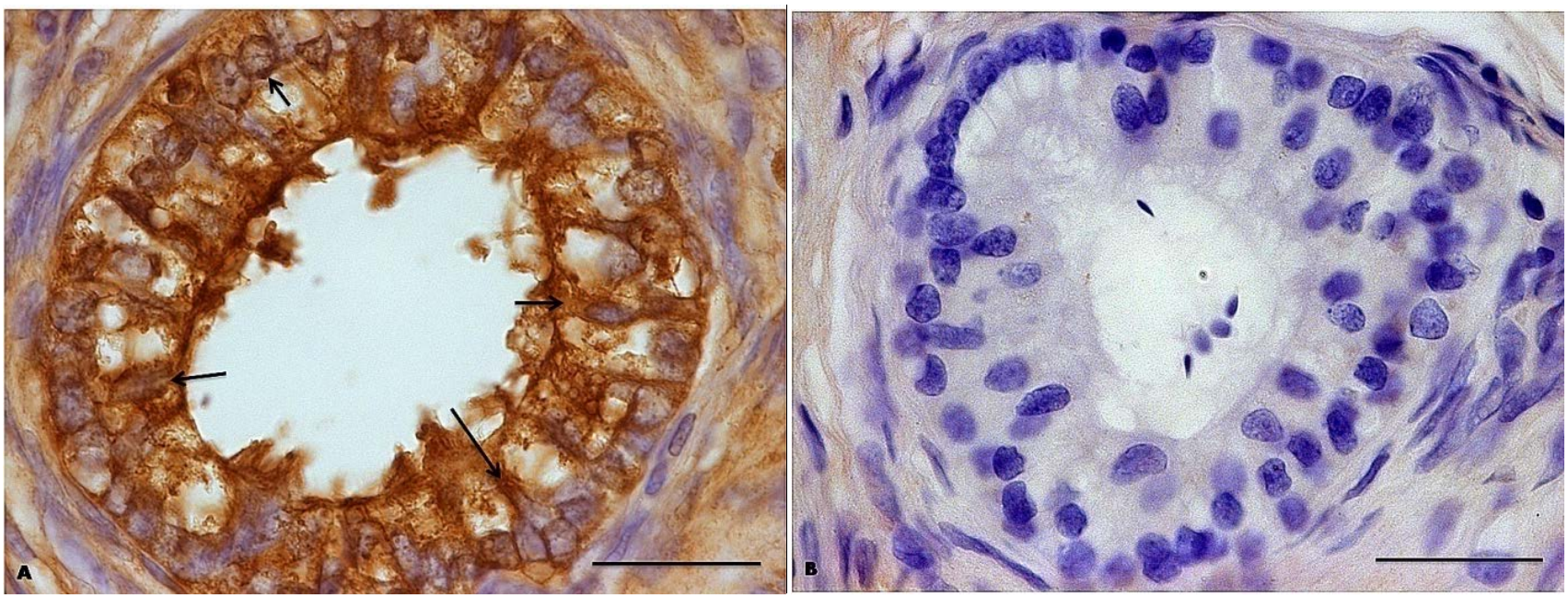

Figure 59: Photomicrographs of the ERβ immunohistochemistry in the efferent duct of the greater cane rat. Figure A showed the strong ERβ-positive staining in both the ciliated (thin long arrows) and non ciliated (thick short arrows) cells while Figure B was the negative control. Mag. X400, **Scale bar: 50µm**

4.3.3.3 Epididymis

Estrogen and Progesterone receptors Immunostaining

In the greater cane rat, the immunohistochemistry revealed no nuclear labeling for ERα throughout the epididymal epithelium. However, whereas low-intensity staining was observed in the cytoplasm of initial segment, caput and corpus epididymis (Fig. 60, 61&62), appreciable cytoplasmic labeling was seen at the cauda epididymis (Fig. 63). Immunostaining for ERα was also present in the stroma of the initial segment, caput and cauda epididymis but very weak in that of corpus epididymis (Fig 60, 61, 62 & 63).

The ERβ, though immunolocalized throughout the epithelium and stroma of the entire epididymal regions, showed selective nuclear staining for some specific cells (Fig. 64, 65, 66 & 67). In the initial segment, nuclear staining was observed in the narrow and basal cells while cytoplasmic and membrane staining was in the principal cells (Fig. 64A&B). At the caput and corpus epididymis, there were nuclear staining of the apical, clear and basal cells with labeling of the cytoplasm and membrane in the principal cells (Fig. 65, 66). In the cauda epididymis, nuclear staining was seen in the basal cells with intense membrane and cytoplasmic staining of the principal cells. Also, immunostaining was observed at the middle pieces of the sperm cells present in the cauda epididymis (Fig 67A).

A major significant finding in the study was the localization of nuclear PR on the epithelium of the cauda epididymis (Fig. 68A-B).

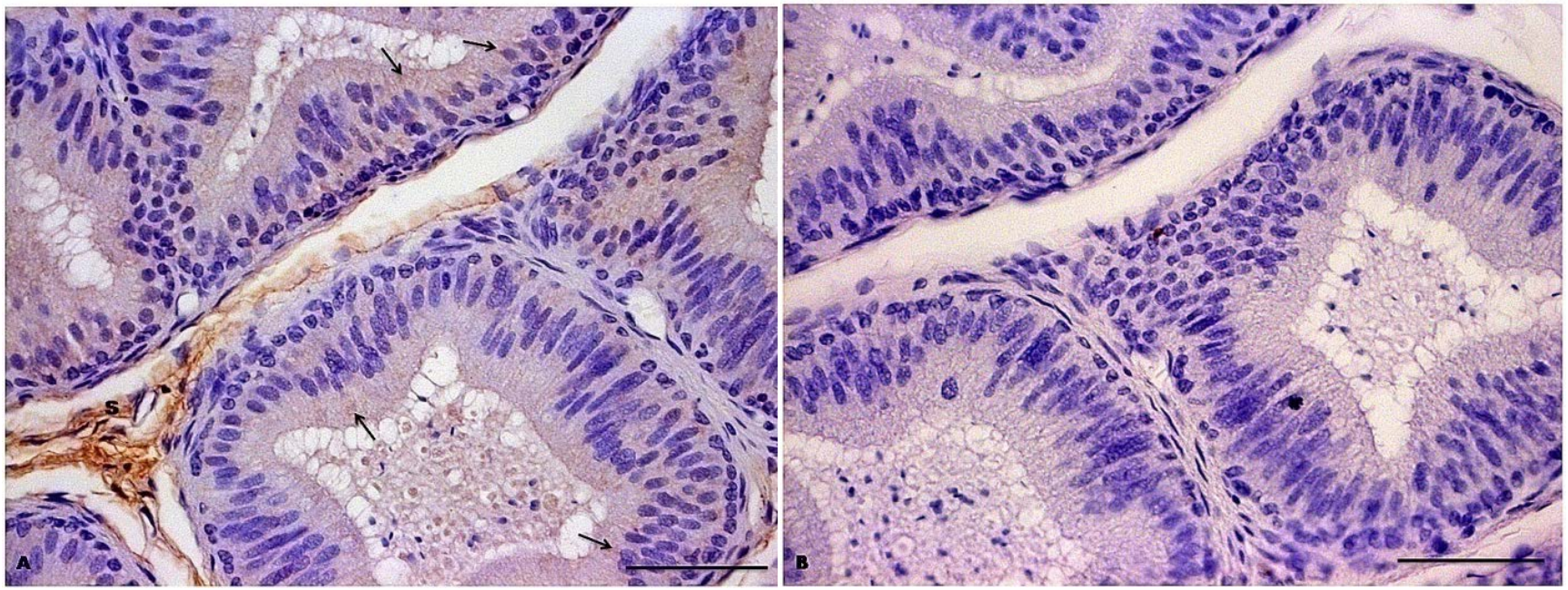

Figure 60: Photomicrographs of the ERα immunohistochemistry in the initial segment of the epididymis of the greater cane rat. Figure A showed the stroma ERα-positive staining (S) with faint labeling of the epithelial cytoplasm (arrows). Figure B was the negative control. Mag. X400, **Scale bar: 50µm**

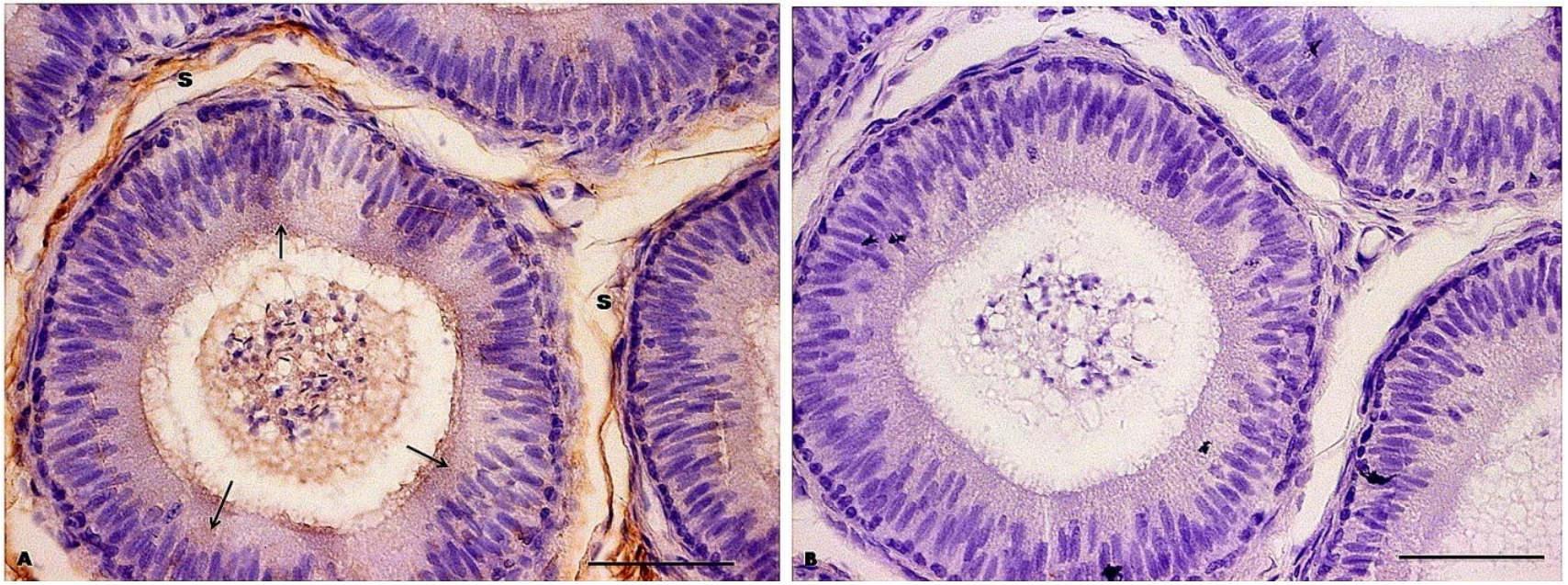

Figure 61: Photomicrographs of the ERα immunohistochemistry in the caput epididymis of the greater cane rat. Figure A showed the stroma ERα-positive staining (S) with faint labeling of the epithelial cytoplasm (arrows). Figure B was the negative control. Mag. X400, **Scale bar: 50µm**

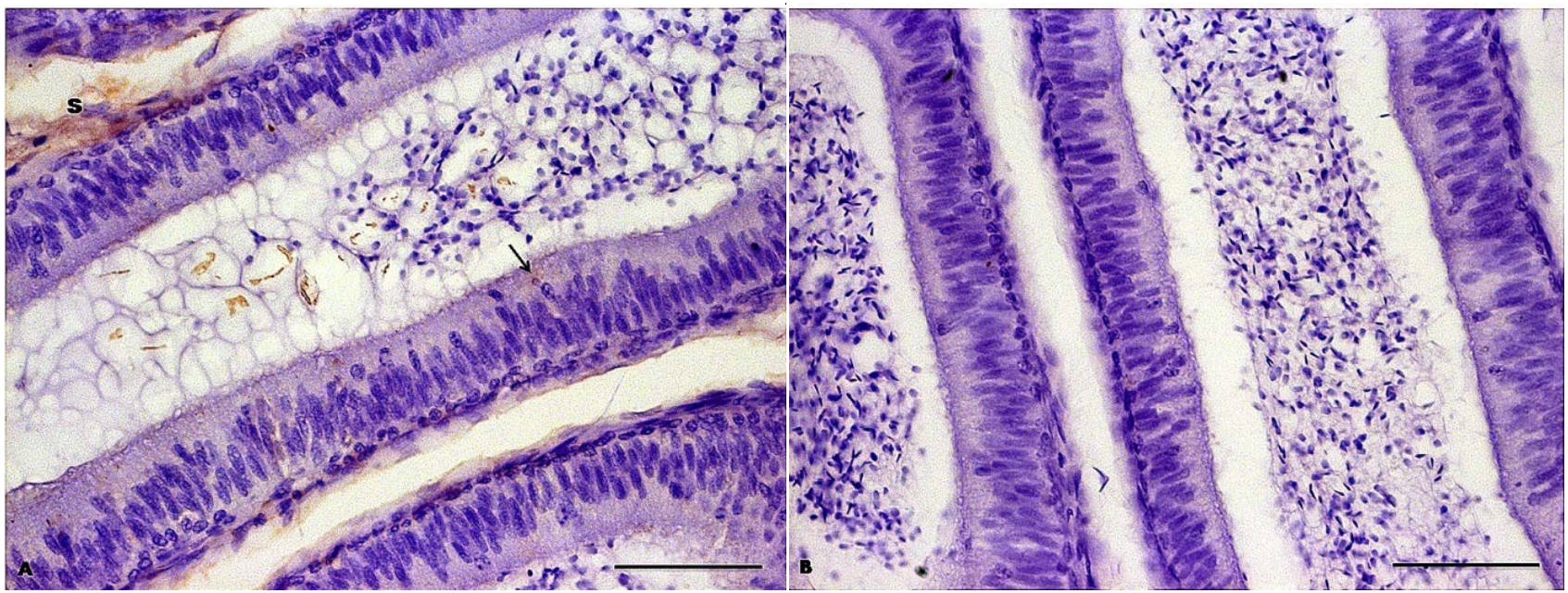

Figure 62: Photomicrographs of the ERα immunohistochemistry in the corpus epididymis of the greater cane rat. Figure A showed the faint labeling of the epithelial cytoplasm (arrows) with very weak stromal labeling (S). Figure B was the negative control. Mag. X400, **Scale bar: 50µm**

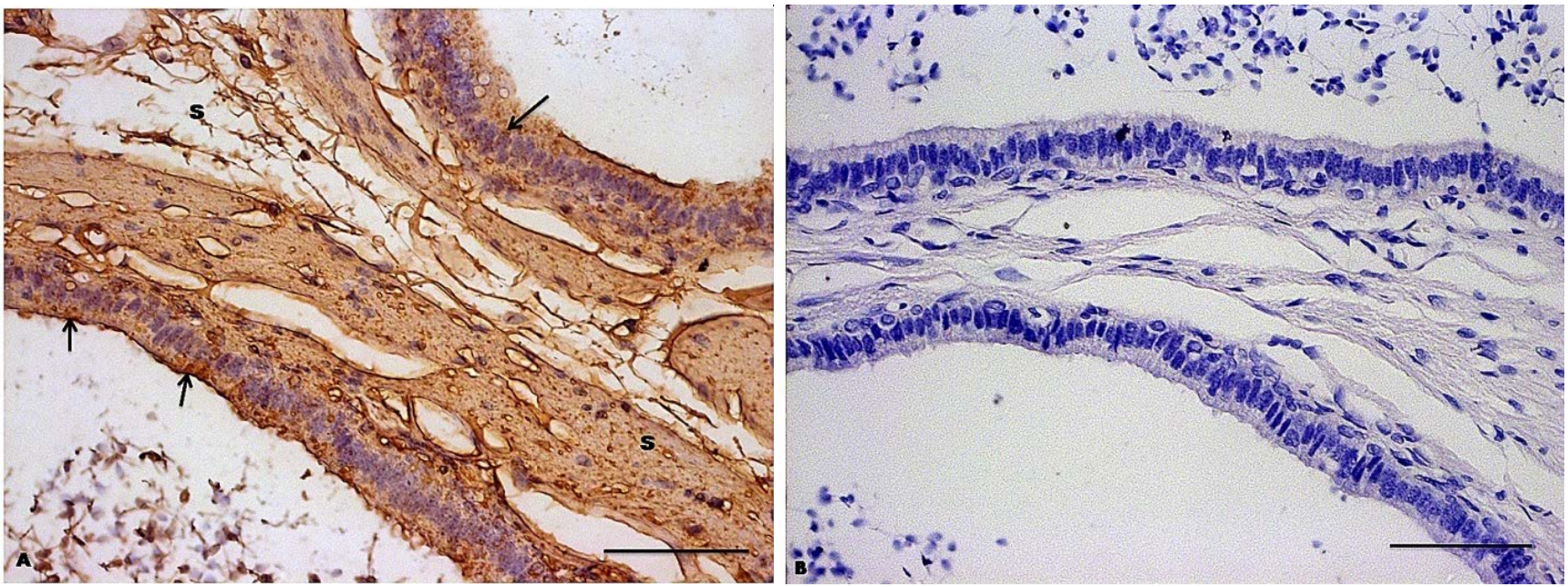

Figure 63: Photomicrographs of the ERα immunohistochemistry in the cauda epididymis in the greater cane rat. Figure A showed the intense cytoplasmic staining of the epithelium (arrows) as well as the strong stromal labeling (S). Figure B was the negative control. Mag. X400, **Scale bar: 50µm**

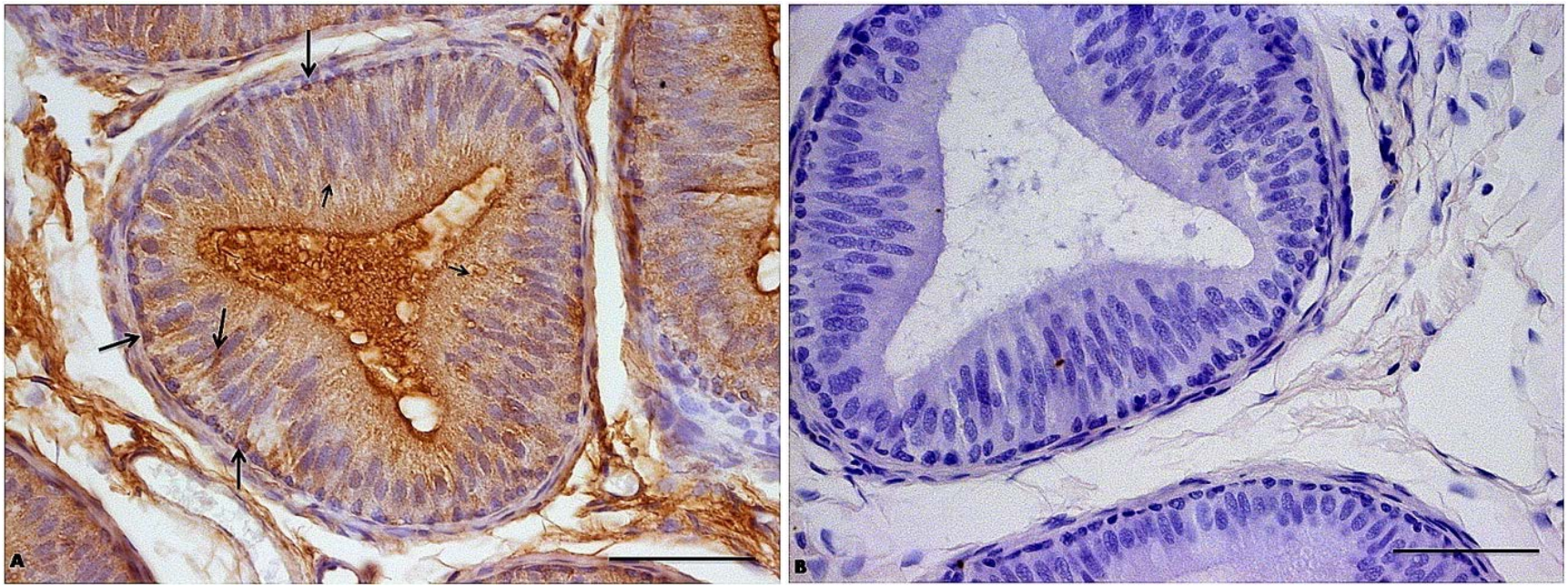

Figure 64: Photomicrographs of the ERβ immunohistochemistry in the initial segment of the epididymis of the greater cane rat. Figure A showed the selective ERβ-positive nuclear staining of the narrow and basal cells (long arrows) and the labeling of the epithelial cytoplasm (short arrows). Figure B was the negative control. Mag. X400, **Scale bar: 50µm**

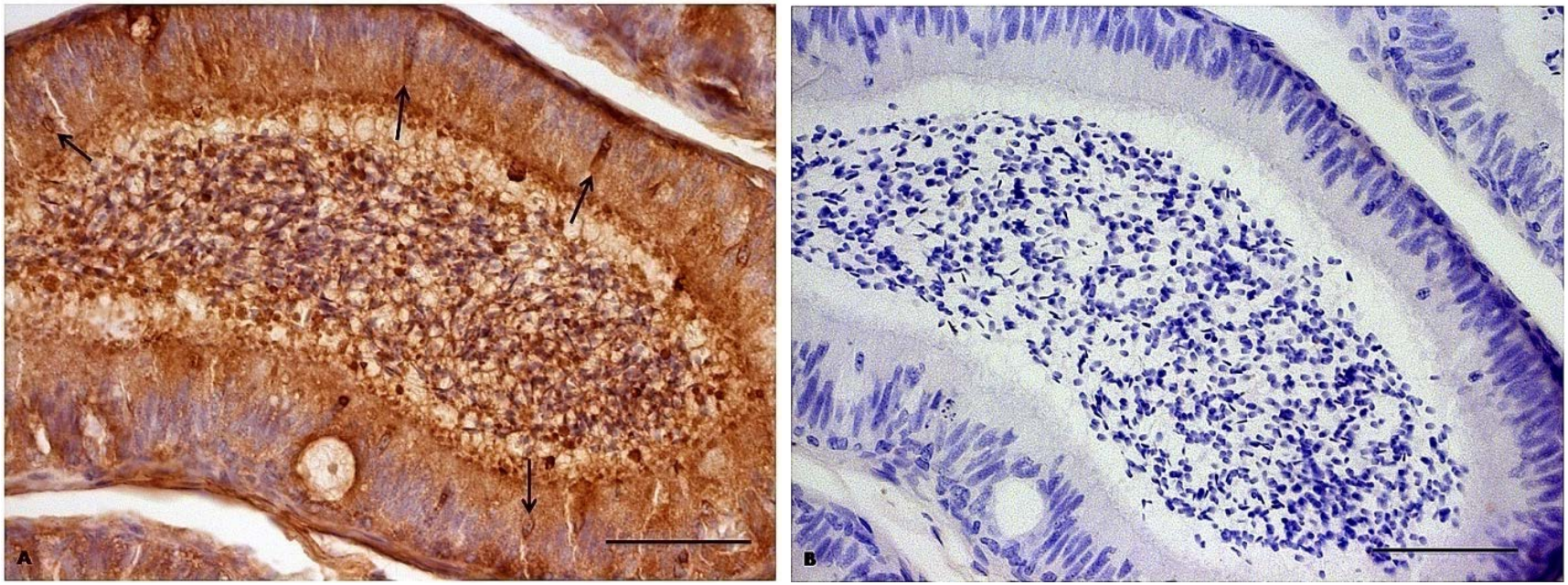

Figure 65: Photomicrographs of the ERβ immunohistochemistry in the caput epididymis of the greater cane rat. Figure A showed the selective ERβ-positive nuclear staining of the apical cells (arrows) and the labeling of the epithelial cytoplasm. Figure B was the negative control. Mag. X400, **Scale bar: 50µm**

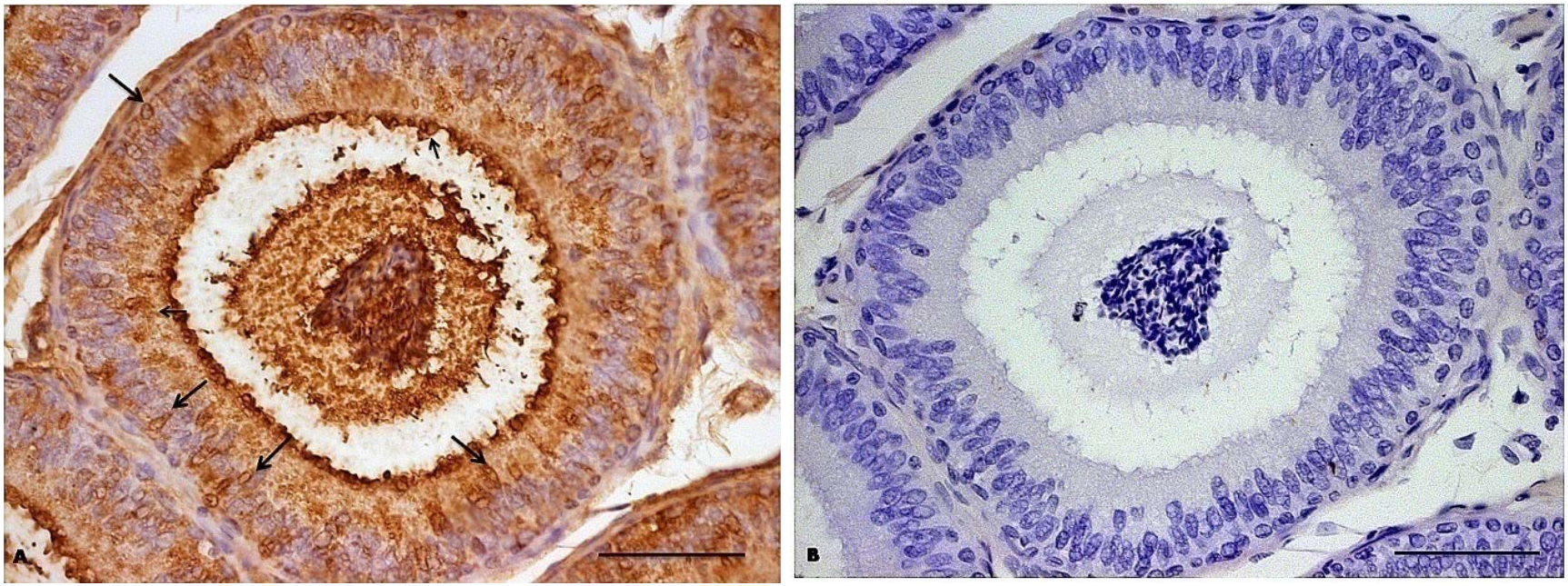

Figure 66: Photomicrographs of the ERβ immunohistochemistry in the corpus epididymis of the greater cane rat. Figure A showed the selective ERβ-positive nuclear staining of the apical and basal cells (arrows) and the labeling of the epithelial cytoplasm. Figure B was the negative control.

Scale bar: 50µm

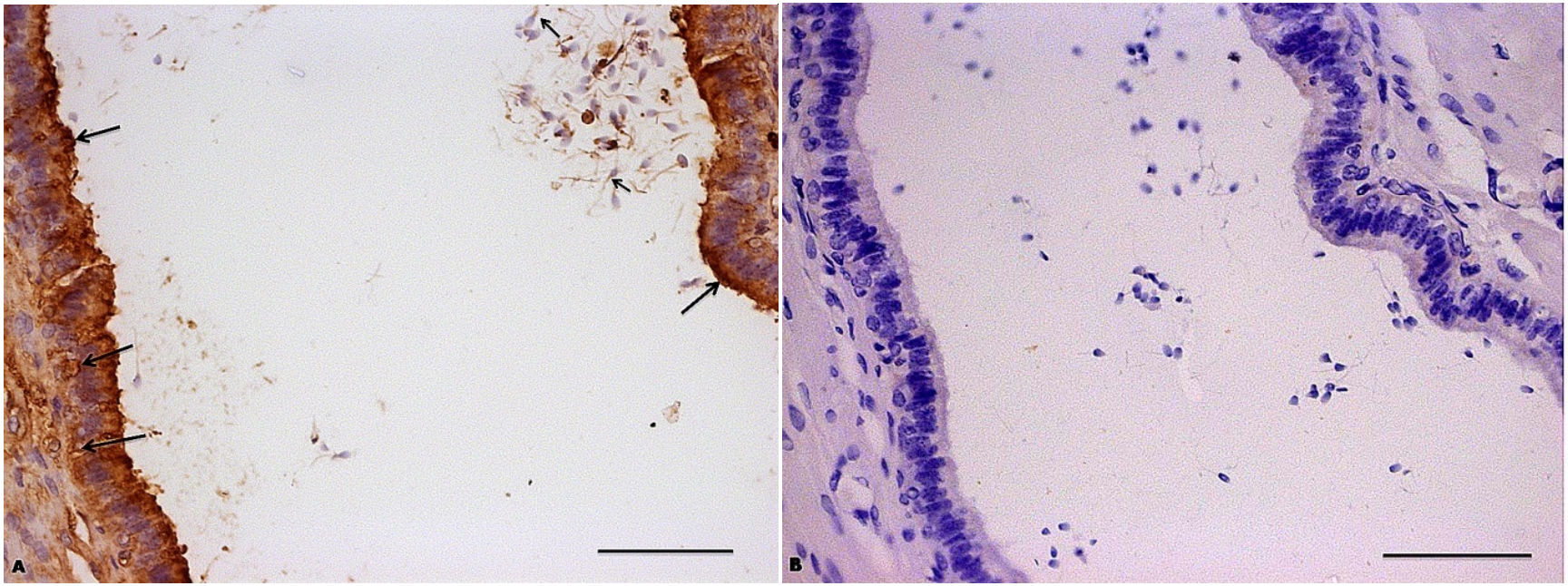

Figure 67: Photomicrographs of the ERβ immunohistochemistry in the cauda epididymis of the greater cane rat. Figure A showed the ERβ-positive nuclear staining of the basal cells (thin long arrow), cytoplasmic and membrane labeling (thick long arrows) as well as the labeling of the midpiece of the sperm cells (short arrows). Figure B was the negative control. Mag. X400, **Scale bar: 50µm**

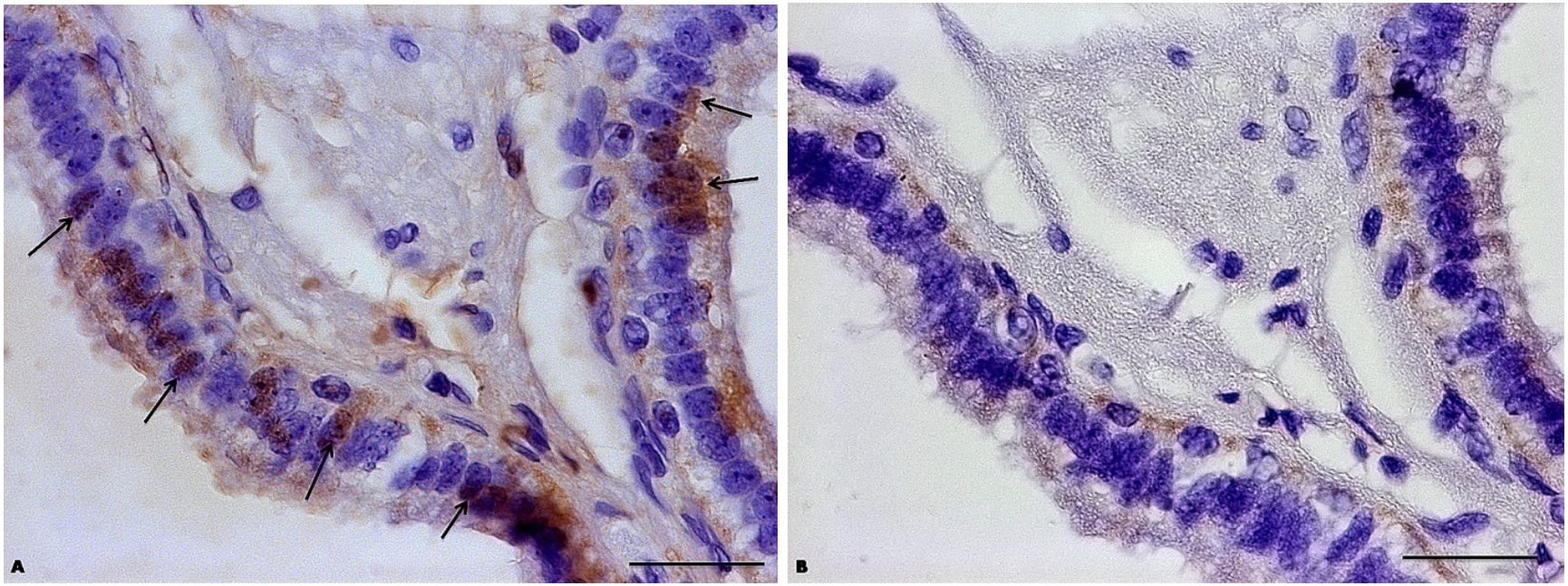

Figure 68: Photomicrographs of the progesterone receptor (PR) immunohistochemistry in the cauda epididymis of the greater cane rat. Figure A shows the PR-positive nuclear staining of the principal cells (arrows). Figure B was the negative control. Mag. X1000, **Scale bar: 50µm**

4.3.3.4 Vas deferens

Estrogen and Progesterone receptors Immunostaining

In the greater cane rat, the immunolocalization of the ERα was predominantly in the stroma with no epithelial labeling (Fig. 69) while there was intense nuclear, cytoplasmic and membrane staining for ERβ in the epithelium as well as the stroma of the vas deferens (Fig 70). PR labeling was not detected in the vas deferens of the cane rat.

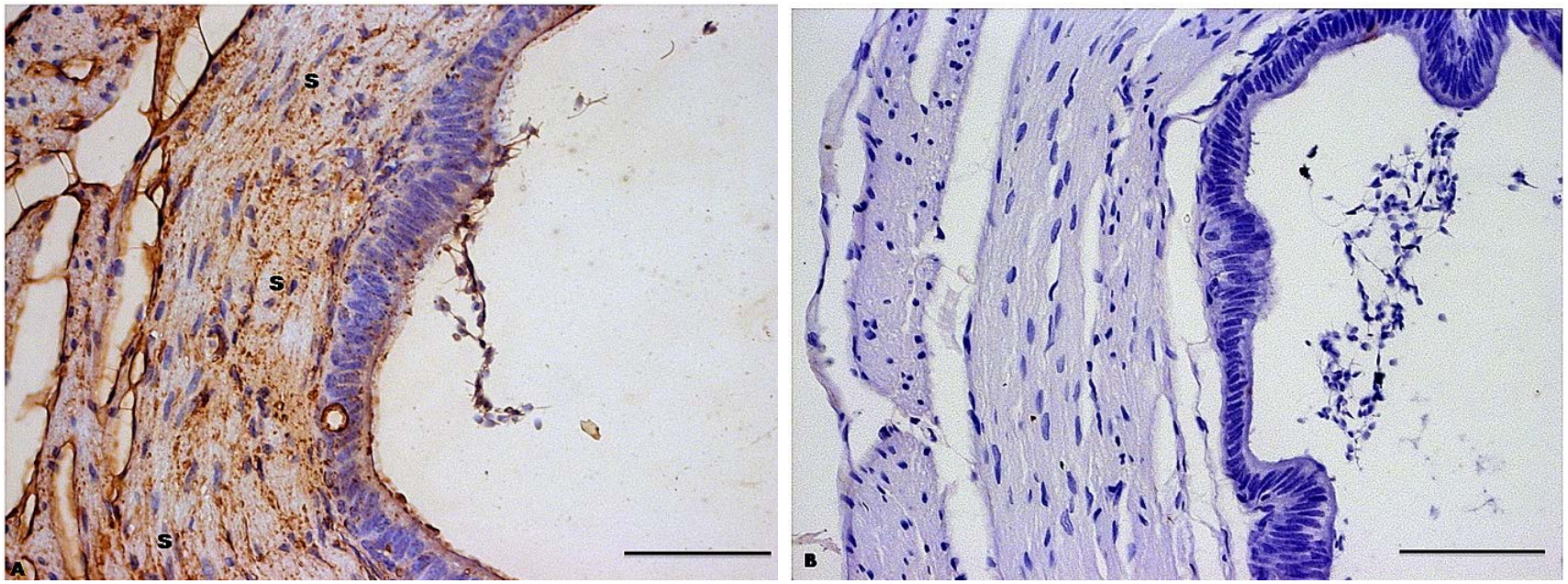

Figure 69: Photomicrographs of the ERα immunohistochemistry in the vas deferens of the greater cane rat. Figure A showed the predominant stroma ERα-positive staining (S). Figure B was the negative control. Mag. X400, **Scale bar: 50µm**

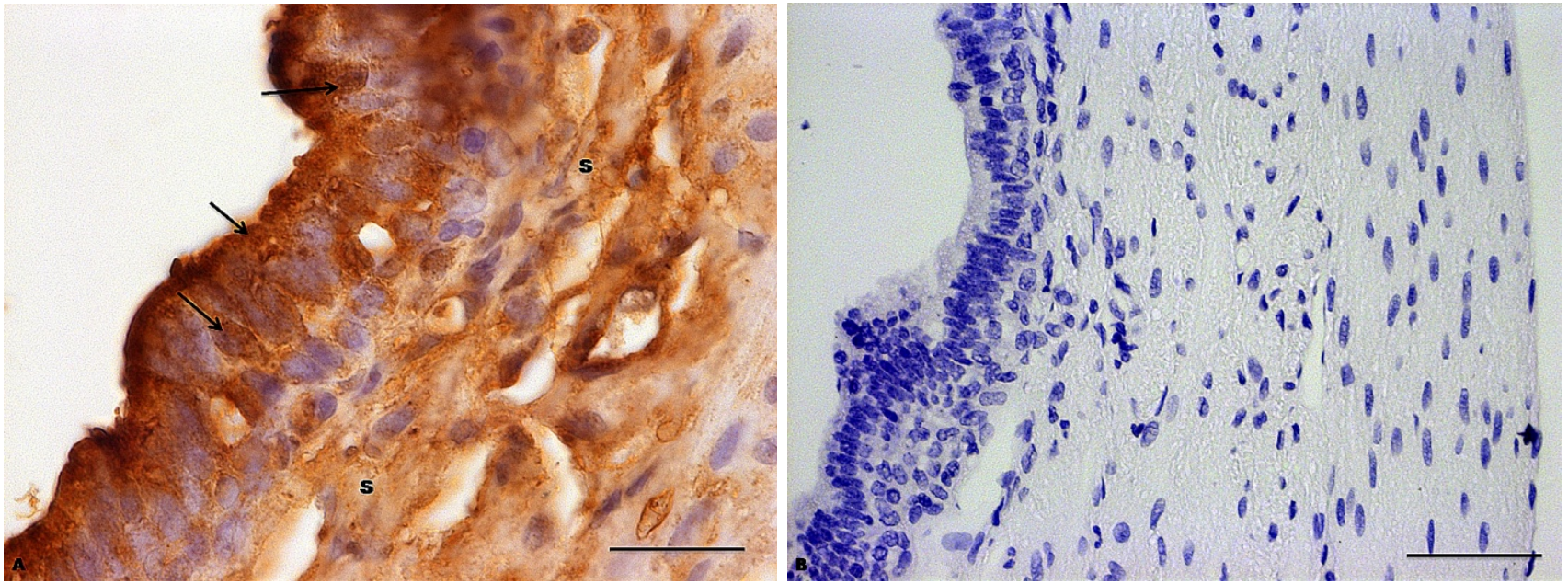

Figure 70: Photomicrographs of the ERβ immunohistochemistry in the vas deferens of greater cane rat. Figure A showed the ERβ-positive nuclear, cytoplasmic and membrane labeling (arrows) as well as stroma staining (S). Figure B was the negative control. Mag. X400, **Scale bar: 50µm**

4.3.3.5 Prostate gland

Estrogen and Progesterone Immunolabellings

The immunohistochemistry of the prostate gland in the cane rat showed positive nuclear staining for estrogen alpha and beta receptors (ERα and ERβ) in the cuboidal epithelial cells. There were positive immunostaining for ERβ in the stroma. In contrast, there was less intense staining for ERα in the stroma (Fig. 71A-D). The prostate did not show positive immunostaining for progesterone receptor (Fig. 71E-F).

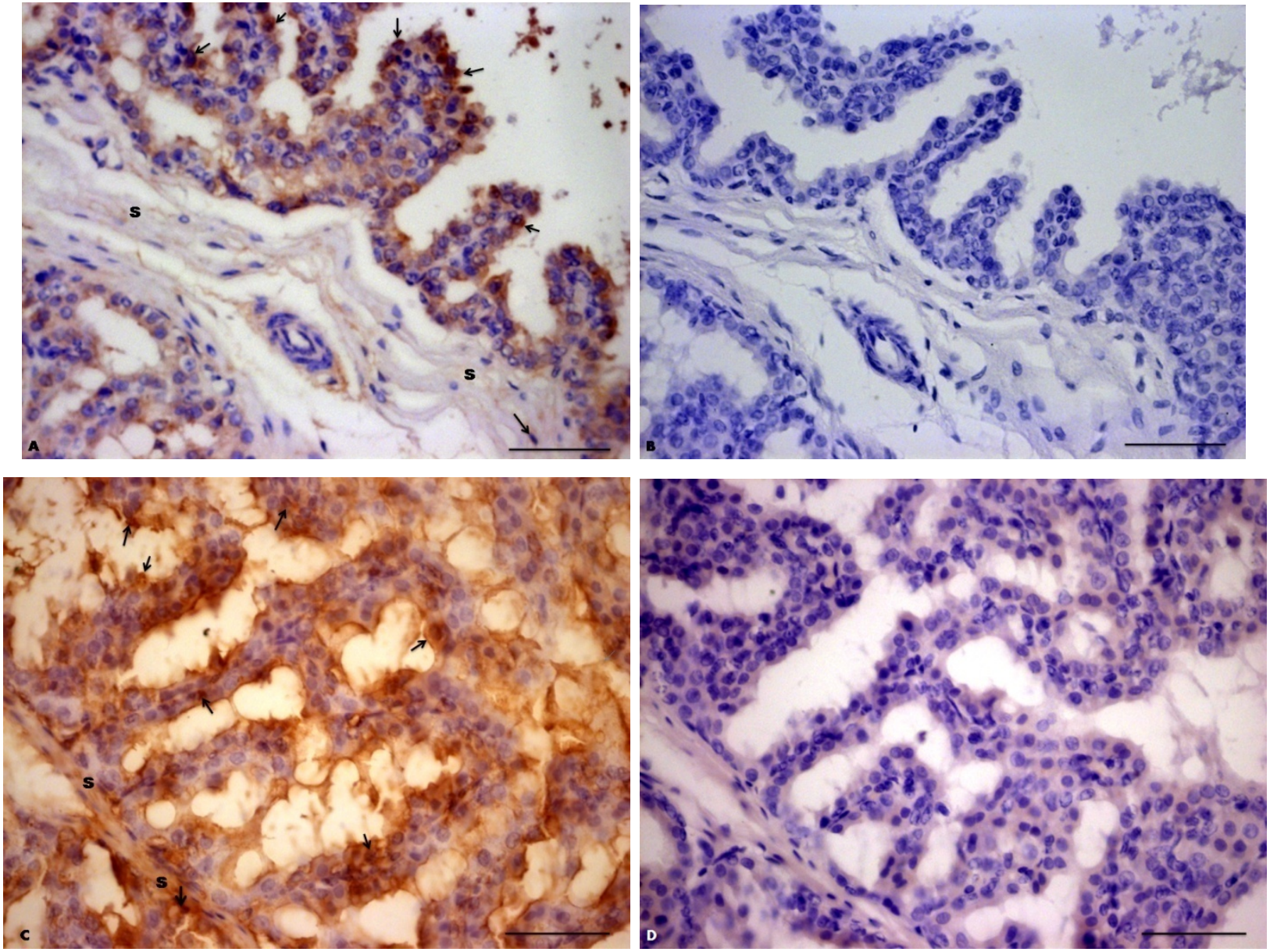
S
S
A
B
S
S
C
D

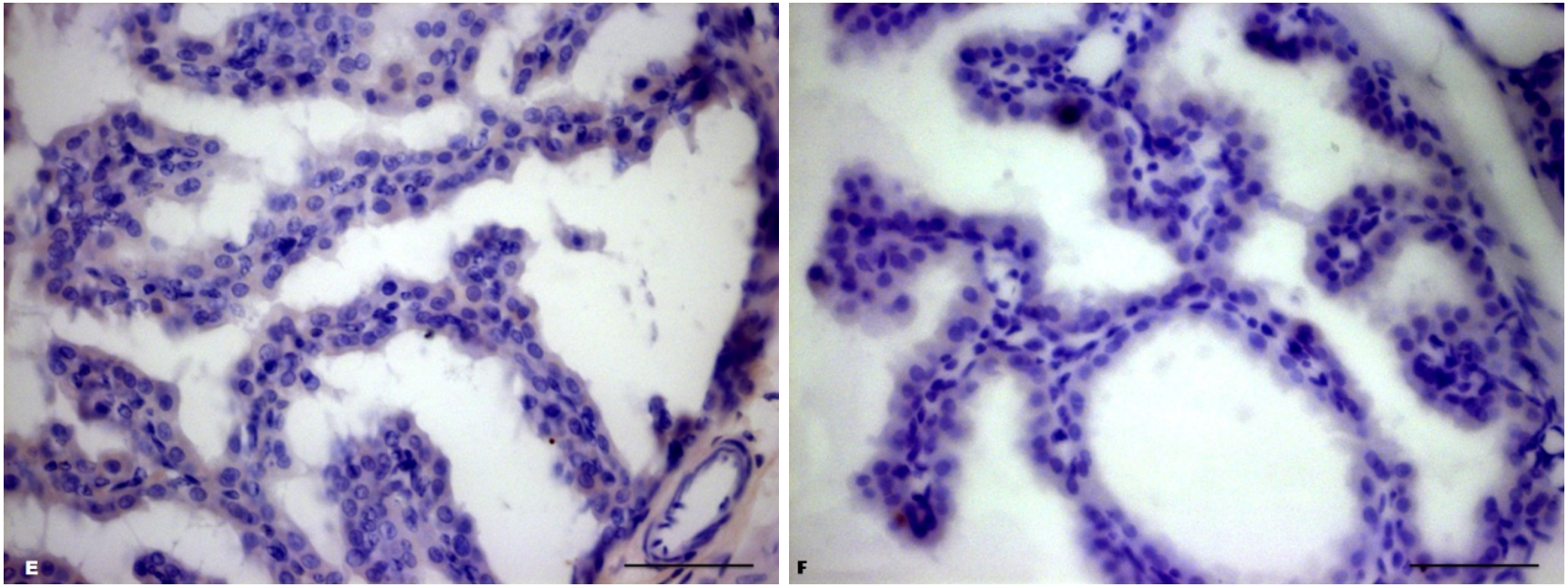

Figure 71: Photomicrographs of the ERα &β and PR immunohistochemistry in the prostate gland of the greater cane rat. Figure A showed the ERα-positive staining on the epithelium (arrows) with some faint stroma (S) staining while Figure B was the negative control. Figure C reveals the ERβ-positive staining of both the epithelium (arrows) and the stromal (S) and Figure D was the negative control. Figure E and F showed the PR-negative and its negative control respectively. Mag. X400, **Scale bar: 50µm**

4.3.3.6 Coagulating gland

Estrogen receptors Immunolabellings

Positive immunostaining for both estrogen receptor alpha and beta (ERα and ERβ) at the glandular epithelium and stroma were observed in the coagulating gland of the cane rat (Fig. 72a&c). ERα was expressed in the nucleus and the apical bleb of secreting cells as well as the nucleus and surrounding tissues in the stroma (Fig. 72a). There was immunostaining for ERβ in the nucleus and cytoplasm of the epithelial cells irrespective of their secretory stages and in the surrounding stroma (Fig. 72c). Figures 72b and d are negative controls in the absence of primary antibodies.

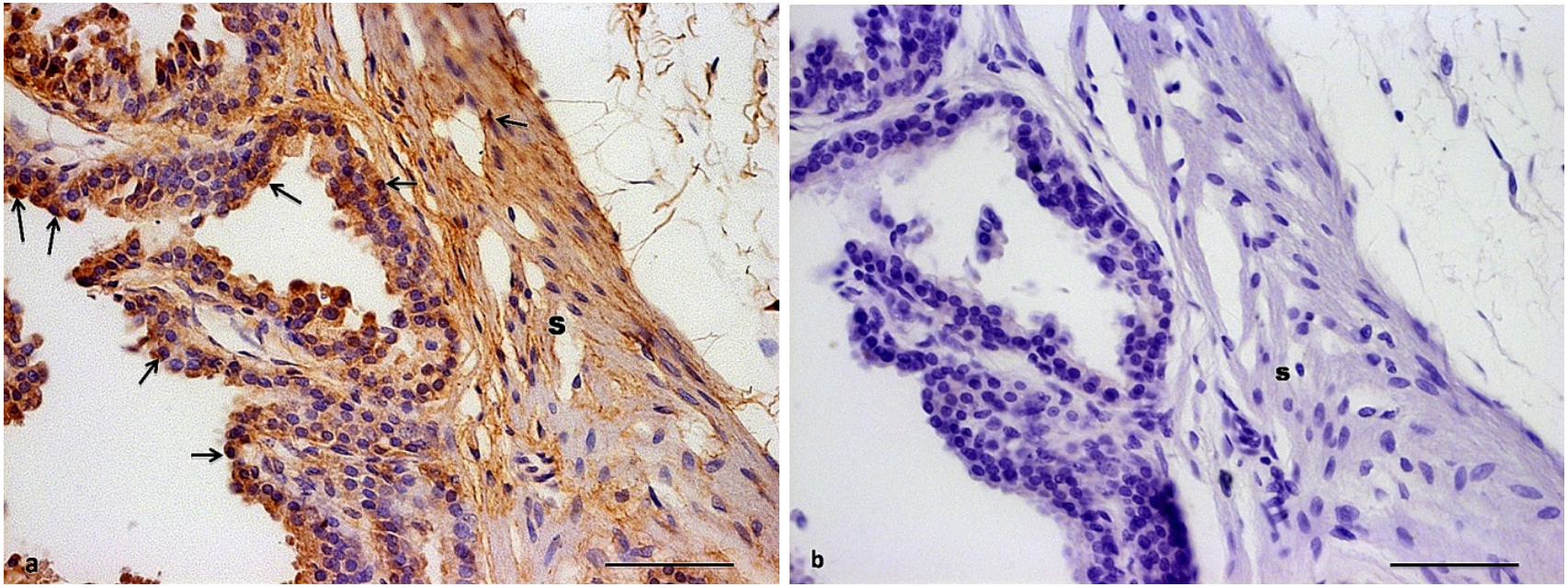

Figure 72a&b: Photomicrograph of immunostaining for estrogen α receptor in the coagulating gland of the greater cane rat. Figures A showed positive immunostaining of estrogen receptor alpha in the columnar cell nuclei and apical blebs (arrows) as well as the stroma (S) and figure B was the negative control. Mag. X400, **Scale bar: A – B = 50 µm**

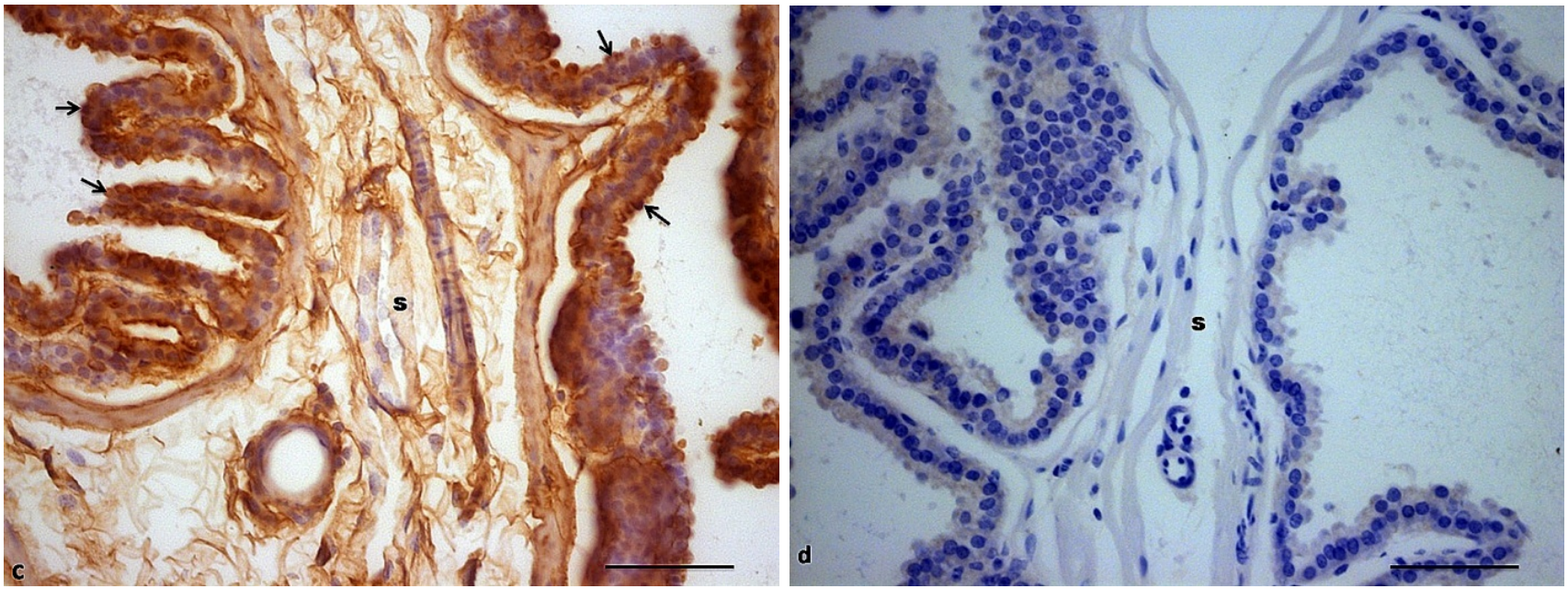

Figure 72c&d: Photomicrograph of immunostaining for estrogen β receptor in the coagulating gland of the greater cane rat. Figure C showed positive immunoexpression for estrogen beta receptor at the nuclei and apical blebs (arrows) of the glandular epithelium as well as the stroma (S) while figure D was the negative control. Mag. X400, **Scale bar: C – D = 50 µm**

4.3.3.7 Vesicular gland

Estrogen Receptors Immunostaining

The vesicular gland in the cane rat showed positive immunostaining for both estrogen receptors alpha (ERα) & estrogen receptor beta (ER β). The ERα expression was located at the nucleus of the basal cells of the glandular epithelium and in the stroma (Figs. 73A&B) while the ERβ showed strong immunoexpression at the cytosol and apical blebs of the glandular epithelium as well as in the stroma (Figs. 73C&D).

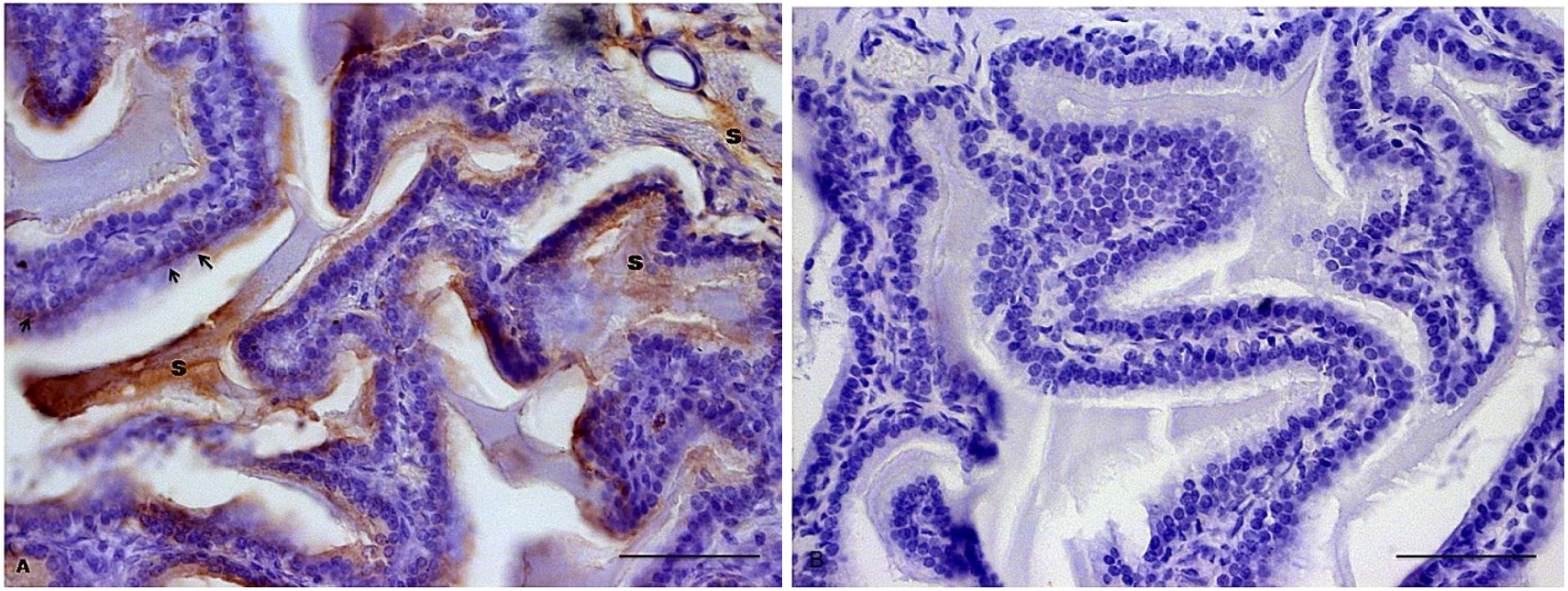

Figure 73A&B: Photomicrograph of immunostaining for estrogen α receptor in the vesicular gland of the greater cane rat. Figure (***A)*** showed weak positive immunostaining of estrogen receptor alpha in the basal cell nuclei (arrows) and the stroma (S) and (***B)*** was the negative control. Mag. X400, **Scale bar**: A – B = 50 µm

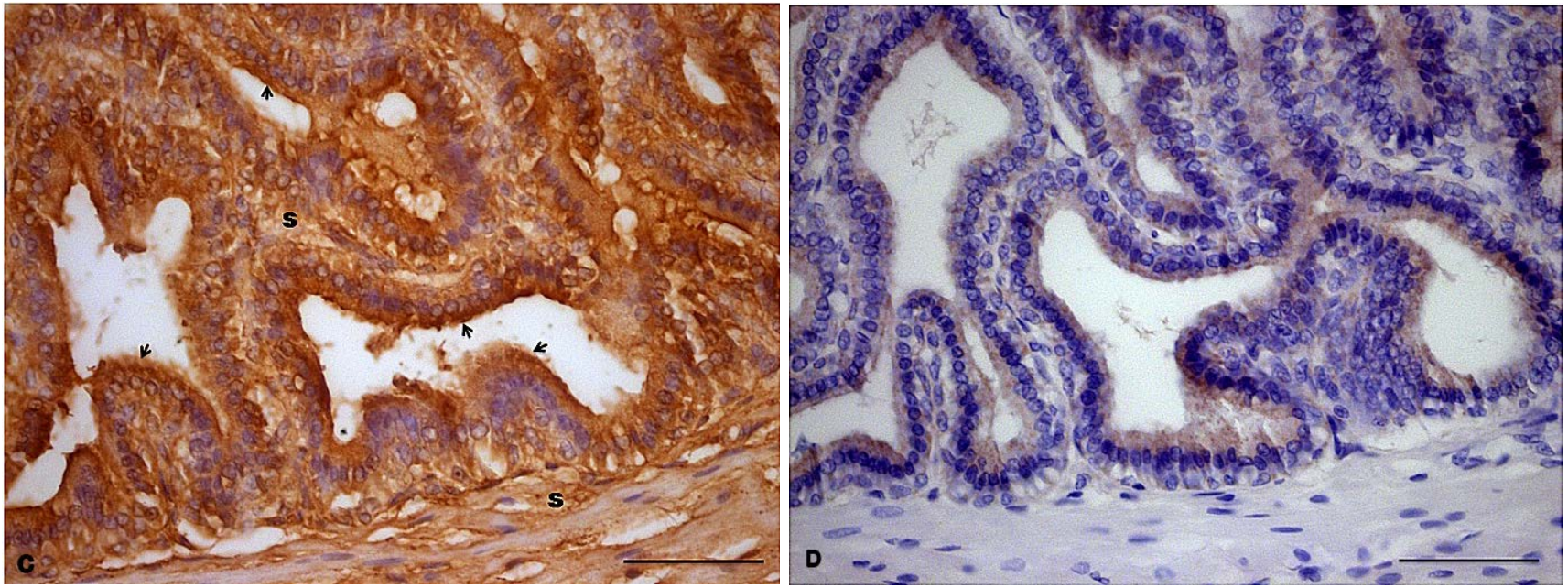

Figure 73C&D: Photomicrograph of immunostaining for estrogen β receptor in the vesicular gland of the greater cane rat. Figure (***C*)** showed strong positive immunostaining for estrogen beta receptor at both the cytosol and apical blebs (arrows) of the glandular epithelium as well as the stroma (S) and (***D*)** was the negative control. Mag. X400, **Scale bar**: C– D = 50 µm

4.3.3.8 Bulbourethral gland

Estrogen and Progesterone Immunohistochemistry

The bulbourethral gland showed no labeling for neither of the two estrogen receptors (ERα and ERβ) nor for the progesterone receptor. Figure 74 is the representative photomicrographs for the immunohistochemistry of the three receptors in the cane rat bulbourethral gland.

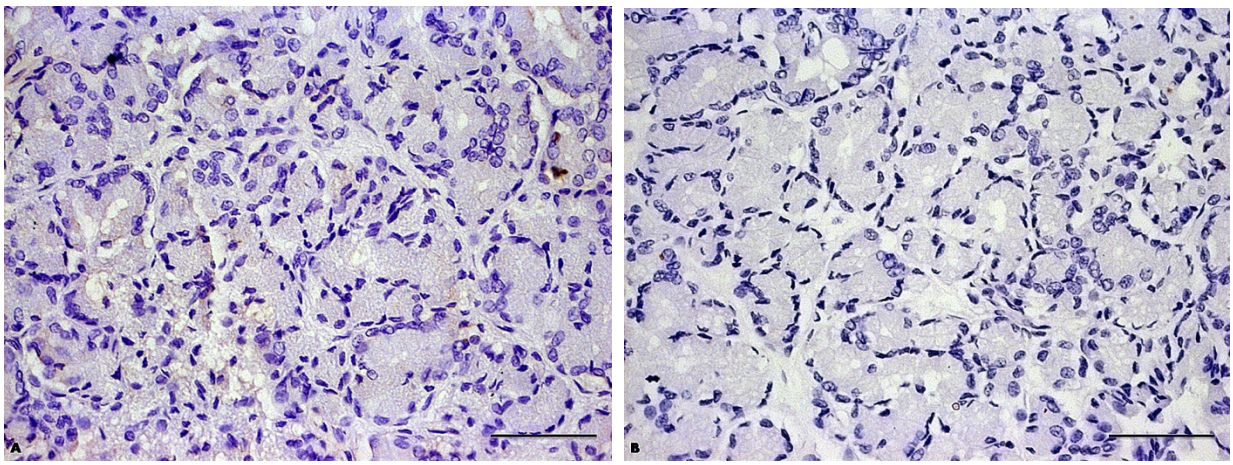

Figure 74: Photomicrographs showing no labeling for ERα, ERβ and PR in the bulbourethral gland in the greater cane rat. Mag. X400, **Scale bar: 50µm**

4.4 DISCUSSION

Hormonal profiles in the greater cane rat

The range and mean value of serum testosterone observed in the greater cane rat is comparable to that earlier reported for cane rat (Alogninouwa *et al,* 1999) as well as for the rat (Lee *et al.*, 1975; Khaki *et al.*, 2009), cat (Genaro *et al.*, 2007), dog (Frank *et al*., 2003) and goat (Jaszczak *et al*., 2010), most of which were determined using radioimmunoassay techniques. The wide range observed in the serum testosterone levels indicated variations in the individual testosterone levels in the male cane rat which had also been reported by Alogninouwa *et al,* (1999). A significant individual variation in the testosterone plasma level had been reported in the buck (Lofstedt *et al.,* 1994). Several factors can affect serum testosterone levels in a given normal male animal species. Time of blood collection has been found to affect testosterone levels in goats and man (Jejuna *et al.*, 1991; Jaszczak *et al.*, 2010). Gottreich *et al,* (2000) has also reported that captivity tended to lower serum testosterone levels in the mole. Since the blood samples used in this work were taken randomly and from animals in captivity, the serum testosterone values presented here can serve as baseline data and basis of comparison with the wild cane rat as well as tool in establishing seasonality of breeding in the captive cane rat.

The mean value and range of estradiol in the serum of the greater cane rat were presented in this work. According to de Ronde *et al,* (2003), only 2-3% of the circulating estradiol is free, with the remaining bound to albumin or sex hormone binding proteins. The serum estrogen level presented in this work was the mean concentration of the free estradiol present in the serum of the male cane rat.

The serum estrogen level observed in this study was similar to that observed in the rat (Farrell *et al.,* 1988), dog (Frank *et al*., 2003) and man (Longcope *et al*., 1990; de Ronde *et al*.,

2003). Reports on circadian variation in the serum estrogen level in man had been contradictory. While Jejuna *et al*., (1991) found variations in the estradiol values between the morning and afternoon readings, de Ronde *et al*, (2003) observed no difference throughout the day and further suggested that a single measurement of estradiol in peripheral blood will give a good indication of the estrogen level for the day. Based on the submission of de Ronde *et al.*, (2003), circadian variation in estrogen secretion was not considered in the estimation of the serum estrogen values in the greater cane rat.

As reported by *Lazari et al*., (2009) optimal serum estrogen level is important for normal male reproductive development and functioning. Apart from the gross and histological abnormalities caused by either under- or over exposure of estrogen on the male reproductive organs, exposure to exogenous estrogen may also result in 'reprogramming' of gene expression, i.e., induction of expression of a gene or its encoded protein in a tissue which does not normally express it (Williams *et al*., 2000; Walker *et al*., 2012). The serum estrogen value reported in this work can serve as basis for the identification and evaluation of the possible abnormal gene/protein induced in the male reproductive tract of the cane rat.

The presence of physiological serum level of progesterone observed in the male cane rat has equally been reported in rat, guinea pig, dog and man (Kalra and Kalra, 1977; Connolly and Resko, 1989; Alollio *et al*., 1995; Frank *et al*., 2003). In these species, progesterone was said to be involved in the modulation of species-specific androgen-dependent sexual behavior in the male through its effect on the hypothalamus (Witts *et al*., 1994). Recent studies have also shown that, in humans, this hormone stimulates Ca^{2+} influx in the sperm and thereby involved in the control of chemotaxis, hypermotility and acrosomal exocytosis of sperm in the female reproductive tract (Baidi *et al*., 2011, Timo *et al.*, 2011). According to Witts *et al*, (1994) the

physiological role of progesterone in the regulation of sexual behaviors became clear only after the establishment of the serum level and the localization of the progesterone receptors in the medial preoptic and ventro-medial nuclei of the hypothalamus. The serum progesterone level established in this work will aid the understanding of the role of this hormone in the physiology of the male reproductive tract in the greater cane rat.

This work presents the mean and ranges of luteinizing and follicular stimulating hormones in the serum of the cane rat. The presence and normal serum levels of both hormones have been established in several mammalian male species (Lee *et al.*, 1975; Perkins and Fitzgerald, 1992; Genaro *et al*., 2007; Khaki *et al*., 2009; Jaszczak *et al.*, 2010) and serves as veritable tools for assessing normal physiological condition as well as serve as complementary diagnostic tools for some reproductive abnormalities in the male goat (Jaszczak *et al*., 2010). Physiological variations in the serum levels of LH and FSH have been observed in the rat (Lee *et al*., 1975) and cat (Genaro *et al*., 2007) due to age, level of functional development of the hypothalamo-hypophysial unit as well as the stage of spermatogenesis in these species. The observed variation in the serum levels of LH and FSH in the cane rat is minimal as sexually matured animals were used. The values presented in this work can therefore serve as baseline data for the serum LH and FSH levels in the greater cane rat.

Anthropometrical Indices – Body mass (BMI) and Lee (LI) Indices

This work establishes the body mass and Lee indices for the sexually active male greater cane rat raised in captivity. With the current increase in the stocking levels and the intensification of production practices in cane rat farming (Adu *et al*, 2005), there is bound to be improved diet which will consequently lead to increased growth rate accompanied by a number of negative

consequences, including an increase in fat deposition (Zerehdaran *et al*., 2005). The estimated anthropometrical parameters in this work are expected to serve as standard obesity markers in the greater cane rat.

Anthropometric indices are ratios of linear body measurements used to estimate body fat and define obesity in man, animals and birds (Pala *et al*., 2005; Mendes *et al*., 2007; Engeland *et al*., 2007). Several other indices such as waist circumference, weight: length ratio, thoracic and abdominal circumference have been used to estimate increasing fat level and define obesity (Ng and Shih-Wei, 2004; Jeyakumar *et al*., 2009) as well as for investigating metabolic abnormalities such as hypertension and impaired fasting glucose (Choy *et al*., 2011). However, the choice to estimate BMI and Lee indices in this work was because these two indices have been adjudged the most accurate, inexpensive and most commonly used anthropometric indices particularly in rodents (Roger and Webbs, 1980; Novelli *et al*., 2007; Jeyakumar *et al*., 2009).

The estimated BMI obtained in this work was calculated using the standard formula for rodents as done by Bernardis (1970) and adapted by Novelli *et al*, (2007): weight of animal divided by square of its length (Novelli et al, 2007). Other formulae have been adapted in other mammals. In humans, the height is used instead of the length (Bahk *et al*., 2010) while in the dogs and cats, BMI is calculated either by using the human formula (Nijland *et al*, 2009) or usually by dividing the weight by the product of the body length and height (Anderson, 1973; Mc Greevy *et al*., 2005)

Age and puberty are important factors in the determination of normal BMI and Lee Index in sexually matured males (Novelli *et al*., 2007; Bahk *et al.,* 2010). In establishing the normal range of values for BMI and Lee Index in adult rat, Novelli *et al*, (2007), based it on the age of cessation of growth and development in rat as well as the age from when the mean BMI values

became constant. Although the age of cessation of growth and development was yet to be determined in the greater cane rat, it was observed from this work that at sexual maturity, there was no significant relationship between ages of these animals and these indices. It can therefore be inferred that the observed BMI and Lee Index in this work represent the normal values in sexually matured male greater cane rat. These observed values were also comparable with the BMI and Lee Index values in the rat (Novelli *et al*., 2007).

In the greater cane rat, it was observed that testicular volume and weight correlate with the height but not the body weight or length of the animal. Testicular weight and volume are indicators of normal seminal profile as they correlate with both sperm quality and quantity (Sakamoto *et al.,* 2007; Bahk *et al.,* 2010). Whereas close relationship between orchidometric parameters and height had also been reported in humans (Handelsman and Staraj, 1985; Bahk *et al*., 2010), their relationship with body weight is controversial in humans. Wikramanayake, (1995) and Spyropoulos *et al*, (2002) reported relationship between testicular volume and body weight while Sobowale and Akinwunmi (1989) and Bahk *et al*, (2010) reported no correlation. The observation in the cane rat reported in this work is consistent with our previous findings (Adebayo *et al*., 2009b).

In this study there was no correlation between either BMI or Lee index and testicular weight or volume. This was similar to what had been reported in young sexually active human adults (Bahk *et al*., 2010). In the same vein, the observed lack of relationship between BMI and the serum levels of testosterone, progesterone, LH and FSH as well as the low correlation between BMI and the serum estradiol level in the greater cane rat was consistent with what obtained in man (Aggerholm *et al*., 2008; MacDonald *et al.,* 2010). In man, increased adipose tissue which showed as higher BMI is associated with changes in the male reproductive hormone

profile causing alterations in the levels of testosterone and estrogens as well as sex-hormone binding globulin (SHBG) (Pasquali *et al*., 2007). These hormonal abnormalities were said to be due to increased peripheral conversion of androgen to estrogen associated with the increased adipose tissue present at a higher BMI (Schneider *et al*., 1979; Pasquali *et al*., 2007). In the light of the above observations in humans, the relationship between the BMI and the serum estradiol seen in the cane rat is plausible giving the lack of correlation between these indices and serum testosterone level.

Immunohistochemistry in the greater cane rat

The observed presence of the estrogen receptors in the testes of the greater cane rat had been reported in several mammalian species (Carreau *et al*., 2010). Reports on the expression of ERα and ERβ in the testes were highly variable with major differences between species and even within individuals of the same species (Saunders *et al*., 2001; Hess and Carnes 2004; Carreau *et al*., 2007). In mouse (Kotula-Balak *et al*., 2005), rat (Oliveira *et al*., 2003) and boar (Mutembei *et al*., 2005), ERα was reported to be localized only in the Leydig and peritubular myoid cells of the testis. However, Lucas *et al*, (2008) had revealed the presence of this same receptor in Sertoli and some germ cells in rat using frozen sections and new antibodies against its amino- or carboxyl terminal regions. While some reports suggested no labeling for ERα in any of the testicular cell in man (Makinen *et al*., 2001; Sierens *et al*., 2005), others suggested it could be found in germ cells, particularly spermatocytes, spermatids and sperm cells (Pentikainen *et al*., 2000; Lambard *et al*., 2004). According to Carreau, *et al*, (2010) these differences could be primarily due to differences in tissue preservation techniques and antibodies used for immunohistochemistry. From this work, the ERα had been found in the Sertoli, Leydig and

peritubular myoid cells while the ERβ were localized in the Sertoli, Leydig and some germ cells particularly the spermatocytes and spermatids. While these observations seem comparable to that of rat and mice, further techniques such as mRNA analysis and *in-situ* hybridization will be necessary to more accurately determine oestrogen responsive cell types in the different testicular tissues in the greater cane rat.

The observed immunolocalization of the estrogen receptors (ERα & ERβ) in the efferent duct of the greater cane rat was consistent with what had been observed across all mammalian species (Hess, 2003; Joseph *et al*., 2011), thereby implicating this duct as an estrogen responsive organ in the cane rat. Not only was the efferent duct a conduit pipe for sperm transport from the testis to the epididymis, it was also involved in the re-absorption of testicular fluids and proteins thereby influencing sperm concentration and seminal fluid composition (Hess and Carnes, 2004; Lazari *et al*., 2009). It has been established that estrogen, through its receptors, ERα and ERβ, played a crucial role in the maintenance of the structure and function of the efferent duct (Lazari *et al*., 2009; Joseph *et al*., 2011). The presence of these receptors in the cane rat efferent duct suggests that estrogen also regulates the structural and functional status of this duct in the greater cane rat.

In the rat and mouse (Oliviera *et al*., 2004), ERα and ERβ are expressed in both the ciliated and non ciliated cells of the efferent duct epithelium. Whereas ERβ is sometimes found in the peritubular and stromal cells in the rat (Oliviera *et al*., 2004), there were cases in humans where the epithelial cells were stained negative for ERα but the stromal cells were stained positive (Hess, 2003). The observed immunolocalization pattern in the cane rat seems to follow that of the rat as well as the occasional human pattern. The significance of this pattern as well as

the presence of positive staining in the ciliated cell cytoplasm of the cane rat efferent duct is yet to be elucidated.

The immunoexpression of the three receptors, estrogen alpha and beta (ERα and ERβ) and progesterone (PR) receptors presented unique pattern of distribution in various regions of the epididymis in the greater cane rat. The expression of ERα in the epididymis is highly variable among mammalian species (Joseph *et al*., 2011). While nuclear labeling of ERα was completely lacking in the epididymal epithelium of several species, it was present in mouse, cat and monkey (Nie *et al*., 2002; Hess, 2003; Lazari *et al*., 2009; Joseph *et al*., 2011). Where present, ERα was said to participate in the regulation of narrow cells in the initial segment and clear cells in the remaining epididymal segments (Hess *et al*., 2001; Lazari *et al*., 2009). In some other species like Marmoset, ERα labeling had been shown in the cytoplasm (Lucas *et al.,* 2008; Schon *et al*., 2009), but its significance at this location was yet unknown. From this work, it can be said that the greater cane rat belonged to the class of mammals without nuclear labeling for ERα. Although the import of the cytoplasmic and stromal labeling for ERα particularly at the cauda epididymis of the cane rat is yet to be elucidated, such cytosol immunostaining for this receptor at the cauda epididymis had been reported in Marmoset monkey (Shayu *et al*., 2005). According to Joseph *et al*, (2011), these variations can sometimes be as a result of differences in antibodies and tissue processing techniques.

The expression of estrogen beta (ERβ) throughout the epididymis in the cane rat is similar to that reported for most studied species (Nie *et al*., 2002; Zhou *et al*., 2002). However the pattern of labeling of ERβ in the cane rat was unique because of its selective nuclear staining for narrow and apical cells in the epididymal epithelium. Selective localization of the ERβ had been observed in boar where only the principal and basal cells of all three epididymal regions were

labeled (Pearl *et al*., 2007). Although selective intense staining of the epididymal narrow, apical and clear cells for ERα had been associated with the involvement of this receptor in the regulation of these cells in mouse (Lazari *et al*., 2009), the implication of selective labeling of these cells for ERβ in the cane rat is yet unknown. However the ERβ localization in the stroma is consistent with that observed in the rat (Atanassova *et al*., 2001)

The observed immunolocalization of the ERβ in the middle pieces of spermatozoa and the nuclear labeling for progesterone receptor (PR) in the cauda epididymis of the greater cane rat were unusual. According to Carreau *et al*, (2011) estrogen receptors have only been localized in the spermatozoa of primates and man but not rodent spermatozoa. As reported by Solakidi *et al*, (2005) and Carreau *et al*, (2011), the localization of aromatase and estrogen receptors in the midpiece of the human spermatozoa could be related to a potential role for estrogen in mitochondria and energy production for motility, as well as for participation in capacitation and/or the acrosomal reaction of sperm. In the same vein, the presence of ERβ especially in the middle pieces of cane rat spermatozoa opens new considerations about the possible role of estrogen in mobility and fertilizing ability of spermatozoa not only in humans but also in this rodent. Similarly, with the localization of PR in the cauda epididymis of the cane rat, which has never been reported in any mammalian species, it is possible that progesterone might be involved in the modulation of epididymal function as it was with sperm hypermotility and fertilization (Baldi *et al*., 2011).

The observed immunolabeling for ERα in the greater cane rat was consistent with the report of Hess and Carnes (2004) where this receptor was said to be absent in the epithelium of the vas deferens in most species. The expression of ERα in the vas deferens stroma had also been reported in rat (Atanassova *et al*., 2001). In the same vein, the expression of ERβ in the vas

deferens of the cane rat was similar to that observed in the rat (Atanassova *et al.*, 2001) where this receptor was said to be present in the vas deferens at all ages.

The immunolocalization of ERα in the epithelial cells of prostate gland in the greater cane rat was uncommon. According to Ellem and Risbridger, (2009) and Lazari *et al*, (2009), in man, monkey, dog and rodent, the ERα subtypes were usually localized in the stromal cells of adult prostate but can be found in the epithelium in humans only upon treatment with estrogen. Even in the stromal cells, it had been reported that only a fraction of the cells are normally positive for ERα while a lot remain ERα negative (Prins and Korach, 2008). While the presence of ERα in the stroma may indicate functional interactions between the stroma and the epithelium in the response of prostate gland to estrogen as it was in other species, the functional importance of the epithelial presence of this receptor in the prostate gland is unknown. However, moderate immunostaining for ERα in the prostatic glandular epithelium had also been reported in California sea lion (Colegrove *et al*., 2009).

The localization of ERβ in the epithelial cells and stroma of the cane rat prostate gland was consistent with that of rat, mouse and humans (Ellem and Risbridger, 2009, Lazari *et al.*, 2009). Fixemer *et al*, (2003) had reported high expression of ERβ in both basal and luminal epithelial cells of the adult human prostate. With the pattern of localization observed in the rat and mouse, where the ERα was primarily localized in the stroma and ERβ localized in the epithelium, Prins and Korach, (2008) suggested the possible formation of ERα : ERβ heterodimer in this organ in the rodent. However, this pattern was not observed in the cane rat.

The absence of progesterone receptor (PR) in both the epithelium and stroma of the cane rat prostate is similar to what obtained in the prostate of rodents and man (Williams *et al.*, 2000), and monkey (Brenner *et al*., 1990). Generally, PR expression is normally absent in the prostate

gland except in the parasympathetic ganglia of the prostate (Williams *et al*., 2000). But where there is exposure to exogenous estrogen, there is induction of immunoexpression of PR and increased expression of the ERα in the prostate stroma together with some gross changes in the prostate tissue (Chang *et al*., 1999; Williams *et al*, 2000., 2001). Whereas the present study outlines the normal structural and ultrastructural features of the cane rat prostate gland, the absence of the PR substantiates the uniqueness of the immunostaining of ERα in epithelial cells of the prostate gland of this animal. Further work, on the expression of the ERα mRNA in the epithelium and its role in the adult prostate gland of the cane rat under normal and disease conditions, is highly recommended.

In this work, we presented the immunoexpression of the two estrogen receptors (ERα & ERβ) in the coagulating gland of the greater cane rat. Generally, literature on the immunolocalization of estrogen receptors (ERα & ERβ) in the coagulating gland was scarce since the gland was usually considered as part of the prostate gland in the laboratory animals commonly used for the study of these receptors. The expression of ERα in the nucleus and the apical bleb/cytoplasm of the secretory epithelium in the cane rat coagulating gland were unusual. As reported by Prins and Korach, (2008), ERα was principally localized in the stroma in the prostate gland of rodent, dog monkey and man where it played a role in stroma-epithelium interactions of prostate in response to estrogen. Although the functional significance of the ERα in the secretory epithelium of this gland in the cane rat is still under investigation, epithelial ERα has been observed in developing human prostate (Shapiro *et al*., 2005) and adult California seal prostate gland (Colegrove *et al*., 2009). The localization pattern of ERβ in the coagulating gland of the greater cane rat is comparable to what is reported in prostate of rodents (Prins and Korach, 2008). However, further work using other validation techniques is recommended.

In the seminal vesicles of rat (Pelletier *et al.,* 2000) and mouse (Yamashita, 2004), immunostaining for ERα was reportedly found in the nuclei of epithelial and stromal cells. Similarly, in rat, weak staining for ERβ was localized in the epithelial cells of seminal vesicles even though ERβ mRNA could not be detected by *in situ* hybridization (Pelletier *et al.,* 2000). In the same vein, significant increases in cytosolic ER levels had been reported in mouse seminal vesicles following neonatal exposure to Diethylstilbestrol (Turner *et al.,* 1989; Walker *et al.,* 2012). Our findings are different as they reveal ERα immunostaining only of the basal cell nuclei and stroma. Also, the apical blebs of the glandular epithelium, the cytosol and the stroma all showed strong positive immunoreactivity to ERβ. According to Lazari, *et al*, (2009), where there is close proximity of ERα positive stromal cells to epithelial cells as in the prostate, there is the possibility of paracrine effects of estrogens on the epithelium. It is therefore possible that estrogen might be involved in the normal functioning of the basal cells and stroma of the vesicular gland in the greater cane rat.

CHAPTER 5

MONTHLY MORPHOMETRIC EVALUATIONS OF THE TESTIS AND EPIDIDYMIS AND THE SEASONAL PATTERN OF BREEDING IN THE MALE GREATER CANE RAT (*Thryonomys swinderianus*)

5.1 INTRODUCTION

In recent years, the application of morphometric and stereological techniques has increased in biomedical research and is now being recognized as the new approach in morphological studies (Mukerjee and Rajan, 2006). Morphometry, which implies the use of quantitative data in the description of structural features (gross, tissue, cell or organelle), derives its justification from the recognition that all orderly function must have an organized structural basis of a size that is adequate but not less or excessive (Ichihara and Pelliniemi, 2007).

In male reproductive biology, accurate morphometric information can be valuable for correlation of spermatogenic processes with physiological and biochemical findings (Gaytan *et al.*, 1986; Franca and Russel, 1998). It has also been used to characterize basic reproductive parameters needed to enhance reproductive efficiency (Segatelli, *et al*., 2002; Gomendio, *et al.*, 2006) and to evaluate reproductive structural behaviors under different environmental (seasons, light, temperature, etc.), pathological and pharmacological (drugs) conditions (Lu *et al.,* 2008; Abdelmalik, 2011; Machado Junior *et al*., 2011). Gross- and histo-morphometric values of the different segments of the male reproductive tract are not only species specific they tend to vary with seasons depending on the seasonality of breeding (Oke, 1988, Chaves *et al.,* 2011). This part of the work, therefore, reports the seasonal variations in the reproductive activities by evaluating the effect of seasons on serum hormonal levels and testicular and epididymal morphometric parameters in the male greater cane rat.

5.2 MATERIALS AND METHODS

5.2.1 Animals

The same animals used in part 2 (chapter four) of this work were used in this part – a total of seventy two (72) sexually matured adult male greater cane rats, obtained from Good health Farms Igbesa, Ogun State and Pavemgo Grasscutter Farm, Ibereko, Badagry, Lagos state. Six (6) males were used every month from March, 2012 – February, 2013. The animals were kidded and raised in captivity with known reproductive and medical records. Their ages ranged from 15 – 24 months and they weighed between 2kg – 3.5kg (2000 – 3500g). All the animals have brownish perineal staining which is usually used as index of sexual maturity in male cane rat (Adu and Yeboah, 2003). They were left to acclimatize for three weeks at the Grasscutter domestication unit, College of Veterinary Medicine, Federal University of Agriculture, Abeokuta and maintained on the combination of maize, cassava and ground nut cake with salt to taste. They were also provided with Elephant grass stems and water was given *ad libitum*.

5.2.2 Location Climates

The animals were raised at Igbesa and Ibereko, Badagry in Lagos state, Nigeria. These coastal areas lie few kilometers west of Lagos metropolis and on 6^0 25'N 2^0 53'E coordinates. The climate of these areas is tropical humid with predominant wet season (March – November) and few months of dry season (December - February). Rainfall in this area usually starts at about February, but sporadic rains have also been reported in January.

The animals were used in Abeokuta where they were allowed to acclimatize for fourteen days. Abeokuta, the Ogun state capital, is situated in the south western region of Nigeria, about

70 km north of Lagos. The area lies between latitudes 7º08' and 7º12'N, and longitudes 3º13' and 3º25'E. It is located in a general hummocky terrain, varying in altitude. The climate of the area is tropical sub-humid (dry) with distinct wet season (April – October) and dry season (November – March). The climate is controlled by the prevailing South-West-wind reaching the land from the limit of Guinea and the dry continental North-East wind originating from the Sahara desert. The wet season has two peak regimes which are separated by the August break. The average monthly rainfall for the peak regimes are about 190 mm (April – July) and 170 mm (September – October) and the range annual rainfall is 130 mm. The dry season is characterized by a retardation of vegetational growth and a decline in the availability of grains and pastures. There is a general lack of rainfall, except occasional rains. The dry, dust-laden winds blow from the Sahara desert between December and January. This period, a part of the dry season known as the harmattan period, is characterized by dustiness, low humidity and general fall in temperature.

The latitudinal location of the state has given her an average higher temperature of 26.6ºC throughout the year with a mean minimum temperature of 21ºC. The maximum temperature varies between 29ºC during the peak of the wet season and 34ºC at the onset of the wet season. The annual relative humidity is about 81%. This is attributable to the prevalence of moisture-laden tropical climate over the state for about 9 months in the year combined with the fact that there is a high rate of temperature and dense vegetational cover in this region

5.2.3 Morphometry

5.2.3.1 Gross morphometry

The weight and linear measurements, which comprise length, width and circumference of the testis and epididymis, were taken using analytical weighing balance and vernier caliper respectively (Chapter four). The volumes of the testes, epididymis and the accessory organs were found by water displacement method as described by Scherle, (1970) and adapted by Hughes (2005). Where the organ is curved, the measurement is taken using thread and ruler. The average of the left and right measurements were taken and recorded as each organ's measurement.

5.2.3.2 Histo-morphometry

Samples of these organs were processed using the automatic tissue processor (Shandon Citadel1000, Rankin Biomedical Co. USA). To achieve dehydration, the tissues were passed through graded concentrations of alcohol: 70% for 1hour, 90% thrice for 1hour each, and absolute alcohol (100%) thrice for 1 hour, 2 hours, and 1 hour respectively. They were then cleared twice in chloroform for 2 hours each and embedded by passing through the four changes of paraffin wax at 60^{o}C. Serial paraffin sections of 4µm thick were obtained on the microtome (Leica, 2035 Biocut, Germany). These were mounted on clear albuminized slides after floating on a warm water bath and then dried in an oven and stained with haematoxylin & eosin (H & E). All the slides were examined under the light microscope (Axioskop 2 plus, Carl Zeiss, Germany).

For tubular organs, twenty tubular profiles that were round or nearly round were chosen randomly and measured for each animal. The epithelial height was obtained in the same tubule sections utilized to determine tubular diameter. Linear measurements of tubular diameters and

epithelial heights were taken at x 100 magnification, using a photomicroscope (Axio-Skop-2-Plus, ZEISS, Germany) fitted with digital camera (Axio-Cam HRC, ZEISS, Germany). The measurements were made with AxioVision Release 4.8.1 software package installed on a computer (Mercury, South Africa).

5.2.4. Hormonal Assay

The serum levels for testosterone, estrogen, progesterone, luteinizing and follicle stimulating hormone were assayed for each of the six animals in each month of the year using the Microplate Immunoenzymometric assay kits specific for each hormone. The test procedure according to the user instruction for each kit, which is almost the same for all the five hormones, was duly followed in this work. 25 µl of each of the calibrators, control serum and sample serum of each of the six cane rats for each month, were pipetted into appropriately labeled microtitre wells in duplicate. 10 µl of the conjugate was added to each well, swirled for 20-30 seconds to mix, covered and incubated for 60minutes at room temperature. After 60 minutes the content of the microtitre were decanted and blot-dried with absorbent tissue paper. To each well, 300 µl of reconstituted washing solution (prepared by mixing the concentrated Washing Solution and distilled water at ratio 1:25 in a separate jar) was then added, decanted and blot-dried. This washing was repeated four (4) additional times, after which 100 µl of TMB-Substrate was pipetted into each well at timed intervals and incubated for 15-20 minutes at room temperature in a dark cupboard. The reaction was then stopped by the addition of 150 µl of the stopping reagent into each well at timed intervals and the microtitre wells read on an ELISA reader (Elx 800, BioTek, England).

A 4-parameter calibrator curve was plotted with the optic densities/Absorbance on the Y-axis and calibrator concentration on the X-axis. The serum concentration of the hormone in each sample was estimated by locating the average absorbance of the sample duplicates on the vertical axis of the graph, finding the intersection point on the curve and reading the concentration from the horizontal axis of the graph. All the test validation criteria for each of the assay were met in this work in accordance with the kit manufactures' instructions.

5.2.5 Statistical Analysis

Values obtained were expressed in mean ± standard deviation (SD) and evaluated with ANOVA. The mean differences were sorted using Duncan post hoc test. Data were also subjected to Pearson's correlation analysis. All stastical analyses were carried out using Paleontological statistics version 2.15 (PAST) data analysis tool.

5.3 RESULTS

Table 17: Monthly variations in the gross morphometry of the testicular and epididymal parameters in the greater cane rat.

	Testicular Parameters (mean ±SD)			***Epididymal Parameters (Mean ±SD)***		
	Weight (g)	**Volume (cm^3)**	**Diameter (cm)**	**Weight (g)**	**Volume (cm^3)**	**Length (cm)**
January	1.76 ±0.56*	1.40 ±0.17*	1.26 ±0.15*	0.32 ±0.09**	0.63 ±0.40**	2.81 ±0.42*
February	1.77 ±0.57*	1.47 ±0.16*	1.27 ±0.16*	0.33 ±0.10**	0.65 ±0.41**	2.50 ±0.40*
March	1.29 ±0.40*	1.37 ±0.49*	1.10 ±0.06*	0.24 ±0.06**	0.30 ±0.16**	2.97 ±0.58*
April	1.40 ±0.29*	1.43 ±0.27*	1.08 ±0.04*	0.25 ±0.04**	0.30 ±0.12**	2.80 ±0.60*
May	1.32 ±0.31*	1.40 ±0.25*	1.03 ±0.05*	0.47 ±0.38**	0.43 ±0.08**	2.37 ±0.56*
June	1.43 ±0.07*	1.33 ±0.10*	0.96 ±0.05*	0.22 ±0.02**	0.33 ±0.20**	2.50 ±0.39*
July	1.41 ±0.08*	1.31 ±0.13*	1.00 ±0.05*	0.23 ±0.03**	0.30 ±0.21**	2.51 ±0.40*
August	1.40 ±0.20*	1.23 ±0.19*	1.06 ±0.10*	0.57 ±0.48**	0.26 ±0.16**	2.75 ±1.34*
September	1.43 ±0.25*	1.21 ±0.21*	1.02 ±0.08*	0.55 ±0.40**	0.27 ±0.17**	2.70 ±1.28*
October	1.42 ±0.16*	1.20 ±0.20*	1.08 ±0.11*	0.59 ±0.45**	0.26 ±0.16**	2.71 ±1.30*
November	1.25 ±0.10*	1.13 ±0.12*	1.08 ±0.04*	0.24 ±0.03**	0.30 ±0.10**	2.50 ±0.41*
December	1.30 ±0.12*	1.15 ±0.16*	1.06 ±0.05*	0.25 ±0.04**	0.32 ±0.11**	2.51 ±0.40*

*p > 0.05; **p < 0.05

	Testicular Parameters (mean ±SD)		***Epididymal Parameters (Mean ±SD)***							
	Seminiferous Tubule		**Initial Segment**		**Caput**		**Corpus**		**Cauda**	
	T. diameter (µm)	*E. height (µm)*	*T. diameter (µm)*	*E. height (µm)*	*T. diameter (µm)*	*E. height (µm)*	*T. diameter (µm)*	*E. height (µm)*	*T. diameter (µm)*	*E. height (µm)*
January	173.7 ±7.2	57.9 ±2.7	226.6 ±22.9	61.2 ±7.3	260.5 ±34.9	51.6 ±5.2	267.6 ±31.8	41.4 ±3.1	319.3 ±60.7*	16.5 ±3.2
February	171.9 ±7.4	55.8 ±3.0	225.7 ±21.8	61.3 ±7.4	250.7 ±35.0	50.8 ±5.3	265.7 ±32.1	42.5 ±3.0	320.7 ±58.8*	15.4 ±3.1
March	170.1 ±6.5	55.6 ±2.9	209.9 ±20.4	53.3 ±4.9	228.6 ±14.3	44.7 ±5.3	236.1 ±27.2	36.9 ±5.9	486.4 ±97.4*	17.1 ±2.4
April	176.4 ±6.8	58.6 ±3.9	207.6 ±32.7	54.2 ±8.9	234.5 ±28.8	38.8 ±4.2	231.3 ±29.4	29.1 ±3.7	647.9 ±145.7*	17.9 ±1.5
May	184.7 ±7.7	57.7 ±4.3	238.6 ±19.2	66.2 ±12.1	224.9 ±28.9	52.4 ±8.1	256.4 ±42.5	37.2 ±7.8	515.3 ±61.8*	18.4 ±3.5
June	170.1 ±8.9	59.2 ±4.4	204.7 ±28.5	52.2 ±10.9	216.2 ±24.2	44.1 ±6.1	229.9 ±33.2	38.3 ±3.5	519.1 ±89.6*	17.9 ±2.5
July	171.2 ±9.1	58.8 ±4.2	208.6 ±26.6	55.4 ±9.1	210.3 ±21.5	48.2 ±5.5	235.1 ±29.4	37.9 ±3.3	530.6 ±85.5*	18.5 ±2.1
August	178.1 ±13.4	58.9 ±5.1	218.5 ±49.7	61.5 ±7.5	215.5 ±22.2	54.1 ±4.3	259.8 ±20.7	48.9 ±4.2	512.5 ±97.9*	14.6 ±1.7
September	184.1 ±4.8	52.1 ±3.6	210.6 ±38.6	58.2 ±5.4	228.5 ±14.7	50.6 ±6.5	227.9 ±28.4	32.8 ±2.2	521.5 ±84.1*	16.5 ±1.2
October	194.0 ±8.5	63.8 ±3.1	205.5 ±23.3	57.5 ±1.1	218.7 ±15.9	45.1 ±4.5	236.1 ±25.2	38.3 ±2.0	523.6 ±89.1*	16.9 ±2.1
November	157. 8 ±5.1	52.8 ±4.3	216.7 ±34.1	60.8 ±3.5	230.7 ±22.2	44.2 ±3.5	246.5 ±20.4	36.8 ±4.3	510.2 ±61.5*	15.8 ±2.4
December	192.3 ±10.4	63.8 ±3.1	221.8 ±21.1	61.1 ±6.5	245.8 ±20.3	46.8 ±3.2	247.3 ±22.7	37.6 ±2.5	485.6 ±80.3*	16.3 ±3.0

T. diameter means tubular diameter; *E. height* means epithelial height.

*$p < 0.05$

Table 18: Monthly variations in the histo-morphometry of the testicular and epididymal parameters in the greater cane ra

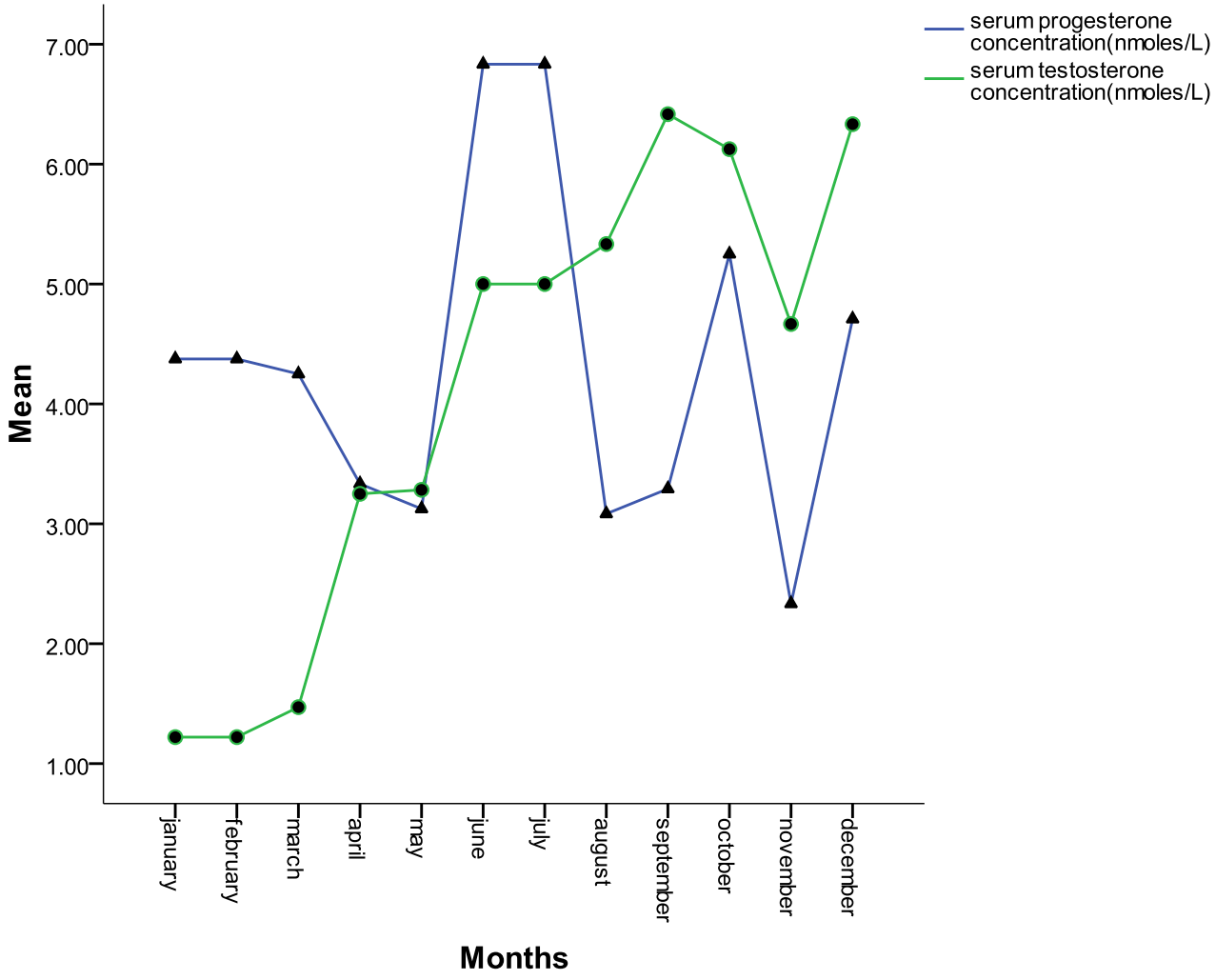

Figure 75: Line graphs showing the monthly variations of the mean serum levels of testosterone and progesterone concentrations in the greater cane rat.

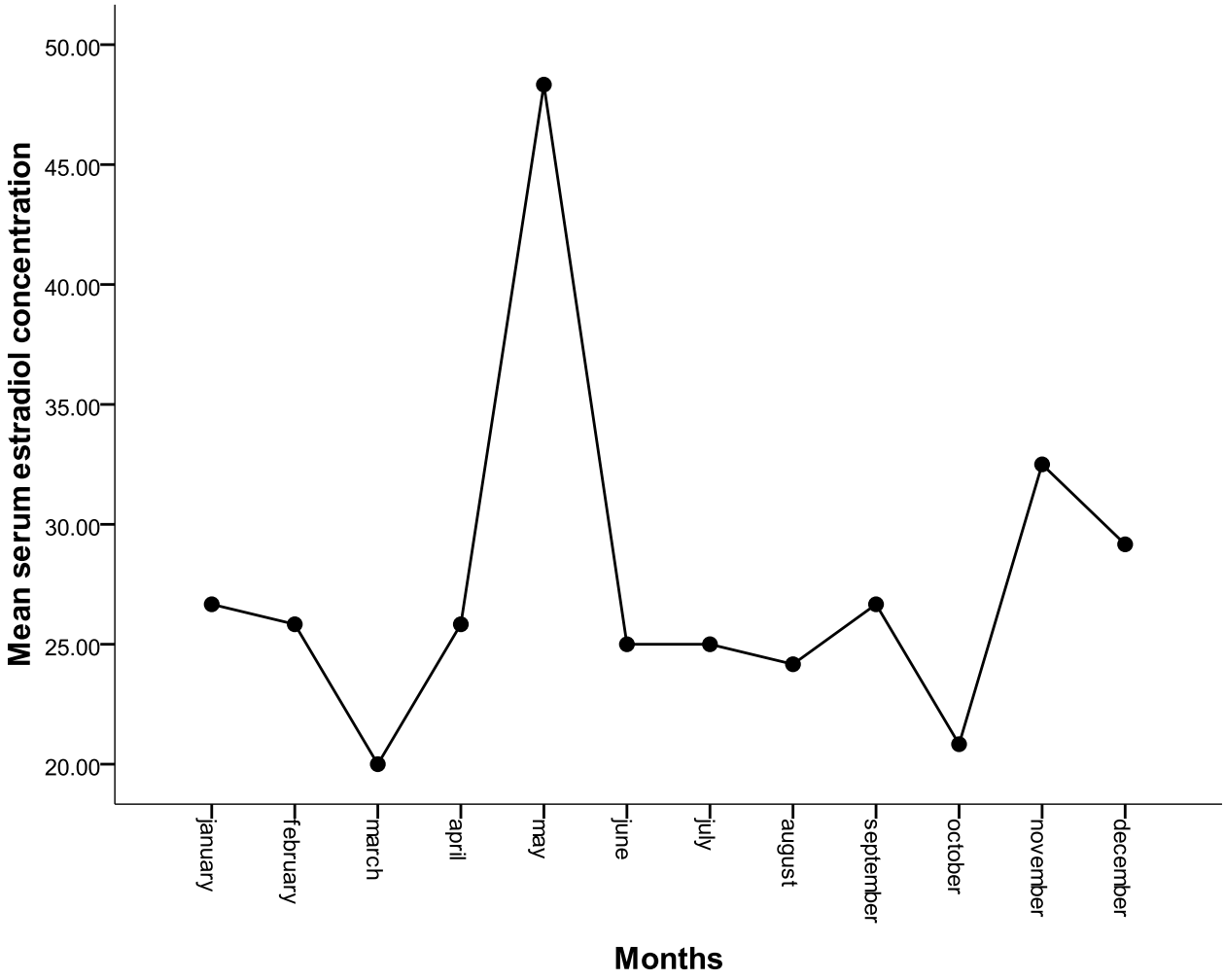

Figure 76: Line graphs showing the monthly variations of the mean serum estradiol concentrations in the greater cane rat.

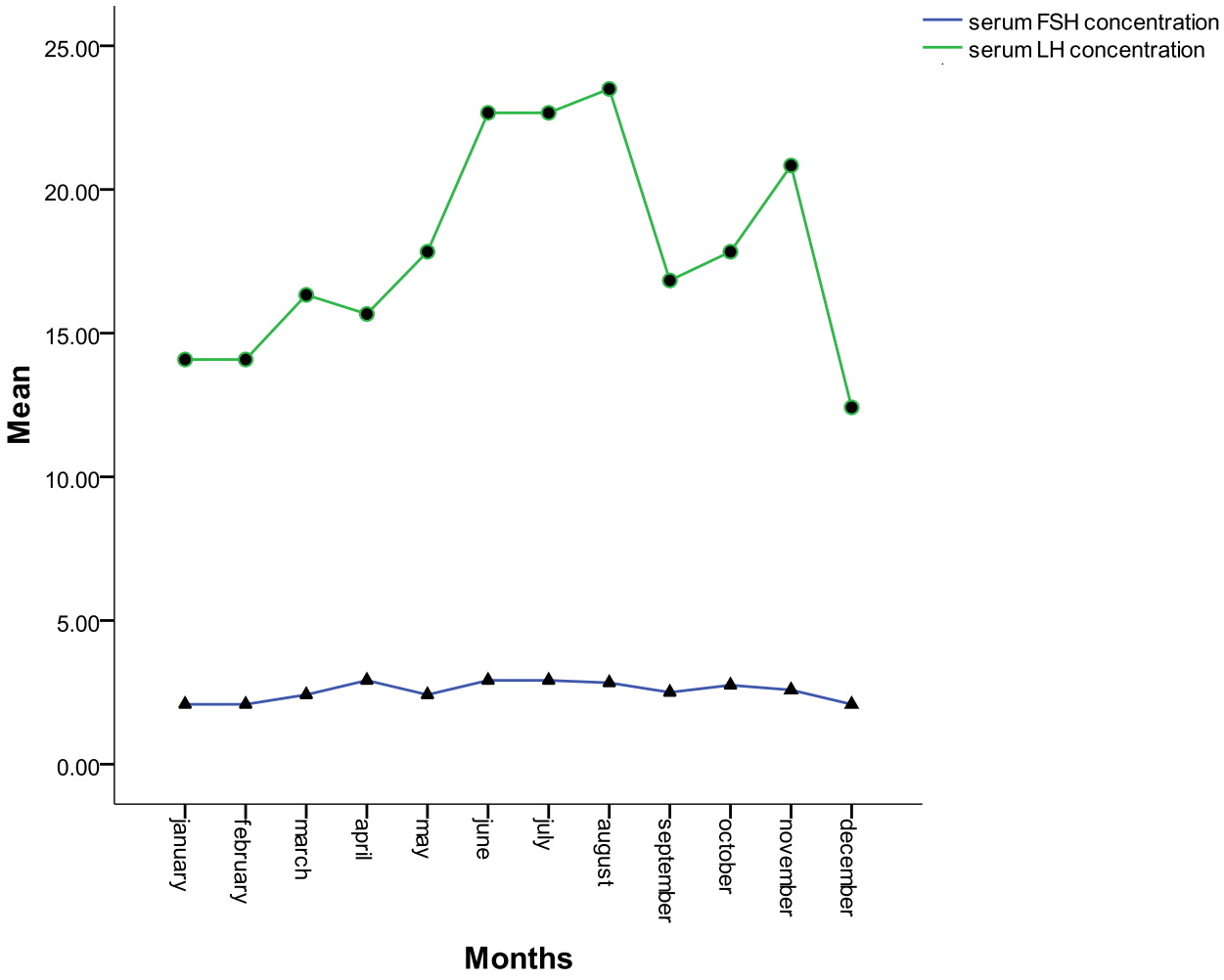

Figure 77: Line graphs showing the monthly variations of the mean serum levels of luteinizing and follicle stimulating hormone concentrations in the greater cane rat.

Table 17 showed the monthly mean ±standard deviation of the testicular and epididymal gross morphometric values in the greater cane rat. It was observed that there was no statistically significant difference ($p > 0.05$) in the testicular weight, volume and diameter within the months suggesting no seasonal variation with these testicular parameters. However, while the epididymal lengths were not significantly different, there were significant variations in the epididymal weight and volume within the months. The epididymal volume and weight were higher between November and March than between April and October.

In Table 18, the monthly mean ±standard deviation of the tubular diameters and epithelial heights of both the seminiferous tubules and the four epididymal regions were shown. From the table, no seasonal variation was observed in the testicular histo-morphometry. Whereas, the first three regions of the epididymis; the initial segment, the caput and corpus epididymis showed no significant differences within the months, monthly variations that follows seasonal pattern was observed in the morphometric values of the cauda epididymis.

Figure 75 showed the monthly variations of the serum testosterone and progesterone levels while Figure 76 showed how the mean serum levels of estradiol varies with the different months of the year. Figure 77 revealed the monthly variations of the serum LH and FSH concentrations in the greater cane rat. Of the five hormones assayed, only testosterone and LH showed some seasonal variations in its serum concentrations increasing during the rainy season (March – October) but gradually decreasing during the dry season (November - February)

5.4 DISCUSSION

This work presented the monthly morphometric variations of the testes and epididymis as well as the monthly hormonal values in the greater cane rat. Gross, histo- and ultrastructural morphometry were valuable tools in the evaluation of the effects of seasons, drugs and hormones on spermatogenesis in several rodents (Ichihara and Pelliniemi, 2007) especially those undergoing domestication and captive-rearing (Oke, 1988; Busso *et al*., 2005; Chaves *et al*., 2012). By analyzing monthly gonadal and hormonal parameters across seasons, Oke, (1988) and Akinloye, (2009) have ostensibly established the seasonality of breeding in the male and female African giant rat while Fuentes *et al*., (1993) and Busso *et al*., (2005) have done the same for viscacha (*Lagostomus maximus maximus*) and chinchilla (*Chinchilla laniger*) respectively. The morphometric values provided in this work therefore served as normative data-basis for further work on testicular and epididymal morphometry as well as for the characterization of seasonality of breeding which will help improve the management strategies of male greater cane rat.

In the greater cane rat, it was observed that while the testicular morphometric parameters were not different within the months, epididymal parameter showed some monthly variations in weight and volume as well as in tubular diameter and epithelial heights of the cauda epididymis. According to Fuentes *et al*, (1991) and Bahk *et al*, (2010) testicular and epididymal volumes and weights were generally regarded as indices representative of spermatogenesis or semen profile. As measures of gonadal activity, marked differences have been reported in both gross and histo-morphometric values of these segments of reproductive organs at different seasons of the year in seasonally breeding animals (Oke, 1988; Ichihara and Pelliniemi, 2007; Chaves *et al*., 2012). Based on the monthly morphometric evaluations of these segments, seasonality of breeding has been reported in several wild rodents (Oke, 1988; Busso *et al*, 2005; Chaves *et al.*, 2012). While

Oke, (1988) reported increased gonadal activity in the wild male African giant rat during the dry season (October – March), data obtained from captive chinchilla males showed decrease in testicular volumes in mid-summer than the rest of the year (Busso *et al*., 2004). The report of Busso *et al*, (2005) revealed that wild rodents such as viscacha and chinchilla reproduce continuously in captivity but have seasonal reproductive patterns in the wild. The observation in the cane rat is consistent with that of viscacha and chinchilla. Giving the current level of captive rearing and domestication of the greater cane rat, the observed seasonal variation in the epididymal parameters might simply be an ontogenic echo of the seasonality of its reproductive activity which will subsequently fade away with increasing level of domestication.

In this work, it was observed that the levels of serum testosterone and luteinizing hormones in the male cane rat showed some seasonal variations with the levels increasing during the rainy season (March – October) but beginning to decrease during the dry season. The level of serum testosterone had been reported to rise during the active reproductive seasons in seasonally breeding animals like viscacha (Chaves *et al*., 2012). Chaves *et al*, (2012) had also observed that the rising testosterone levels was caused by increasing testicular sensitivity to luteinizing hormone (LH) stimulation, the level of which was equally expected to increase during the active reproductive season. The testosterone and LH patterns observed in the greater cane rat were similar to that reported in viscacha (Chaves *et al*., 2012).

It has long been established that testosterone plays the important role of stimulating Sertoli cells to maintain spermatogenesis (Weddington *et al*., 1976). Gendt *et al*, (2004) found that Sertoli cells regulate the spermatogenic process crucially through the spermatocyte meiotic processes and the subsequent process of developing spermatids by their intracellularly synthesized testosterone. This had also been confirmed by the work of Ichihara and Pelliniemi,

(2007) which showed that alteration in the serum levels of testosterone and luteinizing hormone might not cause morphometric changes in the testis or in the process of spermatogenesis in rat. On the background of the above observations, the lack of variation in the monthly testicular morphometric parameters even with the variation in the serum testosterone levels seen in the greater cane rat was conceivable. It is therefore not unlikely that while the varied testosterone levels reflect the seasonality of breeding in this animal, the unchanged testicular morphometry might be as a result of intracellularly synthesized androgen that continuously maintained spermatogenesis in the face of changing serum testosterone levels.

In conclusion, with the lack of monthly variation in the gonadal activity but the seasonal variations in the epididymal morphometry as well as the serum testosterone and LH levels, the male greater cane rat showed increased reproductive activities during the rainy season. However, factors responsible for the possible seasonality of breeding and role of captivity and domestication in the modification of these factors in the male greater cane remain a subject of further research.

CHAPTER SIX

SUMMARY, CONCLUSION AND RECOMMENDATIONS

6.1 Summary

The present work provides information on the morphometry and morphology of the male reproductive system at gross, histological and ultrastructural levels highlighting the peculiarities of organs, cells and organelles in the greater cane rat.

At gross appearance, the oblong-shaped, cream-coloured testis was covered by transparent capsule that is uniformly ramified by blood vessels arranged in a distinctive pattern. It is equally attached to the gubernaculum that makes scrotal, inguinal and abdominal testicular locations possible. The epididymis has an inverted S shape with two distinct divisions of cranial and caudal parts. The prostate is made up of four separate lobes on the right and three attached lobes on the left. The Y-shaped with short cranial branches of the vesicular gland make up the inimitable gross appearance of the reproductive apparatus in this animal.

Histologically, the testis presents normal histo-architecture typical of rodent species with nine stages of seminiferous epithelium cycle. Whereas the epididymis has six discrete zones on its four typical regions, the vas deferens was found to have three zones with each having different luminal diameters, degrees of mucosal folding and amount of muscle layers that surrounds it. Histologically, the prostate has two distinct zones but the coagulating, vesicular and bulbourethral glands exhibit normal histological features typical of other rodentia species. Gross and histometric values were also determined for each segment of the tract.

At the ultrastructural level the process of spermatogenesis and acrosomal formation together with the fine structures of the other segments of the reproductive tract were analyzed in

the cane rat. Most of the organs have several distinctive features some of which are: the peculiar acrosomal formation in the seminiferous tubules; the specific pattern of arrangement of the lymphoid sinuses, Leydig cells and the macrophages in the testicular interstitium; the unique distribution of organelles among the different cells of the various epididymal regions; the distinct presence of the intraepithelial macrophages only in the vas deferens; the peculiar mechanism of secretion in the coagulating gland and the distinct electron-dense strands radiating from the secretory granules of the bulbourethral gland which have not been reported in any rodent species yet studied. This aspect of the work therefore provides the needed baseline information on the morphology of the male reproductive tract in the greater cane rat.

As a basis for the understanding of the normal functioning of these reproductive structures and how these functions are regulated in the male cane rat, the second aspect of this work characterized the serum levels of five sex hormones – testosterone, estrogen, progesterone, luteinizing and follicle stimulating hormones as well as immunolocalize the distribution patterns of the receptor proteins of two of these hormones, that are, apart from testosterone, now being reported as having direct role on the normal functioning of male reproductive structures – estrogen and progesterone. Anthropometric indices – body mass and Lee indices for the normal functioning of these proteins were also determined. The serum hormonal levels were within the normal range for most rodents but the distribution pattern of the estrogen and progesterone receptors in some of the reproductive structures were specific and unique to the male cane rat. While the immunolabelling of the estrogen alpha and beta (ERα and ERβ) receptors followed the normal rodent pattern in the testes and accessory sex glands, the epididymis showed some peculiar selective staining of its narrow, apical and basal cells. In the same vein, progesterone receptor (PR) was also localized in the cauda epididymis, a finding which to the best of our

knowledge has not been reported in any rodent under normal condition. The full imports of these distribution patterns are yet to be determined. The estimated anthropometrical indices in this work varied with the different reproductive parameters in the manner typical of the *rodentia* species.

Finally the study provided information on the possible impact of seasons on the morphology and the functioning of the male reproductive organs through the evaluation of the variation of the testicular and epididymal morphometric parameters as well as the serum hormonal levels within the twelve calendar months of the year. The result from this aspect of the work showed the male cane rat as having increased reproductive activity during the rainy season.

6.2 Conclusion

This work has bridged some of the information gap on the reproductive biology of the male greater cane rat by providing the much needed baseline data on some aspects of the morpho-physiology of reproductive tract. This information will serve as basis for further research on the reproductive biology, enhance and hasten the domestication process as well as aid the intensive management practices of this important, African based rodent

6.3 Recommendations

1. To further the understanding of the significant and functional interpretation of some of the structures and the ultra-structures in the male reproductive tract, it is necessary to investigate the morphology of the reproductive tract in the female greater cane rat.

2. To advance the understanding of the spermatogenic process in the cane rat, morphometric analysis at ultrastructural level is recommended

3. There is the need to further validate the distribution pattern of the receptors using more advance techniques of Polymerase Chain Reaction, Western blotting and In situ hybridization as a way of elucidating the possible roles of these hormones in the male reproductive processes.

4. The age variation in both the distribution pattern of the receptors and the anthropometric indices should be a subject of research so as to understand the roles of these receptors and other factors on the development of the male reproductive tract.

5. Comprehensive studies on the components of the different secretions of the accessory sex glands and how they impact on sperm morphology and fertilization is also a veritable area of research.

REFERENCES

Abdelmalik, S. W. 2011. Histological and ultrastructural changes in adult albino rat testes following chronic crude garlic consumption. *Annals of Anatomy*, 193:134-141

Abercrombie M. 1946. Estimation of nuclear population from microtome sections. *Anatomical Records* 94: 238 -248.

Abou-haila A and Tulsiani D. R. 2009. Signal transduction pathways that regulate sperm capacitation and the acrosome reaction. *Arch Biochem Biophys* 485: 72–81

Adamali H. I and Hermo L. 1996. Apical and Narrow cells are distinct cell types differing in their structures, distribution and function in the Adult rat Epididymis. *Journal of Andrology* 17: 208-222

Adams, C.E. 1989. The laboratory rabbit. In: Trevor, B. Poole (editor), UFAW Handbook on the care and management of laboratory animals. 6th ed. England; Longman Scientific & Technical 415 – 435.

Adaro, L., Mendoza, J. Cepeda R and Oro´ stegui. P. 2001. Anatomo-radiographic study of the seminal vesicles of chinchilla (Chinchilla laniger) in captivity. *Rev. Chil. Anat.* 19: 297–300.

Addo, P., Dodoo, A., Adjei., S. and Awumbila, B. 2003. Optimal duration of male-female exposure to optimize conception in the Grasscutter (*Thryonomys swinderianus*). *Livestock Research for Rural development* 11. 1: 1-3

Addo, P.G., Awumbila, B., Awotwi, E. and Ankrah N-A. 2007. Reproductive characteristics of the female grasscutter (*Thryonomys swinderianus*) and formulation of colony breeding strategies. *Livestock research for rural development* **15**. 1: 1-3.

Adebayo, A. O., Oke, B. O. and Akinloye, A. K. 2009a. Characterizing the gonadosomatic index and its relationship with age in the greater cane rat (*Thryonomys swinderianus* Temminck). *Journal of Veterinary Anatomy. 2. 2:* 53-59.

Adebayo, A. O., Oke, B. O. and Akinloye, A. K.. 2009b. The Gross Morphometry and Histology of the Male Accessory Sex glands in the Greater cane rat (*Thryonomys swinderianus* Temminck) *Journal of Veterinary Anatomy. 2. 2:* 41-51.

Adebayo, A.O. and Olurode S. A. 2010. The morphology and morphometry of the Epidydimis in the greater cane rat (*Thryonomys swinderianus* Temminck). *Folia morphologia*. 69. 4.: 246-252

Adebayo, A.O**.,** Akinloye, A.K., Olurode, S.A., Anise, E.O and Oke, B.O. 2011. The structure of the penis and the associated baculum in the greater cane rat (*Thryonomys swinderianus* Temminck). *Folia Morphologica* 70. 3**:** 197-203.

Adjanohoun, E. 1989. Contribution au developpment de l'élevage de l'aulacode (*Thryonomys swinderianus* – Temminck, 1827) et a l'étude de sa reproduction. Agence de Coopération Culturelle et Technique du Bénin. Para Graphic 31240 L'Union Toulouse, France. 211.

Adu, E. K and Yeboah, S**.** 2003. On the use of perineal stain as an index of sexual maturity and breeding condition in the male greater cane rat (*Thryonomys swinderianus*, Temminck). *Tropical Animal Health and Production*, 35.5: 433-439

Adu, E. K, Otsyina, R.H and Agyei A. D. 2005. The efficacy of different dose levels of albendazole for reducing fecal worm egg count in naturally infected captive grasscutter (*Thryonomys swinderianus*, Temminck). *Livestock research and rural development* 17 .11: 1-6

Adu, E.K. 2003. Patterns of Parturition and mortality in weaned greater cane rat (*Thryonomys swinderianus* – Temminck). *Tropical Animal Health and Production*. 35.5**.**: 425 – 431.

Adu, E.K., Alhassan, W.S and Nelson, F.S. 1999. Small holder farming of the greater cane rat, *Thryonomys swinderianus* Temminck, in Southern Ghana: a baseline survey of management practices. *Tropical Animal Health and Production*, 31: 223 – 232.

Afolayan, T.A. and Anadu, P.A. 1981. Preliminary observations on the ecology and domestication of the Grasscutter. *J. Inst. Ani. Tech. (London)* 31 .1: 31 – 38.

Aggerholm A. S., Thulstrup A. M., Toft G., Ramlau-Hansen C. H, Bonde J. P (2008): Is overweight a risk factor for reduced semen quality and altered serum sex hormone profile? *Fertility and Sterility* 90:619–626.

Aguilera-merlo C., Munoz E., Dominguez S., Scardapane L and Piezzi R. 2005. Epididymis of Viscacha (*Lagostomus maximus maximus*): Morphological Changes During the Annual Reproductive Cycle. *Anatomical Records* 282: 83-92

Aire, T.A. 2006. Anatomy of the testis and Male reproductive tract in birds. *A review*. 1 – 100

Aire, T.A. 1980. The ductuli efferentes of the Epididymal region of birds. *Journal of Anatomy* 130: 707 – 723.

Aire, T.A. 1997. The structure of the interstitial tissues of the active and resting avian testis. *Onderstepoort Journal of Veterinary Research* 64: 291 – 299.

Aire, T.A. and van der Merwe, M. 2003. The ductuli efferentes of the greater cane rat (*Thryonomys swinderianus*). *Anatomy and Embryology* 206: 409 – 417.

Aire, T.A., Ayeni, J.S and Olowookorun, M.O. 1979. The structure of the excurrent ducts of the testis of the guinea-fowl (*Numida meleagris*). *Journal of Anatomy* 129: 633 – 643.

Aitken, R.N.C. 1959. Observations on the development of the seminal vesicles, prostrate and bulbourethral glands in the ram. *Journal of Anatomy* 93: 43 – 51.

Ajayi, S.S and Tewe, O.O. 1980. Food preferences and carcass composition of the Grasscutter (*Thryonomys swinderianus*) in captivity. *African Journal of Ecology* 18 .2 & 3: 133 – 140.

Ajayi, S.S. 1994. Ensuring sustainable management of wildlife resources: The case of Africa: FAO Forestry Paper No. 122, Rome 1994.133 – 140.

Akingbemi, B. T., Ge, R.S and Hardy, M.P. 1999. Leydig cells. In E. Knobil and J.D Neill (eds.), *Encyclopaedia of Reproduction.* Academic Press, San Diego, California. 1021 – 1033

Akinloye, A.K.. 2001.Effects of *Calotropis procera* on the development of the reproductive organ, accessory sex glands and some other organs in male wister rats. M.Sc. Thesis, University of Ibadan.

Akinloye, A.K.. 2009. Structural and Hormonal studies of the Female African Giant rat (*Cricetomys gambianus* Waterhouse) at different stages of the oestrus. Ph.D. Thesis, University of Ibadan.

Alberts, B., Bray, D., Lewis, J., Raff, M., Roberts, K. and Watson, J. D. 2002. Molecular Biology of the Cell. Garland Publishing, New York, 1463.

Allolio B., Oremus M., Reincke M., Schaeffer H. J., Winkelmann W., Heck G and Schulte H. M 1995. High-dose progesterone infusion in healthy male: evidence against antiglucocorticoid activity of progesterone. *European.Journal of Endocrinology*., 133.6: 696 – 700

Almeida F. F., Leal M. C and França L. R. 2006 .Testis morphometry, duration of spermatogenesis, and spermatogenic efficiency in the wild boar (*Sus scrofa scrofa*). *Biology of Reproduction* 75:792-799.

Alogninouwa T., Kpodekon M. and Yewadan L. T. 1999. Effect of castration on growth and endocrine pattern in the grascutter (*Thryonomys swinderianus* Temminck), *Ann. Zootech* 48:225-230

Aly A. E, Abdo M. S and Khabir A. 1991.The fine structure of the camel prostate gland. *Anat. Anz.* 172 (3); 223-229

Amann R. P and Veeramachaneni D. N. 2007. Cryptorchidism in common eutherian mammals. *Reproduction*; 133: 541 –561

Amann R. P. 1962. Reproductive capacity of dairy bulls. III. The effect of ejaculation frequency, unilateral vasectomy, and age on spermatogenesis. *American Journal of Anatomy* 110: 49 -67

Amann R. P., Hay S. R and Hammerstedt R. H. 1982. Yield, characteristics, motility and cAMP content of soerm isolated from seven regions of ram epididymis. *Biology of Reproduction.* 27: 723-733

Amann, R.P., Johnson, L. and Pickett, B.W. 1977. Connection between the seminiferous tubules and the efferent ducts in the stallion. *American Journal of Veterinary Research* 38: 1571 - 1579

Amselgruber, W and Feder, F.H., 1986. Licht- und elektronenmikroskopische untersuchungen der samenblasendr¨use (*Glandula vesicularis*) des bullen. *Anatomia Histolologia Embryologia*. 15: 361–379.

Amubode, F.O. and Oduro, W. 1989. Performance and some nutritional indices in Grasscutter (*Thryonomys swinderianus*) Fed varying food combinations. In Okojie, J.A. and Obiaga, C. (eds.). Proceedings of conference of the Forestry Association of Nigeria (F.A.N.). 309 – 317.

Anderson M. 1994. *Sexual selection*. Princeton: Princeton University Press

Anderson M. J and Dixson A. F. 2002. Sperm competition: motility and mid-piece in primates. *Nature* 416: 496.

Anderson M. J., Nyholt J and Dixson A. F. 2004. Sperm competition affects the structureof the mammaliam vas deferens. *J. Zool., Lond.* 264: 97–103.

Anderson R., Garcia-Castro M., Heasman J and Wylie C. 1998. Early stages of male germ cell differentiation in the mouse. *APMIS* 106:127–133

Anderson, R. S. 1973. Obesity in the dog and cat. *Veterinary Annual* 14**:** 182-186

Arey, L. B. 1974.Developmental Anatomy; A textbook and Laboratory manual of Embryology, 7th edition, W.B Sanders Company, Philadelphia and London. Pp 315-325

Arrighi S., Romanello M. G and Domeneghini C. 1993. Ultrastructural study on the epithelium lining ducts epididymis in adult cats (*Felis catus*). *Arch Biol* 97: 7–24.

Arrington, L.R. 1972. Management of laboratory animals. In: The breeding, care and management of experimental animals.. Interstate Printers and Publishers, Danville, Illinois. 141 – 159

Arrotéia K. F., Garcia P. V., Barbieri M. F., Justino M. L and Pereira L. A. V. 2012.The Epididymis: Embryology, Structure, Function and Its Role in Fertilization and Infertility, Embryology - Updates and Highlights on Classic Topics, Prof. Luis Violin Pereira (Ed.), ISBN: 978- 953-51-0465-0, InTech, Available from: http://www.intechopen.com/books/embryology-updates-and-highlightson- classic-topics/the-epididymis-embryology-structure-function-and-its-role-in-fertilization-and-infertility

Arthur, G.H., Noakes, D.E. and Pearson, H. 1989. The oestrous cycle and its control. In: *Veterinary reproduction and obstetrics.* (6th edition) 3-45. ELDS.

Asibey, E.O.A and Addo P.G 2000. The Grasscutter; a promising animal for meat production. In: Turnham D, (editor) African perspectives. Practices and policies supporting sustainable development. (Scandinavian Seminar College, Denmark, in association with Weaver Press, Harare, Zimbabwe). 120

.

Asibey, E.O.A and Eyeson K. K. 1975. Additional information on the importance of wildlife animals as food source in Africa south of the Sahara. *Bongo Journal of the Ghana Wildlife Society* 1: 13-17

Atanassova N, McKinnell C, Williams K, Turner K. J, Fisher J.S, Saunders P.T. 2001. Age-, cell-and region-specific immunoexpression of estrogen receptor alpha (but not estrogen receptorbeta) during postnatal development of the epididymis and vas deferens of the rat and disruption of this pattern by neonatal treatment with diethylstilbestrol. *Endocrinology*;142.2: 874-86

Aum¨uller, G., Wilhelm, B., Seitz, J. 1999. Apocrine secretion – fact or artifact? *Anat. Anz*. 181: 437–446.

Aumu¨ ller G and Seitz J. 1990. Protein secretion and secretory proccess in male accessory sex gland. *Int Rev Cytol* 121: 127–231.

Ayres de Menezes D. J, Assis Neto A. C, Oliveira M. F, Miglino M. A., Pereira G. R, Ambr_osio C. E, Ferraz M. S and Carvalho M. A. 2010. Morphology of the male agouti accessory genital glands (Dasyprocta prymnolopha Wagler, 1831). *Pesq Vet Bras* 30: 793–797

Baccari, G.C., Chieffi, G., Di Matteo, L., Dafnis, D., De Rienzo, G., Minucci, S. 2000 Morphology of the Harderian gland of the Gecko, *Tarentola mauritanica*. *J. Morphol*. 244: 137–142.

Backhouse, K.. M. 1966. The natural history of testicular descent and maldescent. *Proc R Soc Med* 59: 357–360.

Badia E., Briz M., Pinart E., Garcia-Gil N., Bassols J., Pruneda A., Bussalleu E., Yeste M., Casas I and Bonet S. 2006. Structural and ultrastructural features of boar seminal vesicles. *Tissue and cell* 38: 79–91.

Badia, E., Briz, M. D., Pinart, E., Sancho, S., Garcia, N., Bassols, J.,Pruneda, A., Bussalleu, E., Yeste, M., Casas, I., Bonet, S. 2006. Structural and ultrastructural features of boar bulbourethral glands. *Tissue and cell* 38: 7- 18

Bagnis C, Marsolais M, Biemesderfer D, Laprade R, Breton S. 2001. Na(þ)/ H(þ)-exchange activity and immunolocalization of NHE3 in rat epididymis. *Am J Physiol Renal Physiol **280***: F426–F436.

Bahk, J. Y., Jae H. Jung J. H., Lee M. Jin L. M. and Min S. K. 2010 Cut-off Value of Testes Volume in Young Adults and Correlation among Testes Volume, Body Mass Index, Hormonal Level, and Seminal Profiles. *Urology* 75: 1318-1323

Baldi E., Luconi M., Krausz C and Forti G. 2011. Progesterone and Spermatozoa: a long-lasting liaison comes to definition. *Human Reproduction*, doi:10.1093/humrep/der289

Balinsky, B.I. 1981. An introduction to Embryology, 5th edition Sanders college publishing. Philadelphia.

Banks, W.J 1974. Histology and Comparative organology: A test atlas. The Williams and Wilkins Co. Baltimore.

Baptist R. and Mensah G. A 1986. Benin and West Africa: The cane rat farm animal of the future. *World Anim. Rev.* 60: 2-6.

Barr A. B. 1973. Timing of spermatogenesis in four nonhuman primate species. *Fertil Steril.* **24**: Pp 381 -389

Bartsch G and Rohr H.P. 1980. Comparative light and electron microscopic study of the human, dog and rat prostate. *Urol Int.* 35: 91-104.

Bedford J. M and Nicander L 1971. Ultrastructural changes in the acrosome and sperm membranes during maturation of spermatozoa in the testis and epididymis of the rabbit and monkey. *Journal of Anatomy*. 108 .3: 527-543

Bedford, J. M. 1978. Anatomical evidence for the epididymis as the prime mover in the evolution of the scrotum. *American Journal of Anatomy* 152: 483 – 508

Beil R.E and Hart R.G 1973. Cowper's gland secretion in rat semen coagulation. II. Identification of the potentiating factor secreted by the coagulating glands *Biology of Reproduction* 8: 613-617

Bergh, A. 1987.Treatment with HCG increases the size of Leydig cells and testicular macrophages in unilaterally cryptorchid rats. International *Journal of Andrology* 10: 765 – 772.

Bernardis L. L. 1970. Prediction of carcass fat, water and lean body mass from Lee's nutritive ratio in rats with hypothalamic obesity. *Experientia* 26: 789–90

Berndtson W.E . 1977. Methods for quantifying mammalian spermatogenesis: a review. *J Anim Sci*. **44**: 818 -833

Betteridge, K. .J. 1986. Increasing Productivity in Farm Animals. In: Austin, C.R and Short, R.V. (editors), Reproduction in mammals: Manipulating reproduction 2nd edition. University Press. Cambridge, 1 – 47.

Birkhead, T. R. 2000. *Promiscuity: an evolutionary history of sperm competition and sexual selection*. London: Faber and Faber.

Bloom, W. and Fawcett, D.W. 1975. A textbook of histology. W.b. Saunders Company Philadelphia. London. Toronto

Bonkhoff H, Stein U and Remberger K. 1994. The proliferative function of basal cells in the normal and hyperplastic human prostate. *The Prostate* 24 .3; 114-118

Bormann C. L., Smith G. D., Padmanabhan V and Lee T. M. 2011. Prenatal testosterone and dihydrotestosterone exposure disrupts ovine testicular development. *Reproduction* 142**:** 167–173

Bouin, P. and Ancel, P 1903. Sur la significanyt de la glande interstitiele du testicle cubrayonnaire. *Compt. Rend. Soc. Biol.* 55: 1682-1684.

Brandes D and Portela A. 1960. The fine structure of the epithelial cells of the mouse prostate. II.Ventral lobe epithelium. *Journal of Biophysical and Biochemical Cytology* 7: 511-514.

Brenner, R.M., West, N.B., McClellan, M.C., 1990. Oestrogen and progestin receptors in the reproductive tract of male and female primates. *Biology of Reproduction*. 42: 11–19.

Brooks J. E., Busch R. D., Patanelli D. J and Steelman S. L.(1973. A study of the effects of a new anti androgen on the hyperplastic dog prostate. *Proc Soc Exp Biol Med* 143: 647–655.

Brooks, D.E. 1973. Epididymal and testicular temperature in the unrestrained conscious rat. *Journal of Reproduction and. Fertility*. 35: 157 – 160.

Budras K. D and Meier, U. 1981. The epididymis and its development in ratite birds (Ostrich, Emu, Rhea). *Anatomy and Embryology* 162: 281 – 299.

Burgos, M.H., Vitale-Calpe, R. and Aoki, A. 1970. Fine structure of the testis and its functional significance. In A.D. Johnson, W.R. Gomes and N.L. Vandemark (eds.), *The Testis. Development, Anatomy and Physiology*. Vol. I. Academic Press, London. 552 – 649.

Burnes, R.K. 1961Role of hormones in the differentiation of sex. In sex and internal secretions, W.C. Young Ed. (Baltimore, Williams and Wilkins Co.), 76 – 158.

Busso, J. M., Ponzio M. F., Fiol de Cuneo M. and Ruiz R. D. 2012. Reproduction in Chinchilla (*Chinchilla lanigera*): Current status of environmental control of gonadal activity and advances in reproductive techniques. *Theriogenology* 78: 1-11.

Busso, J. M., Ponzio, M. F., Dabbene, V., Fiol de Cuneo, M and Ruiz, R. D. 2004 Assessment of urine and fecal testosterone metabolite excretion in Chinchilla lanigera males. *Animal Reproduction Science*. doi:10.1016/j.anireprosci.2004.08.001.

Busso, J. M., Ponzio, M. F., Fiol de Cuneo, M and Ruiz, R. D. 2005. Year-round testicular volume and semen evaluation in captive *Chinchilla lanigera*.., *Animal Reproduction Science*. 90: 127 – 134.

Busto-Obregon E., Courol M., Flechon J. E., Hochereau-De Revier M. T and Hostein A. F. 1975. Morphological appraisal of gametogenesis. Spermatogenetic process in mammals with particular reference to man. *Andrologia*. 7: 142-163

Cakir, M. and Karatas A. 2004. Histo-anatomical studies on the accessory reproductive glands of the Anantolian Souslik (Spermophilus xanthoprymmus) (Mammalia: Sciuridae). *Anatomia Histologia. Embryologia.* 33: 146–150.

Calvo A., Pastor L. M., Martı´nez E., Va´zquez J. M and Roca J. 1999. Age related changes in the hamster epididymis. *Anatomical Record* 256: 335–346.

Capel B. 2000. The battle of the sexes. *Mech Dev*, 92: 89-103

Carballada, R and Esponda, P. 1992. Role of fluid from seminal vesicles and coagulating glands in sperm transport into the uterus and fertility in rats. *J Reprod Fertil* 95:639–648.

Cardoso, F.M., Godinho, H.P., Nogueira, J.C. 1979. Age-related changes in the seminal vesicles of a Brazilian (Nelore) zebu. *Acta Anat.* (Basel) 103: 327–335.

Carpino, A., Bilinska, B., Siciliano, L., Maggiolini M and Rago, V. 2004. Immunolocalization of estrogen receptor β in the epididymis of mature and immature pigs. *Folia histochemica et cytobiologica* 42.1: 13-17

Carreau S., Delalande C., Silandre D., Bourguiba S and Lambard S. 2006. Aromatase and estrogen receptors in male reproduction. *Mol Cell Endocrinol*. 246: 65–8.

Carreau S., Silandre, D., Bois, C., Bouraima, H., Galeraud-Denis, I. and Delalande C. (2007) Estrogens: a new player in spermatogenesis. *Folia Histochem. Cytobiol*. 45 Suppl. 1: 5–10.

Carreau, S. and Hess R. A. (2010): Oestrogens and spermatogenesis. *Philosophical Transanction Royal Society* B; 365: 1517–35.

Carreau, S., Bois, C., Zanatta L., Silva F. R. M. B., Bouraima-Lelong H and Delalande, C. 2011. Estrogen signaling in testicular cells. *Life sciences* 89: 584-587

Carreau, S., de Vienne, C. and Galeraud-Denis, I. 2008. Aromatase and estrogens in man reproduction: a review and latest advances. *Adv. Med. Sci*. 53: 139–144. (doi:10.2478/v10039-008-0022-z)

Carvalho, C. A. F., Camargo, A. M., Cagnon, V. H. A and Padovani, C. R. 2003. Effects of experimental diabetes on the structure and ultrastructure of the coagulating gland of C57BL/6J and NOD mice. *Anatomical Record*. 270A: 129-136

Cavazos F. 1975. Fine structure and functional correlates of male accessory sex gland of rodents. *Am Physiol Soc* 5:353–380

Cepeda R., Adaro L and Pen˜ailillo G 2006. Morphometric variations of Chinchilla laniger prostate and plasmatic testosterone concentration during its annual reproductive cycle. *Int. J. Morphol.* 24: 89–97

Chang, W. Y., Wilson, M. J., Birch, L., Prins, G. S 1999. Neonatal oestrogen stimulates proliferation of periductal fibroblasts and alters the extracellular matrix composition in the rat prostate. *Endocrinology* 140: 405–415.

Chaves, E. M., Aguilera-Merlo, C., Filippa, V., Mohamed, F., Dominguez., S and Scardapane, L. 2011 Anatomical, Histological and Immunohistochemical Study of the Reproductive System Accessory Glands in Male Viscacha (*Lagostomus maximus maximus*). *Anatomia Histologia Embryologia* 40: 11–20**.**

Chaves, E.M., Aguilera-merlo, C., Crucen˜ o, A., Fogal, T., Piezzi, R., Scardapane, L and Dominguez, S. 2012. Seasonal Morphological Variations and Age-Related Changes of the Seminal Vesicle of Viscacha (*Lagostomus maximus maximus*): An Ultrastructural and Immunohistochemical Study *Anatomical Record* 295: 886–895

Cheng, C.Y. and Mruk, D.D. 2002. Cell junction dynamics in the testis: Sertoli-Germ cell interactions and male contraceptive development. *Physiol Rev* 82: 825 – 874.

Cheung K. H., Leung G. P., Leung M. C., Shum W. W., Zhou W. L and Wong P. Y. 2005. Cell-cell interaction underlies formation of fluid in the male reproductive tract of the rat. *J Gen Physiol* 125: 443–454.

Choy C, Chan W, Chen T, Shih C, Wu L and Liao C. 2011. Waist circumference and risk of elevated blood pressure in children: a cross-sectional study. *BMC Public Health* doi:10.1186/1471-2458-11-613

Christensen, A.K. 1975. Leydig cells. In: Handbook of physiology V. Male reproductive system. Eds E.B. Ashwood and R.O. Greep. The American Physiological Society, Washington, 57 – 94.

Christensen, A.K. and Fawcett, D.W. 1977.The structure of testicular interstitial cells in mice. *American Journal of Anatomy* 118: 551 – 572.

Chughtai B., Sawas A., O'malley R. L., Naik R. R., AliKhan S. and Pentyala, S. 2005. A neglected gland: a review of Cowper's gland. *International Journal of Andrology* 28**:** 74 – 77

Claudio L., Bearer C. F and Wallinga D. 1999. Assessment of the U.S. Environmental Protection Agency methods for identification of hazards to developing organisms, part I: the reproduction and fertility testing guidelines. *Am J Ind Med* 35: 543–553.

Clermont Y and Hermo L. 1988. Structure of the complex basement membrane underlying the epithelium of the vas deferens in the rat. *Anatomical Record* 221: 482-493.

Clermont Y. 1972. Kinetics of spermatogenesis in mammals seminiferous epithelium cycle and spermatogonial renewal. *Physiol Rev***.** 52: 198 -236

Clermont Y. 1954. Cycle de l'epith6lium seminal et mode de renouvellement des spermatogonies chez le hamster. Rev Can Biol. 13: 208-245.

Clermont, Y. and Antar, M. 1973. Duration of the cycle of the seminiferous epithelium and the spermatogonial renewal in the monkey *Macaca arctoides. American Journal of Anatomy* 136: 153 -166.

Clulow J., Jones R. C., Hansen L. A and Man S. Y. 1998. Fluid and electrolyte reabsorption in the ductuli efferentes testis. *J Reprod Fert* Supp 53: 1-14

Clulow, J. and Jones, R.C. 1988. Studies of fluid and spermatozoal transport in the extratesticular ducts of the Japanese quail. *Journal of Anatomy* 157: 1 – 11.

Clulow, J., Jones, R.C. and Hansen, L.A. 1994. Micropuncture and cannulation studies of fluid composion and transport in the ductuli efferentes testis of the rat: comparisons with the homologous metanephric proximal tubule. *Experimental Physiology* 79: 915 – 928

Colegrove, K. M., Gulland, F. M. D., Naydan, D. K. and Lowenstine, L. J. 2009: Normal Morphology and Hormone Receptor Expression in the Male California sea lion (*Zalophus californianus*) Genital Tract. *Anatomical Record* (Hoboken*);* 292.11: 1818–1826. doi:10.1002/ar.21008.

Comizzoli P., Mermillod P and Mauget R. 2000. Reproductive biotechnologies for endangered mammalian species. *Reprod Nutr Dev***.** 40: 493 –504.

Connell C.J. 1980. Blood-testis barrier formation and the initiation of meiosis in the dog. In: Steinberger A, Steinberger E, ed. *Testicular development, structure, and function*. New York: Raven Press. 71–78.

Connolly P. B and Resko J. A. 1989 Progestins affect reproductive behavior and androgen receptor dynamics in male guinea pig brain. *Brain Research*. 305: 312-316

Cornwall, G.A. 2009. New insights into epididymal biology and function, *Human Reproduction Update* 15 . 2: 213-227

Corradi L. S, Jesus M. M., Fochi R. A., Justulin-Jr L. A., Goes R. M., Felisbino S. L and Taboga S. R. 2013. Structural and Ultrastructural evidence for Telocytes in the prostate stroma. *J.cell.Mol. Med*. 17 .3: 398-406

Cortes D., Muller J. and Skakkebaek N.E. 1987. Proliferation of Sertoli cells during development of the human testis assessed by stereological methods. *International Journal of Andrology* 10: 589–596.

Costa G. M. J., Chiarini-Garcia, H., Morato, R.G., Alvarenga, R. L. L. S. and França, L. R. 2008. Duration of spermatogenesis and daily sperm production in the jaguar *(Pantheronca) Theriogenology* 70: 1136-1146.

Costa G. M. J., Leal M. C., Ferreira C. S., Guimarães D. A. and França L. R 2010. Duration of Spermatogenesis and Spermatogenic Efficiency in 2 Large Neotropical Rodent Species: The Agouti (*Dasyprocta leporina*) and Paca (*Agouti paca*). *Journal of Andrology*, 31.5:DOI: 10.2164/jandrol.109.009787

Crabo, B. 1965. Studies on the composition of Epididymal content in bulls and boars. *Acta Veterinaria Scandinavica* 6 (Suppl. 5): 8 – 94.

Cunha, G.R. and Lung, B. 1979. In: Accessory glands of the male reproductive tract. Vol. 6. Eds.: E.S.E. Hafez and E. Spring-Mills. Ann Arbor Scientific Publishers Inc. Ann Arbor Michigan.

Da Silva N., Shum W. W., El-Annan J., Paunescu T. G., McKee M., Smith P. J, Brown D and Breton S. 2007. Relocalization of the V-ATPase B2 subunit to the apical membrane of epididymal clear cells of mice deficient in the B1 subunit. *Am J Physiol Cell Physiol* 293: C199–C210.

Dacheux J. L., Castella S., Gatti L. J and Dacheux F. 2005. Epididymal cell secretory activities and the role of the proteins in boar sperm epididymis. *Theriogenology* 63 .2: 319-341

Davis, J.R., Langford, G.A. and Kirby, P.J. 1970. The testicular capsule. In: The Testis, Vol. 1. Academic Press, New York.

de Ronde W., Pols H. A. P., van Leeuwen J. P.T.M and de Jong F. H. 2003. The importance of oestrogens in males. *Clinical Endocrinology* 58: 529–542

De Rooij D. G. 1973. Spermatogonial stem cell renewal in the mouse. in. Normal situation. Cell Tissue Kinetics 6: 281-287.

Demoulin, A., Koulischer, L., Hustin, J., Hazee-Hagelstein, M.T., Lambotte,R and Franchimont, P. 1979. Organ culture of mammalian testis III. Inhibin secretion. *Hormone Research* 10: 117 – 190.

Dhingra, L.D. 1977. "Mediastinum testis". In: The Testis (A.D. Johnson and W.R. Gomes, eds.). Vol. IV : 451-460. Academic Press. New York.

Di Fiore M.S.H 1989. Atlas of Normal Histology. In: Male reproductive system 6th edition. Edited by Victor P. Eroschenko. Philadelphia. London (Indian Edition: KM Varghese Company, Bombay, India. 212-13.

Dukelow, W.R. 1978. Ovulation detection and control relative to optimal time of mating in non-human primates. Symposium of the Zoological Society of London. 43**:** 195 – 206.

Dunker, N and Aumuller, G. 2002. Transforming growth factor beta 2 heterozygous mutant mice exhibit Cowper's gland hyperplasia and cystic dilations of the gland ducts (Cowper's syringoceles). *Journal of Anatomy* 201: 173–183.

Dyce, K.M., Sack, W.O and Wensing, C.J.G 2002. Text book of Veterinary Anatomy, 3rd edition, Saunders, Pennsylvania. 183 – 192

Dyce, K.M., Sack, W.O., Wensing, C. J. G. 1999. Anatom´ıa Veterinaria. McGraw-Hill Interamericana, M´exico. 178-199

Dym, M. and Fawcett, D.W. 1970. The blood-testis barrier in the rat and the physiological compartmentation of the seminiferous epithelium. *Biology of Reproduction* 3: 308 – 326.

Eddy E. M., Washburn T. F., Bunch D. O., Goulding E. H., Gladen B. C., Lubahn D. B and Korach K. S 1996 Targeted disruption of the estrogen receptor gene in male mice causes alteration of spermatogenesis and infertility. *Endocrinology* 137: 4796–4805. (doi:10.1210/en.137.11.4796)

El-Alfy, M., Pelletier, G., Hermo, L.S., Labrie, F. 2000. Unique features of the basal cells of human prostate epithelium. *Microscopic Research Techniques*. 51: 436–446.

Ellem S. J and Risbridger G. P. 2009. The dual, opposing roles of estrogen in the prostate. *Steroid Enzymes and Cancer* 1155: 174-86.

Emmanuella, N. V and Emmanuella, M. A. (2002): Alcohol and the Male reproductive system. *NIAAA Research Monograph No. 25*, Bethesda, MD: National Institute on Alcohol Abuse and Alcoholism. 282–287

Engeland A., Tretli S., Hansen S and Bjorge T 2007. Height and body mass index and risk Lymphohematopoietic Malignancies in two million Norwegian men and women. *American Journal of Epidemiology*, 165 .1: 44-52.

English, H.F. and Dym, M. 1981. The time required for materials injected into the rete testis to reach points in the caput epididymidis of the rat and observations on the absorption of cationic ferritin. *Annals of New York Academy of Sciences* 383: 445 – 446.

Ezeasor, D.N. 1986. Ultrastructural observations on the terminal segment epithelium of the seminiferous tubule of West African dwarf goats. *Journal of Anatomy* 144: 167 – 179.

Fargeix, N., Didier, E. and Didier, P. 1981. Early sequential development in avian gonads: An ultrastructural study using selective glycogen labeling in the germ cells. *Reproduction, Nutrition and Development* 21: 479-496

Farrell G. C., Koltai A and Murray M. 1988. Sources of raised serum estrogen in male rat with portal by-pass. *J. Clin Invest.* 81: 221-228

Fawcett D. W, Neaves W. B and Flores M. N. 1973. Comparative observations on intertubular lymphatic and the organization of the interstitial tissue of the mammalian testis. *Biology of Reproduction.* 9: 500 -532

Fawcett, D.W and Burges, M.H. 1956. Ciba Foundation College on Ageing. 2: 86-98

Fawcett, D.W and Dym, M. 1974. A glycogen-rich segment of the tubuli recti and proximal portion of the rete testis in the guinea pig. *Journal of Reproduction and Fertility* 38: 401 – 409.

Fawcett, D.W. 1975. Ultrastructure and function of the Sertoli cell. In R.O.Greep (ed.) *Handbook of Physiology*. Section 7, Volume 5. Williams and Wilkins. Baltimore. 21 – 55

Fawcett, D.W. 1981 The Cell, second edition. W.B. Saunders Company, Philadelphia, London, Toronto. 862

Fixemer, T, Remberger K and Bonkhoff H. 2003. Differential expression of the estrogen receptor beta (ERbeta) in human prostate tissue, premalignant changes, and in primary, metastatic, and recurrent prostatic adenocarcinoma. *Prostate* 54**:** 79–87.

Flickinger C. J. 1975. Fine structure of the rabbit epididymis and vas deferens after vasectomy. *Biology of Reproduction* 13: 50-60.

Flickinger, C.J. 1977. The influence of anti-fertility agents on the fine structure of the male reproductive tract. In: Male reproductive system, R. Yates and M. Gordon, Eds. New York, Masson, Publishers 57 – 78.

Flickinger, C.J. and Fawcett, D.W. 1967. The Junctional specifications of the Sertoli cells in the seminiferous epithelium. *Anatomical Record* 158: 207 – 222.

Flickinger, C.J., Howards, S.S and English, H.F. 1978. Ultrastructural differences in efferent ducts and several regions of the epididymis of hamster. *American Journal of Anatomy* 152: 557-586

Foote R. H., Swierstra E. E and Hunt W. L. 1972. Spermatogenesis in the dog *Anatomical Record* 173: 341–350.

Fox, R.R 1987. Taxonomy and genetics. In: Weisbroth, S.H., Flatt, R.E. and Kraus, A.L. (editors). The biology of laboratory rabbit, Academic Press Incorporated. Orlando, Florida. 1 – 22.

França L. R, and Godinho C. L. 2003. Testis morphometry, seminiferous epithelium cycle length, and daily sperm production in domestic cats (*Felis catus*). *Biology of Reproduction* 68: 1554 -1561.

França L. R. and Russell L. D 1998. The testis of domestic mammals. In: Martínez-Garcia F, Regadera J, eds. *Male Reproduction.* Spain: Churchill Communications Europe España: 197 -219.

França L. R., Avelar, G. F and Almeida F. F. L. 2005. Spermatogenesis and sperm transit through the epididymis in mammals with emphasis on pigs. *Theriogenology* 63.2: 300-318.

França L. R.., Becker-Silva S. C. and Chiarini-Garcia H. 1999. The length of the cycle of seminiferous epithelium in goats (*Capra hirais*). *Tissue Cell* 31: 274-280

França, L. R 1992. Daily sperm production in Piau boars estimated from Sertoli cell population and Sertoli cell index. In: *Proceedings of the 12th International Congress on Animal Reproduction and Artificial Insemination,* The Hague; 4: 1716-1718

Frandson, R.D. 1974. Anatomy and Physiology of Farm animals 2nd ed. Library of Congress Cataloging in Publication Data. 348 – 359.

Frank L. A., Rohrbach B. W., Bailey E.M., West J. R and Oliver J. W. 2003. Steroid hormone concentration profiles in healthy intact and neutered dogs before and after cosyntropin administration. *Domestic Animal Endocrinology* 24: 43-57

Fuentes, L. B., Calvo, J. C., Charreau, E. H and Guzm´an, J. A 1993. Seasonal variations in testicular LH; FSH, and PRL receptors; in vitro testosterone production; serum testosterone concentration in adult male vizcacha (*Lagostomus maximus maximus*). *Biology of Reproduction* 47: 133–141.

Fuentes, L. B., Caravaca, N., Pelzer, L. E., Scardapane, L. A., Piezzi, R. S and Guzm´an, J. A 1991 Seasonal variations in the testis and epididymis of vizcacha (*Lagostomus maximus maximus*). *Biology of Reproduction* 45: 493–497.

Gaytan F, Lucena M.C, Muñoz E, Paniagua R. 1986. Morphometric aspects of rat testis development. *Journal of Anatomy* 145: 155 -159.

Gayton, F., Bellido C., Aguilar, E. and van Rooijen, N. 1994 Requirement for testicular macrophages in Leydig cell proliferation and differentiation during prepubertal development in rats. *Journal of Reproduction and Fertility* 102: 393 – 399

.

Genaro G., Moraes W., Silva J. C.R., Adania C. H, Franci C. R. 2007. Plasma hormones in neotropical and domestic cats undergoing routine manipulations. *Research in Veterinary Science* 82: 263 – 270

Gendt D. K., Swinnen J. V., Saunders P. T. K., Schoonjans L., Dewerchin M., Devos A., Tan K., Atanassova N., Claessens F., Lecureuil C., Heyns W., Carmeliet P., Guillou F., Sharpe R. M and Verhoeven G 2004. A Sertoli cell-selective knockout of the androgen receptor causes spermatogenic arrest in meiosis, *Proc. Natl. Acad. Sci.* 101: 1327–1332

Ghana Export Promotion Council (GEPC) 1995. Report on comparison of export performance of non-traditional products for the period of January to December 1993 and 1994.

Ghodesawar M. A. G, Ahamed R. N and Aladakatti R. H. 2004. Ultrastructural changes in prostate gland and vas deferens induced by *Azadirachta indica* leaves in Albino rat. *Journal of natural remedies.* 4.2:160-168

Ghosh S., Sinha-Hikim A. P and Russell L. D. 1991. Further observations of stage-specific effects seen after short-term hypophysectomy in the rat, *Tissue Cell* 23: 613–630

Gier H.M and Marion G.B 1969 Development of mammalian testes and genital ducts. *Biology of Reproduction* 1: 1–23

Glauert, A. M. 1972. Practical methods in electron microscopy. Vol. 1 – 17. Amsterdam: North Holland.

Glover T. D and Nicander L. 1971. Some aspects of Structure and Function in mammalian Epididymis. *Journal of Reproduction and. Fertility* (Suppl.) 13: 39-50

Gomendio, M., Martin-Coello, J., Crespo, C., Magaña, C. and Roldan, E.R.S 2006. Sperm competition enhances functional capacity of mammalian spermatozoa. *Proc Natl Acad Sci USA* 103: 15113–15117

Gordon, M. 1969. Localisation of the 'apical body' in guinea pig and human spermatozoa with phosphotungstic acid. *Journal of Reproduction and. Fertility* 19: 367-370.

Gottreich A., Zuri I., Barel S., Hammer I and Terkel J. 2000. Urinary testosterone levels in the male blind mole rat (*Spalax ehrenbergi*) affect female preference. *Physiology and Behavior.* 3: 309–315.

Goyal H. O and Williams C. S. 1991. Regional differences in the morphology of the goat epididymis: a light mycroscope and ultrastructural study. *American Journal of Anatomy* 190: 349–369.

Goyal H. O. 1985. Morphology of the bovine epididymis. *American Journal of Anatomy* 190. 172: 155–172.

Goyal H. O. 1989 Application of regional differences in sperm concentration in predicting absorptive and secretory function of the epididymis in the goat. *Anatomia Histolologia Embryologia* (abstr. In press).

Goyal H. O., Braden T. D., Williams C. S and Williams J. W. 2007. Role of estrogen in induction of penile dysmorphogenesis: a review. *Reproduction* 134: 199–208. [PubMed: 17660230]

Goyal, H.O. and Hrudka, F. 1981. Ductuli efferentes of the bull – a morphological, experimental and developmental study. *Andrologia* 13: 292 – 306.

Goyal, H.O., Hutto, V. and Robinson, D. D. 1992. Reexamination of the morphology of the extratesticular rete and ductuli efferentes in the goat. *The Anatomical Record* 233: 53 – 60.

Gray, B.W., Brown, B.G., Ganjam, V.K. and Whitesides, J.F. 1983. Effect of deprival of the rete testis fluid on the morphology of efferent ducts. *Biology of Reproduction* 29: 525 – 534

Groos, S., Wilhelm, B., Renneberg, H., Riva, A., Reichelt, R., Seitz, J., Aum¨uller, G. 1999. Simultaneous apocrine and merocrine secretion in the rat coagulating gland. *Cell Tissue Research*. 295: 495–504.

Gupta A.N. and Singh Y. 1982. Histological and histochemical studies on the bulbourethral glands of normal and castrated goats. *Indian Journal of Animal Science*. 52:758–763.

Guttroff, R.F., Cooke, P.S. and Hess, R.A. 1992. Blind-ending tubules and branching patterns of the rat ductuli efferentes. *The Anatomical Record* 232: 423–431

Hafez, E.S.E and Spring-Mills E. 1979. Accessory glands of the male reproductive tract. In: *Perspective in Human Reproduction*. 1st edition Ann Arbor Science Publisher Michigan. 40-49.

Hafez, E.S.E. 1980. Reproduction in Farm Animals. Lea and Feibger. Philadelphia.

Hafez, E.S.E. 1987. Reproductive cycles. In: Reproduction in Farm Animals. 5th edition Lea and Febiger. Philadelphia. 107-129.

Hagenas L. 1977. Sertoli cell regulation of spermatogenesis. Ph.D. thesis, Stockholm. Pp 9 – 17.

Hagenas, L. and Ritzen, E.M. 1976. Impaired Sertoli functions in experimental cryptorchidism in the rat. *Molecular and cell Endocrinology* 98: 918 – 921.

Hahnel, A.C and Eddy, E.M. 1986. Cell surface markers of mouse primodial germ cells defined by two monoclonal antibodies. *Gamete Research*, 15: 918-921

Hamilton S. W and Cooper T. G 1978. Gross histological variations along the length of the rat vas deferens. *The Anatomical Record* 190: 795-810.

Hamilton, D.W. 1971. Steriod function in the mammalian epididymis. *Journal of Reproduction and Fertility*. (Suppl.) 13: 89-97

Hamilton, D.W. 1975. Structure and function of the epithelium lining the ductuli efferentes, ductus epididymidis and ductus deferens in the rat. In: Handbook of Physiology. Section 7, Vol. V American Physiological Society, Washington D.C. 259 -301.

Handelsman D. J and Staraj S. 1985. Testicular size: the effects of aging, malnutrition, and illness. *Journal of Andrology* 6:144-151.

Hannema S .E and Hughes, I. A. 2007. Regulation of Wolffian duct development. *Hormone Research* 67 .3: 142-151

Hansson, V., Weddington, S.C., French, F.S., Mclean, W., Smith, A., Nayfeh, S.N., Ritzen, E.M. and Hagenas, L. 1976. Secretion and role of androgen binding proteins in the testis and epididymis. *Journal of Reproduction and Fertility* 24: 17 – 33.

Hargrove, J.L., Mc Indoe, J.H. and Ellis, L.C. 1977. Testicular contractile cells and sperm transport. *Fertility and Sterility* 38: 1146 – 1157.

Harmelin A, Danon T, Kela I and Brenner O. 2005. Biopsy of the mouse prostate. *Laboratory Animals* 39: 215–220

Hasan, M.H., Singh, D.R. and Glees, P. 1974. Diagnostic histology In: The Male reproductive system. 1st Ed. Anita Prakashan, Lucknow, India: 300-01.

Hawkins, W. E and Geuze, J. J. 1977. Secretion in the rat coagulating gland (Anterior prostate) after copulation. *Cell and Tissue Research* 181: 519-529

Hayashi, N., Y. Sugimura, J. Kawamura, A. Donjacour, and G. Cunha, 1991. Morphological and functional heterogeneity in the rat prostatic gland. *Biology of. Reproduction* 45, 308–321.

Hayward, S.W., Brody, J.R., Cunha, G.R. 1996. An edgewise look at basal epithelial cells: three-dimensional views of the rat prostate, mammary gland and salivary gland. *Differentiation* 60: 219– 227

Hees, H., Wrobel, K.-H., Kohler, T., Abou Elmagd, A. and Hees, I. 1989. The mediastinum of the bovine testis. *Cell and Tissue Research* 255: 29 – 39.

Hees, H., Wrobel, K.-H., Kohler, T., Leiser, R. and Rothbacher, I. 1987. Spatial topography of the excurrent duct system in the bovine testis. *Cell and Tissue Research* 248: 143 – 151.

Hermo L and Papp S 1996. Effects of ligation, orchidectomy, and hypophysectomy on expression of the Yf subunit of GST-P in principal and basal cells of the adult rat

epididymis and on basal cell shape and overall arrangement. *The Anatomical Record* 244: 59–69.

Hermo L. and Dworkin, J. 1988. Transitional cells at the junction of seminiferous tubules with the rete testis of the rat: their fine structure, endocytic activity and basement membrane. *American Journal of Anatomy* 181: 111 – 131.

Hermo L., Adamali H. I and Andonian S. 2000. Immunolocalization of CA II and Hþ V-ATPase in epithelial cells of the mouse and rat epididymis. *Journal of Andrology*; 21: 376–391.

Hermo L. 1995.Structural features and functions of principal cells of the intermediate zone of the epididymis of adult rats. *The Anatomical Record* 242: 515-530

Hermo L., Chong D. L., Moffatt P., Sly W.S., Waheed A. and Smith, C.E. 2005. Region – and cell – specific differences in the distribution of carbonic anhydrases II, III, XII, and XIV in the adult rat epididymis. *The Journal of Histochemistry and Cytochemistry*, 53 .6: 699-713

Hermo L., Dworkin J and Oko R 1988. Role of epithelial clear cells of the rat epididymis in the disposal of the contents of cytoplasmic droplets detached from spermatozoa. *American Journal of Anatomy* 183: 107–124.

Hermo L., Oko R and Morales C. R. 1994. Secretion and endocytosis in the male reproductive tract: a role in sperm maturation. *Int. Rev. Cytol* 154: 106–189

Hess R. A and Bassily N. 1988. Structure of the ductuli efferentes in the dog. *J Vet Med C* 17:85. Abstract

Hess R. A. 1990. Quantitative and qualitative characteristics of the stages and transitions in the cycle of the rat seminiferous epithelium: light microscopic observations of perfusion-fixed and plastic-embedded testes. *Biology of Reproduction* 43: 525-542.

Hess R. A., Cooke P. S., Bunick D and Kirby J. D. 1993. Adult testicular enlargement induced by neonatal hypothyroidism is accompanied by increased Sertoli cell and germ cell number. *Endocrinology*. 132: 2607 -2613.

Hess R.A., Zhou Q., Nie R., Oliveira C., Cho H., Nakai M and Carnes K. 2001. Estrogens and epididymal function. *Reprod Fertil Dev* 13: 273– 283.

Hess, R. A. & Carnes, K. 2004. The role of estrogen in testis and the male reproductive tract: a review and species comparison. *Animal Reproduction* 1: 5–30.

Hess, R. A. 2003. Estrogen in the adult male reproductive tract: A review. *Reproductive Biology and Endocrinology* 1: 52

Hess, R. A. and Moore, B. J. 2001 Histological Methods for Evaluation of the Testis and Perfusion techniques in Rat. S. Lincoln, Urbana-Champaign, Illinois 217/333-8933. 1-38

Hess, R. A., Schaeffer, D. J., Eroschenko V. P. and Keen J. E. 1990. Frequency of the stages in the cycle of the seminiferous epithelium in the rat. *Biology of Reproduction* 43**:** 517 -24

Heyns C. F., Human H.J., Werely C.J., DeKlerk D.P (1990): The glycosaminoglycans of the gubernaculum during testicular descent in the fetus. *Journal of Urology* 143: 612–617

Heyns C.F (1987): The gubernaculum during testicular descent in the human fetus. *Journal of Anatomy* 153: 93–112.

Hinton, B.T.; Galdamez, M.M.; Sutherland, A.; Bomgardner, D.; Xu, B.; Abdel-Fattah, R. and Yang, L. 2011. How Do You Get Six Meters of Epididymis Inside a Human Scrotum? *Journal of Andrology*, In press,

Hinton, B.T and Turner, T.T. 2003. Third International Conference on the Epididymis. Van Doren Press, Charlottesville.

Hoffer A. P and Karnovsky M. L 1981. Studies on zonation in the epididymis of the guinea pig. I. ultrastructural and biochemical analysis of the zone rich in large lipid droplets (zone II). *The Anatomical Record* 201: 623-633

Hoffer, A.P. and Greenberg, J. 1978. The structure of the epididymis, efferent ductules and ductus deferens of the guinea-pig: A light microscope study. *The Anatomical Record* 190: 659-677.

Holstein A. F 1969. Morphologische studien am Nebenhoden des Menschen. Zwanglose Abhandl. *Gebiet Norm. Pathol. Anat*, 20: 1-91

Holtz, W.H. 1972. Structure, function and secretions of reproductive organs in the male rabbit. Ph.D Thesis, Cornell University, U.S.A. 13-27

Hughes I. A and Acerini C. L. 2008. Factors controlling testis descent *European Journal of Endocrinology* 159: 75–82

Hughes, S. W. 2005. Archimedes revisited: a faster, better, cheaper method of accuratel measuring the volume of small objects. *Phys Educ* 40**:** 468

Hutson, J. M., Hasthorpe, S and Heyns, C.F 1997. Anatomical and Functional Aspects of Testicular Descent and Cryptorchidism. *Endocrine Reviews* 18 .2: 259-280

Ichihara I., Kawamura H and Pelliniemi L. J. 1993. Ultrastructure and morphometry of testicular Leydig cells and the interstitial components correlated with testosterone in aging rats, *Cell Tissue Research* 271: 241–255.

Ichihara, I. and Pelliniemi, L. J. 2007. Morphometric and Ultrastructural analysis of stage specific effects of Sertoli and spermatogenic cells seen after testosterone treatment on young adult rat testis, *Annals of Anatomy*. 189: 413–426

Ilio, K.Y. and Hess, R.A. 1994. Structure and function of the ductuli efferentes: a review. *Microscopy Research and Technique* 29: 432 – 467.

Jaszczak K., Sysa P., Romanowicz K., Boryczko Z., Parada R., Sacharczuk M., Witkowski M., Kawka M and Horbańczuk K. 2010. Cytogenetic, histological, hormonal and semen studies in male goats with developed udders. *Animal Science Papers and Reports,* 28 .1: 71-80

Jejuna, H.S., Karanth, S., Dutt, P. and Meherjee, P. 1991. Diurnal variation and temporal coupling of bioactive and immunoactive luteinizing hormone, prolactin, testosterone and 17β estradiol in adult men. *Hormone Research* 35: 89–94.

Jequier, A. M. 1995. Clinical disorders affecting semen quality. In: Yovich, J.L. (Ed.), Gametes—TheSpermatozoon. University Press, Cambridge 175–191.

Jesik, C., J. Holland, and C. Lee 1982. An anatomic and histologic study of the rat prostate. *Prostate* 3: 81–97

Jeyakumar S. M, Lopamudra P, Padmini S, Balakrishna N, Giridharan N. V and Vajreswari A. 2009. Fatty acid desaturation index correlates with body mass and adiposity indices of obesity in Wistar NIN obese mutant rat strains WNIN/Ob and WNIN/GR-Ob. *Nutrition & Metabolism* 6:27 doi:10.1186/1743-7075-6-27

Jiang, F.X., Temple-Smith, P., Wreford, N.G. 1994. Postnatal differentiation and development of the rat epididymis: a stereological study. *The Anatomical Record* 238. 191–198.

Johnson L. 1995. Efficiency of spermatogenesis. *Microsc Res Tech.* 32: 385 -422.

Jones R., Hamilton D. W and Fawcett D. W. 1979. Morphology of the epithelium of the extratesticular rete testis, ductuli efferentes and ductus epididymis of the adult male rabbit. *American Journal of Anatomy* 156: 373-400.

Jones, R.C. 1980. Luminal composition and maturation of spermatozoa in the genital ducts of the African elephant, *Loxodonta africana. Journal of Reproduction and Fertility* 60: 87 – 93.

Jones, R.C. 1988. Evolution of the vertebrate epididymis. *Journal of Reproduction and Fertility*, Supplement 53: 161 – 181.

Joseph, A., Shur, B. D. and Hess, R. A. 2011. Estrogen, Efferent Ductules, and the Epididymis. *Biology of Reproduction* 84. 207–217

Joseph, A., Yao, H., and Hinton, B.T 2009. Development and morphogenesis of the Wolffian/Epididymal duct, more twists and turns. *Developmental Biology* 325**:** 6-14.

Jost, A. 1953. Problems of fetal endocrinology: the gonadal and hypophyseal hormones. *Rec. Prog. Horm. Res*. 8: 379–418.

Kalra P.S and Kalra S.P 1977. Circadian periodicities of serum androgen, progesterone, gonadotropins and luteinizing hormone-releasing hormone in male rat: The effect of deafferentation, castration and adrenalectomy. *Endocrinology* 10 (16): 1821-1827

Kalra, P. S. and Kalra. S. P. 1979. Regulation of gonadal steroid rhythms in rats. *Journal of Steroid and Biochemistry* 11: 981–987.

Kennedy S. W and Heidger Jr., P. M. (1979): Fine structural studies of the rat vas deferens. *The Anatomical Record* 194: 159-180.

Khaki A., Fathiazad F., Nouri M., Khaki A. A., Ozanci C.C., Ghafari-Novin M., Hamadeh M. 2009. The effects of Ginger on spermatogenesis and sperm parameters of rat. *Iranian Journal of Reproductive Medicine* 7.1: 7-12

Khan, A.A., Zaidi, M.T and Faruqi, N.A. 2003. Ductus deferens- a comparative histology in mammals, *J. Anat. Soc. India* 52. *2.* 163 – 165.

Kianifard D., Sadrkhanlou R. A. and Hasanzadeh S. 2012. The Ultrastructural Changes of the Sertoli and Leydig Cells Following Streptozotocin Induced Diabetes. *Iranian Journal of Basic Medical Sciences* 15: 623-635

Kotula-Balak, M., Gancarczyk, M., Sadowska, J. and Bilinskai, B. (2005): The expression of aromatase, estrogen receptor alpha and estrogen receptor beta in mouse Leydig cells in vitro that derived from cryptorchid males. *European Journal of Histochemistry*. 49: 59–62.

Kumar V. L and Majumder P. K 1995. Prostate gland: Structure, Functions and Regulations. *Int.Urol and Nephrol*. 27.3: 231-243

Kurita, T., Medina, R. T., Mills, A. A. and Cunha, G. R. 2004. Roles of p63 and basal cells in prostate. *Development* 131: 4955-4964.

Lambard, S., Galeraud-Denis, I., Saunders, P. T. and Carreau, S. 2004. Human immature germ cells and ejaculated spermatozoa contain aromatase and oestrogen receptors. *Journal of Molecular Endocrinology* 32: 279–289. (doi:10.1677/jme.0.0320279)

Larios, H.M and Mendoza, N.M. 2001. Onset of sex differentiation. Dialog between genes and cells. *Archives of Medical Research,* 32 .6: 553-558

Larsson, K., Einarsson, S., Nicander, L. 1976. Influence of thawing diluents on vitality, acrosome morphology, ultrastructure and enzyme release of deep frozen boar spermatozoa. *Acta Vet. Scand.* 17: 83–100

.

Lasnitzki, I. and Mizuno, T. 1977. Induction of the rat prostate gland by androgens in organ culture. *Journal of Endocrinology* 74: 47–55.

Lasserre, A., Barrozo, S., Tezón, J. G.,Miranda, P. V and Vazquez-Levin, M. H. 2001. Human epididymal proteins and sperm function during fertilization: an update. *Biological Research,* 34 .3-4: 165-178

Lazari, M.F.M., Lucas, T.F.G., Yasuhara, F., Gomes, G.R.O., Siu, E.R., Royer, C., Sheilla Alessandra Ferreira Fernandes, S.A. F. and Porto., C.S. 2009. Estrogen receptors and function in the male reproductive system *Arq Bras Endocrinol Metab*.; 53.8:923-933

Leal M. C., Cardoso, E. R., Nobrega, R. H., Batlouni, S. R., Bogerd, J., França, L. R. and Schulz, R. W. 2009. Histological and stereological evalution of the Zebrafish (*Danio rerio*) spermatogenesis with an emphasis on spermatogonial generation. *Biology of Reproduction* 81: 177-187

Leblond, C.P and Clermont, Y. 1952. Definition of the stages of the cycle of the seminiferous epithelium in the rat. *Ann NY Acad Sci* 55: 548 – 573.

Lee V. W. K., De Kretser M., Hudson D. M. B and Wang, C. 1975. Variations in Serum FSH, LH and Testosterone levels in male rats from birth to sexual maturity. *Journal of Reproduction and Fertility* 42: 121-126

Lemasters G.K., Perreault S.D., Hales B.F., Hatch M., Hirshfield A.N., Hughes C.L., Kimmel G.L., Lamb J.C., Pryor J.L., Rubin C. and Seed J.G. 2000. Workshop to identify critical windows of exposure for children's health: reproductive health in children and adolescents work group summary. *Environ Health Perspective*. 108.Suppl 3: 505–509.

Leong S. K. and Singh G. 1990. Ultrastructure of the monkey vas deferens. *Journal of Anatomy* 171: 93-104.

Leydig, F. 1850. Zur anatomia der mannlichen Geschlechtsorgane und Analdrusen der Saugetiere. Z. wiss. *Zool*. 2

Ljungvall K.., Veeramachaneni D. N., Hou M., Hulte´n F and Magnusson U. 2008. Morphologyand morphometry of the reproductive organs in prepubertal and

postpubertal male pigs exposed to di(2-ethylhexyl) phthalate before puberty: precocious development of bulbourethral glands. *Theriogenology* 70: 984–991.

Lofstedt R.M., Laarveld B and Ihle S.L. 1994. Adrenal neoplasia causing lactation in a castrated male goat. *Journal of Veterinary Internal Medicine*, 8: 382-384.

Lok D., Weenk D and De Rooij D. G. 1982. Morphology, proliferation and differentiation of undifferentiated spermatogonia in the Chinese hamster and the ram. *The Anatomical Record* 203: 83-99.

Longcope, C., Goldfield, S.R.W., Brambilla, D.J and McKinlay, J. 1990. Androgens, oestrogens and sex hormone-binding globulin in middle aged men. *Journal of Clinical Endocrinology and Metabolism* 71:1442–1446.

Lu, Y. D, Li, Y., Bi, Z. W., Yu, H. M and Li, X. J. 2008. Expression and immunolocalization of Aquaporin-1 in male reproductive organs of the mouse. *Anatomia, Histologia, Embryologia*. 37: 1-8

Lucas, T. F., Siu, E. R., Esteves, C. A., Monteiro, H. P., Oliveira, C. A., Porto, C. S. and Lazari, M. F. 2008. 17beta-estradiol induces the translocation of the estrogen receptors ESR1 and ESR2 to the cell membrane, MAPK3/1 phosphorylation and proliferation of cultured immature rat Sertoli cells. *Biology of Reproduction*. 78, 101–114. (doi:10.1095/biolreprod.107.063909)

Luetjens, C. M., Didolkar, A., Kliesch, S., Paulus, W., Jeibmann, A., Bocker, W., Nieschlag, E. and Simoni, M. 2006. Tissue expression of the nuclear progesterone receptor in male non-human primates and men. *Journal of Endocrinology* 189: 529–539.

Luke M and Coffey D. 1994. The male sex accessory tissue. Structure, androgen, action, and physiology. In: Knobil E, Neil J, editors. The physiology of reproduction. New York: Raven Press. 1435–1487

Lumpkin, M., Negro-vilar, A., Franchimont, P. and McCann, S. 1981. Evidence for a hypothalamic site of action of inhibin to suppress FSH release. *Endocrinology*, 108: 1101 – 1104.

MacDonald A. A., Herbison G. P., Showell M, and C.M. Farquhar C. M. 2010. The impact of body mass index on semen parameters and reproductive hormones in human males: a systematic review with meta-analysis. *Human Reproduction Update* 16 .3: 293–311

Machado-Junior, A. A. N., Assis Neto, A. C., Sousa Junior, A., Menezes, D. J. A., Alves, F. R., Sousa, A. L. and Carvalho, M. A. M. 2011. Daily sperm production and testicular

morphometry in goats according to external scrotal conformation. *Animal Reproduction Science*, doi:10.10.1016/j.anireprosci.2011.06.008

Makinen, S., Makela, S., Weihua, Z., Warner, M., Rosenlund, B., Salmi, S., Hovatta, O. and Gustafsson, J. K. 2001. Localization of oestrogen receptors alpha and beta in human testis. *Molecular Human Reproduction* 7: 497–503. (doi:10.1093/molehr/7.6.497)

Man, S.Y., Clulow, J., Hansen, L. A. and Jones, R.C. 1997. Adrenal independence of fluid and electrolyte reabsorption in the ductuli efferentes testis of the rat. *Experimental Physiology* 82: 283 – 290.

Maneely, R.B. 1959. Epididymal structure and function: a historical and critical review. *Acta Zool.* 40. 1–21

Marengo S. R and Amann R. P. 1990. Morphological features of principal cells in the ovine epididymis: a quantitative and qualitative study. *Biology of Reproduction* 42: 167–179.

Marty, M.S., Chapin, R. E., Parks, L.G., Thorsrud, B.A. 2003. Development and maturation of the male reproductive system. *Birth defect research* (Part B) 68: 125-136.

Massanyi, P., Jancova, A. and Uhrin, V. 2003. Morphometric study of male reproductive organs in the rodent species *Apodemus sylvaticus and Apodemus flavicollis, Bull. Vet. Inst. Pulawy* 47**:** 133 – 138.

Mata, L.R. 1995. Dynamics of the seminal vesicle epithelium. *Int. Rev. Cytol*. 160: 267–302.

Matsumoto T., Takeyama K.., Sato T and Kato S. 2005. Study of androgen receptor functions by genetic models. *Journal of Biochemistry* 138: 105–110. (doi:10.1093/jb/mvi118)

McGreevy P. D., Thomson P. C., Pride C., Fawcett A., Grassi T and Jones B. 2005. Prevalence of obesity in dogs examined by Australian veterinary practices and the risk factors involved. *Veterinary Record* 156**:** 695-702

McNeal J. E. 1981. The zonal anatomy of prostate. *Prostate.* 2: 35-49.

Melo, S. R., Melo-Jr, W., Garcia, P. J and Cagnon, V.H.A. 1997. Ultrastructural study of the coagulating gland epithelium of the rat (*rattus norvegicus*) after vasectomy. *Rev.Chil. Anat*. 15. doi: 10.4067/S0716-98681997000200008

Mendeş M, Dinçer E and Arslan E. 2007. Profile Analysis and Growth Curve for Body Mass Index of Broiler Chickens Reared Under Different Feed Restrictions in Early Age *Arch. Tierz., Dummerstorf* 50 .4: 403-411

Mendis-Handagama S. M., Zirkin B. R., Scallen T. J and Ewing L. L. 1990. Studies on perioxisomes of adult rat Leydig cell *Journal of Andrology* 11: 270–278

Merchant-Larios, H. 1979. Origin of the somatic cells in the rat gonad: An auto-radiographic approach. *Annals of Biology, Animal Biochemistry and Biophysics*, 19: 1219 – 1229.

Min, T. and Lee, K. 2010. The Roles of Estrogens in the Efferent Ductules of the Male Reproductive System: A Review. *Asian-Aust. J. Anim. Sci*. 23 .8: 1118 - 1126

Mollineau W M., Adogwa, A O. and Garcia G W. 2009. The gross and micro anatomy of the accessory sex glands of the male agouti (Dasyprocta leporina). *Anatomia Histologia Embryologia* 38: 204–207.

Møller, A.P. 1989. Ejaculate quality, size and sperm production in mammals. *Functional Ecology* 3: 91 – 96.

Moore, K .L and Persaud T.V.N. 2003. Urogenital System. In: *The Developing Human: Clinical Oriented Embryology*, Saunders Elsevier, (Ed.):Pp. 246-285, Elsevier, ISBN: 978-85-

Morales, C. and Hermo, L. 1983. Demonstration of fluid-phase endocytosis in epithelial cells of the male reproductive system by means of horseradish peroxidase-colloidal gold complex. *Cell and Tissue Research* 230: 503 – 510.

Mori H and Christensen A.K. 1980. Morphometric analysis of Leydig cells in normal rat testis. *Journal of Cellular Biology* 84: 340-354

Mori H., Hiromoto N., Nakahara M and Shiraishi T 1982. Stereological analysis of Leydig cell ultrastructure in aged human. *J. Clin. Endocrinol Metab*. 55: 634-641

Morita, J. 1966. Some observations on the fine structure of the human ductuli efferentes testis. *Archivum Histologicum Japonicum* 26: 341 – 365.

Mukerjee B and Rajan T. 2006. Morphometric Study of Seminal Vesicles of Rat in Normal Health and Stress Conditions. *J.Anat.Soc. India* 55 .1 : 31-36.

Muller J. and Skakkebaek, N.E. 1992. The prenatal and postnatal development of the testis. *Bailliere's Clin Endo Metab* 6: 251–271.

Muńoz, E.M., Fogal, T., Dominguez, S., Scardapane L., Guzma N. J., Cavicchia J. C and Piezzi R. N S. 1998. Stages of the cycle of the seminiferous epithelium of the Viscacha (*Lagostomus maximus maximus*). *The Anatomical Record* 252**:** 8-16.

Murakami, M., Yokoyama, R. 1989. SEM observations of the male reproductive tract with special reference to epithelial phagocytosis. *Prog. Clin. Biol. Res.* 296: 207–214.

Mutembei, H., Pesch, S., Schuler, G. and Hoffmann, B. 2005. Expression of oestrogen receptors alpha and beta and of aromatase in the testis of immature and mature boars. *Reproduction of Domestic Animals*. 40: 228–236. (doi:10.1111/j.1439-0531.2005.00586.x)

Neaves, W.B. 1975. Leydig cells. *Contraception* 11: 571 – 606.

Neves E. S.,Chiarini-Garcia H., França L. R. 2002. Comparative testis morphometry and seminiferous epithelium cycle length in donkeys and mules. *Biology of Reproduction* 67: 247 -255.

Ng K and Shih-Wei L. 2004. Application of anthropometric indices in Childhood obesity. *Southern Medical Journal* 97.6: 566-570

Nicander, L. 1957. On the regional histology and cytochemistry of the ductus epididymis in rabbits. *Acta Morph. Neerl-Scand*. 1: 99-118.

Nie, R., Zhou, Q., Jassim, E., Saunders, P. T. & Hess, R. A. 2002. Differential expression of estrogen receptors alpha and beta in the reproductive tracts of adult male dogs and cats. *Biology of Reproduction* 66: 1161–1168. (doi:10.1095/biolreprod66.4.1161)

Nijland M. L., Stam F and Seidell J. C. 2009. Overweight in dogs, but not in cats, is related to overweight in their owners. *Public Health Nutrition* 13.1: 102–106

Nistal M., Santamaria L and Ricardo Paniagua R. 1992. The ampulla of the ductus deferens in man: morphological and ultrastructural aspects. *Journal of Anatomy* 180: 97-104.

Niu, Y. J., T. X. Ma, J. Zhang, Y. Xu, R. F. H and Sun G. 2003. Androgen and prostatic stroma. *Asian Journal of Andrology* 5: 19–26.

Notides A. C and Williams-Ashman H. G. 1967. The basic protein responsible for clotting of guinea-pig semen Proceedings of the National Academy of Sciences of the USA 58 1991-2022

Novelli, E. L. S., Diniz, Y. S., Galhardi, C. M., Ebaid,G. M. X., Rodrigues, H. G., Mani, F., Fernandes, A. A. H., Cicogna, A. C. and J L V B Novelli Filho, J. L. V. B. (2007): Anthropometrical parameters and markers of obesity in rats. *Laboratory Animals* 41: 111-119

Ntiamoh-Baidu, Y. 1998. Wildlife development plan 1998-2003: Sustainable use of Bushmeat commissioned Wildlife department, Accra ministry of Lands andForestry.

Oakberg E. F. 1956. A description of spermiogenesis in the mouse and its use in analysis of the cycle of the seminiferous epithelium and germ cell renewal. *American Journal Anatomy* 99: 391-414.

Ojeda S.R., Andrews W.W., Advis J.P. and Smith-White S. 1980. Recent advances in the endocrinology of puberty. *Endocrinological Review*. 1: pp 228–257.

Oke B. O and Aire T. A. 1997. The epithelium of the vesicular gland of the African giant rat (*Cricetomys gambianus* Waterhouse): Histology and ultrastructure. *African. Journal of Medicine & Medical Sciences* 26: 69-72

Oke B. O., Aire T. A., Adeyemo O and Heath E 1988. The structure of the epididymis of the giant rat (Cricetomys gambianus, Waterhouse): histological, histochemical and microstereological studies. *Journal of Anatomy* 160: 9-19

Oke, B. O and Aire, T. A. 1996. The coagulating gland of the African giant rat (*Cricetomys gambianus* Waterhouse). *Tropical Veterinarian* 14: 23-29

Oke, B.O. 1988. Some aspects of the reproductive biology of the male African giant rat (Cricetomys gambianus, Waterhouse). Ph.D. Thesis, University of Ibadan.

Oliveira, C. A., Nie, R., Carnes, K., Franca, L. R., Prins, G. S., Saunders, P. T. and Hess, R. A. 2003. The antiestrogen ICI 182,780 decreases the expression of estrogen receptor-alpha but has no effect on estrogen receptorbeta and androgen receptor in rat efferent ductules. *Reproductive Biology & Endocrinology* 1:75. (doi:10.1186/1477-7827-1-75)

Oluwole, O.A. 2008. Effect of cassava peel on the male reproductive system in Wistar rat. MSc. Thesis, University of Ibadan.

Onadeko, S.A. 1996. The reproductive ecology of the Grasscutter (*Thryonomys swinderianus* Temminck) in captivity. Ph.D Thesis, University of Ibadan

Opara, M.N. 2010. The grasscutter I: A livestock of tomorrow. *Res. J. For*. 4: 119-135.

Orsi A. M., De Melo V. R., Ferrerira A. L and Campo V. J. M 1980. Morphology of the epithelial cells of the epididymal duct of the South American Opossum (*Didelphis azarae*). *Anat. Anz*, 148: 7-13

Oud J. L and De Rooij D. G. 1977. Spermatogenesis in the Chinese hamster. *The Anatomical Record* 187: 113-124.

Pala A.; Savaş T., Uğur, F and Daş G 2005. Growth curves of Turkish Saanen Goats' Kids grouped for weight and body mass index. *Arch. Tierz., Dummerstorf* 48 **.**2: 185-193

Pardue, M.L. and Gall, L.G. 1970. Chromosomal localization of mouse. *Satellite DNA Science*, 168: 1356 – 1358.

Parr, M, B., de Franca, L.R., Kepple, L., Ying, L., Parr, E.L andL. D. Russel, L.D. 1994. The urethral glands of male mice in relation to depletion of secretory granules upon mating. *Journal of Reproduction and Fertility* 101: 675-680

Pasquali R., Patton L and Gambineri A. 2007. Obesity and infertility. *Curr Opin Endocrinol Diabetes Obes*. 14:482–487

Patil S. B and Saidapur S. K. 1991. Kinetic of spermatogenesis in wild Squirrel (*Funambulum palmarum* Linnaeus). *Acta Anat*. 141: 352- 363

Patten, B.M. 1959. Embryology of pigs. 3rd Edition, Mcgraw-Hill Book Co. 197 – 226.

Paula T. A. R., Chiarini-Garcia H and França L. R. 1999. Seminiferous epithelium cycle and its duration in capybaras (*Hydrochoerus hydrochaeris*). *Tissue Cell.* 31: 327 -334

Pearl C. A., At-Taras E, Berger T and Roser J. F. 2007. Reduced endogenous estrogen delays epididymal development but has no effect on efferent duct morphology in boars. *Reproduction* 134.4:593-604.

Pelletier, G., Labrie C and Labrie, F. 2000. Localization of oestrogen receptor α, oestrogen receptor β and androgen receptors in the rat reproductive organs. *Journal of Endocrinology* 165**:** 359–370

Pentikainen, V., Erkkila, K., Suomalainen, L., Parvinen, M. and Dunkel, L. 2000 Estradiol acts as a germ cell survival factor in the human testis in vitro. *Journal of Clinical Endocrinology and Metabolism* 85: 2057–2067. (doi:10.1210/jc.85.5.2057

Perkins A and Fitzgerald J. A. 1992. Luteinizing hormone, testosterone, and behavioral response of male-oriented rams to estrous ewes and rams. *Journal Animal Science* 70: 1787-1794

Pholpramool C., Zupp J. L and Setchell B. P. 1985. Motility of undiluted bull epididymal spermatozoa collected by micropuncture. *Journal of Reproduction and Fertility* 75: 413-420

Pierre-point, C. G., Davies, P., Lewis, M.H. and Moffet, A.B. 1975. Examination of the hypothesis that a direct control system exists for the prostate and seminal vesicles. *Journal of Reproduction and Fertility* 35: 149 – 152.

Pochron, S. T.,Wright P.C., Schaentzler, E., Ippolito, M., Rakotonirina, G., Ratsimbazafy, R and Rakotosoa, R. 2002: Effect of Season and Age on the Gonado-somatic Index of Milne Edwards' Sifakas (*Propithecus diadema edwardsi*) in Ranomafana National Park, Madagascar. *International Journal of Primatology*, 23 .2: 355-364

Price D. 1963. Comparative aspects of development and structure in the prostate. NCI *Monograph* 12:1–27

.

Price, D. 1956. Normal development of the prostate and seminal vesicles of the rat with a study of experimental postnatal modifications. *Am. J. Anta*. 60: 79 – 127

Price, D. and Williams-Ashman, H.G. 1961. The accessory reproductive glands of mammals. In: Young, W.C. (ed.). Sex and Internal Secretion. 3rd ed. Williams and Wilkins Co., Baltimore. 336 – 448

Prins G. S and Korach K. S. 2008. The role of estrogens and estrogen receptors in normal prostate growth and disease. *Steroids* 73 .3. 233-44

Prins, G. S. and Putz, O. 2008. Molecular signaling pathways that regulate prostate gland development. *Differentiation* 76: 641-659

Prins, G.S. and Birch, L. 1995. The developmental pattern of androgen receptor expression in rat prostate lobes is altered after neonatal exposure to estrogen. *Endocrinology* 136: 1303–1314.

Prins, G.S., Cooke, P.S., Birch, L., Donjacour, A.A., Yalcinkaya,T.M., Siiteri, P.K. and Cunha, G.R. 1992. Androgen receptor expression and 5a-reductase activity along the proximal-distal axis of the rat prostatic duct. *Endocrinology* 130: 3066–3073

Pucek Z., Jedrzejewski W., Jedrzejewska B., Pucek M. 1993. Rodent population – Dynamics in a primeval deciduous forest (Bialowieza – National-Park) in relation to weather, seed crop, and predation. *Acta Theriologica* 38: 199 – 232.

Pukazhenthi, B. and Wildt D. E. 2004. Which reproductive technologies are most relevant to studying, managing and conserving wildlife? *Reproduction, Fertility and Development.* 16: .33– 46.

Pushkin A., Clark I., Kwon T. H., Nielsen S and Kurtz I. 2000. Immunolocalization of NBC3 and NHE3 in the rat epididymis: colocalization of NBC3 and the vacuolar Hþ-ATPase. *Journal of Andrology* 21: 708–720

Ramos A. S and Dym M. 1977. Fine structure of the monkey epididymis. *American Journal of Anatomy* 149: 501–532.

Recabarren S. E., Rojas-Garcia P. P., Recabarren M. P., Alfaro V. H., Smith R., Padmanabhan V and Sir-Petermann T. 2008. Prenatal testosterone excess reduces sperm count and motility. *Endocrinology* 149: 6444–6448. (doi:10.1210/en.2008-0785)

Reid, B.L. and Cleland, K.W. 1957. The structure and function of the epididymis. In: The histology of the rat epididymis. *Australian Journal of Zoology* 5: 223 – 246.

Rennie P. S, Bouffard R, Bruchovsky N and Cheng H. 1984. Increased activity of plasminogen activators during involution of the rat ventral prostate. *Journal of Biochem istry* 221: 171–178.

Riva, A. and Aum¨uller, G. 1994. Epithelium of the distal portion of the human spermatic pathway: seminal vesicle, ampulla ductus deferentis and ejaculatory duct. In: PM, M. (Ed.), Ultrastructure of the Male Urogenital Glands: Prostate, Seminal Vesicles, Urethral, and Bulbourethral Glands. Kluwer Academic Publishers, New York 35–49.

Robaire B., Hinton B. T and Orgebin-Crist, M. C. 2006. The Epididymis. In: *The physiology of reproduction*, Knobil and J. Neil, (Ed.). 1071-1148, Elsevier, ISBN 978-0-12-515-400, New York.

Robaire B., Syntin P and Jervis, K. 2000. The coming of age of the epididymis. In: *Testis, Epididymis and Technologies in the Year 2000*, Jégou B, Pineau C, Saez J, (Ed.), pp. 229- 262, Springer: Hildenberg, ISBN 978-3-540-67345-3, New York.

Robaire, B and Hinton, B.T. (Eds.) 2002. The Epididymis; From Molecules to Clinical Practice. Kluwer Academic/Plenum Publishers, New York.

Robaire, B. and Hermo, L. 1988. Efferent ducts, epididymis, and vas deferens: Structure, functions, and their regulation. In E. Knobil and J. Neill (eds.). *The Physiology of Reproduction.* Raven Press, New York. 999 – 1080.

Robaire, B., Pryor, J.L. and Trasler, J.M. 1995. How are germ cells produced and what factors control their production? In: *Handbook of Andrology*. San Francisco, CA: *Am Soc Androl*. 13 -15.

Robaire, B., Seenundun, S., Hamzeh, M., Lamour, S. A. 2007. Androgenic regulation of novel genes in the epididymis. *Asian Journal of Andrology*; 9: 545–553

.

Roberts K. P., Ensrud K. M., Wooters J. L., Nolan M. A., Johnston D. S and Hamilton D. W 2006. Epididymal secreted protein Crisp-1 and sperm function. *Mol Cell Endocrinol* 250: 122–127.

Rogers P and Webb G. P 1980. Estimation of body fat in normal and obese rat. Br. J. Nutri. 48: 83-86

Roosen-Runge, E.C. 1961. The rete tstis in the albino rat: its structure, development and morphological significance. *Acta Anat*. 45: 1 – 20.

Roosen-Runge, E.C. and Holstein, A.F. 1978. The human rete testis. *Cell and Tissue Research* 189: 409 – 433.

Rosiepen G, Aslan M, Clemen G, Nieschlag E, Weinbauer G.F 1997. Estimation of the duration of the cycle of the seminiferous epithelium in the nonhuman primate *Macaca mulatta* using the 5-bromodeoxyuridine technique. *Cell Tissue Research.* 288: 365 -369.

Ross, M.H and Romrell, L. J. 1985. Histology: A text atlas. 2nd edition. Williams and Wilkins Coy. Baltimore, Hong Kong, London and Sydney.

Rowley, M.J., Berlin, J.D and Heller, C.G. 1971. The ultrastructure of four types of human spermatogonia. *Z. Zellforsch*. 112: 139.

Russell L. D and Clermont Y. 1977. Degeneration of germ cells in normal, hypophysectomized and hormone-treated hypophysectomized rats *The Anatomical Records* 187: 347–365.

Russell L. D., Ettlin R A., Sinha Hikim A. P and Clegg E. D. 1990. Histological and Histopathological Evaluation of the Testis. Clearwater: Cache River Press: 41-58.

Saidapur S. K and Kamath S. R. 1994. Kinetics of spermatogenesis in Indian desert gerbil (*Meriones hurrianae* Jerdon): seminiferous epithelial cycle, frequency of stages, spermatogonial renewal and germ cell degeneration. *Annals of Anatomy*. 176: 287-295

Sakamoto H., Saito K and Oohta M. 2007. Testicular Volume Measurement: Comparison of Ultrasonography, Orchidometry, and Water Displacement. *Urology*. 69: 152-157.

Samuelson, D.A. 2007. Textbook of Veterinary Histology. (ed.) Saunders Elsevier, St. Louis Missouri 63146. 418 – 441

Sandberg A.A., Karr J.P., Muntzing J. 1980. The prostates of dog, baboon and rat. In: Spring-Mills E, Hafez ESE, editors. Male accessory sex glands. Biology and pathology, New York: Elsevier/North Holland Biomedical Press. 565–608.

Satoh, Y., Ishikawa, K., Oomori, Y., Takede, S., Ono, K.. 1992. Secretion mode of the harderian gland of rats after stimulation by cholinergic secretagogues. *Acta Anat*. (Basel) 143, 7–13.

Saunders, P. T., Sharpe, R. M., Williams, K., Macpherson, S., Urquart, H., Irvine, D. S. & Millar, M. R. 2001. Differential expression of oestrogen receptor alpha and beta proteins in the testes and male reproductive system of human and non-human primates. *Molecular Human Reproduction* 7: 227–236. (doi:10.1093/molehr/7.3.227)

Scherle, W. A 1970. Simple method for volumetry of organs in quantitative stereology. *Mikroskopie* 26**:** 57

Schimming B. C and Vicentini C. A. 2001. Ultrastructural features in the epididymis of the dog (*Canis familiaris, L*). *Anatomia Histologia Embryologia* 30: 327–332.

Schneider G., Kirschner M. A., Berkowitz R and Ertel N. H. 1979. Increased estrogen production in obese men. *J Clin Endocrinol Metab* 48:633–638.

Schon J, Neumann S, Wildt D E, Pukazhenthi B S, Jewgenow K.. 2009. Localization of oestrogen receptors in the epididymis during sexual maturation of the domestic cat. *Reproduction of Domestic Animals* 44 (suppl 2): 294–301.

Schulze, C. 1984. Sertoli cells and Leydig cells in man. In: *Advances in anatomy, embryology and cell biology* 88: 195 – 292.

Segatelli, T. M., França, L. R., Pinheiro, P. F. F., Alemida, C. C. D., Martinez, M. and Martinez, F. E. 2004. Spermatogenic Cycle Length and Spermatogenic Efficiency in the Gerbil (*Meriones unguiculatus*). *Journal of Andrology* 25. 6: 1 – 21.

Segatelli, T. M., Pinheiro P. F. F., Almeida C. C. D., Martinez M., Padovani C. R and Martinez F. E. 2000. Ultrastructural study of acrosome formation in mongolian gerbil (*Meriones unguiculatus*). *Tissue Cell.* 32**:** 1 -10

Segatelli, T.M., Almeida, C.C.D., Pinheiro, P.F.F., Martinez, M., Padovani, C.R., Martinez, F.E. 2002. Kinetics of spermatogenesis in the Mongolian gerbil (*Meriones unguiculatus*). *Tissue and Cell* 34 .1: 7-13.

Setchell, B.P. 1977. Reproduction in male Marsupials. In: Biology of marsupials, eds. D.P. Gilmore and B. Stonehouse, London, Marcmillan, 411 – 457.

Setchell, B.P. (1980): The functional significance of blood-testis barrier. Journal of Andrology **1**: pp 3 – 10.

Shabsigh, A., Tanji, N., D'Agati, V., Burchardt, T., Burchardt, M., Hayek, O., Shabsigh, R. and Buttyan, R. 1999. Vascular anatomy of the rat ventral prostate. *The Anatomical Record* 256: 403–411.

Shapiro E, Huang H, Masch R. J, McFadden D. E, Wilson E. L and Wu X R. 2005. Immunolocalization of estrogen receptor alpha and beta in human fetal prostate *Journal of Urology* 174. 5: 2051–3.

Shayu D, Kesava C. C, Soundarajan R and Rao A. J. 2005. Effects of ICI 182780 on estrogen receptor expression, fluid absorption and sperm motility in the epididymis of the bonnet monkey. *Reprod Biol Endocrinol* 3:10.

Shi, S. R., Key, M. E. and Kalra, K. L. 1991. Antigen retrieval in fomali-fixed paraffin-embedded tissue: an enhancement method for immunohistochemical staining based on microwave oven heating of sections. *Journal of Histochemistry and Cytochemistry* 39: 741 – 748

Short, R.V. 1990. Oestrous and menstrual cycles. In: Austin and Short R.V (Editors) Reproduction in mammals: Hormonal control of reproduction: Volume 3, 2nd Edition 115 – 152. University Press, Cambidge.

Shum W. W., Da Silva N., Brown D and Breton S. 2009. Regulation of luminal acidification in the male reproductive tract via cell-cell crosstalk. *Journal Experimental Biology* 212: 1753–1761.

Sierens, J. E., Sneddon, S. F., Collins, F., Millar, M. R. and Saunders, P. T. 2005. Estrogens in testis biology. Ann. N. Y. Acad. Sci. 1061, 65–76. (doi:10.1196/annals.1336.008)

Sirigu, P., Turno, F., Usai, E., Perra, M.T. 1993. Histochemical study of the human bulbourethral (Cowper's) glands.*Andrologia* 25: 293–299.

Sjostrand, N. O. 1965. The adrenergic innervation of the vas deferens and the accessory male genital gland. *Acta. Physiol. Scand.* 169-75.

Skinner, J.D., Booth, W.D., Rowson, L.E., Karg, H. 1968. The post-natal development of the reproductive tract of the Suffolk ram, and changes in the gonadotrophin content of the pituitary. *J. Reprod. Fertil*. 16: 463–477.

Sluczanowska-Glabowska S, Laszczyñska M, Wylot M, Glabowski W, Piasecka M and Gacarzewichz D. 2010. Morphological and immunohistochemical compare of three rat prostate lobe (lateral, dorsal and ventral) in experimental hyperprolactinemia. *Folia Histochem Cytobiol* 48: 447-454

Smith, R. L. (Ed.) 1984 Sperm competition and the evolution of animal mating system. San Diego: Academic Press.

Smithwick E. B., Young L. G and Gould K. G. 1996. Duration of spermatogenesis and relative frequency of each stage in the seminiferous epithelial cycle of the chimpanzee. *Tissue Cell.* 28: 357 -366

Sobowale O. B and Akiwumi O. 1989. Testicular volume and seminal fluid profile in fertile and infertile males in Ilorin, Nigeria. *Int J Gynaecol Obstet*. 28:155-161

Solakidi, S., Psarra, A. M., Nikolaropoulos, S. & Sekeris, C. E. 2005. Estrogen receptors alpha and beta (ERalpha and ERbeta) and androgen receptor (AR) in human sperm: localization of ERbeta and AR in mitochondria of the midpiece. *Human Reproduction*. 20: 3481–3487. (doi:10. 1093/humrep/dei267)

Soranzo L., Dadoune J. P and Fain-M. 1982. Segmentation of the epididymal duct in mouse: An ultrastructural study. *Reprod. Nutr. Dev*. 22: 999-1012

Spyropoulos E., Borousas D and Mavrikos S 2002. Size of external genital organs and somatometric parameters among physically normal men younger than 40 years old. *Urology* 60: 485-489.

Steinberger, A and Steinberger , E. 1976. Secretion of an FSH-inhibiting factor by cultured Sertoli cells. *Endocrinology* 98: 918 – 921.

Stoltenberg, M., Therkildsen, P., Andreasen, A., Jensen, K.B., Juhl, S., Ernst, E., Danscher, G., 1998. Computer-assisted visualization of the rat epididymis: a methodological study based on paraf.n sections autometallographically stained for zinc ions. *Histochem. J*. 30: 237–244.

Strzezek J., Martı´n-Rillo S., i S_aiz-Cidoncha F. 2000. Glandula vesicular seminal del verraco: su papel en la capacidad de fertilizaci_on. Anaporc 205:59–84.

Sugimura, Y., Cunha, G.R. and Donjacour, A.A. 1986. Morphogenesis of ductal networks in the mouse prostate. *Biology of Reproduction* 34: 961–971.

Sullivan R., Frenette G and Girouard J. 2007. Epididymosomes are involved in the acquisition of new sperm proteins during epididymal transit. Asian Journal of Andrology 9: 483–491.

Sun E. L and Flickinger C. J 1982. Proliferative activity in the rat epididymis during postnatal development. *The Anatomical Records* 203**:** 273-284

Takano H. 1980. Qualitative and Quantitative histology and histogenesis of the mouse epididymis, with special emphasis on the regional difference. *Acta Anat.* (Nippon.) 55: 573-587

Testa-Riva, F., Riva, A., Congiu, T., De Lisa, A., Motta, P.M. 1994. Human bulbourethral and urethral glands. In: Motta, P.M. (Ed.), Ultrastructure of the Male Urogenital Glands: Prostate, Seminal Vesicles, Urethral, and Bulbourethral Glands. Kluwer Academic Publishers, New York, 163–176.

Thompson A. 2001. Role of androgen and fibroblast growth factors in prostatic development. *Reproduction* 121:187–195.

Timms, B.G., Mohs, T.J. and Didio, L .J. 1994. Ductal budding and branching patterns in the developing prostate. *Journal of Urology* 151: 1427–1432.

Timo S., Godwin N., Brenker C., Kashikar N. D., Wenyand I., Seifert R and Kaupp U. B. 2011. The CatSper channel mediates progesterone-induced Ca^{2+} influx in human sperm. Nature doi: 10.1038/nature09769

Toma, J., and Buzzell G. 1988. Fine structure of the ventral and dorsal lobes of the prostate in the young adult Syrian hamster, Mesocricetus auratus. *American Journal of Anatomy* 2: 132–140.

Toshimori, K. 2003. Biology of spermatozoa maturation: an overview with an introduction to this issue. *Microscopy Research and Technique,* 61 .1: 1-6

Tuck, R.R., Setchell, B.P., Waites, G.M.H. and Young, J.A. 1970. The composition of fluid collected by micropuncture and catheterization from the seminiferous tubules and rete testis of rats. *European Journal of Physiology* 31**.** 8: 225 – 243.

Turner T. T. 2002. Necessity's potion: inorganic ions and small organic molecules in the epididymal lumen. In: Robaire B, Hinton BT (eds.). The Epididymis: from Molecules to Clincal Practice. New York: Kluwer Academic/Plenum Publishers; 49–80.

Turner T., Edery M., Mills K. T and Bern H. A. 1989. Influence of neonatal diethylstilbestrol treatment on androgen and estrogen receptor levels in the mouse anterior prostate, ventral prostate and seminal vesicle. *J Steroid Biochem* 32: 559–564.

Turner, T.T. 2008. De Graaf's thread: the human epididymis. *Journal of Andrology* 29 .3: 237-50

Ueno H and Mori H. 1990. Morphometrical analysis of Sertoli cell ultra-structure during the seminiferous epithelial cycle in rat. *Biology of Reproduction*. 43**:** 769-776

UFAW Handbook on the care and management of laboratory animals 1989. (Poole, B.P. ed) 6th Ed. Longman Scientific and Technical.

Umar A., Ooms M.P., Luider T. M., Grootegoed J. A.and Brinkmann A. O. 2003. Proteomic Profiling of Epididymis and Vas Deferens: Identification of Proteins Regulated during Rat Genital Tract Development. *Endocrinology* 144 .10): 4637–4647

Va´squez, B. and del Sol, M. 2002. Prostatic complex in the rabbit (Oryctolaguscuniculus). *Rev. Chil. Anat*. 20: 175–180.

Van Haaster L. H and de Rooij D. G. 1993. Spermatogenesis is accelerated in the immature Djungarian and Chinese hamster and rat. *Biology of Reproduction* 49: 1229 –1235

Veermachaneni, D.N.R. and Amann,R.P. 1991. Endocytosis of androgen-binding protein, clusterin, and transferrin in the efferent ducts and epididymis of the ram. *Journal of Andrology* 12: 288 – 294

Veneziale, C.M., Brown, A.L.J. and Prendergast, F.G. 1974. Histology and fine structure of guinea pig seminal vesicle. *Mayo Clin. Proc*. 49: 309–313

.

Verhagen, A.P., Aalders, T.W., Ramaekers, F.C., Debruyne, F.M. and Schalken, J.A. 1988. Differential expression of keratins in the basal and luminal compartments of rat prostatic epithelium during degeneration and regeneration. *Prostate* 13: 25–38.

Vierula M. E., Rankin T. L and Orgebin-Crist M. C. 1995. Electron microscopic immunolocalization of the 18 and 29 kilodalton secretory proteins in the mouse epididymis: evidence for differential uptake by clear cells. *Microsc Res Tech* 30: 24–36.

Vincentini C. A., Orsi A. M and Gregorio E. A. 1990. Fine structure of the ductuli efferentes of the hamster (Mesocricetus auratus). Gegenbaurs morpho Jahrb Leipzig 136:111–118

Walker, V. R., Jefferson, W. N., Couse, J. F and Korach, K. S. 2012. Estrogen Receptor-α Mediates Diethylstilbestrol-Induced Feminization of the Seminal Vesicle in Male Mice. *Environmental Health Perspectives*, 120 .4: 560-565

Weber, J.E., Russell, L.D., Wong, V and Paterson, R. N. 1983. Three-dimensional reconstruction of a rat stage Sertoli cell II. Morphometry of Sertoli and Sertoli-germ cell relationships. *American Journal of Anatomy* 167: 163 – 179.

Weddington S. C., Hansson V., Purvis K., Varaas T., Verjans H. L., Eik-nes K. B., Ryan W. H., French F. S and Ritzén E. M. 1976. Biphasic effect of testosterone propionate on Sertoli cell secretory function, *Mol. Cell. Endocrinol.* 5 : 137–145.

Weinbauer G. F., Aslam H., Krishnamurthy H., Brinkworth M. H., Einspanier A, Hodges I. K.. 2001. Quantitative analysis of spermatogenesis and apoptosis in the common marmoset (*Callithrix jacchus*) reveals high rates of spermatogonial turnover and high spermatogenic efficiency. *Biology of Reproduction* 64: 120 -126

Weiss, L. 1983. Histology, Cell and Tissue Biology 5th edition. Elsevier Science Publishing Co. Inc, New York 10017, pp 1001 – 1053.

Wendell S. C. 2000. Terminology of prostate and related structures. *Clinical Anatomy* 13:207-213.

Wensing C.J.G. 1986. Testicular descent in the rat and a comparison of this process in the rat with that in the pig. *The Anatomical Records* 214: 154–160

Wheater, P.R., Burkitt, H.G. and Daniels, V.G. 1990. Male reproductive system. In: Functional Histology. A text and colour atlas. ELBS (2^{nd}) edition, 18: 277 – 288.

Wiesner, B. 1934. The post-natal development of the genital organs in the albino rat. *Journal of Obstetrics and Gynaecology* British Empire 41: 867 – 922.

Wikramanayake E. 1995. Testicular size in young adult Sinhalese. *Int J Androl*. 18(Suppl 1): 29-31.

Williams K, Saunders P.T.K, Atanassova N, Fisher J.S, Turner K.J, Millar M.R, McKinnell C, Sharpe R.M. 2000. Induction of progesterone receptor immunoexpression throughout the male reproductive tract after neonatal estrogen treatment of rats. *Mol Cell Endocrinol* 164: 117–131.

Williams K., Fisher J S., Turner K J., McKinnell C., Saunders P T, Sharpe R M. 2001. Relationship between expression of sex steroid receptors and structure of the seminal vesicles after neonatal treatment of rats with potent or weak estrogens. *Environmental Health Perspectives* 109: 1227–1235.

Williams M.P.L and Hutson J.M. 1991. The phylogeny of testicular descent. *Pediatr Surg Int* 6: 162–166.

Wislocki, G.B. (1949): Seasonal changes in the testis, epididymal and seminal vesicles of deer investigated by histochemical methods. *Journal of Anatomy* 44: 167 – 189.

Witts D. M., Young L. J and Crew D. 1994. Progesterone and sexual behavior in male. *Psychoneuroendocrinology* 19 .5-7: 553-562

Wong Y. C and Tse M. K. 1981. Fine structural and functional study of the prostate complex in the guinea pig. *Acta Anat*. 109 .4: 289-312

Wrobel, K.H and Bergmann, M. 2006. In: Eurell, J.A and Frappier, B.L. Dellman's textbook of histology, 6^{th} Ed. Blackwell Publishing Ltd. Iowa. 233-255.

Wrobel, K.H., 1970: Zur morphologie des samenblasenepithels der ziege. *Zentralbl Veterinarmed A* 17: 634–643.

Yamashita S. 2004: Ontogenic expression of estrogen receptor coactivators in the reproductive tract of female mice neonatally exposed to diethylstilbestrol. *Reprod Toxicol* 18: 275–284.

Yanagimachi R., Kamiguchi Y., Mikamo, K., Suzuki, F and Yanagimachi, H. 1985. Maturation of spermatozoa in the epididymis of the Chinese hamster. *American Journal of Anatomy*, 172 .4: 317-330, ISSN 0002-9106

Yeboah, S. and Adamu, E.K**.** 1995. The cane rat. *Biologist* 42 .2: 86 – 97. 352-2662-1, Philadelphia: Saunders.

Zaviacic, M., Jakubovska, V., Belosovic, M., Breza, J. 2000. Ultrastructure of the normal adult human female prostate gland (Skene's gland). *Anatomy and Embryology*. (Berl) 201: 51–61.

Zerehdaran, S., Vereijken, A. L. J., Van Arendonk, J. A. M and Van Derwaaij, E.H. 2005. Estimation of Genetic Parameters for Fat Deposition and Carcass Traits in Broilers. *Poultry Science* 83: 521–525

Zeuner, F.E. 1963. A history of domestic animals. London, Hutchinson. 560p

Zhou Q, Nie R, Prins G. S, Saunders P. T, Katzenellenbogen B. S and Hess R. A. 2002. Localization of androgen and estrogen receptors in adult male mouse reproductive gtract. *Journal of Andrology* 23: 870–881.